

SOME STUDIES OF COMPLEXES OF  
TRANSITION METALS WITH HETEROCYCLIC LIGANDS

A Thesis  
submitted for the  
Degree of Doctor of Philosophy  
of the University of London

by

Maxwell John Weeks

Department of Chemistry  
Imperial College  
LONDON, S.W.7.

July 1966

## ABSTRACT

In these studies there were two main aims of a general nature. The first was to determine the factors that are of significance in the adoption of a given structure for nickel (II) complexes. The second was the study of the spectral and magnetic properties of nickel (II) complexes of a particular structure. More specifically, an examination was made of the general chemistry, electronic spectra, and magnetic properties of the complexes formed by nickel (II) with benzimidazole, a ligand of some biological importance.

Complexes with a number of heterocyclic ligands have been prepared, and from the trends observed, and the electronic spectra, it appeared that steric effects were the dominant factor in determining structure.

The polymeric complexes of stoichiometry  $\text{NiLX}_2$ , and  $\text{NiL}_2\text{X}_2$  (L = heterocycle, X = halide), were found to give Curie-Weiss  $\theta$  values of ferromagnetic sign. The tetrahedral complexes of the type  $\text{NiL}_2\text{X}_2$ , gave electronic spectra that suggested marked distortion from  $T_d$  symmetry. These latter complexes showed Curie-Weiss behaviour in the region 80-300°K, with small negative values of  $\theta$ . The proton n.m.r. contact shifts for these

tetrahedral complexes in solution were investigated, for ligands of the imidazole type. Predominantly  $\sigma$  delocalisation was found.

The magnetic and spectral properties of  $\text{Ni}(\text{benzimidazole})_4\text{X}_2 \cdot 2 \text{ Acetone}$  ( $\text{X} = \text{Cl}$ , (3 forms);  $\text{Br}$ ), and the various desolvation products, were found to be critically dependent on the conditions of preparation. The anomalous magnetic behaviour seen in a number of these complexes was rationalised in terms of antiferromagnetism, spin state equilibria, and phase changes.

## ACKNOWLEDGEMENTS

I should like to express my thanks to Dr. Margaret Goodgame for her guidance, and continued interest, in the supervision of the studies presented here.

During the past three years there have been numerous helpful discussions with Dr. David Goodgame, for which gratitude is extended.

My thanks are due also to Dr. D. Forster who constructed the variable temperature Gouy balance, and to Dr. M.B. Hursthouse, Mr. W.E. Finkle, and Mr. J. Foy for the development of the low temperature X-ray powder pattern apparatus.

I am indebted to Imperial College Computer Unit for the use of computing facilities.

The award of an S.R.C. grant is gratefully acknowledged.

## CONTENTS

	Page
Introduction	7
Abbreviations	13
CHAPTER I.            Polymeric 1:1 and 2:1 Nickel Halide Complexes	
Preparation	15
Electronic Spectra	16
Magnetic Properties	35
CHAPTER II.           Tetrahedral 2:1 Nickel Halide Complexes	
Preparation	45
Electronic Spectra	50
Magnetic Properties	72
CHAPTER III.          The 4:1 Complexes of Benzimidazole with Nickel (II) Halides	
Preparation	81
X-Ray Powder Patterns	89
Electronic Spectra	95

CONTENTS (continued)

	Page
Infrared Spectra	114
Magnetic Properties	116
CHAPTER IV.            Structural Factors in Nickel (II) Complexes	
Introduction	150
Six Coordinate Iron (II) Complexes	165
Six Coordinate Nickel (II) Complexes	176
Structural Factors	205
CHAPTER V.            Contact Shifts in the Proton N.M.R. Spectra of the Tetrahedral 2:1 Nickel (II) Complexes	
Introduction	218
Contact Shift Spectra	224
Pseudocontact Terms	244
CHAPTER VI.           Experimental	
Physical Measurements	250
Preparation of Compounds	256
References	282

INTRODUCTION

In these studies there are basically three main aims. Two are of a general nature. The first is an investigation of the factors which might be of significance in determining the structures adopted by nickel (II) complexes. The second is a study of the magnetic and spectral properties associated with compounds of a given structure. Various ligands have been used within this framework, one of which was benzimidazole (see p.13 ). This latter ligand has some biological importance, though the complexes formed with metal ions have been little investigated. Thus the third aspect of these studies has been an examination of the general chemistry, and electronic and magnetic properties of the nickel (II) complexes with benzimidazole, substituted benzimidazoles, and to a lesser extent the complexes with imidazole, substituted imidazoles, and benzothiazole. An outline is given below of the previous work relating to the two general topics mentioned above, and some background is given to both the biological importance of imidazole type heterocycles, and to earlier studies of the complexes formed by these ligands.

Nickel (II) forms complexes within each of the main structural classes seen for the first row transition metals, octahedral, tetrahedral, and planar. It was considered of interest to examine, in a general manner, the factors which might be of significance in determining which of these structures a nickel (II) complex would adopt with a given heterocyclic ligand, and anion. At the time of starting the present work, there had been no systematic study of this question, only a limited number of tetrahedral complexes, of the 2:1 type, being known. Tetrahedral and planar structures for complexes of the type nickel (tertiary phosphine)<sub>2</sub>X<sub>2</sub> (X = halide) had been described.<sup>1</sup> Octahedral, tetrahedral, and planar complexes in the system nickel (quinoline)<sub>2</sub>X<sub>2</sub> (X = halide) were also known<sup>2</sup>, it being suggested that structural changes might be connected with varying contributions of σ- and π- bonding.

Recently however there have been contributions in a number of publications which have added considerably to the information relating to the question of structural factors. Studies on the complexes formed with methyl substituted pyridine and quinoline type ligands,<sup>3,4,4(a),5</sup> have indicated the importance



of steric factors. On the basis of the studies on the substituted pyridine complexes,<sup>4,5</sup> and the electronic spectra of various nickel (II) complexes,<sup>6,7</sup>  $\sigma$ - and  $\pi$  bonding, and lattice energies,<sup>4,7</sup> have also been cited as possible causes of differences in structure between closely related compounds. Complexes within the various stereochemical systems have been prepared in this work, and these are examined to see if they throw any light on the structural factors, the data obtained being mainly interpreted in terms of the factors outlined above.

The electronic<sup>8,9,10</sup>, and magnetic<sup>11,13</sup> properties of nickel (II) in regular octahedral and tetrahedral symmetries are fairly well understood. There have been some studies of the effects of low symmetry on the electronic spectra of octahedral nickel (II)<sup>12</sup>, and of distortion on the magnetic properties of tetrahedral nickel (II)<sup>14</sup>. There was however little experimental data relating to these topics.

The low energy bands in the electronic spectra of both octahedral, and tetrahedral nickel (II) appear to be sensitive to distortion, and thus fairly extensive investigations were made of the electronic spectra of

complexes in various symmetries in the range 4,000-28 000  $\text{cm}^{-1}$ . The magnetic properties of the 2:1 polymeric octahedral complexes, the 2:1 tetrahedral complexes, and certain of the 4:1 complexes, were examined over the temperature range 80-300°K.

Imidazole, and the imidazole ring are considered to play a part of some importance in biological systems, mainly in connection with enzyme units, this role has been reviewed in the literature in some detail<sup>15</sup>. It has recently been suggested that the coordination possibilities of imidazole, and the delocalisation within the ring, may enable it to act as a bridge for rapid electron transfer in biological systems.<sup>16</sup>

Imidazole is found in the histidine molecule, and coordinated to iron in haemoglobin. Benzimidazole occurs in vitamin B<sub>12</sub>, where a 5,6 dimethylbenzimidazole molecule is coordinated to a cobalt ion. Benzimidazoles have been suggested as possible virus action inhibitors<sup>17</sup>, and fluorinated benzimidazoles have been shown to act as uncouplers of oxidative phosphorylation.<sup>18</sup>

The ability of benzimidazole to form salts with metals was first noted in the 1870's<sup>19,20</sup>. Most of the subsequent work was done in Germany, concerned

mainly with the preparation of the inner complexes<sup>21,22</sup>. The inner complexes with cobalt, nickel and copper (II), and the 4:1 and 2:1 vanadyl complexes have been described since 1950 by workers in India<sup>23,24</sup>. The only recent study of the complexes with this ligand was concerned with the electronic spectra, and room temperature magnetic properties, of the 2:1 tetrahedral complexes with cobalt (II) salts.<sup>25</sup>

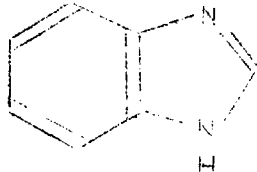
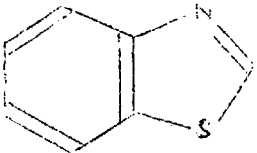

The inner complexes formed by imidazole with nickel, copper, zinc and silver have been prepared<sup>26,27</sup>, also a hydrated 6:1 complex with nickel chloride<sup>27</sup>. The interaction of imidazole with metal ions in solution is considered of importance in understanding the action of proteins, and several stability constant studies have been made<sup>28,29,30,31</sup>.

Imidazole has two possible sites for coordination, in the secondary (pyrrole type), and tertiary (pyridine type) nitrogens. The various investigations to date have suggested that coordination takes place through the tertiary nitrogen. This was based on, changes in the N-H stretching frequency on coordination,<sup>32</sup> differences in stability constants between complex formation with benzimidazole and N-substituted benzimidazole<sup>33</sup>, and n.m.r. studies on the imidazole group in histidine complexes<sup>34</sup>.

There appears to be very little published material on the complexes formed by benzothiazole (see p.13 ), though very recently there has been a contribution from Russia on the copper complexes with 2-substituted benzothiazoles.<sup>35</sup>

Various techniques have been used in the course of this present work. The theoretical principles are not in general given here, as there is not space available to give an adequate coverage of each, and also as there are several excellent reviews and textbooks relating to these subjects, electronic spectra<sup>36,37,38</sup>, magnetism<sup>38, 11,39</sup> and n.m.r. contact shifts<sup>40,41</sup>. This latter topic is less well documented than the first two, and is dealt with briefly in the introduction to Chapter V. An outline is also given, in Chapter IV, covering some of the main references to the crystal field and molecular orbital treatments of the splitting of electronic spectral bands arising on the lowering of symmetry.

Abbreviations used in Text

<u>Ligand</u>		<u>Abbreviation</u>
Acetone		Ac
Benzimidazole		bz
2-Methylbenzimidazole		2-mebz
5,6-Dimethylbenzimidazole		5,6-dimebz
5,6-Dichlorobenzimidazole		5,6-diClbz
Benzothiazole		bth
2-Methylbenzothiazole		2-mebth
Imidazole		im
2-Methylimidazole		2-meim
N-Methylimidazole		N-meim
Isoquinoline		isoqn
3-Methylisoquinoline		3-meisoqn

Abbreviations (continued)

<u>Ligand</u>	<u>Abbreviation</u>
2,5-Lutidine (2,5-Dimethylpyridine)	2,5-lut
Pyridine	py
4-Cyanopyridine	4-CNpy
3,5-Dichloropyridine	3,5-diClpy
Quinoline	qn

<u>Anion</u>	<u>Abbreviation</u>
Tetramethylammonium	$[\text{Me}_4\text{N}]^+$
Tetraethylammonium	$[\text{Et}_4\text{N}]^+$
Methyltriphenylarsonium	$[\text{MePh}_3\text{As}]^+$

Abbreviations relating to spectral data

s ; strong	sh ; shoulder
m ; medium	n.r ; not resolved (for two
w ; weak	bands of similar intensity)
	br ; broad
v ; very	sp ; sharp

CHAPTER I

Polymeric 1:1 and 2:1 Nickel Halide Complexes

Preparation

Complexes were prepared of the type  $NiLX_2$ , (L = imidazole, benzimidazole, quinoline, 2-methylbenzothiazole, and 3-methylisoquinoline, X = Cl, Br ; L = pyridine, X = Cl); and  $NiL_2X_2$ , (L = pyridine, benzothiazole, X = Cl, Br). The 2:1 complexes with benzimidazole and 3-methylisoquinoline were tetrahedral, and with 2-methylbenzothiazole, planar, these complexes are described in Chapter II.

The 1:1 complexes  $NiLX_2$  (L = imidazole, benzimidazole, X = Cl, Br ; L = 2-methylbenzothiazole, X = Cl), were prepared by evaporating to dryness a 1+1 ethanolic solution of ligand and nickel halide. The other 1:1 complexes were obtained by heating the 2:1 complex. The colours of the 1:1 complexes are described on p.

The 2:1 complexes were prepared by mixing ethanolic solutions of ligand and nickel halide, in 2:1 mole ratio, when the complexes precipitated. The 2:1 complexes with pyridine were yellow-green, and those

with benzothiazole, pale yellow.

### Electronic Spectra.

The electronic spectra of the compounds were measured by the diffuse reflectance technique in the range 4,000 - 28,000  $\text{cm}^{-1}$  (Table 1.1, Fig. I.1). The spectra may be interpreted in terms of the energy levels arising for nickel (II) in an essentially octahedral environment. Calculations have been done<sup>8</sup> for the energy levels in nickel (II) in  $O_h$  symmetry, using the crystal field approximation, including spin-orbit coupling, the results are given in Fig. I.2.

The compound  $[\text{Me}_4\text{N}][\text{NiCl}_3]$  may be used to give a value for the ligand field parameter,  $\Delta$ , arising from an octahedral arrangement of chloride ions about a nickel ion. (This compound had been prepared previously<sup>42</sup>). Little distortion would be expected, and the spectrum may be assigned in  $O_h$  symmetry:

${}^3A_{2g} \rightarrow {}^3T_{2g}$ , [ $\nu_1$ ] at 6,600  $\text{cm}^{-1}$  ;  ${}^3A_{2g} \rightarrow {}^3T_{1g}$  ( ${}^3F$ ), [ $\nu_2$ ] at 11,200 ;  ${}^3A_{2g} \rightarrow {}^1E_g$  ( ${}^1D$ ) at  $\sim 12,800$  ;  ${}^3A_{2g} \rightarrow {}^1T_{2g}$  ( ${}^1D$ ) at  $\sim 18,200$  ;  ${}^3A_{2g} \rightarrow {}^3T_{1g}$  ( ${}^3F$ ), [ $\nu_3$ ] at 21,200.

While the assignments fit well in the Liehr and Ballhausen scheme for  $\lambda = -275\text{cm}^{-1}$  and  $F_4 = 90\text{cm}^{-1}$  (Fig. I.2). This does not rationalise the weak shoulder at  $\sim 14,300\text{cm}^{-1}$ .



Table 1.1

Electronic Absorption Spectra<sup>\*</sup>

<u>Compound</u>	<u>Absorption Maxima (cm.<sup>-1</sup>)</u>
[Me <sub>4</sub> N][NiCl <sub>3</sub> ]	21,200 ; ~18,200(sh) ; ~14,300(w.sh) ; ~12,800(sh) ; 11,200 ; 6,600
Ni(py) <sub>2</sub> Cl <sub>2</sub>	24,100 ; ~22,200(sh) ; ~13,900 ; ~12,200(sh) ; 8,400 ; 6,000
Ni(py) <sub>2</sub> Br <sub>2</sub>	23,350 ; ~21,400(sh) ; ~19,800(sh) ; 13,700 ; ~11,600(sh) ; 8,000 ; 5,800
Ni(bth) <sub>2</sub> Cl <sub>2</sub>	23,300 ; ~19,700(sh) ; 13,700 ; ~12,300(sh) ; 8,100 ; ~6,700(sh)
Ni(bth) <sub>2</sub> Br <sub>2</sub>	22,300 ; ~18,700(sh) ; 13,200 ; ~11,600(sh) ; 7,800 ; ~6,300(sh)
Ni(qn) <sub>2</sub> Cl <sub>2</sub> <sup>***</sup>	22,700 ; ~19,200(sh) ; 13,150 ; ~12,000 ; 7550 ; ~6,000(sh)
Ni(py)Cl <sub>2</sub>	22,400 ; ~18,900(sh) ; 13,100 ; ~12,200(sh) ; 7,800 ; ~6,500(sh)
Ni(im)Cl <sub>2</sub>	22,100 ; ~18,700(sh) ; 12,950 ; 12,000 ; 7,700 ; ~6,300(sh)
Ni(im)Br <sub>2</sub>	21,400 ; ~18,700(sh) ; ~18,000(sh) ; 12,300 ; ~11,300(sh) ; 7300 ; ~5900(sh)
Ni(im)Br <sub>2</sub> 77°K	21,600 ; 19,400 ; ~18,300(sh) ; 12,700 ; ~11,800(sh) ; 7,700 ; 6,450
Ni(bz)Cl <sub>2</sub>	21,700 ; ~18,500(sh) ; ~16,000(sh) ; 13,000 ; 11,800 ; 7,450 ; ~6,100(sh)
Ni(bz)Br <sub>2</sub>	20,900 ; ~17,900(sh) ; 12,200 ; ~11,100(sh) ; 7,200 ; ~6,00(sh)

\* At room temperature unless otherwise stated

\*\*\* Yellow form, previously prepared<sup>2</sup>.

Table 1.1 (continued)

<u>Compound</u>	<u>Absorption maxima (cm<sup>-1</sup>)</u>
Ni(qn)Cl <sub>2</sub>	21,100 ; ~18,500(sh) ; 11,100 ; ~10,200(sh) 6,400
Ni(qn)Br <sub>2</sub>	20,000 ; ~17,500(sh) ; 14,500(sh) ; 10,800 ; ~9,500(sh) ; 6,250
Ni(2-mebth)Cl <sub>2</sub>	21,200 ; ~18,900(sh) ; ~16,300(w.sh) ; 11,000 ; ~9,000(sh) ; ~7,400(w)
Ni(2-mebth)Cl <sub>2</sub>	77°K 21,200 ; ~20,100(sh) ; ~19,000(sh) ; 17,450 ; 16,000(w) ; 11,300 ; ~9,500(sh) 7,600 ; 6,000
Ni(2-mebth)Br <sub>2</sub>	19,700 ; ~17,000(sh) ; 10,500 ; 6,100
Ni(2-mebth)Br <sub>2</sub>	77°K 19,800 ; ~18,700(sh) ; 17,700 ; ~10,600 ~9,500(sh) ; 6,200
Ni(3-meisoqn)Cl <sub>2</sub>	21,200 ; ~19,200(sh) ; ~16,700(w.sh) 11,000 ; ~9,100(sh) ; ~7,400(w)
Ni(3-meisoqn)Br <sub>2</sub>	20,100 ; ~18,200(sh) ; 14,500(w) 10,700 ; ~8,700(sh) ; 7,200
Ni(3-meisoqn)Br <sub>2</sub>	77°K 20,200 ; 18,200 ; 16,800(w) ; 14,500 11,000 ~9,000(sh) ; 6,900 ; 6,100

Fig. I.1 Spectra of: A. Ni(pyridine)<sub>2</sub>Cl<sub>2</sub>  
 B. Ni(pyridine)Cl<sub>2</sub>  
 C. Ni(quinoline)Cl<sub>2</sub>

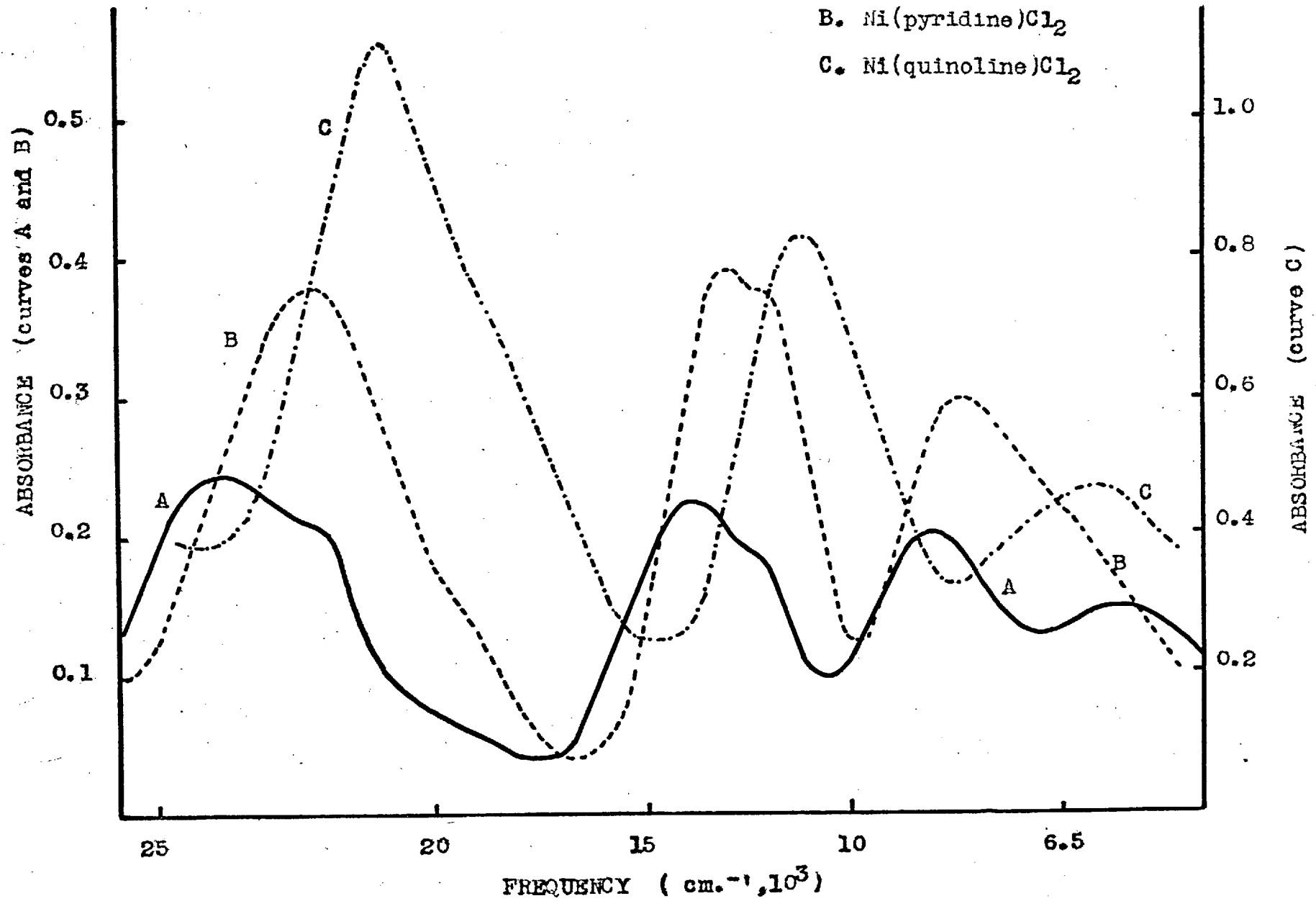
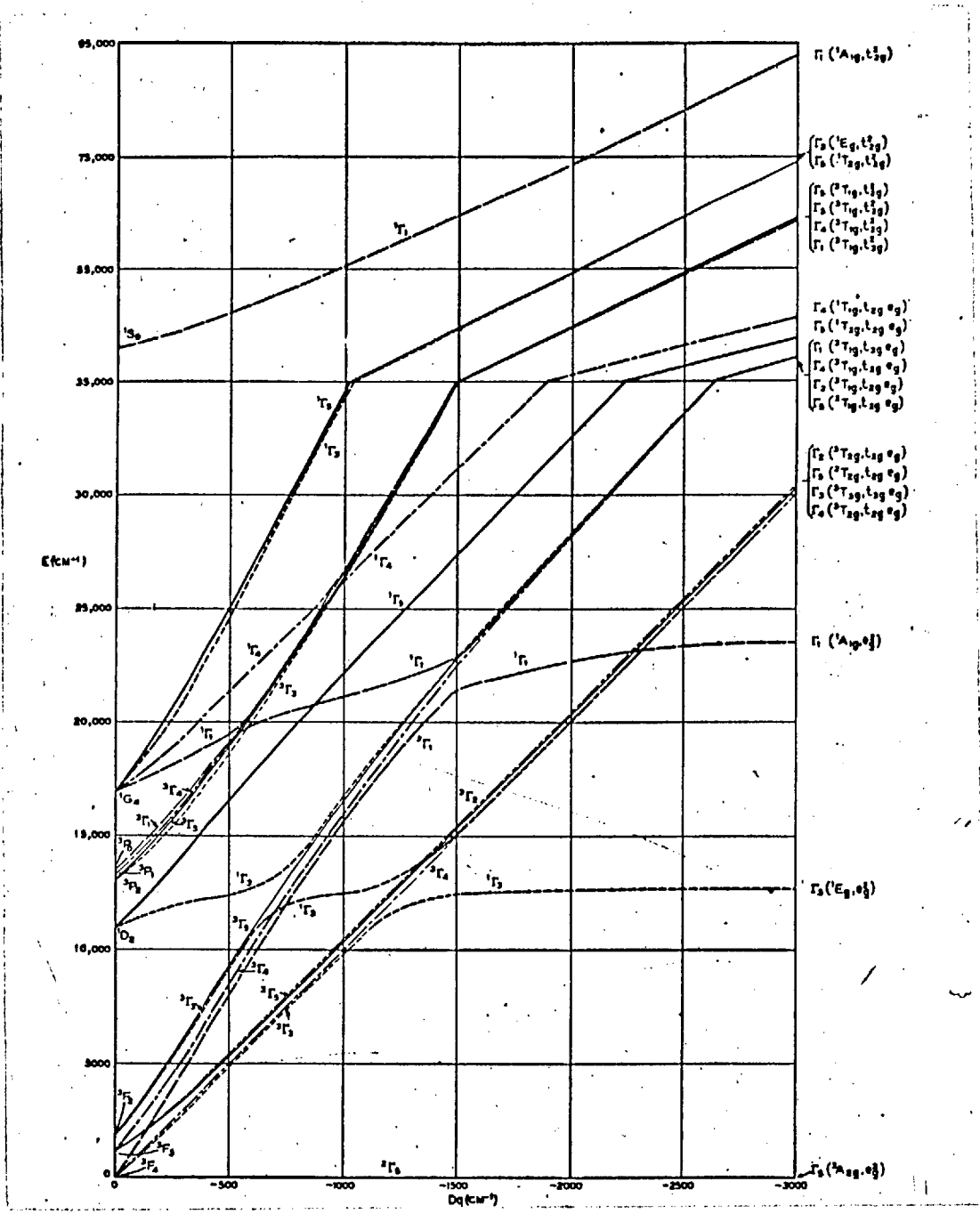


Fig. I.2



Energy level curves for a  $d^8$  electronic system in an octahedral field for  $\lambda = -275 \text{ cm}^{-1}$ , and  $F_4$  equal to  $90 \text{ cm}^{-1}$  ( $F_2 = 14F_4$ )

(from ref. 8)

A possibility is that the field is in fact distorted from  $O_h$  symmetry, and that the bands at 11,200, and 12,800  $\text{cm}^{-1}$ , are spin allowed components of a split  $v_2$  band, when the shoulder at  $\sim 14,300 \text{cm}^{-1}$  would be assigned as the  ${}^3A_{2g} \rightarrow {}^1E_g({}^1D)$ . The value of  $\Delta$  is given by the energy of the  ${}^3A_{2g} \rightarrow {}^3T_{2g}$  transition, i.e. 6,600  $\text{cm}^{-1}$ . The interelectronic repulsion parameter in the complex, B', may be found from the relationship:<sup>43</sup>

$$15B' = \text{Energy } {}^3T_{1g}({}^3F) + \text{Energy } {}^3T_{1g}({}^3P) - 3\Delta$$

For the above complex the value of B' is found to be  $\sim 840 \text{cm}^{-1}$ , compared with  $\sim 1030 \text{cm}^{-1}$  for the free ion.

For the 2:1 complex  $\text{Ni}(\text{pyridine})_2\text{Cl}_2$ , each nickel ion has been shown to be surrounded by four halide ions and two nitrogen atoms, in a transconfiguration.<sup>44</sup> In the resultant approximately  $D_{4h}$  symmetry, the electronic states of symmetry  $E_g$ ,  $T_{1g}$  and  $T_{2g}$ , arising in  $O_h$  symmetry, for nickel (II) will be split:

$$\begin{aligned} E_g &\longrightarrow A_{1g} + B_{1g} \\ T_{1g} &\longrightarrow A_{2g} + E_g \\ T_{2g} &\longrightarrow B_{2g} + E_g \end{aligned}$$

The ground state symmetry will be  $B_{1g}$ . In discussing the spectra of the distorted octahedral nickel (II) complexes the symbols  $\nu_1$ ,  $\nu_2$ , and  $\nu_3$ , as given above for the spin allowed transitions, in regular  $O_h$  symmetry, will be used to describe the bands arising from the transitions to the groups of levels arising from the splitting of the orbital triplet levels by low symmetry. Thus in  $D_{4h}$  symmetry the  $\nu_1$  band will have components of  $B_{2g}$  and  $E_g$  symmetry.

Assignments may be made for the spectrum of  $Ni(\text{pyridine})_2Cl_2$ ;  ${}^3B_{1g} \rightarrow {}^3B_{2g}$  at  $6,000\text{ cm}^{-1}$ ;  ${}^3B_{1g} \rightarrow {}^3E_g$  at  $8,400$ ; the latter band being the more intense (Fig. I.1). The bands seen in the region of  $\sim 13,500\text{ cm}^{-1}$ , and  $\sim 24,000$ , may be generally assigned to  $\nu_2$  and  $\nu_3$  respectively, or to components of these bands if split. The splitting expected is however not known, and it is not clear whether the shoulders seen on the low energy side of the main bands, (Fig. I.1), arise from orbital singlet components, or from spin forbidden transitions, or both superimposed. Thus tentative assignments could be made:  ${}^3B_{1g} \rightarrow {}^1A_{1g}$  and  ${}^1B_{1g}$ , or  ${}^3B_{1g} \rightarrow {}^3A_{2g}$ , at  $\sim 12,800\text{ cm}^{-1}$ ;  ${}^3B_{1g} \rightarrow {}^1B_{2g}$  and  ${}^1E_g$  or  ${}^3B_{1g} \rightarrow {}^3A_{2g}({}^3P)$ , at  $\sim 22,200$ ; and  ${}^3B_{1g} \rightarrow {}^3E_g({}^3P)$  at  $24,100$ .

The complexes  $\text{Ni L}_2 \text{X}_2$  (L=quinoline, X=Cl; L=benzothiazole, X=Cl,Br) gave electronic spectra which were similar in form to the spectra of  $\text{Ni}(\text{pyridine})_2\text{Cl}_2$ , suggesting that they have the same trans-octahedral structure. The  $\nu_1$  band energy may be used to obtain a value for  $\Delta$ , as described above. The weighted average of the energies of the components of  $\nu_1$  will be taken, to give a value of  $\Delta$  for the field taken as spherically symmetric, the 'average ligand field'. In the case of the 2:1 benzothiazole and quinoline complexes, the splitting of  $\nu_1$  was less than that seen for the pyridine complexes, and it was not clear exactly where the  ${}^3\text{B}_{1g} \rightarrow {}^3\text{B}_{2g}$  transition should be placed, it being seen as a broadening to low energy of the main component. This rendered the value of  $\Delta$  for these complexes rather less reliable. The differences in the splittings of the  $\nu_1$  bands will be discussed further in Chapter IV. The  $\Delta$  values are given in Table 1.2.

The effective value of  $\Delta$  appears to be similar for the 2:1 complexes with pyridine and benzothiazole, suggesting that the latter is bonded via the nitrogen atom, as low fields might be expected if the sulphur was coordinated. The lower  $\Delta$  value seen in the quinoline complex may be a reflection of the greater steric

hindrance that might be associated with this ligand. The calculation of B' values, as described above, if carried out for the 2:1 complexes would require mean  $\nu_2$  and  $\nu_3$  band energies, from the weighted averages of component energies. The values obtained are rather sensitive to the assignments taken, and in view of the general uncertainty on this latter point, B' values are not given, but they appear to be of the same order as seen in  $[\text{Me}_4\text{N}][\text{NiCl}_3]$ .

The 1:1 complexes with the ligands pyridine, imidazole, and benzimidazole, (to be termed pyridine type ligands), give electronic spectra similar to those seen for the 2:1 complexes described above, but with smaller splittings of  $\nu_1$  and  $\nu_2$ , and with the bands lying to lower energy. For the complex  $\text{Ni}(\text{pyridine})\text{Cl}_2$  the value of  $\Delta$  lies about half-way between that seen for  $\text{Ni}(\text{pyridine})_2\text{Cl}_2$  and  $[\text{Me}_4\text{N}][\text{NiCl}_3]$ . (Table 1.2). The splitting of the  $\nu_1$  band also appears to be about half that for the 2:1 complex (Table 1.1, Fig. I.1). It thus seems reasonable to suppose a polymeric structure for the 1:1 complex, in which halide ions occupy five coordination positions, and the heterocycle the sixth. Band assignments may thus be made as for  $\text{Ni}(\text{pyridine})_2\text{Cl}_2$ , but with the components of  $\nu_1$  no



longer resolved. The symmetry in the 1:1 complex is lower than  $D_{4h}$ , and is probably approximating to  $C_{4v}$ , when the g suffix given to the symmetry symbols in  $D_{4h}$  is dropped i.e. in  $C_{4v}$  ,  $B_{1g} \rightarrow B_1$  etc.

The electronic spectra of  $NiLCl_2$  (L=imidazole, benzimidazole) are as that for  $Ni(pyridine)Cl_2$ , suggesting that they have similar structures. The imidazole groups do not appear to be bridging, as if this were the case, and the bridging were such that the nitrogens were trans-, then splittings of the same order of magnitude as seen in  $NiL_2X_2$  might be expected. If the nitrogens were cis- then the splitting would be small, but the bands would be expected at higher energy. While the  $\Delta$  values, (Table 1.2), seen in the 1:1 complexes are probably not very sensitive indicators of ligand field strength for the heterocycle, in that the latter occupy one coordination position, it seems that imidazole and pyridine give similar fields, with benzimidazole rather weaker, probably due to steric effects.

The complexes of the form  $NiLX_2$  (L=pyridine, X=Cl ; L=imidazole, benzimidazole, X=Cl,Br) are pale yellow for the chloride complexes, and pale

Table 1.2  
Spectral and Magnetic Parameters

Compound	$\Delta$ ( $\text{cm}^{-1}$ )	Diamag. corr. $\times 10^6$ (c.g.s.u.)	T.I.P. $\times 10^6$ (c.g.s.u.)	$\theta$ ( $^\circ\text{K}$ )	$\mu_{\text{eff.}}^{\#}$ (B.M.)	$-\lambda'$ ( $\text{cm}^{-1}$ )
$[\text{Me}_4\text{N}][\text{NiCl}_3]$	6600	213	318	0 $\pm$ 2	3.20 $\pm$ 0.03	220 $\pm$ 20
$\text{Ni}(\text{py})_2\text{Cl}_2$	7600	165	272	19	3.17	230
$\text{Ni}(\text{py})_2\text{Br}_2$	7250	180	288	13	3.14	200
$\text{Ni}(\text{bth})_2\text{Cl}_2$	7600					
$\text{Ni}(\text{bth})_2\text{Br}_2$	7300					
$\text{Ni}(\text{qn})_2\text{Cl}_2$	7050	213	297	19	3.22	240
$\text{Ni}(\text{py})\text{Cl}_2$	7200	110	290	34	3.32	300
$\text{Ni}(\text{in})\text{Cl}_2$	7200					
$\text{Ni}(\text{in})\text{Br}_2$	6800					
$\text{Ni}(\text{bz})\text{Cl}_2$	7000	125	299	30	3.31	300
$\text{Ni}(\text{bz})\text{Br}_2$	6800	150	307	20	3.17	210
$\text{Ni}(\text{qn})\text{Cl}_2$	6400	135	327	18	3.22	220
$\text{Ni}(\text{2n})\text{Br}_2$	6250	160	336	5	3.24	230

$\#$  corrected for  $\theta$  and T.I.P.

yellow-brown for the bromide complexes. However the complexes  $\text{NiLX}_2$  (L=quinoline, 2-methylbenzothiazole, 3-methylisoquinoline, X=Cl,Br) are all pinkish red. The electronic spectra of  $\text{Ni(quinoline)Cl}_2$  is shown in Fig. 1.1. The band positions may be rationalised in terms of the transitions in an essentially octahedral environment, as for  $\text{Ni(pyridine)Cl}_2$ . There are however three main differences between the spectra of the 1:1 chloride complexes with pyridine and quinoline. For the complex with the latter ligand, the bands lie at lower energy, the  $\nu_1$  and  $\nu_2$  bands are less split, and the spectrum is generally more intense for  $\nu_2$  and  $\nu_3$ . These three features will be considered in turn.

The  $\Delta$  value for  $\text{Ni(quinoline)Cl}_2$  is less than that for  $[\text{Me}_4\text{N}][\text{NiCl}_3]$ , (Table 1.2). This might be due to the steric effect of quinoline causing it to lie further from the metal ion than for pyridine. This however does not seem adequate to explain the low  $\Delta$  value. It is possible that the steric effects of the quinoline cause a distortion of the lattice, such that the halide trans- to the quinoline is further from the metal than the inplane halide ions. As a result the net axial field is less than that for two halide ions. In the limit of such a distortion a five coordinate complex

is formed. If an approximate value for the  $\Delta$  of a single halide ion, of  $\sim 1,100\text{cm}^{-1}$ , is taken from  $\Delta$  for  $[\text{NiCl}_3]^-$ , and then that for quinoline, of

$1,300\text{cm}^{-1}$ , from  $\Delta$  for  $\text{Ni}(\text{quinoline})_2\text{Cl}_2$ , then for the five coordinate complex  $\Delta$  would be expected  $5,800\text{cm}^{-1}$ . While only approximate, comparison with the observed value of  $6,400\text{cm}^{-1}$ , suggests that the sixth halide is coordinated, if only weakly.

Crystal field calculations have been made for the energy levels arising in square pyramidal, five coordinate nickel (II)<sup>45</sup>. These predict that if there is a strong band,  ${}^3B_1 \rightarrow {}^3E({}^3F)$  at  $6,400\text{cm}^{-1}$ , then  ${}^3B_1 \rightarrow {}^3A_2({}^3F)$  and  ${}^3B_2$  at  $\sim 10,000$ ;  ${}^3B_1 \rightarrow {}^3E({}^3F)$  at  $\sim 15,000$ ,  ${}^3B_1 \rightarrow {}^3A_2({}^3F)$  at  $\sim 24,000$  and  ${}^3B_1 \rightarrow {}^3E({}^3P)$  at  $\sim 27,000$ . These values are not similar to those observed for the present complexes, consistent with the six coordinate structure suggested above.

If the axial field from the quinoline is thus taken as weak, then there may be less difference between the axial and inplane fields, than in the case of  $\text{Ni}(\text{pyradine})\text{Cl}_2$ , and hence the band splittings may be less in  $\text{Ni}(\text{quinoline})\text{Cl}_2$ , as observed.

The complexes  $\text{NiLX}_2$  (L=quinoline, 2-methylbenzothiazole, X=Br) give spectra which are similar in intensity and

outline to that seen for Ni(quinoline)Cl<sub>2</sub>, (Fig. I.3) though with the bands shifted to lower energies. It therefore seems likely that these complexes also have a distorted structure, similar to that postulated above for Ni(quinoline)Cl<sub>2</sub>. The other pink 1:1 complexes while essentially similar to Ni(quinoline)Cl<sub>2</sub>, showed some differences and are described below.

The difference in intensity between the spectra of Ni(pyridine)Cl<sub>2</sub> and Ni(quinoline)Cl<sub>2</sub> is an aspect of a general trend seen in the intensity of the spectra of the complexes examined in this chapter, and this will be discussed generally.

In D<sub>4h</sub> symmetry all electric dipole transitions are symmetry forbidden, and vibronically allowed, electronic spectra then being expected to be weak, as seen for the 2:1 complexes. If however the center of symmetry is removed, as in C<sub>4v</sub>, then the transition  ${}^3B_1 \rightarrow {}^3E$  becomes symmetry allowed, while the transitions  ${}^3B_1 \rightarrow {}^3A_2$  and  ${}^3B_1 \rightarrow {}^3B_2$  remain symmetry forbidden. The 2:1 complexes give spectra which are somewhat less intense than the spectra of the 1:1 complexes with the pyridine type ligands, while the latter spectra are about half as intense as the 1:1 complexes with quinoline, (Fig. I.1).

Fig. 1.3

Spectrum of: Ni(2-methylbenzothiazole) Br<sub>2</sub>

A. at RT

B. at 77°K

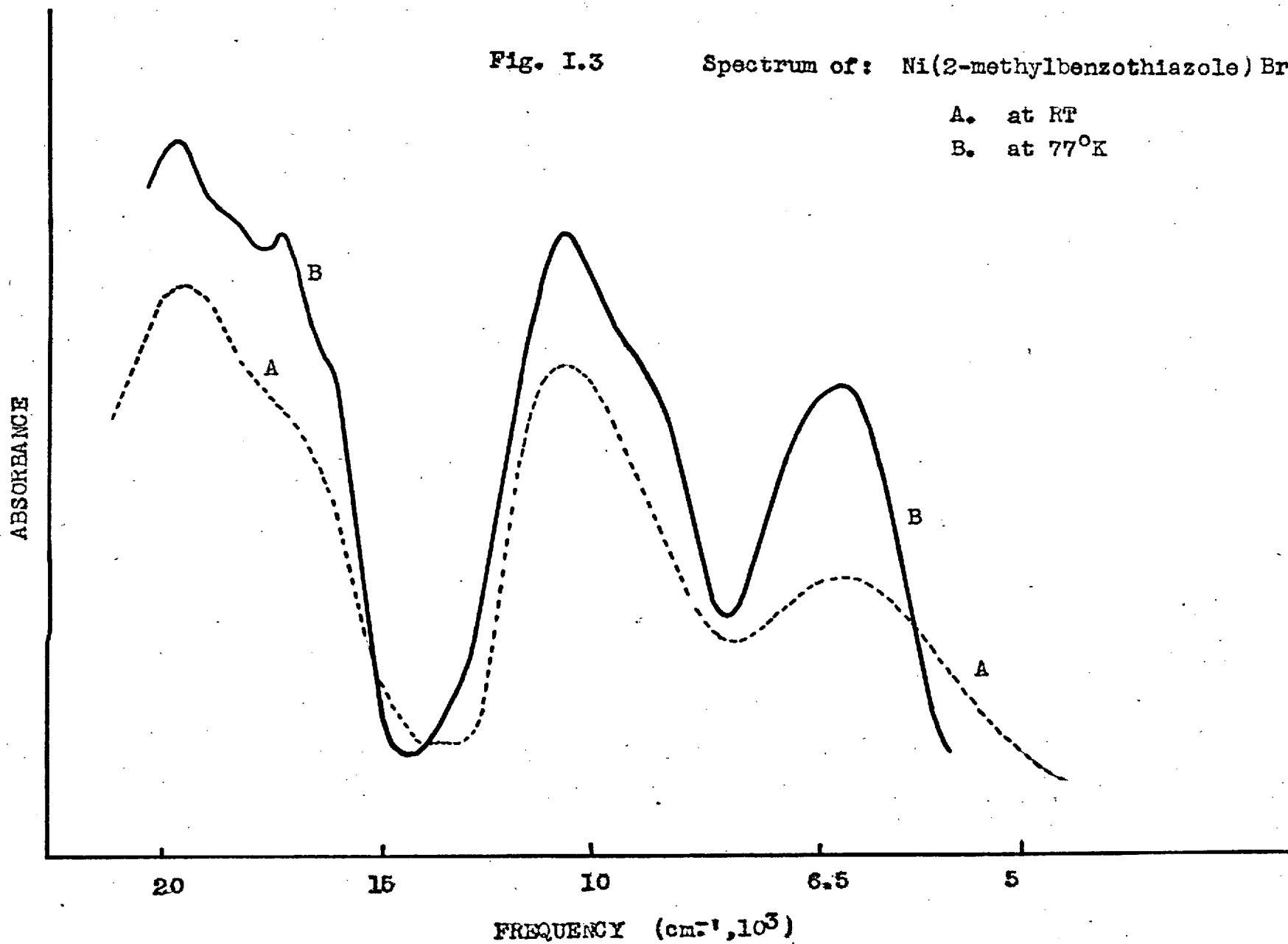
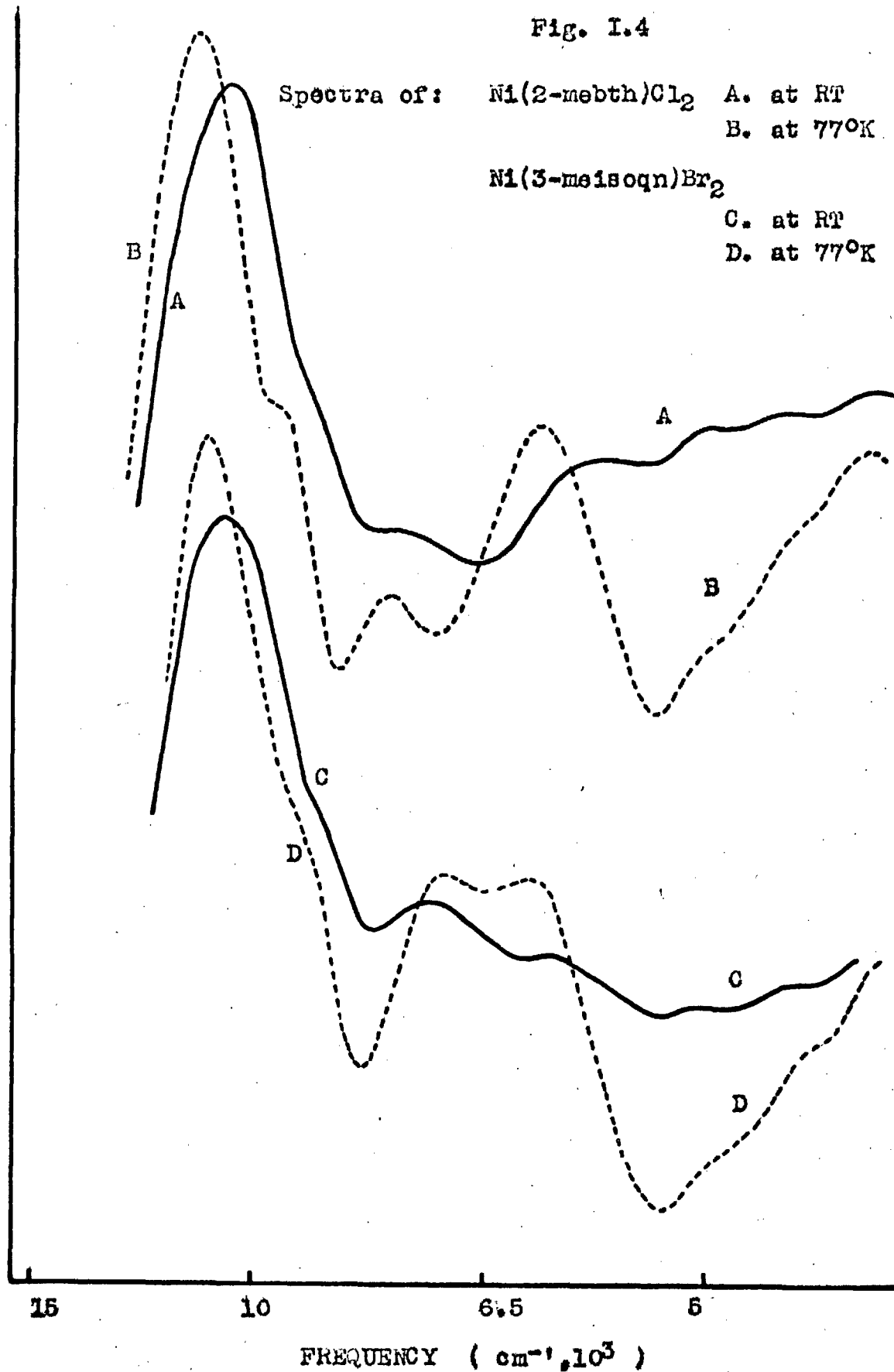


Fig. I.4

Spectra of:  $\text{Ni}(2\text{-meth})\text{Cl}_2$  A. at RT  
B. at 77°K

$\text{Ni}(3\text{-meisoqn})\text{Br}_2$  C. at RT  
D. at 77°K

ABSORBANCE



Intensity measurements from reflectance spectra must be treated with some caution, intensities being dependant on factors such as crystallinity. The present spectra were however all measured on samples in the form of fine powders, and it seems probable that the above generalisations are meaningful. The changes in intensity may be associated with a progressive loss of centrosymmetry in the complexes. The 1:1 complexes with quinoline, through the large distortions discussed above, giving the most intense spectra. The loss of centrosymmetry will increase the intensity of the E components of  $\nu_1$ ,  $\nu_2$  and  $\nu_3$ , as these become associated with more symmetry allowed transitions. The apparently smaller splittings in the 1:1 complexes may be due in part to the more intense E component rendering the orbital singlet component less conspicuous.

An examination was made of the ratios of the maximum intensities of the  $\nu_1$ ,  $\nu_2$  and  $\nu_3$  bands, for certain of the complexes, (Table 1.3). Where the bands are clearly split the ratio of the maximum intensities of the main components is given. There appears to be little change in the relative intensities of the bands in passing from the 2:1 to the 1:1 complexes with the pyridine type ligands. In the



Table 1.3

Relative intensities of electronic spectral bands for polymeric 2:1 and 1:1 nickel halide complexes

	Ni(py) <sub>2</sub> Cl <sub>2</sub>	Ni(py)Cl <sub>2</sub>	Ni(im)Cl <sub>2</sub>	Ni(im)Br <sub>2</sub>	
$\nu_3/\nu_2$	1.2	1.2	1.2	(RT) 1.4	(77°K) 1
$\nu_2/\nu_1$	1.2	1.0	1.0	1.4	0.9
	Ni(qn)Cl <sub>2</sub>	Ni(qn)Br <sub>2</sub>	Ni(2-mebth)Br <sub>2</sub>		
$\nu_3/\nu_2$	1.4	1.2	(RT) 1.2	(77°K) 1.2	
$\nu_2/\nu_1$	2.5	2.1	2.1	1.2	

complexes Ni(quinoline)X<sub>2</sub> (X=Cl,Br) the  $\nu_2$  and  $\nu_3$  bands have both gained considerably in intensity, and to about the same extent, while  $\nu_1$  remains relatively weaker. A similar effect is seen in the room temperature spectrum of Ni(2-methylbenzothiazole)Br<sub>2</sub>, however at 77°K the  $\nu_1$  band has gained relative intensity (Fig. I.3), and the ratios of band intensities approach those seen in the 2:1 and 1:1 complexes with the pyridine type ligands. The origin of the intensity differences, and of the changes with temperature are not at present clear.

The pink complexes  $\text{NiLX}_2$  ( $\text{L}=2\text{-methylbenzothiazole}$ ,  $\text{X}=\text{Cl}$  ;  $\text{L}=3\text{-methylisoquinoline}$ ,  $\text{X}=\text{Cl,Br}$ ) give spectra in the  $\nu_2$  and  $\nu_3$  regions that were very similar to the spectra in these regions of  $\text{Ni}(\text{quinoline})\text{X}_2$  ( $\text{X}=\text{Cl,Br}$ ), (Fig. I.4), and may be assigned in an essentially octahedral environment as described above. The  $\nu_1$  region was however different in that the clear band seen at  $\sim 6,300 \text{ cm}^{-1}$  in the 1:1 quinoline complexes, was not present in the room temperature spectra. On cooling to  $77^\circ\text{K}$  two distinct bands were seen, at  $6,000 \text{ cm}^{-1}$  and  $7,600 \text{ cm}^{-1}$ , in the spectrum of  $\text{Ni}(2\text{-methylbenzothiazole})\text{Cl}_2$  (Fig. I.4), and the spectrum of  $\text{Ni}(3\text{-methylisoquinoline})\text{Cl}_2$  appears to be similar. For  $\text{Ni}(3\text{-methylisoquinoline})\text{Br}_2$ , at  $77^\circ\text{K}$ , two bands were again seen in the  $\nu_1$  region, but close together and not resolved, (Fig. I.4). A possible explanation is that for these complexes, the symmetry is rather lower than  $\text{C}_{4v}$ , such that the E component of  $\nu_1$  is split into two orbital singlet components. If the two components seen at  $77^\circ\text{K}$  in the spectrum of  $\text{Ni}(3\text{-methylisoquinoline})\text{Br}_2$  are superimposed, then the ratio of the intensity maximum of  $\nu_2$  to that of the superimposed band is  $\sim 1.2$ , which is the same as that seen for  $\text{Ni}(\text{quinoline})\text{Br}_2$ .

If low symmetry is the cause of this splitting, then the sensitivity of  $\nu_1$  to distortion is shown by the fact that no differences are seen in the  $\nu_2$  and  $\nu_3$  bands for these complexes, and those such as Ni(quinoline) $\text{Cl}_2$ , where the  $\nu_1$  band is not appreciably split.

It appeared initially that the differences in the spectra in the  $\nu_1$  region for the pink 1:1 complexes might be connected with the method of preparation. The 1:1 complexes with unsplit  $\nu_1$  coming from heating the 2:1 complex, and those with split  $\nu_1$  coming from solution evaporation. However, samples of Ni(2-methylbenzothiazole) $\text{Br}_2$  were prepared by both methods, and no differences in spectra were found.

### Magnetic Properties

The magnetic susceptibilities of a number of 1:1 and 2:1 complexes were examined over a temperature range of 80-300<sup>o</sup>K, using a (Gouy balance, with a cryostat arrangement, (see Chapter VI). Susceptibility measurements were made at eight temperatures, and on two packings. The observed susceptibilities were corrected for ligand and metal ion diamagnetism, using Pascal constants, and for temperature independent paramagnetism, (T.I.P.), calculated from the

relationship<sup>46</sup>;

$$\text{T.I.P.} = 8N\beta^2/\Delta \approx 2.09/\Delta \text{ e.g.s.u.}$$

where  $N$  = Avogadro's number,  $\beta$  = Bohr magneton, and  $\Delta$  = the energy of the first excited state, being mixed into the ground state. In these complexes when low symmetry splits the orbital triplet levels, the T.I.P. contribution is taken to be the same as that for an unsplit  ${}^3T_{2g}$  level at the position given by the weighted average of the component positions. In these compounds the T.I.P. amounts to  $\sim 300 \times 10^{-6}$  e.g.s.u., or about 7% of the room temperature susceptibility.

Plots of  $1/\chi_A(\text{corr.})$  against  $T$  were made, when for all the complexes examined, excellent straight line graphs were obtained. The results of a typical plot are shown in Fig. I.5. (Some discussion of the errors expected for the magnetic data is given in Chapter VI).

The linear plots indicate that the compounds obey the Curie-Weiss law:

$$\chi = C/T - \theta$$

Fig. I.5

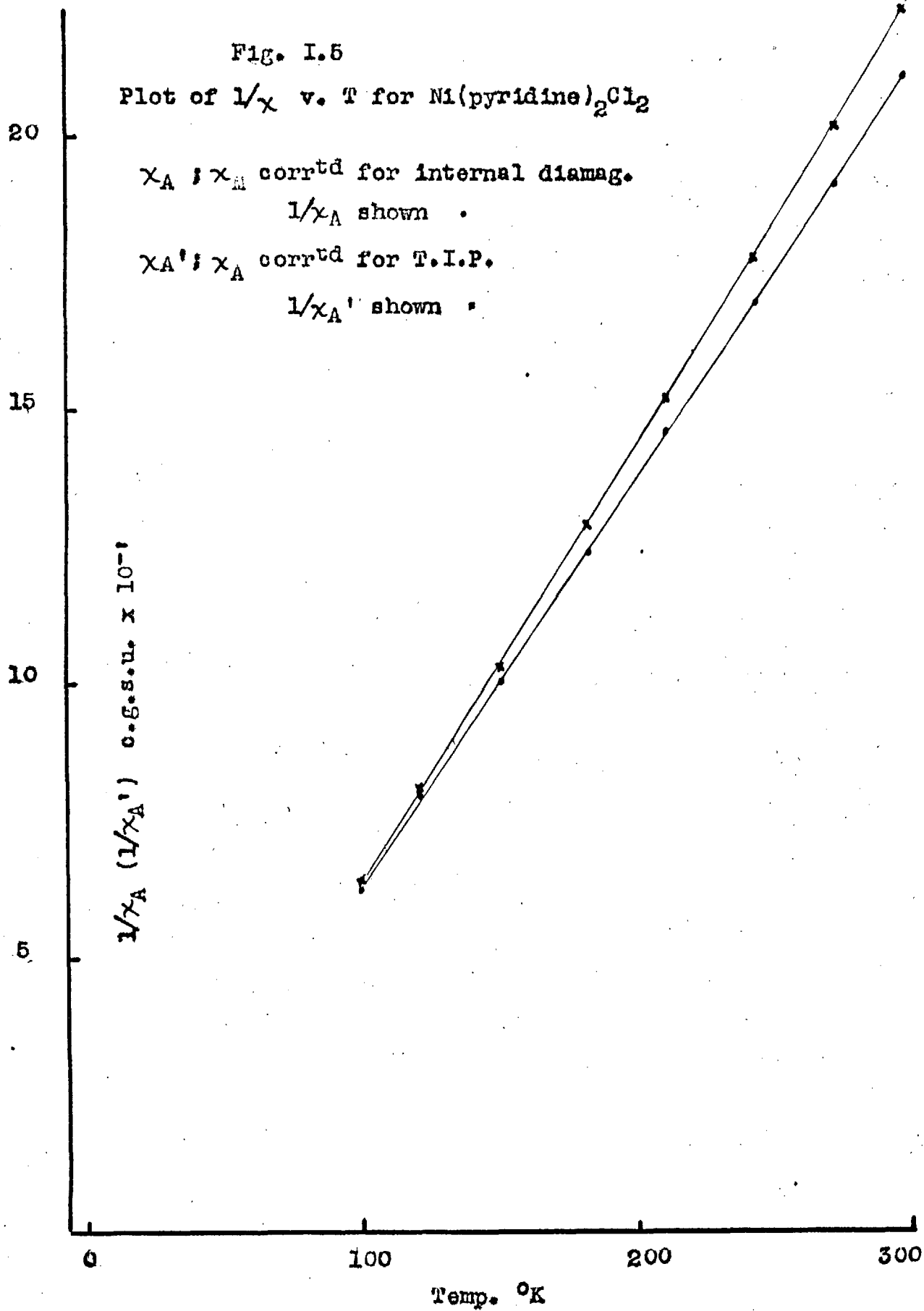
Plot of  $1/\chi$  v.  $T$  for  $\text{Ni}(\text{pyridine})_2\text{Cl}_2$

$\chi_A$  ;  $\chi_M$  corrd for internal diamag.

$1/\chi_A$  shown .

$\chi_A'$  ;  $\chi_A$  corrd for T.I.P.

$1/\chi_A'$  shown .



in this temperature range. This type of behaviour is expected for nickel (II) in an essentially octahedral environment, when there is an orbital singlet ground state. The tetragonal, or other distortions, in the present complexes, will lead to a splitting of the orbital triplet excited levels, when by the action of spin-orbit coupling, the spin degeneracy of the ground state will be raised<sup>47</sup>. However, this latter splitting is expected to be small, less than  $10 \text{ cm}^{-1}$ , and thus non-Curie-Weiss behaviour, from this cause, would only be expected at temperatures below  $50^\circ\text{K}$ .

The values of  $\theta$  found for magnetically dilute nickel (II) in an essentially octahedral environment, are generally of the order of  $-10^\circ$  <sup>11</sup>. For all the present complexes however, positive  $\theta$  values were found, ranging from  $5-34^\circ$  (Table 1.2). Comparison of the data for the 2:1 chloride complexes, with that for the 1:1 chloride complexes with the non sterically hindered ligands, suggests that the  $\theta$  value depends on the number of heterocyclic ligands present, rather than on their nature. Thus for  $\text{NiL}_2\text{Cl}_2$  (L=pyridine, quinoline),  $\theta \approx 20^\circ$ , and for  $\text{NiLCl}_2$  (L=pyridine, imidazole, benzothiazole),  $\theta \approx 30-35^\circ$ . In  $\text{Ni}(\text{quinoline})\text{Cl}_2$  the  $\theta$  value is markedly smaller at  $18^\circ$ , agreeing

with the indications from the electronic spectra that the coordination system is rather different from that with the pyridine type ligands. For the bromide complexes less data is available, but the results seem to follow similar trends to those seen in the chloride complexes, with the  $\theta$  values somewhat reduced.

The sign and magnitude of  $\theta$  may be indicative of magnetic coupling. For non-magnetically dilute materials, at temperatures above the Curie point, long range coupling ceases, and Curie-Weiss behaviour is followed, the value of  $\theta$  being negative for anti-ferromagnetic interaction, and positive for ferromagnetic.<sup>11, 39</sup> Small values of  $\theta$  must be interpreted with caution, thus the  $\theta$  value of about  $-10^\circ$ , often seen for octahedral magnetically dilute nickel (II), is not regarded as indicating any definite interaction.<sup>11</sup> Positive  $\theta$  values are however somewhat unusual, and the origins of some magnetic coupling in the present complexes may possibly be seen in the descriptions given of the magnetic interactions in anhydrous nickel halides.

Anhydrous nickel chloride has a  $\theta$  value of  $68^\circ$ , for temperatures above the Curie point at  $50^\circ\text{K}$ .<sup>48</sup> The anhydrous chlorides of the iron group form cubic

close packed structures, with the cations occupying alternate interstitial planes. The magnetic properties of anhydrous nickel chloride have been interpreted in terms of an intralayer ferromagnetic interaction, of greater magnitude than an antiferromagnetic interaction between layers<sup>49</sup>. A ferromagnetic interaction of this type is considered likely on the basis of qualitative symmetry considerations<sup>49</sup>. Thus in the chloride complexes examined here it may be considered that while magnetic interactions, both within and between layers, are reduced as a result of the distortion caused by the introduction of the heterocyclic ligands, effective intralayer ferromagnetic coupling is still retained. The larger  $\Theta$  values seen for the 1:1 complexes, compared with the 2:1 complexes, are consistent with the lesser distortion of the halide lattice expected for the former complexes.

For anhydrous nickel bromide a  $\Theta$  value of  $-20^\circ$  is found<sup>50</sup>, and a larger interlayer antiferromagnetic interaction has been postulated<sup>50</sup>. Thus if a qualitative extension is carried over these present complexes, a lower  $\Theta$  value might be expected for the bromide complexes compared with the chloride complexes, as observed.



As the magnetic studies given here are at temperatures well above the Curie points for the complexes, which exhibit paramagnetism, no dependence of susceptibility on field strength would be expected. This was found to be the case for fields between 2,400 - 6,700 gauss, except for one sample of Ni(benzimidazole)Br<sub>2</sub>, which showed a small field dependence at all temperatures. This sample had good analyses, and an electronic spectrum indistinguishable from other samples of this compound which showed no field dependence. It was found that, for this sample, graphs of susceptibility against reciprocal field strength gave straight lines at all temperatures. The susceptibilities at infinite field, when any contribution from saturated ferromagnetism would be insignificant, were found to agree well with the susceptibilities observed for other samples. This behaviour indicated the presence of ferromagnetic impurity.

There will be a contribution to the magnetic moment arising from spin-orbit coupling mixing the excited orbital triplet electronic states into the ground state. The first excited state is primarily mixed in, this state having symmetry  ${}^3T_{2g}$  in fields of O<sub>h</sub> symmetry, but which is split into  ${}^3B_2$  and  ${}^3E$

components in  $C_{4v}$  symmetry. It appears however that the contribution to the magnetic moment is effectively that of an orbital triplet at the position of the weighted average of the two components.

The magnetic moment,  $\mu_{\text{eff.}}$ , is given by:<sup>46</sup>

$$\mu_{\text{eff.}} = 2.83 \quad [\chi_{A(\text{corr.})}(T-\theta)] = 2.83(1-4\lambda'/\Delta)$$

where  $\chi_{A(\text{corr.})}$  is the observed susceptibility, corrected for ligand and metal ion diamagnetism, and T.I.P., and  $\lambda'$  is the spin-orbit coupling constant in the complex. Thus values of  $\lambda'$  may be found, and are given in Table 1.2. The values should not be taken as quantitatively significant, but indicate that the  $\lambda'$  values are about 75% of the free ion value of  $-315 \text{ cm.}^{-1}$

For octahedral magnetically dilute nickel (II) complexes, the room temperature magnetic moments based on the observed susceptibility, corrected only for ligand diamagnetism, are usually found to be in the region of 3.15 B.M.<sup>11</sup> When calculated in this way rather larger magnetic moments of 3.4 - 3.6 B.M. are found for the 1:1 complexes with pyridine type ligands, and of 3.3 - 3.45 B.M. for the 2:1 complexes. Similar magnetic moments have been seen for other 2:1 polymeric

halide complexes.<sup>51</sup> The high values of the uncorrected magnetic moments for some of the complexes are given in Table 1.4, together with the contributions to the magnetic moment due to the positive  $\theta$  value, and from the T.I.P.

Table 1.4

Contributions of T.I.P. and  $\theta$  to the magnetic moments,  
at 298°K, of some polymeric 1:1 and 2:1 complexes.

Compound	$\chi_A \times 10^6$ (c.g.s.u.)	$\mu_{\text{eff.}}^*$ (B.M.)	$\chi_A \times 10^6$ corr. T.I.P. <sup>***</sup> (c.g.s.u.)	$\mu_{\text{eff.}}$ corr. T.I.P. (B.M.)	$\theta$ (°K)	$\mu_{\text{eff.}}$ corr. T.I.P. $\theta$ (B.M.)
Ni(py) Cl <sub>2</sub>	5500	3.62	5210	3.52	34	3.32
Ni(bz) Br <sub>2</sub>	4820	3.39	4510	3.28	20	3.17
Ni(py) <sub>2</sub> Cl <sub>2</sub>	4770	3.37	4500	3.28	19	3.17
Ni(py) <sub>2</sub> Br <sub>2</sub>	4600	3.32	4310	3.21	13	3.14
Ni(qn) <sub>2</sub> Cl <sub>2</sub>	4960	3.45	4660	3.34	19	3.22

\* observed susceptibility corrected for ligand and metal ion diamagnetism.

\*\*\* see Table 1.2 for T.I.P. values.

CHAPTER IITetrahedral 2:1 Nickel Halide ComplexesTetrahedral ComplexesPreparation

As discussed in the introduction (p. 8 ), up to 1963 the number of tetrahedral nickel (II) complexes known was small. It was thus considered of interest to make an examination of the properties of complexes of this type, in particular the 2:1 complexes with heterocyclic ligands that may be prepared from non-aqueous solvents.

The compounds examined were of the type  $NiL_2X_2$  (L=N-methylimidazole, 2-methylimidazole, X=Br; L=benzimidazole, X=Br, I<sup>x</sup>; L=benzothiazole, X=I; L=2-methylbenzimidazole, X=Cl<sup>x</sup>, Br<sup>x</sup>, I; L=3-methylisoquinoline, X=Cl<sup>x</sup>, Br<sup>x</sup>), and also  $[Et_4N][Ni(\text{benzimidazole})Br_3]^x$ . To permit comparison with the electronic spectrum, and magnetic properties, of a complex with regular tetrahedral symmetry,  $[MePh_3As]_2[NiCl_4]$  was prepared following the method of Goodgame et al.<sup>53</sup>.

A number of the 2:1 complexes had previously been prepared by Dr. M. Goodgame, and are indicated

<sup>x</sup> Prepared by Dr. M. Goodgame

in the above list. The same general method was used for the preparation of the benzimidazole and 2-methylbenzimidazole complexes. Ligand and nickel halide, in 2:1 mole ratios, were dissolved in acetone, the solution filtered, and hot carbon tetrachloride added to the hot filtrate. The oil formed was triturated with successive portions of hot carbon tetrachloride till a crystalline solid was obtained. This technique of rapid removal from the hot solution was necessary owing to the high solubility of the tetrahedral complex, and also in the case of the benzimidazole nickel bromide complex, a 4:1 solvated compound formed on cooling. No complex  $\text{Ni}(\text{benzimidazole})_2 \text{Cl}_2$  has been obtained in any configuration. Although a tetrahedral complex of this type exists in acetone solution, attempts to prepare the solid compound by the above technique resulted in the formation of a 4:1 solvated complex.

The less soluble 3-methylisoquinoline complexes crystallised out on cooling a hot concentrated acetone solution of ligand and nickel halide in 2:1 mole ratios. The other complexes were prepared by specific methods, the details of which may be found in the collected experimental data in Chapter VI.

The complexes had intense colours, the chloride

and bromide complexes being blue, and the iodide complexes green, except in the case of Ni(benzothiazole)<sub>2</sub>I<sub>2</sub> which was dark brown. The complexes were hygroscopic, this being less marked for the benzothiazole and 3-methylisoquinoline complexes.

Some tetrahedral 2:1 cobalt complexes have been examined in connection with the n.m.r. studies in Chapter V, and they will be introduced at this point as their electronic spectra may be usefully related to the electronic spectra of the nickel complexes.

The complexes examined were of the type CoL<sub>2</sub>X<sub>2</sub> (L=N-methylimidazole, 2-methylimidazole<sup>✕</sup>, benzimidazole<sup>✕✕</sup>, 2-methylbenzimidazole, X=Cl, Br), and [E]L<sub>4</sub>N [Co(benzimidazole)Br<sub>3</sub>]<sup>✕✕</sup>. The cobalt complexes either crystallised from acetone, or ethanol, solutions containing ligand and cobalt halide in 2:1 mole ratios, or the solutions were evaporated to a small bulk, benzene added, and the oil formed triturated with further benzene. These complexes were all an intense blue colour, and hygroscopic, though to a lesser extent than the nickel (II) complexes.

✕- Prepared by Miss K.A. Price of this Department

✕✕ Prepared by Dr. M. Goodgame<sup>62</sup>

X-ray powder patterns were taken for the following compounds to determine whether the cobalt and nickel analogs were isomorphous.  $ML_2X_2$  (M=cobalt or nickel; L=N-methylimidazole, X=Br; L=2-methylimidazole, X=Br; L=benzimidazole, X=Br, I; L=2-methylbenzimidazole, X=Cl, Br). The d spacings of the more intense lines are given in Table 2.1.

From the above complexes only the cobalt and nickel analogs of  $M(\text{benzimidazole})_2 \text{Br}_2$  and  $M(\text{benzimidazole})_2 \text{I}_2$  were found to be essentially isomorphous.  $[\text{Et}_4\text{N}] [M(\text{benzimidazole})\text{Br}_3]$ , (M=Co or Ni) have previously been shown to be non-isomorphous<sup>56</sup>.



Table 2.1  
X-Ray Powder Data

<u>Ni(bz)<sub>2</sub>Br<sub>2</sub></u>		<u>Co(bz)<sub>2</sub>Br<sub>2</sub></u>		<u>Ni(bz)<sub>2</sub>I<sub>2</sub></u>		<u>Co(bz)<sub>2</sub>I<sub>2</sub></u>	
<u>d</u>	<u>Inten-</u> <u>sity</u>	<u>d</u>	<u>Inten-</u> <u>sity</u>	<u>d</u>	<u>Inten-</u> <u>sity</u>	<u>d</u>	<u>Inten-</u> <u>sity</u>
7.45	m	7.53	m	7.87	ms	8.17	ms
6.82	s	6.80	s	7.17	ms	7.23	ms
5.74	vw	5.78	vw	4.975	w	5.26	w
5.33	ms	5.45	m	4.79	vs	4.85	vs
5.11	vw	5.19	vw	4.21	w	4.26	w
4.77	vs	4.78	vs	4.035	ms	4.12	ms
3.91	w	3.96	w	3.875	vw	3.89	vw
3.57	vw	3.46	vw	3.67	s	3.66	s
3.43	ms	3.37	ms			3.51	s
3.35	mw			3.39	ms	3.40	ms
3.09	w	3.13	w	3.235	w	3.25	w
2.95	w	3.01	w	3.11	mw	3.10	mw
2.85	w	2.83	vw	2.69	ms	2.69	w
2.56	m	2.57	m	2.28	m	2.28	m
2.275	m			1.99	ms	2.00	ms

### Electronic Spectra

The spectra of the 2:1 nickel (II) complexes are given in Table 2.2, and may be interpreted in terms of an essentially tetrahedral environment, the high molar extinction coefficients of the solution spectra are consistent with the high intensity of absorption expected for noncentrosymmetric tetrahedral species. In discussing the spectra of the tetrahedral complexes the notation used will be  ${}^3T_1({}^3F) \rightarrow {}^3T_2 = \nu_1$  ;  ${}^3T_1({}^3F) \rightarrow {}^3A_2 = \nu_2$  ;  ${}^3T_1({}^3F) \rightarrow {}^3T_1({}^3P) = \nu_3$ . Calculations of the energy levels for nickel (II) in a regular tetrahedral environment, have been carried out by Liehr and Ballhausen<sup>8</sup>, the resultant energy level diagram, for a given value of  $\lambda$  and  $F_4$  in Fig. II.1.

For  $[\text{MePh}_3\text{As}]_2 [\text{NiCl}_4]$  the bands at  $7,200 \text{ cm}^{-1}$ , and  $14,550 \text{ cm}^{-1}$  may be assigned to  $\nu_2$  and  $\nu_3$ , giving a good fit within the energy level diagram of Fig. II.1 for a  $\Delta$  value of  $3580 \text{ cm}^{-1}$ . The  $\nu_1$  band is not seen as it lies below  $4000 \text{ cm}^{-1}$ , the lower limit of the instrument used. At  $77^\circ\text{K}$  there is considerable sharpening of the spectrum, and a band is resolved on the low energy side of  $\nu_3$ , separated from it by  $\sim 2,500 \text{ cm}^{-1}$ . Weakliem has made a study of the spectra of nickel (II) in tetrahedral sites, including  $[\text{NiCl}_4]^{2-}$ ,

Table 2.2

Electronic Absorption Spectra for the  
Tetrahedral 2:1 Nickel (II) Complexes

<u>Compound</u>	<u>Phase</u>	<u>Absorption maxima (cm.<sup>-1</sup>)</u> <u>(<u>⊗</u> molar for solutions)</u>
Ni(N-meim) <sub>2</sub> Br <sub>2</sub>	solid	~17,600(sh); 16,350; ~11,950(sh); 10,730; 8,700; 5,700
Ni(2-meim) <sub>2</sub> Br <sub>2</sub>	solid	17,600; ~16,100(sh); ~11,700(sh); 10,100; ~6,700(br)
Ni(bz) <sub>2</sub> Br <sub>2</sub>	solid	~21,700(sh); 17,250; ~11,700(sh); 10,420; ~6,760(br)
	solid (77°K)	24,000(w); ~21,600(w.sh); 17,300; ~11,700(sh); 7,800; 6,300
	acetone (0.0025M)	17,500(200); ~11,900(sh); 10,350(60);
	MeNO <sub>2</sub> (0.0025M)	17,500(170); ~11,900(sh); 10,370(50)
Ni(bz) <sub>2</sub> I <sub>2</sub>	solid	16,200; ~10,800(sh); 9,950; 6,800(br)
	solid (77°K)	16,300; ~10,950(sh); 9,900; 7,620; 6,470; ~5,600(sh)
	acetone (0.0025M)	16,600(280); ~15,400(sh); ~10,900(sh); 10,050(80)
	MeNO <sub>2</sub> (0.0025M)	16,700(200); ~15,400(sh); ~10,900(sh); 10,050(55)

⊗ At room temperature unless otherwise stated.

Table 2.2 (continued)

<u>Compound</u>	<u>Phase</u>	<u>Absorption Maxima (cm.<sup>-1</sup>)</u> (← molar for solutions)
Ni(bth) <sub>2</sub> I <sub>2</sub>	solid	~16,300(sh); ~14,000(sh); ~10,400(n.r) ~9,900(n.r); 7,300
	solid (77°K)	~16,150(sh); 13,650; 9,800; 7,250
Ni(2-nebz) <sub>2</sub>	solid	18,300; 15,500; ~12,100(sh); 10,000; 6,750
	solid (77°K)	18,000; 15,550; ~12,100(sh); 10,100; ~7,100(br); ~5,900(sh)
	acetone (0.0025M)	17,700(150); ~16,500(sh); ~12,200(sh); 10,120(45)
	meNO <sub>2</sub> (0.0025M)	17,700(145); ~16,500(sh); ~12,200(sh); 10,120(45)
Ni(2-nebz) <sub>2</sub> Br <sub>2</sub>	solid	18,000; 14,800; ~11,800(sh); 9,900; 6,830
	solid (77°K)	18,000; 15,000; ~12,000(sh); 10,000; 7,000
	acetone (0.0025M)	17,100(188); ~15,800(sh); ~11,700(sh); 9,900(50)
	meNO <sub>2</sub> (0.0025M)	17,400(175); ~15,800(sh); ~11,700(sh); 9,900(40)

Table 2.2 (continued)

<u>Compound</u>	<u>Phase</u>	<u>Absorption Maxima (cm.<sup>-1</sup>)</u> <u>(← molar for solutions)</u>
Ni(2-mebz) <sub>2</sub> I <sub>2</sub>	solid	16,800; 14,500; ~11,000(sh); 10,000; 7,070
	solid (77°K)	16,800; 14,500; ~11,000(sh); 10,000; 7,270
	acetone (0.0025M)	16,530(280); ~14,600(sh); ~10,800(sh); 9,900(80)
Ni(3-meisoqn) <sub>2</sub> Cl <sub>2</sub>	solid	~18,200-16,700(br); ~11,900(sh); 10,100; ~6,800(br)
	solid (77°K)	* 10,200; 7,300; ~6,000(sh)
Ni(3-meisoqn) <sub>2</sub> Br <sub>2</sub>	solid	~17,700-15,750(br); ~11,600(sh); 9,900; 6,800(br)
	solid (77°K)	~17,300-16,250(br); ~11,250(sh); 9,950; 7,100; ~6,000(sh)
	CHCl <sub>3</sub>	17,100; 15,900(sh); ~11,600(sh); 10,100; ~8,900(sh)
	acetone	~16,800(sh); 15,500; ~11,600(sh); ~10,100(sh); 8,900

\* High energy values not obtained.

Table 2.2 (continued)

<u>Compound</u>	<u>Phase</u>	<u>Absorption Maxima (cm.<sup>-1</sup>)</u> <u>(<math>\epsilon</math> molar for solutions)</u>
[Et <sub>4</sub> N][Ni(bz)Br <sub>3</sub> ]	solid	15,650; 8,700; 5,100(br)
	solid (77°K)	15,700; ~10,800(sh); 8,700; 6,300; ~4,400(br)
	acetone (0.001M)	15,900(210); 8,700(40)
	MeNO <sub>2</sub> (0.001M)	16,250(210); ~10,200(sh); 8,800(40)
[MePh <sub>3</sub> As] <sub>2</sub> [NiCl <sub>4</sub> ]	solid	22,900(w); 20,100(w); ~19,350(w.n.r); 18,500(w); ~15,000(s.sh); 14,550; ~13,050(sh); ~11,850(sh); ~8,850(w.sh); 7,200
	solid (77°K)	15,050; 12,550; ~10,000(v.w); ~8,850(w.sh); 7,150



from nickel (II) doped into  $\text{Cs}_2\text{ZnCl}_4$ <sup>54</sup>. The orbital triplet levels are split by the action of spin-orbit coupling, into four components, grouped into two pairs, and the spectrum of the above doped complex at room temperature, showed  $\nu_3$  split into two components separated by rather less than  $1000 \text{ cm}^{-1}$ . This splitting is considerably smaller than that seen in the present complex.

The observed splitting is not due to low symmetry, as preliminary crystallographic data has indicated that in  $[\text{MePh}_3\text{As}]_2[\text{NiCl}_4]$  the  $[\text{NiCl}_4]^{2-}$  ion has an almost regular tetrahedral structure<sup>55</sup>. Thus the observed band may be due to a spin forbidden transition to  ${}^1\text{T}_2({}^1\text{D})$  or  ${}^1\text{E}({}^1\text{D})$ , which gains intensity by the close proximity of the like symmetry components of  $\nu_3$ .

Turning to the complex  $[\text{Et}_4\text{N}][\text{Ni}(\text{benzimidazole})\text{Br}_3]$ , this may be considered to have a distorted tetrahedral structure, with effectively  $\text{C}_{3v}$  symmetry. This compound is of interest in that it is the only one known at present, in which three halides and a nitrogen donor are tetrahedrally coordinated to nickel (II). In  $\text{C}_{3v}$  symmetry the degenerate levels of  $\text{T}_d$  symmetry will split;



$$T_1 \rightarrow A_2 + E$$

$$T_2 \rightarrow A_1 + E$$

The band at  $15,650 \text{ cm}^{-1}$  may be assigned to  $\nu_3$ , no splitting being resolved, and that at  $8,700$  to  $\nu_2$ . Only broad absorption is seen in the  $\nu_1$  region at room temperature, but at  $77^\circ\text{K}$  two components of  $\nu_1$  are resolved, with a splitting of  $\sim 2000 \text{ cm}^{-1}$ .

The stronger component, assigned to the transition to the  $\bar{3}E$  level, lies lowest. This splitting would then be of the same sign, but  $\sim 1000 \text{ cm}^{-1}$  less than that seen in  $[\text{Et}_4\text{N}][\text{Ni}(\text{C}_6\text{H}_5)_3\text{P Br}_3]^{56}$ .

The 2:1 complexes may be considered to have distorted tetrahedral structures with effectively  $C_{2v}$  symmetry, when the degenerate levels will split:

$$T_1 \rightarrow A_2 + B_1 + B_2$$

$$T_2 \rightarrow A_1 + B_1 + B_2$$

Following previous assignments,<sup>2,3</sup> the bands in the region  $15,000-17,000 \text{ cm}^{-1}$  may be assigned to  $\nu_3$ , or components of  $\nu_3$ , and the comparatively sharp band at  $\sim 10,000 \text{ cm}^{-1}$  to  $\nu_2$ . The shoulder seen at  $\sim 12,000 \text{ cm}^{-1}$  may be assigned to the spin forbidden transition to  ${}^1E({}^1D)$ .

There have been a number of publications of the spectra of tetrahedral 2:1 nickel (II) complexes,

only the  $\nu_2$  and  $\nu_3$  bands being given however, owing to machine limitations.<sup>2,3,4,5,53</sup> These two bands were seen to be unsplit, and the band energies were found to fit well into the energy level scheme for nickel (II) in a regular tetrahedral environment.<sup>4,53</sup> This is also found to be the case for the present complexes. In the spectra of the 2:1 complexes with the benzimidazole type ligands, the  $\nu_2$  and  $\nu_3$  bands for the chlorides will be found to fit, in Fig. II.1, for a  $\Delta$  of  $\sim 5,500 \text{ cm}^{-1}$ ; the bromides,  $\sim 5,000$ ; and the iodides  $\sim 4,500$ . It might be anticipated that these  $\Delta$  values would be intermediate between the value seen for four nitrogen donors, and the value for four halide ions. For  $[\text{Ni}(\text{NCO})_4]^{2-}$  and  $[\text{Ni}(\text{NCS})_4]^{2-}$ , (both tetrahedral) the  $\Delta$  value is found to be  $\sim 4,600-4,000 \text{ cm}^{-1}$ ,<sup>57,58</sup> and for  $[\text{NiCl}_4]^{2-}$   $\Delta$  is  $\sim 3,600 \text{ cm}^{-1}$ .<sup>53</sup> Thus the values of  $\Delta$  indicated above for the 2:1 complexes seem larger than expected. A further indication that the energy level diagram can not be used directly in the case of these  $\text{C}_{2v}$  complexes, is in the position of the  $\nu_1$  band. For most of the complexes a single broad band is seen in the  $\nu_1$  region (Figs. II.2 and II.3). A more detailed examination of the nature of this band is given after the spectra of the cobalt complexes

Fig. II.2

Spectra of:  $\text{Ni}(\text{benzimidazole})_2\text{I}_2$

A. at RT

B. at 77°K

$\text{Ni}(\text{benzimidazole})_2\text{Br}_2$

C. at RT

D. at 77°K

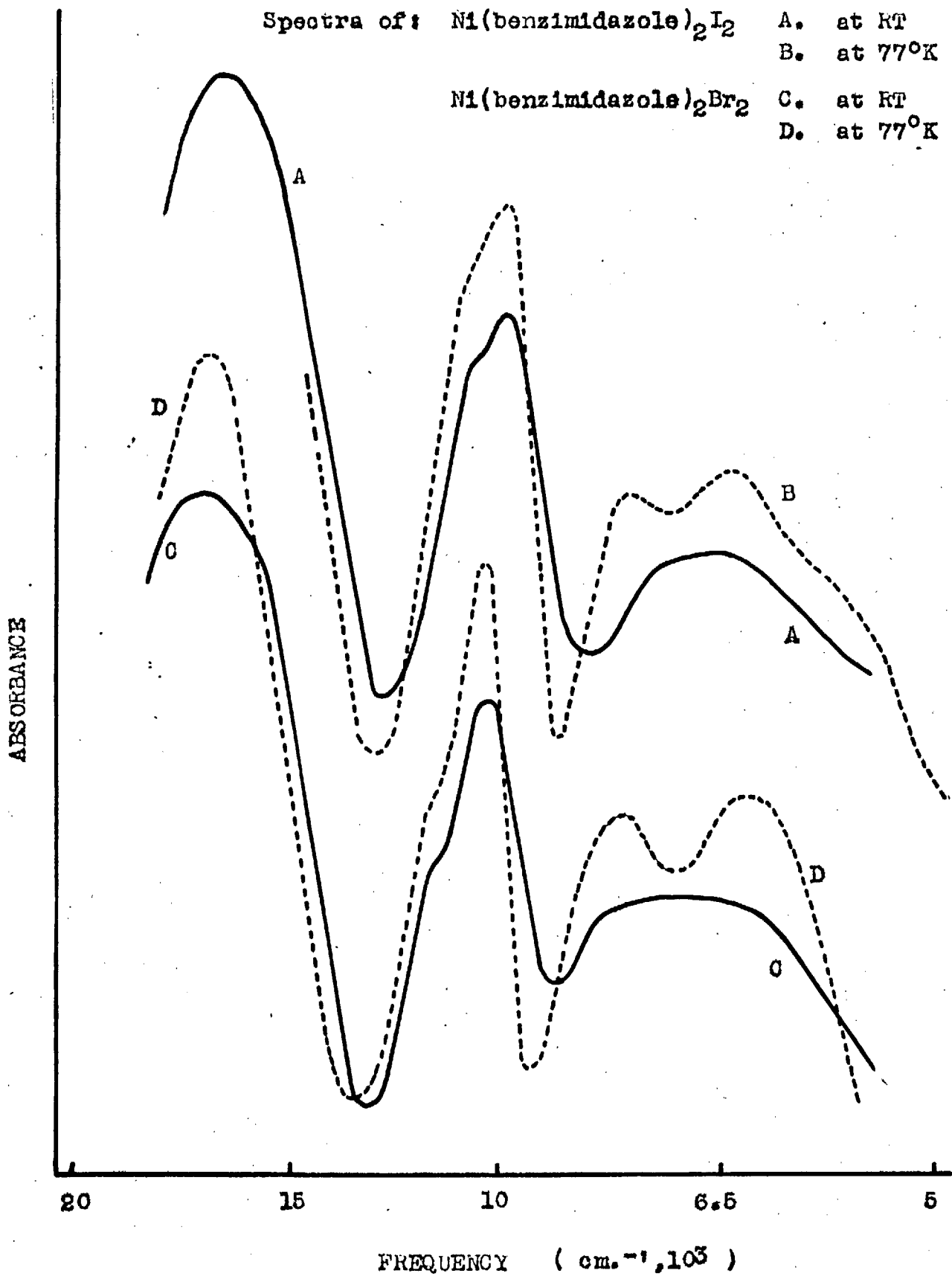
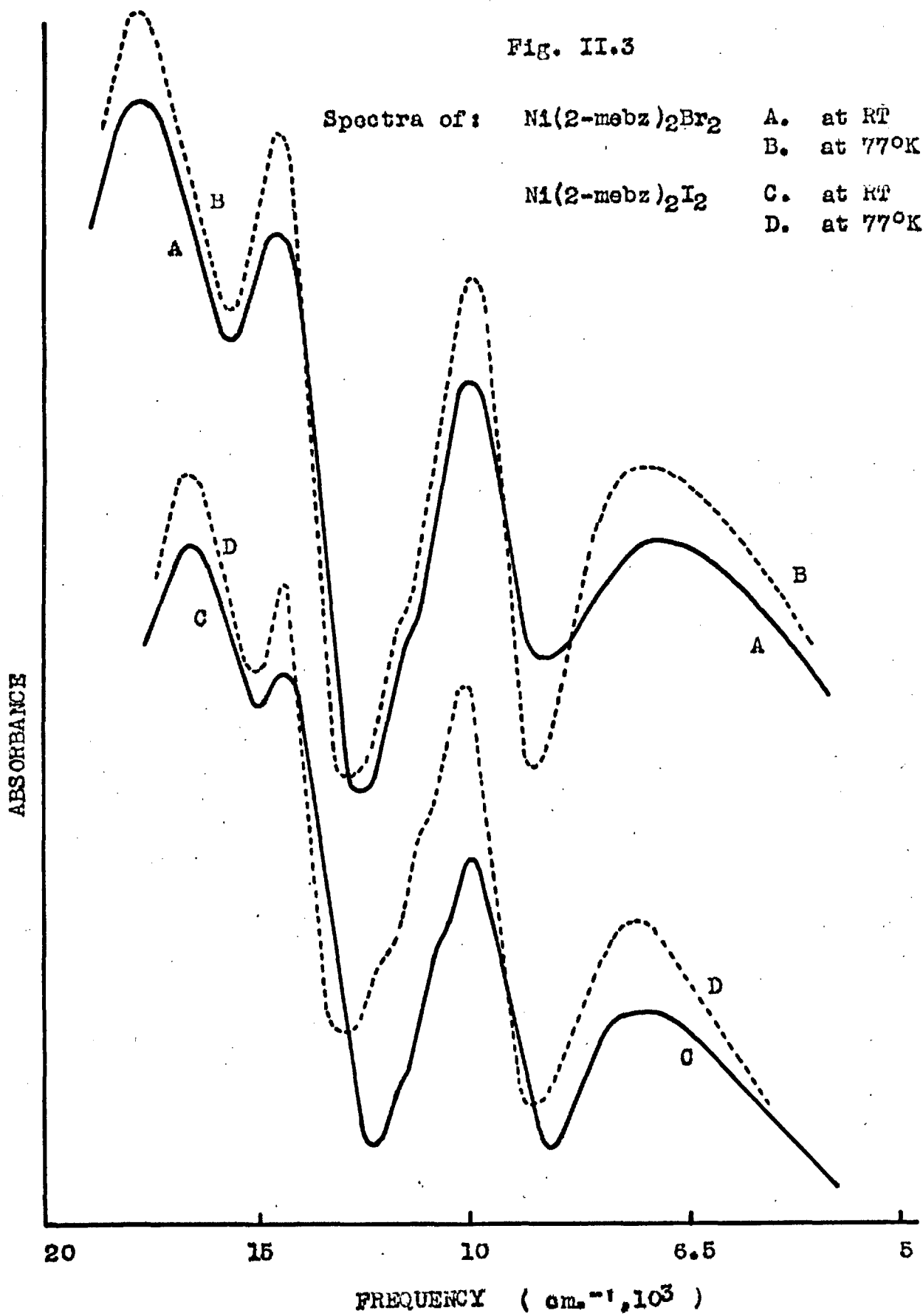


Fig. II.3



have been introduced, but it will be taken that this band contains the observable components of  $\nu_1$ , which are in general not resolved at room temperature. It seems unlikely that there would be other components lying below  $4,100 \text{ cm}^{-1}$ .

The average energy of the  $\nu_1$  bands would be expected to occur at the same energy as the  $\Delta$  values given above, and to drop in energy on going from  $\text{NiL}_2\text{Cl}_2$  to  $\text{NiL}_2\text{I}_2$ . However the  $\nu_1$  bands are found at around  $7,000 \text{ cm}^{-1}$ , this energy showing little change between the complexes with the various anions. A possible explanation of these observed energies, is that they are significantly affected by distortion. Any splitting of the ground state would raise the energy of all transitions, the effect being relatively greater the lower the energy of the transition.

Thus if the band energies for the electronic spectra of the  $\text{C}_{2v}$  complexes are to be fitted into the energy level diagram for  $T_d$  symmetry, a value of  $\Delta$  may be taken that is reasonable for two nitrogen donors and two halide ions, and the transition energies increased by a suitable amount, due to the ground state splitting. A good fit can not be immediately obtained however, and it is found necessary to make

empirical reductions in term separation energies calculated for  $F_4 = 90 \text{ cm}^{-1}$  (The energy separations of the free ion terms may be expressed as functions of the radial integrals,  $F_0$ ,  $F_2$  and  $F_4$ , as given by Condon and Shortley<sup>60</sup>, which are linearly related to the Racah parameters<sup>61</sup>).

These effects may be seen through the spectra of  $[\text{Et}_4\text{N}][\text{Ni}(\text{benzimidazole})\text{Br}_3]$  and  $\text{Ni}(\text{benzimidazole})_2\text{Br}_2$ . For these bromide complexes the term separation energy between,  $^3\text{F}$  and  $^1\text{D}$  has to be reduced to 78%, and  $^3\text{F}-^3\text{P}$  to 94%, of the separation calculated for  $F_4 = 90 \text{ cm}^{-1}$ . The effects on the energies for Td symmetry, arising from the distortion, and the above arbitrary changes in term separation, are given in Table 2.3.

The spectra of the other complexes may be similarly treated by suitable variation of the parameters. The spectral band energies can thus be made to look reasonable, but the question remains as to whether the arbitrary alterations in term separations have any meaning. The fact that the same reductions are needed for complexes with the same anion indicates that they may not be completely random, but the differing reductions that are needed for different

Table 2.3

Band Energies from the Spectra of Distorted Tetrahedral Nickel(II) Complexes

		Band Energies ( $\text{cm}^{-1}$ )	Band Energies ( $\text{cm}^{-1}$ )	Band Energies ( $\text{cm}^{-1}$ )	Observed
		Td : $F_4 = 90$ $\text{cm}^{-1}$	Reduced Term Sep <sup>ns</sup> (a)	with effect of G/S <sup>(b)</sup> splitting	Spectrum ( $\text{cm}^{-1}$ )
<u>[Ni(bz)Br<sub>3</sub>]</u>					
Average $\Delta$	$\nu_1$	4,000	4,000	5,100	5,100
3,800 $\text{cm}^{-1}$	$\nu_2$	7,800	7,800	8,900	8,700
Lowering from	s.f. <sup>(c)</sup>	~12,000	~9,400	~10,500	~10,500
G/S <sup>(b)</sup> split <sup>ng</sup>	$\nu_3$	15,500	14,600	15,700	15,700
1,100 $\text{cm}^{-1}$					
<u>Ni(bz)<sub>2</sub>Br<sub>2</sub></u>					
Average $\Delta$	$\nu_1$	4,250	4,250	5,550	6,700
4,000 $\text{cm}^{-1}$	$\nu_2$	8,100	8,100	10,400	10,400
Lowering from	s.f. <sup>(b)</sup>	~12,100	~9,400	~11,700	~11,700
G/S <sup>(b)</sup> split <sup>ng</sup>	$\nu_3$	16,000	15,000	17,300	17,250
2,300 $\text{cm}^{-1}$					

(a) Energy of  ${}^3F-{}^1D$  reduced to 78% of value calculated for  $F_4=90\text{cm}^{-1}$ . (Fig.II.1) (1)

" "  ${}^3F-{}^3P$  " " 94% " " " " " " " " " " " "

(b) G/S = Ground State

(c) s.f. = Spin-forbidden transition,  ${}^3T_{1g}({}^3F) - {}^1T_{2g}({}^1D)$

term separations suggests that no simple correlation with effects such as delocalisation can be made.

In most cases the  $\nu_1$  and  $\nu_3$  bands for the  $C_{2v}$  complexes do not show any significant splitting in the room temperature spectra. However the  $\nu_3$  band for  $Ni(2\text{-methylbenzimidazole})_2X_2$  ( $X=Cl, Br, I$ ) is split by  $2,500 - 3,000 \text{ cm.}^{-1}$  (Fig. II.2). The splittings may be due in part of solid state effects, for in the solution spectra, while the mean  $\nu_3$  band positions are roughly the same as seen in the solid state, the splittings are about halved (Table 2.4). There are no systematic changes in the splitting in the solid state, but in solution the splittings, for complexes with a given anion, are  $I > Br > Cl$ .

The splitting of one of the bands in the electronic spectra of tetrahedral cobalt (II) complexes may give some indication of the likely splitting of the tetrahedral nickel (II) ground state. Hence the spectra of the tetrahedral cobalt (II) complexes will be introduced. The notation used will be:

$${}^4A_2 \rightarrow {}^4T_2 = \nu_1 ; {}^4A_2 \rightarrow {}^4T_1 ({}^4F) = \nu_2 ;$$

$${}^4A_2 \rightarrow {}^4T_1 ({}^4P) = \nu_3. \text{ The diffuse reflectance}$$

spectra are given in Table 2.5, and may be interpreted in terms of an essentially tetrahedral coordination,



Table 2.4

Splittings of the  $\nu_3$  band for complexes of the type  $\text{Ni}(\text{2-methylbenzimidazole})_2\text{X}_2$  in the solid state and in solution.

<u>Complex</u>	<u>Splitting of <math>\nu_3</math> (<math>\text{cm}^{-1}</math>)</u>		<u>Weighted Mean <math>\nu_3</math> Position (<math>\text{cm}^{-1}</math>)</u>	
	Solid	Solution	Solid	Solution
$\text{Ni}(\text{2-mebz})_2 \text{Cl}_2$	2,800	1,200	17,350	17,300
"	$\text{Br}_2$ 3,200	1,300	16,900	16,700
"	$\text{I}_2$ 2,300	1,900	16,000	15,900

the high intensity of the spectra, as for the nickel (II) complexes, again being consistent with a noncentro-symmetric configuration. The band, or group of bands, seen in the region  $5,000 - 9,000 \text{ cm}^{-1}$  may be assigned to  $\nu_2$ , or components of  $\nu_2$ , and the band, or group of bands, in the region  $15,000 - 17,000 \text{ cm}^{-1}$  to  $\nu_3$ , or components of  $\nu_3$ . The  $\nu_1$  band is not usually seen, lying below  $4,000 \text{ cm}^{-1}$ . The  $\nu_2$  band in the spectra of the tetrahedral cobalt complexes arises from the transition to a level of  $T_1$  symmetry, which is the

Table 2.5

Electronic Absorption Spectra of the  
Tetrahedral 2:1 Cobalt (II) Complexes

<u>Compound</u> <sup>*</sup>	
Co(N-neim) <sub>2</sub> Cl <sub>2</sub>	~17,300(s.sh); 16,600; 16,100; 9,100; 7,000 ~6,400(s.sh)
Co(N-neim) <sub>2</sub> Br <sub>2</sub>	~17,150(sh); 16,400; 15,200; 8,700; 6,800 ~6,300(s.sh)
Co(2-neim) <sub>2</sub> Cl <sub>2</sub>	~17,900(s.sh); 17,050; ~16,500(s.sh); 9,900 ~7,700(n.r); ~7,100(n.r)
Co(2-neim) <sub>2</sub> Br <sub>2</sub>	~17,750(s.sh); 16,850; ~16,200(s.sh); 9,860 ~7,650(n.r); ~6,950(n.r)
Co(bz) <sub>2</sub> Br <sub>2</sub>	16,850(s); 16,100; 15,500; 8,900; 7,200; 6,000
Co(2-mebz) <sub>2</sub> Cl <sub>2</sub>	~17,300(sh); 15,800; 8,700; 7,250; 6,150
Co(2-mebz) <sub>2</sub> Br <sub>2</sub>	17,200; 15,200; 8,650; 6,850; 5,650

\*  
#

All in the solid state

same symmetry as the ground state for tetrahedral nickel (II). Thus any splitting in the  $\nu_2$  band for the former may give some indication of the order of magnitude of the splitting of the ground state, in the latter, though this can not be taken as in any sense quantitative, or as giving the sign of the splitting where this gives rise to A and E components.

The complex  $[\text{Et}_4\text{N}][\text{Co}(\text{benzimidazole})\text{Br}_3]$  is expected to have  $C_{3v}$  symmetry, and the  $T_1$  level will split as given above. The observed bands have been assigned<sup>56</sup> to the  ${}^4A_2$  component of  $\nu_2$  at  $4,900\text{ cm}^{-1}$ , and the E component at  $6,900\text{ cm}^{-1}$ . The cobalt and nickel analogs of this complex are not isomorphous, though it does not necessarily follow that the local symmetry of the metal ions will differ in the complexes with the two metals, and it seems likely that the general symmetry of the complexes with a given anion and heterocycle may be similar. Thus the splitting of  $2,000\text{ cm}^{-1}$  in the  $\nu_2$  band for the cobalt complex indicates that the significant splitting of the ground state in the nickel complex postulated above, (Table 2.3), is reasonable.

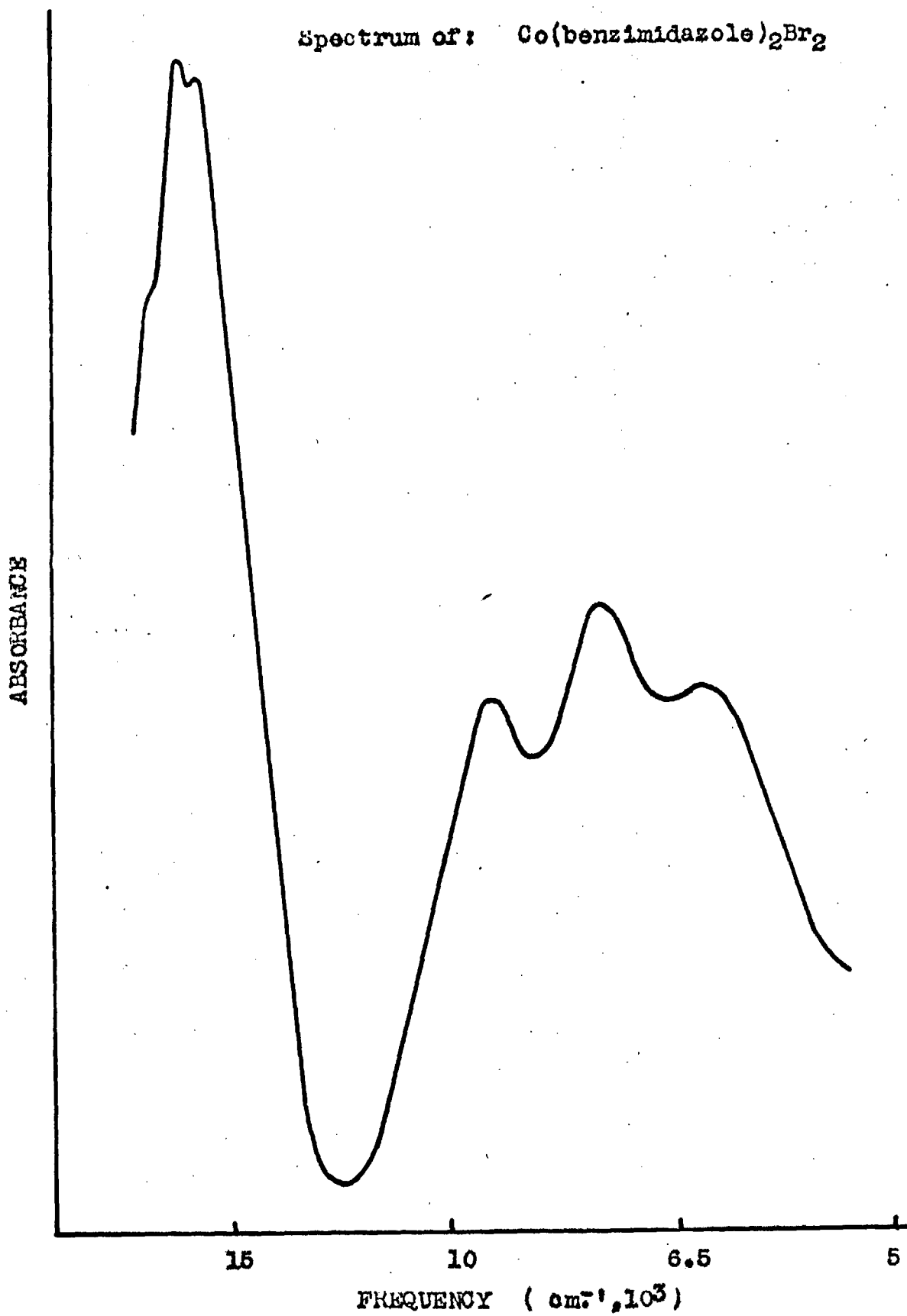
The complexes  $\text{Co}(\text{benzimidazole})_2 X_2$  ( $X=\text{Br}, \text{I}$ ) give spectra<sup>56,62</sup> in which the  $\nu_2$  band is split

into three components, as expected for  $C_{2v}$  symmetry, (Fig. II.4). The X-ray powder patterns (Table 2.1) for  $M(\text{benzimidazole})_2\text{Br}_2$  ( $M = \text{Co, Ni}$ ) indicate that these complexes are virtually isomorphous. Thus again the large splitting suggested above for the ground state in the nickel (II) complex (Table 2.3) seems quite likely. In the spectrum of  $\text{Ni}(\text{benzimidazole})_2\text{Br}_2$  at room temperature  $\nu_1$  appears as a broad band at  $\sim 7,000 \text{ cm}^{-1}$ , which at  $77^\circ\text{K}$  is resolved into two components with a splitting  $\sim 1,500 \text{ cm}^{-1}$ . The appearance of only two components is possibly to be expected for nickel (II) in  $C_{2v}$  symmetry, as whichever of the levels  ${}^3A_2$ ,  ${}^3B_1$ , or  ${}^3B_2$ , of the split ground state, lies lowest, transitions will only be symmetry allowed to two of the levels of the split  $\nu_1$ ,  ${}^3A_1$ ,  ${}^3B_1$ , or  ${}^3B_2$ . (All ground states give symmetry allowed transitions to  $\nu_2$ , ( ${}^3A_2$ ). For the  $\nu_3$  band, if the  ${}^3A_2$  level of the ground state lies lowest, then transitions to all components of  $\nu_3$  are symmetry allowed, while if either of the other levels lies lowest, then transitions to only two components of  $\nu_3$  are symmetry allowed).

The spectra of  $\text{Co}(2\text{-methylbenzimidazole})_2\text{X}_2$  ( $\text{X} = \text{Cl, Br}$ ) are very similar to those for the

Fig. II.4

Spectrum of:  $\text{Co}(\text{benzimidazole})_2\text{Br}_2$



benzimidazole complexes, with  $\nu_2$  clearly split into three components. The cobalt and nickel analogs of the complexes with 2-methylbenzimidazole are not isomorphous, which renders any comparison rather dubious. The splitting of the ground state is likely to be significant, in the nickel (II) complexes, as indicated by the band positions in the electronic spectrum. However no resolution of the  $\nu_1$  band could be obtained at 77°K, while the  $\nu_3$  band shows a clear splitting. This is in contrast to the spectra of the benzimidazole complexes, where the  $\nu_1$  band is split, and  $\nu_3$  fairly sharp and unsplit, at 77°K. This is somewhat surprising as the general symmetry of the complexes with both ligands might have been expected to be similar, and further examination of complexes of this type will be necessary to determine the factors which control the relative splittings of  $\nu_1$  and  $\nu_2$  in the distorted tetrahedral nickel (II) complexes. The complex  $\text{Ni}(\text{benzothiazole})_2\text{I}_2$  has a dark brown colour, in contrast to the 2:1 tetrahedral iodide complexes previously discussed, these latter being dark green. The complex is paramagnetic, and gives an electronic spectrum, (Table 2.2), whose intensity and band positions indicate an essentially tetrahedral

structure.

The origin of the intense dark green colour of the other nickel iodide complexes was in a charge transfer band extending into the visible region. Similarly here the brown colour arises from a charge transfer band extending further into the visible, to the extent of partly obscuring the  $\nu_3$  band. This might indicate that the benzothiazole was bonding through the sulphur atom, sulphur donors tending to cause low energy charge transfer bands<sup>63</sup>. There is however no evidence from the infrared spectrum to establish the mode of bonding, and the electronic spectrum may be interpreted in terms of bonding through the nitrogen atom.

The presence of the electronegative sulphur in the thiazole ring bonded via the nitrogen atom, might cause a flow of charge into the ring, and a low energy charge transfer band. The splitting of the  $\nu_3$  band is similar to that seen for Ni(2-methylbenzimidazole)<sub>2</sub>I<sub>2</sub>, while the average band energy is lower for the benzothiazole complex, which might be a result of the delocalisation into the ring, and a reduced term separation.

The  $\nu_2$  band appears as a doublet, with a splitting

of  $\sim 500 \text{ cm}^{-1}$  this probably arising from the  ${}^1T_2$ , ( $\Gamma_5$  under spin-orbit coupling in tetrahedral symmetry), being energetically close to the  ${}^3A_2$  ( $\Gamma_5$ ), and mixing strongly to gain intensity. The  $\nu_1$  band is sharp, and at high energy, being barely resolved from the  $\nu_2$  band. In general outline it resembles the  $\nu_1$  band of  $\text{Ni}(\text{2-methylbenzimidazole})_2\text{I}_2$ . This similarity is seen more clearly from the spectrum of the benzothiazole complex at  $77^\circ\text{K}$ , when the  $\nu_1$  band is completely resolved from the  $\nu_2$  band.

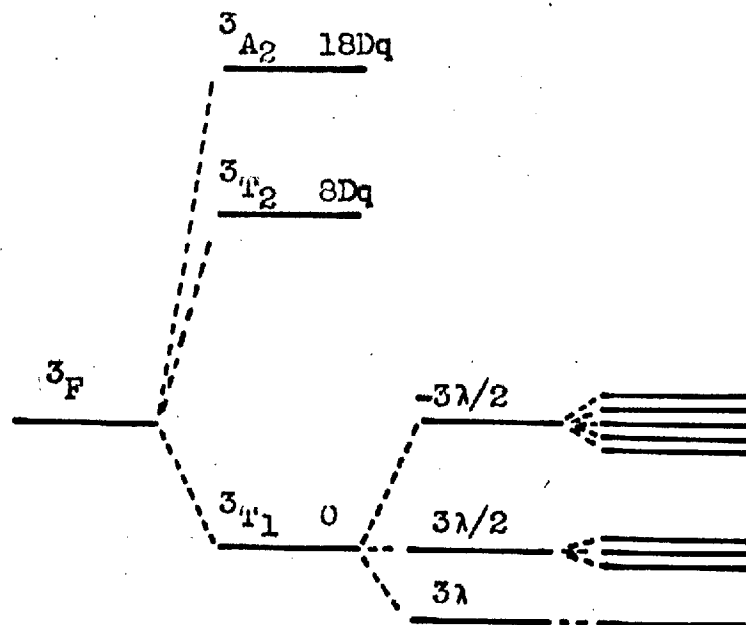
### Magnetic Properties

For the  $d^8$  system in  $T_d$  symmetry the room temperature magnetic moments are expected to be high owing to the contribution to the moment from the orbitally degenerate ground state ( ${}^3T_1$ ). The action of spin-orbit coupling however, is to raise the degeneracy of the  ${}^3T_1$  term, such that the lowest energy state has  $J=0$ , with levels  $J=1$ , and  $J=2$  several multiples of  $\lambda$  above (Fig. II.5). At room temperature there will be appreciable population of all levels, and the magnetic moment will be significantly above the spin only value. On lowering the temperature



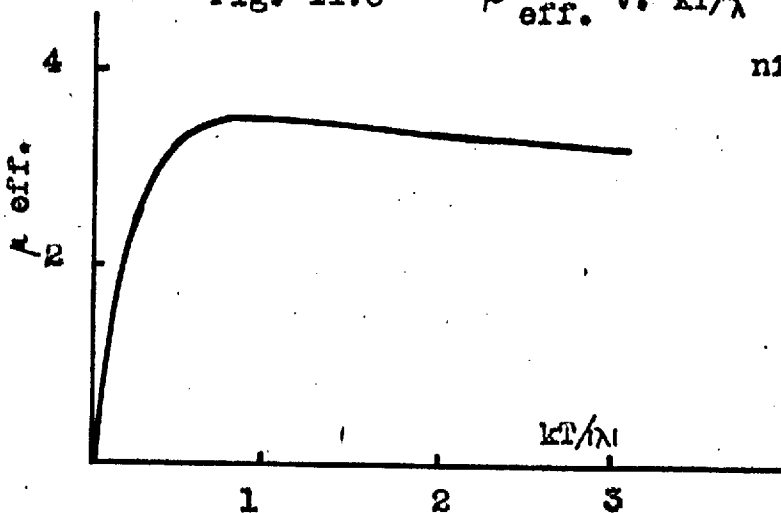
Fig II.5 \*

Free ion F term, for nickel(II), under the successive influences of a weak tetrahedral ligand field, spin-orbit coupling, and a magnetic field.



Term	Ligand Field	Spin-Orbit Coupling	Magnetic Field
$3F$			
$3A_2$	$18Dq$		
$3T_2$	$8Dq$		
$3T_1$	$0$		
$3A_1$		$3\lambda$	
		$3\lambda/2$	
		$-3\lambda/2$	

Fig. II.6 \*  $\mu_{\text{eff.}}$  v.  $kT/\lambda$  for tetrahedral nickel(II)



\* Figs. II.5 and II.6, after Figgis and Lewis, ref. 11.

the electron population will begin to drop into the  $J=0$  level, the moment showing a progressive decrease, Fig. II.6. Nickel (II) in an essentially octahedral environment, where there is an orbital singlet ground state, was found to obey the Curie-Weiss law (see Chapter I, p.36):

$$\chi_A = C / (T - \theta)$$

When this law holds, the magnetic moment, corrected for  $\theta$ , remains constant. Thus for nickel (II) in  $T_d$  symmetry a Curie-Weiss behaviour should not be shown, and plots of  $1/\chi_A$  v.T will show a curvature away from the temperature axis; such plots being linear for octahedral nickel (II). (Fig. I.5).

The action of symmetries lower than  $T_d$  will be to split the orbitally degenerate ground state, when spin-orbit coupling will be reduced. Thus on distortion, the room temperature magnetic moments should be diminished, owing to loss of orbital moment, and the drop in moment on lowering temperature should be less than that seen in  $T_d$  symmetry.

Figgis has calculated the magnetic moments, as a function of temperature for nickel (II) in  $T_d$

symmetry, and in symmetries such as  $C_{3v}$  and  $D_{2d}$ , where the orbital triplet level is split into A and E components<sup>14</sup>.

In making the calculations four variables were used, the spin-orbit coupling constant in the complex, ( $\lambda'$ ); the relative strengths of the ligand field and interelectronic repulsion energies, ( $\Delta$ ); the splitting of the orbital triplet by low symmetry, ( $\Delta$ ); and a delocalisation parameter, ( $k$ ).

Certain generalisations may be taken over from these results. For those distortions which split the orbital triplet into A and E components, if the delocalisation is significant, i.e.  $K \sim 0.5 - 0.7$ , then the drop in moment and deviation from Curie-Weiss type behaviour, are larger when the E component lies lowest. For cases where the orbital singlet lies lowest, and behaviour approximates to Curie-Weiss, then it might be thought that the ' $\theta$ ' value would be larger, the greater the value of the room temperature moment, if spin-orbit coupling is leading to a loss of moment. This however is not the case in general, in that while the room temperature moment decreases the larger the distortion for given values of the other parameters, the detailed behaviour of the

magnetic moment with temperature depends on the interrelation of all the parameters.

Attempts have been made to determine the values of these parameters in some complexes by fitting the magnetic moment data found over a temperature range to the calculated curves<sup>14</sup>. It would seem however, that while such curve fitting gives parameters which would, within the limits of the approximations used, describe a system giving the observed behaviour, the real situation might require other distortion, and bonding characteristics to be considered, which would lead to a greater variation in interpretation of the magnetic data.

Of the present complexes the curve fitting technique might apply to  $[\text{Et}_4\text{N}][\text{Ni}(\text{benzimidazole})\text{Br}_3]$  where the nickel ion is in  $C_{3v}$  symmetry. The magnetic moment and susceptibility of this complex at  $295^\circ$  and  $100^\circ\text{K}$  are given in Table 2.6.

While it was not found possible to make a quantitative fit, the best agreement was obtained with;  $\lambda' = \sim 220 \text{ cm}^{-1}$ ;  $A/\lambda' = \sim -3$  (singlet state lowest);  $A = 1.5$ ;  $K = \sim 0.7$ . The magnetic susceptibility showed an effectively Curie-Weiss behaviour, consistent with the generalisations from the Figgis

calculations. The calculations are strictly only valid for complexes with  $T_d$ , or  $C_{3v}$  and  $D_{2d}$ , symmetries. Attempts have been made however to derive parameters for complexes with  $C_{2v}$  symmetry, where the E component is split into two orbital singlets<sup>14</sup>. The lowest state must then be an orbital singlet, and it was indeed found that applying the calculations for  $C_{3v}$  symmetry to the  $C_{2v}$  complexes, the parameters derived indicated a singlet ground state in all cases<sup>14</sup>. The parameters found for complexes of  $C_{2v}$  symmetry can not be considered quantitatively meaningful, and are not always in agreement with values obtained by independent methods.<sup>9</sup>

Following the generalisations given above it might be expected that  $C_{2v}$  complexes, with a singlet ground state, would show effectively Curie-Weiss behaviour. This was found to be the case for all the tetrahedral 2:1 complexes examined here. The susceptibilities and magnetic moments at 295 and 100°K are given in Table 2.6. The room temperature moments are seen to increase for complexes with a given ligand, and with the various anions, in the order, chloride > bromide > iodide. This is consistent with the larger distortion expected in the iodide compared with the

chloride complex. The intercepts on the temperature axis for the  $1/\chi_A$  v.T plots (Table 2.6) were apparently random, and could not be correlated with the room temperature moment, a feature suggested by the generalisations from the Figgis calculations. Dr. Leask at the Clarendon Laboratories, Oxford has measured the susceptibilities of  $[\text{MePh}_3\text{As}]_2[\text{NiCl}_4]$ ,  $[\text{Et}_4\text{N}][\text{Ni}(\text{benzimidazole})\text{Br}_3]$ , and  $\text{Ni}(\text{benzimidazole})_2\text{Br}_2$  in the region of liquid helium temperatures Table 2.6. Qualitatively the results are as expected, in that the  $[\text{NiCl}_4]^{2-}$  ion has a much lower moment at these temperatures than the nickel (II) in  $C_{3v}$  and  $C_{2v}$  symmetries. All three show moments at these temperatures below the spin-only value.

Table 2.6

Magnetic Data for the Tetrahedral 2:1 Nickel (II)

<u>Compound</u>	<u>295°K</u>		<u>100°K</u>		<u>Inter- cept<sup>xx</sup></u> (-T°K)
	$10^6 \chi_A^*$	$\mu_{\text{eff.}}$	$10^6 \chi_A$	$\mu_{\text{eff.}}$	
	(c.g.s.u)	(B.M.)	(c.g.s.u)	(B.M.)	
[Et <sub>4</sub> N][Ni(bz)Br <sub>3</sub> ]	5390	3.57	14,780	3.44	11
Ni(bz) <sub>2</sub> Br <sub>2</sub>	5080	3.46	13,950	3.34	13
Ni(bz) <sub>2</sub> I <sub>2</sub>	4550	3.28	12,550	3.17	10
Ni(2-mebz) <sub>2</sub> Cl <sub>2</sub>	5480	3.60	14,500	3.41	19
Ni(2-mebz) <sub>2</sub> Br <sub>2</sub>	4980	3.43	14,080	3.36	7
Ni(2-mebz) <sub>2</sub> I <sub>2</sub>	4780	3.36	13,300	3.26	12
Ni(3-meisoqn) <sub>2</sub> Cl <sub>2</sub>	5400	3.58	14,800	3.45	12
Ni(3-meisoqn) <sub>2</sub> Br <sub>2</sub>	5360	3.56	14,300	3.38	16
Ni(qn) <sub>2</sub> Cl <sub>2</sub>	5220	3.53	15,000	3.47	5
Ni(qn) <sub>2</sub> Br <sub>2</sub>	5050	3.45	13,400	3.28	17

\* Molar susceptibility corrected for ligand and metal ion diamagnetism.

\*\* For  $1/\chi_A$  v.T plots, which are linear over the range of measurements.

Table 2.6 (continued).

Susceptibility measurements in the region of Liquid Helium Temperatures for some Tetrahedral Nickel (II) complexes

<u>Compound</u>	<u>T(°K)</u>	<u><math>\chi_M^*</math>(c.g.s.u)</u>	
[MePh <sub>3</sub> As] <sub>2</sub> [NiCl <sub>4</sub> ]	4.2	1.46x10 <sup>-2</sup>	$\chi_M$ assumed indep. of temp.
[Et <sub>4</sub> N][Ni(bz)Br <sub>3</sub> ]	4.187	2.38x10 <sup>-1</sup>	
	4.005	2.35 "	
	3.502	2.31 "	
	1.430	3.63 "	
Ni(Ph <sub>3</sub> P) <sub>2</sub> Cl <sub>2</sub>	4.2>T>1.4	1.40x10 <sup>-1</sup>	
Ni(bz) <sub>2</sub> Br <sub>2</sub>	4.186	2.40x10 <sup>-1</sup>	
	4.010	2.59 "	
	3.509	2.54 "	
	3.006	2.54 "	
	2.472	2.75 "	
	1.943	3.07 "	
	1.481	3.20 "	

\* Molar susceptibility



CHAPTER IIIThe 4:1 Complexes of Benzimidazole with Nickel (II)HalidesPreparation

The complexes initially prepared were of the type  $\text{Ni}(\text{benzimidazole})_4\text{X}_{2.n}\text{Acetone}$  ( $\text{X} = \text{Cl}, \text{Br}, n = 2;$   
 $\text{X} = \text{I}, n = 3$ ). These solvated compounds were prepared in a number of different forms, and a further series of compounds obtained on desolvation. For discussion purposes a code alphameric will be assigned to each compound. These will be given at the first appearance of the compound in the text, and a general statement of the coding made at this point.

For the solvated complexes the first letter refers to the colour of the complex B = blue, G = green, O = olive-green, and Y = yellow; for the second letter, C = chloride, B = bromide. A prefix  $\Delta$  indicates that the compound has been obtained on desolvation of an acetone containing complex, by heating. For the letter following, C = chloride, B = bromide. The number after the letter indicates to which of three classes of

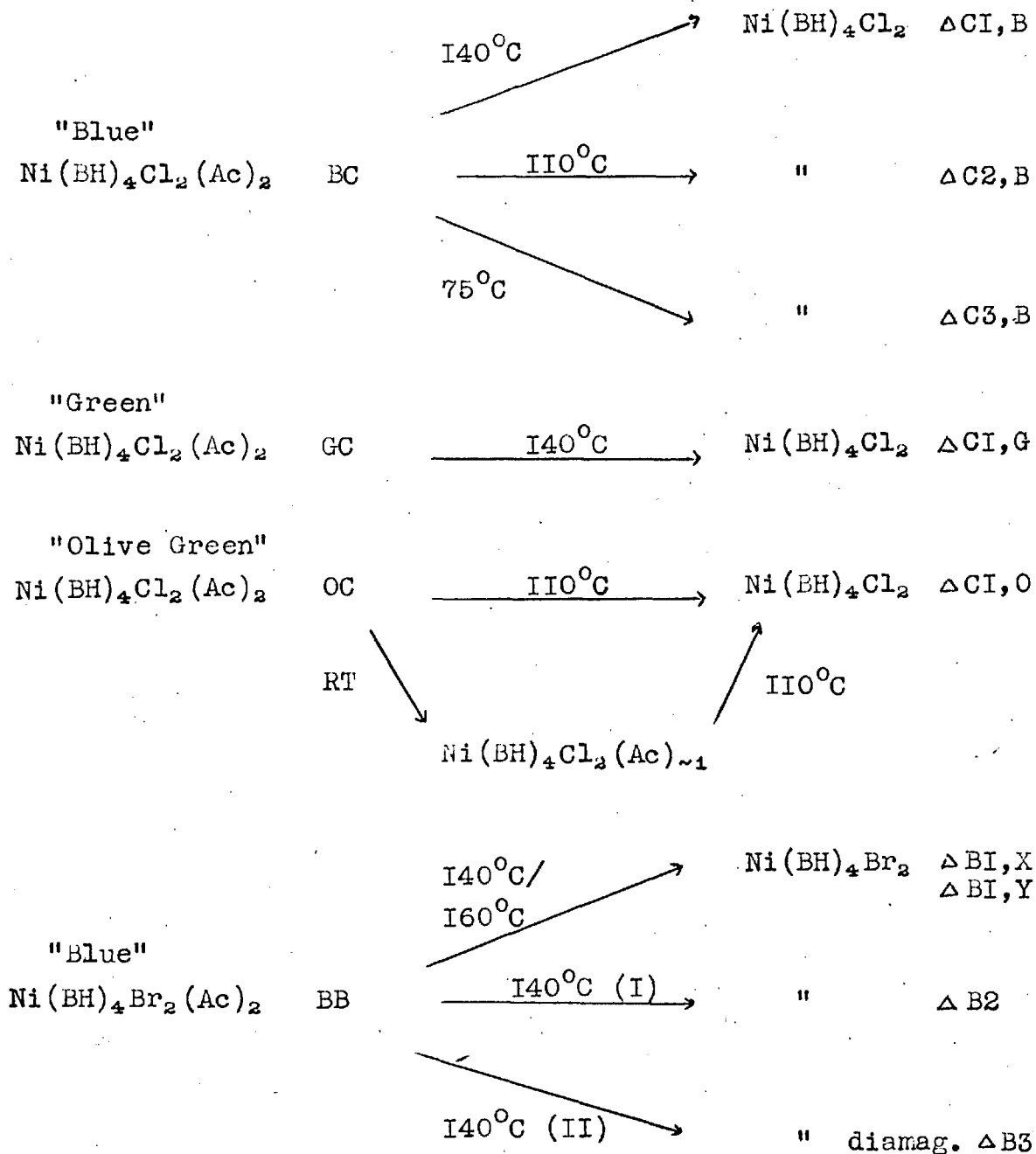
unsolvated chloride, or two classes of unsolvated bromide complexes, the compound belongs. There is in some cases a final letter, which for the unsolvated chloride complexes, indicates the colour of the solvate from which the desolvated complex was obtained. The code assignments are summarised in Fig. III.1.

The presence of acetone in these compounds was indicated by the infrared spectra of the solids, and of the gases evolved on heating the solids. Some difficulty was experienced with carbon analysis for all compounds containing acetone. It appears that the solvent molecules are lost so rapidly under the conditions of the analysis, that incomplete combustion occurs, and low results are obtained. The stoichiometries assigned to the solvated complexes have been checked by analysis for other elements, including oxygen, and also by weight loss on heating, followed by analysis of the desolvated product.

The compound  $\text{Ni}(\text{benzimidazole})_4\text{Cl}_2 \cdot 2 \text{ Acetone}$ , may be found in blue (BC), green (GC), or olive-green (OC) forms. On refluxing a 4:1 mole ratio mixture of benzimidazole and nickel chloride hexahydrate, in acetone, there is an immediate precipitate of a pale green solid. After refluxing for 24 hours the green solid changes to

Fig. III.1

The Acetone Solvates of Ni(BH)<sub>4</sub>X<sub>2</sub> (X= Cl,Br)  
and the Desolvation Products



an olive-green solid (OC). The system is allowed to cool, and stand corked, for up to 12 days, the olive-green crystals slowly altering to a blue crystalline form (BC).

This process may be much hastened if a small quantity of water is added to the initial reaction mixture. The olive-green form is then obtained after 3 hrs. refluxing, and the blue form after standing for 48 hrs. Oxygen analyses indicated that there was no water present in the final compound, prepared either with, or without, any water added to the initial mixture.

If the blue product is dissolved in dry acetone, an excess of benzimidazole added, and the solution allowed to stand, green monoclinic crystals are formed (GC). It was found that this green compound, if placed in acetone containing 1% of water, altered to the blue form. Direct oxygen analysis again showing that no water was present in the blue form.

The compound OC slowly loses acetone at room temperature, changing first to a dark yellow, then to a pale yellow colour, the compound (YC) then containing about one molecule of acetone per molecule of 4:1 complex. The rate of loss of further acetone is greatly

reduced. The forms BC and GC also lose acetone at room temperature, but at a slower rate than OC, and do not appear to form any intermediates.

On desolvation of the acetone containing chloride complexes a number of products may be obtained depending on the temperature. These various products will be differentiated through their magnetic and spectral properties in later sections.

If the solvates BC and GC are heated at 130°C to constant weight, a bright green compound is formed ( $\Delta\text{Cl}$ ). The compound BC on heating at 110°C however, gives a darker green compound ( $\Delta\text{C2}$ ), whereas heating at 75°C gave an olive-green form ( $\Delta\text{C3}$ ). If the solvate OC is heated at either 130, or 110°C, it gives  $\Delta\text{Cl}$ . The compound YC gave  $\Delta\text{Cl}$  on heating at 75°C. (See Fig. III.1). X-ray powder patterns (see next section) showed that the various samples of  $\Delta\text{Cl}$  from different sources, had the same structure.

The compound  $\text{Ni}(\text{benzimidazole})_4\text{Br}_2 \cdot 2 \text{ Acetone}$ , has been found in one blue form (BB). Attempts to produce other forms analogous to the chloride system have not been successful. The blue form may be prepared by refluxing a 4:1 mole ratio of benzimidazole and nickel bromide hexahydrate, in acetone. A pale green solid

is initially formed, this altering to the blue form over about 4 hours. If the pale green solid is removed from the acetone, it immediately changes to a blue form.

A number of desolvation products may again be obtained, from BB, depending on the temperature used. The procedure necessary to obtain any given product is difficult to define precisely. It was found that apparently similar experiments gave different products, and mixtures **were** often obtained. However certain guiding principles emerged from a number of experiments, and these are outlined below.

Rapid removal of acetone, either on desolvation by heating ( $\sim 80-90^{\circ}\text{C}$ ) under vacuum, or by heating the samples to high temperatures ( $\sim 140^{\circ}\text{C}$ ) in an open vessel, such as a watch glass, tended to give mixtures containing tetrahedral  $\text{Ni}(\text{benzimidazole})_2\text{Br}_2$ . On heating the solvate BB at  $140^{\circ}\text{C}$ , in an elongated vessel with a small aperture, such as a drawn off ignition tube, (i.e. the ratio of surface area, to mass, is small), for about 15 minutes, the colour changed to blue-brown. When transferred, without cooling, to a temperature of  $160-165^{\circ}\text{C}$ , there was an alteration to a dark green compound over 1 hour. This latter compound on cooling

changed to a yellow-green form ( $\Delta B1$ ). This change had sometimes not occurred when the sample had cooled to room temperature undisturbed, then on tapping the tube the change took place immediately.

If BB is heated solely at  $140^{\circ}\text{C}$ , in the vessel described above, a pale blue product is obtained ( $\Delta B2$ ). However if heated at  $140^{\circ}\text{C}$  in a more open vessel, such as a weighing bottle, uncapped, an orange diamagnetic form may be produced ( $\Delta B3$ ).

A sample of another orange form was obtained by placing a portion of the acetone solvated complex BB, in chloroform, and sealing the tube. Over a period of some months, the blue crystalline material slowly turned into well formed orange crystals. From analysis, and weight loss on heating, it was found that this orange compound was the 4:1 bromide complex, with three molecules of chloroform per molecule of complex. The product obtained on heating this latter complex at  $110^{\circ}\text{C}$  was a pale blue paramagnetic solid. The electronic spectrum, and X-ray powder pattern (see next section) showed that this compound was the same as that designated  $\Delta B2$  above.

The compound  $\text{Ni}(\text{benzimidazole})_4\text{I}_2 \cdot 3 \text{ Acetone}$  has been found in one pale green form. This was obtained

by dissolving  $\text{Ni}(\text{benzimidazole})_2\text{I}_2$  in acetone, adding an excess of benzimidazole, and allowing to stand. On desolvation an orange diamagnetic compound was obtained, independent of the conditions under which the acetone was removed.



### X-Ray Powder Patterns

The X-ray powder pattern data is collected in the tables below, the results being required at various points in the following sections. The nature of the complexes listed, and the significance of any mixtures, or phase changes, established, will be discussed in the sections on electronic spectra and magnetism that follow.

As some of the complexes occur in isomeric forms fairly full X-ray powder data is given. The d spacings and intensities of some of the stronger lines for the powder patterns of the solvated complexes are given in Table 3.1, and for the desolvated complexes in Table 3.2.

The samples of  $\Delta C1$  from the various sources, i.e.  $\Delta C1$ , B, G and O as in Fig. III.1, gave powder patterns that were indistinguishable.

The complex  $\Delta C2$  (see Fig. III.1) gave a powder pattern that was the same as that for  $\Delta C1$ , except that for an exposure of the same time interval the lines were less intense. The same effect was found to a more marked degree for  $\Delta C3$ , such that for the latter, only the strongest lines from the  $\Delta C1$  powder pattern were

Table 3.1

X-Ray Powder Data : Solvated Complexes

Ni(benzimidazole)<sub>4</sub>Cl<sub>2</sub>·2 Acetone

Ni(bz)<sub>4</sub>Br<sub>2</sub>·2Ac. Ni(bz)<sub>4</sub>Br<sub>2</sub>·3CHCl<sub>3</sub>

<u>BC</u>		<u>GC</u>		<u>OC</u>		<u>BB</u>			
d	inten.‡	d	inten.	d	inten.	d	inten.	d	inten.
9.54	vs	11.57	vs	12.01	vs	10.61	vs	10.87	s
7.96	m	9.15	vw	11.19	vs	9.86	s	9.25	vs
6.47	mw	7.35	w	8.52	w	7.98	ms	7.37	vs
5.85	ms	7.15	w	6.14	w	7.30	ms	7.21	s
5.35	m	7.08	w	5.62	w	4.86	ms	7.05	s
5.03	ms	5.76	w	5.39	ms	4.32	s	6.91	s
3.84	m	4.81	m	5.10	s	3.47	ms	5.96	ms
3.48	m	4.63	w	4.88	w	3.43	ms	4.00	s
3.28	m	4.29	w	4.64	mw	3.22	m	3.70	s
3.23	m	4.24	mw	4.28	w	3.12	m	3.47	s
3.15	mw	4.01	w	4.14	mw	3.04	mw		
2.94	mw	3.84	mw	3.61	m	3.02	mw		
2.88	mw	3.79	w	3.20	w	2.97	mw		
2.63	mw	2.88	w	3.16	vw	2.90	mw		

‡ Intensity

Table 3.2X-Ray Powder Pattern Data : Desolvated Complexes.

Ni(bz) <sub>4</sub> Cl <sub>2</sub>		Ni(benzimidazole) <sub>4</sub> Br <sub>2</sub>					
<u>ΔCl</u>		<u>ΔB1,X</u>		<u>ΔB1,Y</u>		<u>ΔB2</u>	
d	inten.	d	inten.	d	inten.	d	inten.
9.75	vs	10.61	w	10.81	w	10.81	m
6.92	m	10.10	vs	10.10	vs		
6.02	vs			9.27	w	9.27	vs
4.82	s			7.38	w	7.38	ms
4.38	w	7.17	vs	7.17	vs	7.17	m
4.16	vs			7.02	vw	7.02	m
3.80	m			6.93	w	6.93	m
3.46	vw	6.72	vw	6.56	vw	6.56	vw
3.34	w			6.20	vw	6.20	w
3.26	mw	5.35	mw	5.35	mw	5.35	w
3.18	w	5.10	m	5.10	m		
3.10	m	4.51	vs	4.51	vs		
3.07	ms	4.25	vs	4.25	vs		
3.01	vw			4.00	w	4.00	ms
2.72	w	3.81	w	3.81	w		
2.69	w	3.61	m	3.61	m		
2.68	w	3.47	w	3.47	w	3.47	ms
2.45	mw	3.24	s	3.24	s		
2.31	mw	3.07	s	3.07	s		

visible against a fairly strong background. This may indicate that  $\Delta C2$  and  $\Delta C3$  are mixtures of  $\Delta C1$  with another phase that does not give a defined powder pattern.

The complex  $\Delta B1,Y$  appears to be a mixture of  $\Delta B1,X$  with  $\Delta B2$ , (Table 3.2).

The measurements of the magnetic susceptibility of  $\Delta C1$  over a temperature range indicated the possibility of a phase change at  $\sim 180^\circ K$ . X-ray powder patterns were thus taken at low temperature, using the apparatus described in Chapter VI, Physical Measurements.

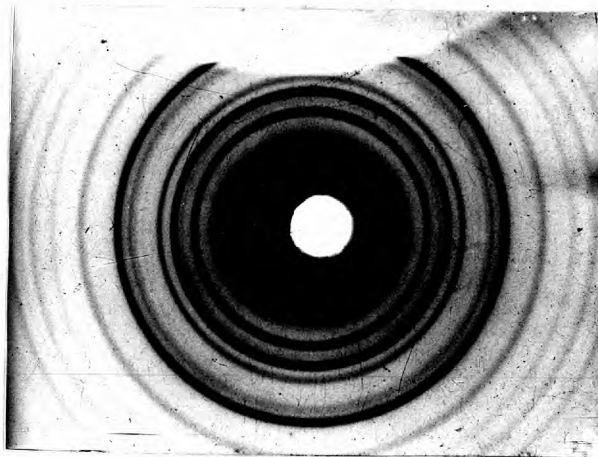
As a control the powder pattern of  $\Delta B2$ , for which there was no indication of any phase change from the magnetic results, was taken at room temperature, and at  $140^\circ K$ . The powder patterns obtained at the two temperatures were identical.

For  $\Delta C1$  there was a clear alteration in the powder pattern on cooling from room temperature to  $130^\circ K$ , as shown in Figure III.2. (The powder photographs were obtained with a front plate camera.)

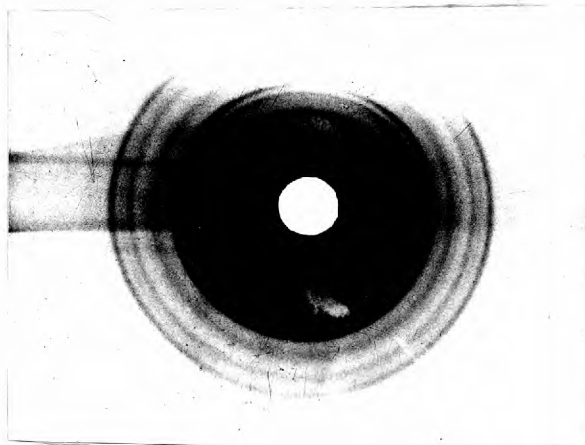
The room temperature powder pattern was qualitatively the same as that obtained using a Guinier camera, (see Chapter VI, Physical Measurements). There was however a shift between the two sets of d spacings

Fig. III.2

X-Ray Powder Patterns (Front Plate Camera) for  
 $\text{Ni}(\text{benzimidazole})_4\text{Cl}_2$ ,  $\Delta\text{Cl}$  at Room Temperature  
and  $\sim 140^\circ\text{K}$ .



Room Temperature



$\sim 140^\circ\text{K}$

from the patterns with the different cameras, this being most marked when the  $d$  spacing was large (i.e. the diffracted angle was small). The origin of this difference is not at present known, but as it is anticipated that the results from the Guinier camera will be the more accurate,  $d$  spacings at room temperature and low temperature from the powder patterns using the front plate camera are not given, though the photographs of Fig. III.2 provide qualitative evidence for a phase change.

## Electronic Spectra

The electronic reflectance spectra are given in Table 3.3. Solution spectra are not reported as the 4:1 complexes dissociate to give the tetrahedral 2:1 species, for solvents in which dissolution may be obtained, such as acetone...

The electronic spectra of the paramagnetic 4:1 complexes may be interpreted in terms of nickel (II) in a tetragonally distorted octahedral field, while the diamagnetic complexes have an essentially square planar field. The transitions expected in a tetragonal field have been given in Chapter I (p.22), and the same notation will be used in this present section.

Considering first the acetone solvated complexes. The blue forms, BC and BB, of  $\text{Ni}(\text{benzimidazole})_4\text{X}_2 \cdot 2$  Acetone (X = Cl or Br), and  $\text{Ni}(\text{benzimidazole})_4\text{I}_2 \cdot 3$  Acetone, give spectra which are alike in appearance, and with similar band energies. The spectrum of BC is shown in Fig. III.3. Band assignments will be made here for this latter complex, which will be considered as typical for the paramagnetic complexes in this chapter. For BC at room temperature  ${}^3\text{A}_{2g} \rightarrow {}^3\text{E}_g$  at  $8,050 \text{ cm}^{-1}$ ;

${}^3A_{2g} \rightarrow {}^3B_{2g}$  at 11,300; either  ${}^3A_{2g} \rightarrow {}^3A_{2g}$ , or  
 ${}^3A_{2g} \rightarrow {}^1E_g^*$ , at  $\sim 13,600$ ,  ${}^3A_{2g} \rightarrow {}^3E_g$  at 16,100;  
 ${}^3A_{2g} \rightarrow {}^1T_{2g}^*$  at 20,800; and  ${}^3A_{2g} \rightarrow {}^3T_{1g}({}^3P)^*$  at  
 25,900  $\text{cm}^{-1}$ .

In that  $\text{Ni}(\text{benzimidazole})_4\text{I}_2$  is known only as  
 an orange diamagnetic complex (Table 3.3), it seems  
 reasonable to suppose that the acetone molecules,  
 in the above solvated complexes, are coordinated in  
 the axial positions. The spectra indicate an average  
 value of  $\Delta$  of  $\sim 9,100 \text{ cm}^{-1}$  for BC and BB, and  $\sim 8,950$   
 $\text{cm}^{-1}$  for  $\text{Ni}(\text{benzimidazole})_4\text{I}_2 \cdot 3 \text{ Acetone}$ .

The green isomer, GC, of  $\text{Ni}(\text{benzimidazole})_4\text{Cl}_2 \cdot 2$   
 Acetone, gives a spectrum in which the bands lie  
 at lower energy than in the blue form BC, (Fig. III.4).  
 This would arise if the halide ions, considered as  
 weaker ligands than acetone, were coordinated in the  
 axial positions in GC. Support for this is found in  
 the similarity of the spectrum of GC to that of one  
 of the desolvated 4:1 complexes,  $\Delta\text{Cl}$  (c.f. Figs. III.4  
 and III.5).

On cooling GC to  $77^\circ\text{K}$ , the bands shifted to  
 higher energies by  $\sim 5\%$ , arising from the expected

\* or components thereof.



Table 3.3Electronic Absorption Spectra.

<u>Compound</u>	<u>Absorption Maxima (cm.<sup>-1</sup>)<sup>‡</sup></u>
Ni(bz) <sub>4</sub> Cl <sub>2</sub> · 2 Acetone	
BC <sup>‡‡</sup>	25,900; ~20,800(w); 16,100; ~13,600(sh); 11,300; 8,000.
BC 77°K	26,500; 21,300(w); 16,850; 14,400; 12,100; 8,400.
GC	25,000; ~20,800(w); 15,400; ~12,800(sh); ~11,400(sh); ~8,800(w.sh); ~6,100(br)
GC 77°K	25,800; 16,000; 12,500; ~8,800(w.sh); 6,400
OC	25,200; 21,300; 15,350; ~12,850(sh); ~11,000(sh); ~6,000(br)
OC 77°K	25,900; 21,600; 16,100; 12,700; ~8,800(w.sh); ~6,600(br)
Ni(bz) <sub>4</sub> Cl <sub>2</sub> · ~1 Acetone	
YC	~25,100(sh); 21,600; 16,100; ~13,000(sh); ~11,500(sh); ~8,800(w.sh); 7,100(br)
YC 77°K	26,000; 21,800; 16,700; 13,100; ~8,850(w.sh); 7,900

<sup>‡</sup> At room temperature unless otherwise stated

<sup>‡‡</sup> See Fig. III.1 for symbols

Table 3.3 (continued)

<u>Compound</u>		<u>Absorption Maxima (cm.<sup>-1</sup>)</u>
	Ni(bz) <sub>4</sub> Br <sub>2</sub> ·2 Acetone	26,300; 20,800(w); 16,250; ~13,700(sh); ~11,900(sh); 7,800
	Ni(bz) <sub>4</sub> I <sub>2</sub> ·3 Acetone	26,100; 20,500; 16,150; ~13,100(sh); ~11,750(sh); 7,520
	Ni(bz) <sub>4</sub> Cl <sub>2</sub>	
	ΔCl	24,900; ~20,800(sh); ~17,700(sh); 15,200; ~12,500(w.sh); ~11,600(w.sh); 9,900; 5,700
	ΔCl            77°K	25,200; ~21,500(w.sh); ~19,400(w); ~17,500(sh); 15,500; 12,400; ~9,700(w); ~6,100(br)
	ΔC2	24,800; ~20,800(w.sh); ~17,700(sh); 15,100; ~12,500(w.sh); 9,900; 5,700
	ΔC3	24,200; ~20,000(sh); 14,400; ~11,650(sh); ~8,800(w.sh); 6,900
	ΔC3            77°K	24,500; 14,700; ~11,700(sh); ~9,100(sh); 7,000
	Ni(bz) <sub>4</sub> Br <sub>2</sub>	
	ΔB1 <sup>***</sup>	27,700; ~25,100(sh); ~19,700(w); 15,300; ~12,600(sh); ~10,500(w.sh); ~8,800(w.sh); ~6,700(br)
	ΔB1            77°K	28,000; 25,300; ~20,800(w); ~18,700(w); 15,800; 12,600; ~8,700(w); (~8,000(sh)) <sup>‡</sup> ; 6,200

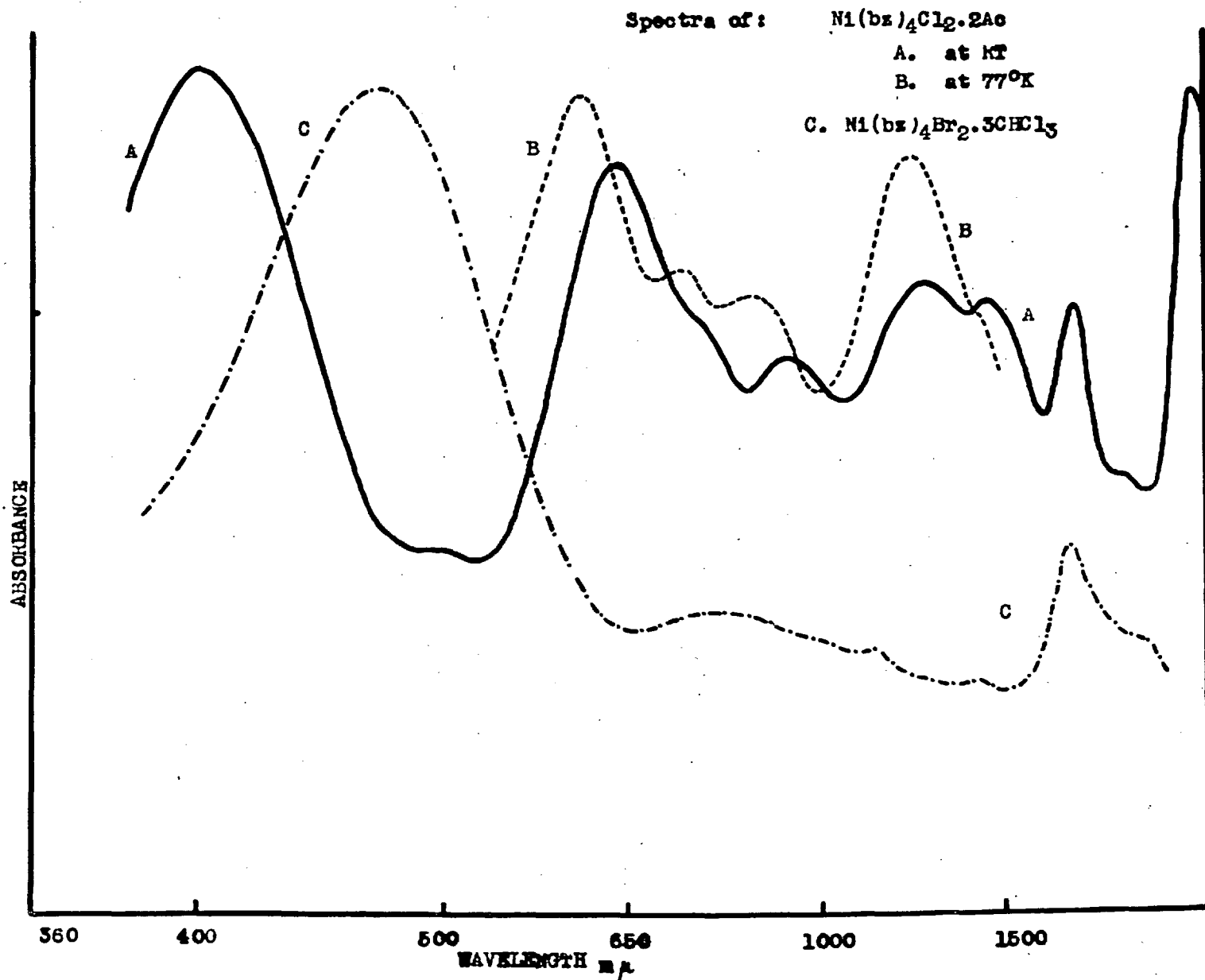
<sup>\*\*\*</sup> Both ΔB1.X and ΔB1.Y

<sup>‡</sup> ΔB1.Y only

Table 3.3 (continued)

<u>Compound</u>	<u>Absorption Maxima (cm.<sup>-1</sup>)</u>
$\Delta B_2$	25,100; $\sim$ 20,000(w); 15,630; $\sim$ 13,000(sh); $\sim$ 11,000(sh); $\sim$ 8,800(w.sh); 7,250
$\Delta B_2$ 77°K	26,500; 21,300(w); 16,850; 14,400; 12,100; 8,400
$\Delta B_3$	21,300; $\sim$ 12,500(br.w)
$Ni(bz)_4Br_2 \cdot 3 CHCl_3$	21,300; $\sim$ 12,700(br.w)
$Ni(bz)_4I_2$	21,300; $\sim$ 12,500(br.w)

Fig. III.3





small increase in  $\Delta$ , owing to a shortening of bond lengths on cooling. It is noticeable that while there are shoulders on the low energy side of  $\nu_2$  at room temperature, only one band appears in this region at 77°K.

The band assignments for GC, and a number of the other compounds examined below, are less certain than for the solvated complexes BC and BB, where the orbital singlet components of  $\nu_1$  and  $\nu_2$  were fairly clear, located between the stronger orbital doublet components (Fig. III.3). In making assignments for these complexes, a feature which is of use is that the position of the  $\nu_1$ ,  $\nu_2$ , and  $\nu_3$  bands, taken from the weighted average positions of the components of these bands, should fit approximately within the Liehr and Ballhausen energy level scheme for nickel (II) in  $O_h$  symmetry, (Fig. I.2). This will be true if the tetragonal distortion is not too great, when configuration interaction, and orbital mixing may occur. (A general discussion of band splittings in distorted nickel (II) complexes is given in Chapter IV).

Thus for GC the spectrum at 77°K suggests that there is essentially one band, at  $\sim 12,500 \text{ cm}^{-1}$ , between the main components of  $\nu_1$  and  $\nu_2$ , at 6,400 and 16,000  $\text{cm}^{-1}$ .

respectively.

This might arise if the splitting of  $\nu_1$  was small, so that the  ${}^3B_{2g}$  and  ${}^3E_g$  components were not resolved, the band at  $12,500 \text{ cm}^{-1}$ , then being assigned to the orbital singlet components of  $\nu_2$ . Alternatively the splitting of  $\nu_1$  might be large so that the orbital singlet components from  $\nu_1$  and  $\nu_2$  overlap, and are seen as a single band at  $12,500 \text{ cm}^{-1}$ .

Taking the average band energies for the second assignment, ( $\nu_1 \sim 8,430 \text{ cm}^{-1}$ ,  $\nu_2 \sim 14,830$ ,  $\nu_3 \sim 25,800$ ), it is found that the energies fit well into the energy level diagram of Fig. I.2. For the first assignment, the  $\Delta$  value indicated by  $\nu_1$ , of  $\sim 6,500 \text{ cm}^{-1}$ , would be very much too low.

In the room temperature spectrum two shoulders are seen on the low energy side of  $\nu_2$ , and it is possible that the orbital singlet components no longer overlap. Assigning the shoulder at  $\sim 11,400 \text{ cm}^{-1}$  to the  ${}^3A_{2g}$  component of  $\nu_2$ , and that at  $\sim 12,800 \text{ cm}^{-1}$  to the  ${}^3B_{2g}$  component of  $\nu_1$ , a good fit may be obtained within the energy level diagram of Fig. I.2. The shoulder at  $12,800 \text{ cm}^{-1}$  might alternatively be assigned to the spin-forbidden transition to one of the components  ${}^1A_{1g}$ ,  ${}^1B_{1g}$ , of the split  ${}^1E_g$ . This band would

not be seen at  $77^{\circ}\text{K}$ , lying on the side of the stronger resolved band at  $12,500\text{ cm}^{-1}$ . The weak shoulder at  $\sim 8,800\text{ cm}^{-1}$  may be assigned to the spin-forbidden transition to the other component of  ${}^1\text{E}_g$ .

Comparison of the electronic spectra of GC and the olive-green isomer, OC, (Fig. III.4) shows that the spectrum of OC is identical to that of GC, both at room temperature and  $77^{\circ}\text{K}$ , with the addition of a band at  $21,300\text{ cm}^{-1}$ . This latter band energy is that at which a planar diamagnetic species would be expected to absorb, as seen from the spectrum of the orange form of  $\text{Ni}(\text{benzimidazole})_4\text{Br}_2$  (Table 3.3). It is further found that the magnetic moment of OC is considerably lower than expected for six coordinate nickel (II) (Table 3.5). It is thus considered that both paramagnetic and diamagnetic nickel (II) ions are present in OC. The X-ray powder pattern of OC, (Table 3.1), did not show any lines that could be attributed to GC, thus indicating that there is no mechanical mixture of GC with a separate diamagnetic species. This might suggest a uniform lattice with nickel ions thermally distributed in different spin states, or a lattice containing nickel ions in two different sites. This will be discussed in the next



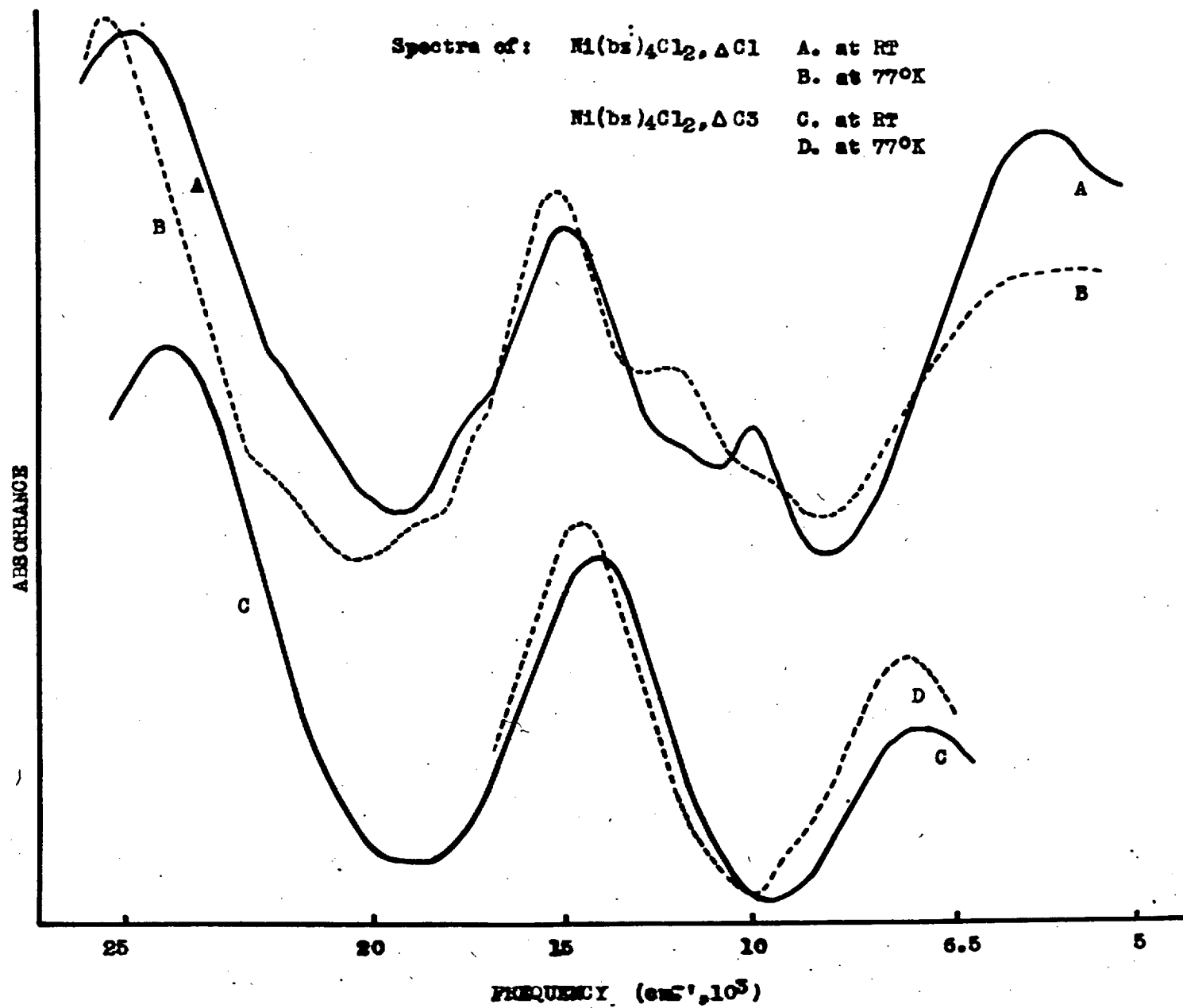
section. While the diamagnetic species appears to be stabilised in this lattice, it has not been found possible to prepare a fully diamagnetic form of  $\text{Ni}(\text{benzimidazole})_4\text{Cl}_2$ .

As the complex OC slowly lost acetone at room temperature, the bands initially at 5,800 and 15,400  $\text{cm}^{-1}$  gradually shifted to higher energies, until the complex YC was obtained, containing one mole of acetone per mole of complex. The strong diamagnetic band was seen in YC, and the spectrum of the paramagnetic portion, in the  $\nu_1$  region, was intermediate between that for BC and GC, it being possible that one molecule of acetone is associated with each molecule of 4:1 complex, and is coordinated to the metal ion.

Turning next to the desolvated complexes the paramagnetic compounds  $\text{Ni}(\text{benzimidazole})_4\text{X}_2$  ( $\text{X} = \text{Cl}, \text{Br}$ ) show spectra which may be considered as arising from nickel (II) in a tetragonal field, the transitions will then be as given above.

Considering first the complex  $\Delta\text{Cl}$ , (see Fig. III.1), it was noted above that GC and the desolvate  $\Delta\text{Cl}$ , have somewhat similar spectra, though for  $\Delta\text{Cl}$  there is a band at 9,900  $\text{cm}^{-1}$  not seen in GC (c.f. Figs. III.5 and III.4).

Fig. III.5



By comparison of the average band energies with the energy level diagram of Fig. I.2, as described above for GC, it was found that the band at  $9,900 \text{ cm}^{-1}$  may be associated with the orbital singlet component ( ${}^3A_{2g}$ ) of  $\nu_2$ , with  ${}^3B_{2g}$  component of  $\nu_1$  lying at higher energies, ( $\sim 12,600 \text{ cm}^{-1}$ ), under the main component of  $\nu_2$ . The shoulder at  $\sim 11,600 \text{ cm}^{-1}$  might be assigned to the spin-forbidden transition to one of the components of  ${}^1E_g$ . The lower energy component would lie on the side of a strong spin-allowed band, and can not be distinguished.

At  $77^\circ\text{K}$  the band at  $9,900 \text{ cm}^{-1}$  appeared to be much reduced in intensity (Fig. III.5). As was evidenced from the X-ray powder pattern data at low temperature (see earlier section in this chapter), and initially indicated by the magnetic results over a temperature, there is a phase change at  $\sim 180^\circ\text{K}$ , and it seems likely that the alteration in the spectrum is due to this change in structure.

It was a possibility that the absorption at  $9,900 \text{ cm}^{-1}$  arose from a hot-band. In this case the band intensity might be expected to diminish gradually on lowering the temperature. Spectra were thus taken at a number of temperatures, using slush baths of various liquids

at their melting points, (n-amyl alcohol, 195°K; toluene, 178°K; iso-amyl alcohol, 156°K). No significant alteration was seen on cooling to 178°K, though on cooling a further 20°, to temperatures in the region of the expected phase change, there was a definite diminution in the intensity of the 9,900  $\text{cm}^{-1}$  band, indicating that the effects are not due to a hot band.

The assignments for the spectrum at 77°K are uncertain. While the band at 9,900  $\text{cm}^{-1}$  appears to have diminished there remains a weaker band at  $\sim 9,700$   $\text{cm}^{-1}$ . This might be due to a spin-forbidden transition, but it is rather stronger than that seen in the spectrum of GC, (c.f. Figs. III.5 and III.4). An alternative explanation might be that the stronger  $E_g$  component of  $\nu_1$  has shifted to higher energies on cooling, and become broader, thus filling in the absorption trough seen on the low energy side of the 9,900  $\text{cm}^{-1}$  band at room temperature, hence rendering this band less conspicuous at 77°K. Thus either both orbital singlet components from  $\nu_1$  and  $\nu_2$  are located at  $\sim 12,500$   $\text{cm}^{-1}$ , or the  ${}^3A_{2g}(\nu_2)$  is at  $\sim 9,700$  and the  ${}^3B_{2g}(\nu_1)$  at  $\sim 12,500$   $\text{cm}^{-1}$ .

The three weak bands between  $\nu_3$  and the main

component of  $\nu_2$ , in the spectrum at  $77^\circ\text{K}$ , may be assigned to spin-forbidden transitions to  ${}^1\text{A}_{1g}$  and the two components of  ${}^1\text{T}_{2g}$ .

In the spectrum of  $\Delta\text{C3}$  the  $\nu_1$  and  $\nu_2$  bands appear to be essentially unsplit, (Fig. III.5). However it seems unlikely that the four nitrogen donors, and two halide ions, would give a symmetrical field with  $\Delta \sim 6,900 \text{ cm}^{-1}$ , which would be only slightly greater than that for six chloride ions (see Chapter I). Thus it seems probable that there is again a significant splitting of the  $\nu_1$  band, such that the orbital singlet component is under the  $\nu_2$  band. There is a shoulder on the low energy side of  $\nu_2$  which if assigned to the orbital singlet component of  $\nu_1$  would give a very reasonable value for,  $\Delta$  average, of  $\sim 8,3000 \text{ cm}^{-1}$ , and also for the band splitting parameters, as discussed in Chapter IV. If this assignment was correct then it might be expected that the orbital singlet component of  $\nu_1$  would be resolved from  $\nu_2$  at  $77^\circ\text{K}$ . This however is not the case, (Fig. III.5), which throws doubt on the above interpretation, unless the splitting of  $\nu_1$  is greater than anticipated. The low in-plane field required for the orbital singlet component of  $\nu_1$  to be located below  $9,000 \text{ cm}^{-1}$ , suggest that in general

the above assignments are more reasonable. Following the latter assignments the band splittings for  $\Delta C3$  are significantly less than for  $\Delta C1$ , ( $\Delta C3$ ,  $\nu_1$  splitting  $\sim 4,700 \text{ cm.}^{-1}$ ;  $\Delta C1$ , ( $T > 180^\circ\text{K}$ ),  $\sim 7,200 \text{ cm.}^{-1}$ ).

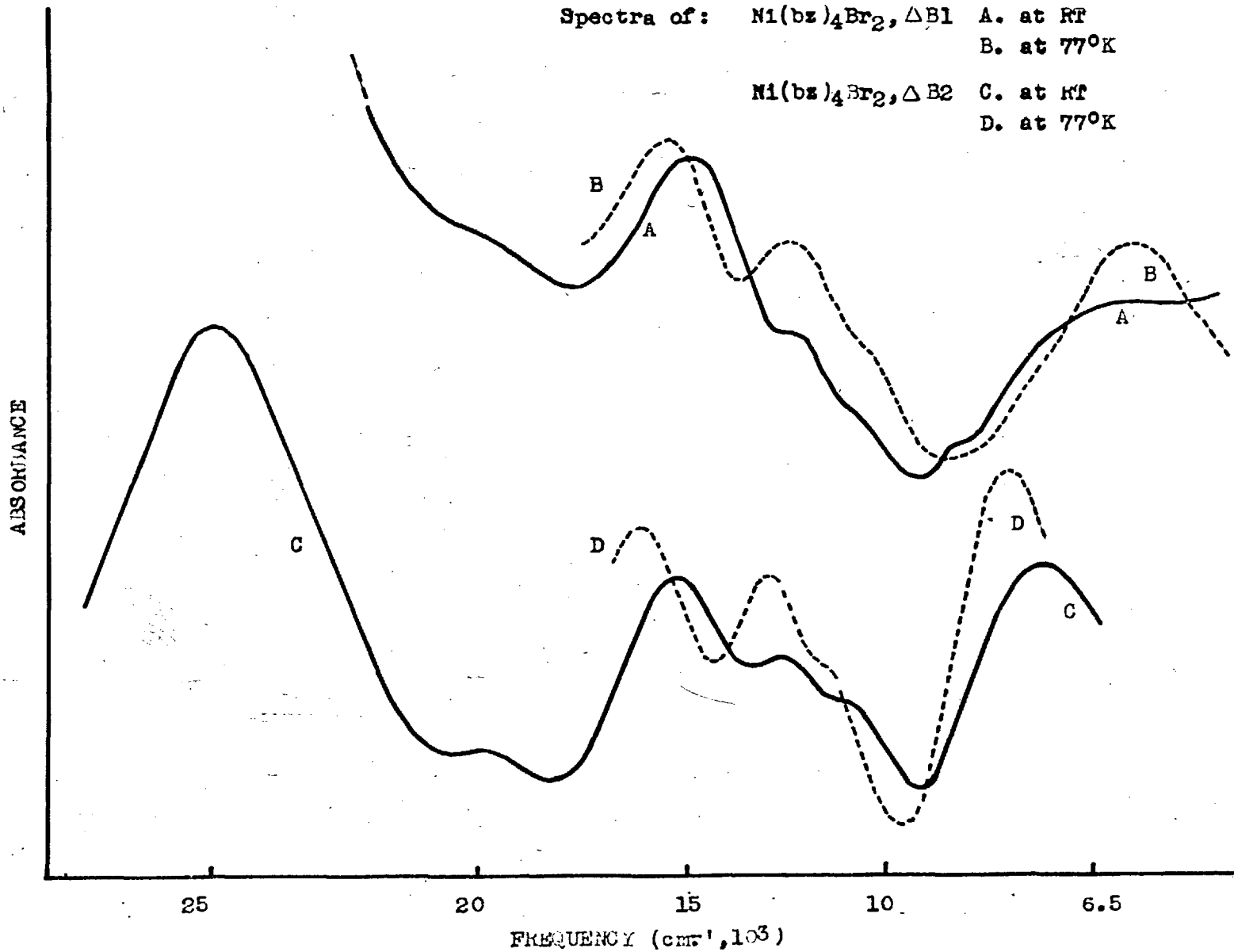
Turning next to the desolvated bromide complexes, and  $\Delta B1$  (see Fig. III.1). The various samples of  $\Delta B1$ , gave electronic spectra which were in general very similar. The common features will be considered first, then any differences. (The samples of  $\Delta B1$  were all prepared by the same method, and differentiated by their magnetic properties, as discussed in the next section).

The spectra show large splittings of  $\nu_1$  and  $\nu_2$  (Fig. III.6) as were seen for GC and  $\Delta C1$ ; and considerations of band assignments, and average band energies may be made as above. At  $77^\circ\text{K}$ , a single band is resolved on the low energy side of the main component of  $\nu_2$ , and the spectrum is very similar to that for GC at  $77^\circ\text{K}$  (c.f. Figs. III.6 and III.4). It may thus be considered that the band at  $12,600 \text{ cm.}^{-1}$  again contains the orbital singlet components of both  $\nu_1$  and  $\nu_2$ .

The spectrum of  $\Delta B1, Y$  shows a shoulder ( $\sim 8,000 \text{ cm.}^{-1}$ ) on the high energy side of the main ( $E_g$ ) component of  $\nu_1$ . This band seems rather too strong for a spin-forbidden

Fig. III.6

Spectra of:  $\text{Ni}(\text{bz})_4\text{Br}_2, \Delta\text{B1}$  A. at RT  
B. at 77°K  
 $\text{Ni}(\text{bz})_4\text{Br}_2, \Delta\text{B2}$  C. at RT  
D. at 77°K



band, and it is likely that the band is due to  $\Delta B_2$ , the presence of which was indicated by the X-ray powder data (Table 3.2), the shoulder then arising from the  $E_g$  component of  $\nu_1$  for that complex, which is expected at  $8,400 \text{ cm}^{-1}$  (Table 3.3).

The spectrum of  $\Delta B_2$  (Fig. III.6) shows considerably smaller band splittings than were seen for  $\Delta B_1$  (splitting  $\nu_1$  for  $\Delta B_2$ ,  $\sim 3,700 \text{ cm}^{-1}$ , for  $\Delta B_1$ ,  $\sim 6,000 \text{ cm}^{-1}$ ). This difference then resembles that between the spectra of  $\Delta C_1$  and  $\Delta C_3$ , as given above. The band splitting parameters for  $\Delta B_2$  are similar to those for  $\text{Ni}(\text{pyridine})_4\text{Br}_2$ , as will be discussed in Chapter IV.

Thus summarising it would seem that  $\Delta C_3$  and  $\Delta B_2$  may give band splittings which are of the order of magnitude expected for a  $D_{4h}$  complex with four nitrogen donors and two halide ions.  $\Delta C_1$ ,  $\Delta C_2$ , and  $\Delta B_1$  show larger splittings, which, as there is no increase in the average field, indicates a weakening of the axial field from the halide ions.

The diamagnetic complexes  $\Delta B_3$ ,  $\text{Ni}(\text{benzimidazole})_4\text{Br}_2 \cdot 3\text{CHCl}_3$ , and  $\text{Ni}(\text{benzimidazole})_4\text{I}_2$ , give identical electronic spectra as might be expected if the in-plane field is the same for each compound. The main band at  $21,300 \text{ cm}^{-1}$  may be assigned as the transition  ${}^1A_g \rightarrow {}^1B_{3g}$ . It seems likely that the weak band seen



to lower energies may be attributed to a spin-forbidden transition, following the assignments given for similar bands in other planar complexes.<sup>2,70</sup>

Infrared Spectra

The infrared stretching frequencies for the C=O group in the acetone of the solvated complexes were examined to see if significant differences could be found between the various forms. The 3,000 - 4,000  $\text{cm}^{-1}$  region was also examined, this being the region where the N-H stretching frequency would be observed.

Table 3.4

<u>Compound</u>	4,000-3,050( $\text{cm}^{-1}$ )	C=O stretch <sup>ng</sup> Freq. ( $\text{cm}^{-1}$ )
Ni(bz) <sub>4</sub> Cl <sub>2</sub> ·2 Acetone		
BC	3,640(sp.w); 3380(m); (~3080(m.sh))	1699(sp.m.s)
GC	~3300(w.sh); 3115(m.br)	1706(" " )
OC	3100(" " )	1706(" " )
YC	~3130(sh)	1708(sp.m)
Ni(bz) <sub>4</sub> Br <sub>2</sub> ·2 Acetone		
BB	3450(w.br)~3,120(br)	1701(sp.m.s)
Ni(bz) <sub>4</sub> I <sub>2</sub> ·3 Acetone	3420(w.br); 3,120(br)	1697(sp.m.s)

In the gas phase the CO stretching frequency for acetone is seen at 1742  $\text{cm}^{-1}$ , and at 1718 in the liquid.

It was suggested on the basis of the electronic spectra that the acetone molecules might be coordinated in the blue solvated forms of the chloride and bromide complexes (BC, BB), and also, (for two of the acetones), in the solvated iodide complex, while being hydrogen bonded in the green solvated form of the chloride complex. The somewhat lower CO stretching frequencies for the former group of complexes could be consistent with this suggestion.

A further indication of possible differences in the modes of acetone bonding is seen in the spectrum in the NH stretching region. The blue solvated chloride complex (BC) shows a number of clear bands between 3050 and 3650  $\text{cm}^{-1}$ , while the green form (GC) gives rather undefined absorption at lower energies.

## Magnetic Properties

### Results

The magnetic susceptibilities of the 4:1 benzimidazole complexes were measured over a temperature range of 80 - 300°K. The Curie-Weiss law (see Chapter I) was obeyed over this range by certain of the compounds, however other of the compounds showed Curie-Weiss behaviour over only part of this range.

The room temperature susceptibilities, magnetic moments, and the  $\theta$  values, with the temperature range over which the  $\theta$  value holds, are given in Table 3.5. For those complexes where Curie-Weiss behaviour was not shown over the full range, the observed susceptibilities, at various temperatures, are given in Table 3.6. The general features of the magnetic properties of these complexes will be given below, and the anomalous magnetic behaviour discussed in the next section.

The two blue solvated complexes, BC and BB, are magnetically normal with room temperature magnetic moments of 3.15 and 3.10 B.M. respectively, and a  $\theta$  value of -8°. Small negative values of  $\theta$ ,  $\sim$ -10°,

Table 3.5  
Magnetic Data for the Acetone Solvates of  
Ni(BH)<sub>4</sub>X<sub>2</sub> (X= Cl,Br), and the Desolvation Products

<u>Compound</u>	$\chi_A \times 10^6 \frac{\text{c.g.s.u.}}{294^\circ\text{K}}$	$\mu_{\text{eff.}} \frac{\text{B.M.}}{294^\circ\text{K}}$	$\theta^\circ$	<u>holds over</u> <u>range <math>^\circ\text{K}</math></u>
Ni(BH) <sub>4</sub> Cl <sub>2</sub> (Ac) <sub>2</sub>				(c)
BC <sup>(b)</sup>	4180	3.15	-8	full range
GC	3940	3.06	-77	200-300
GC/M <sup>(d)</sup>	3810	3.00	-70	" "
OC	2330	2.35	-400	100-300
Ni(BH) <sub>4</sub> Br <sub>2</sub> (Ac) <sub>2</sub>				
BB	4040	3.10	-9	full range
Ni(BH) <sub>4</sub> Cl <sub>2</sub>				
△ CI, B	4220	3.17	-14	190-300
" CI, G	4210	3.17	-10	" "
R " CI, G <sup>(e)</sup>	4320	3.20	-20	" "
" CI, O	4260	3.18	-30	" "
" C2, B	4200	3.16	-42	190-300
			-105	80-110
" C3, B	4115	3.13	-15	full range
Ni(BH) <sub>4</sub> Br <sub>2</sub>				
△ BI, X	2770	2.56	--	χ indep. temp.
" BI, Y	3450	2.86	--	
" B2	4170	3.14	-16	full range

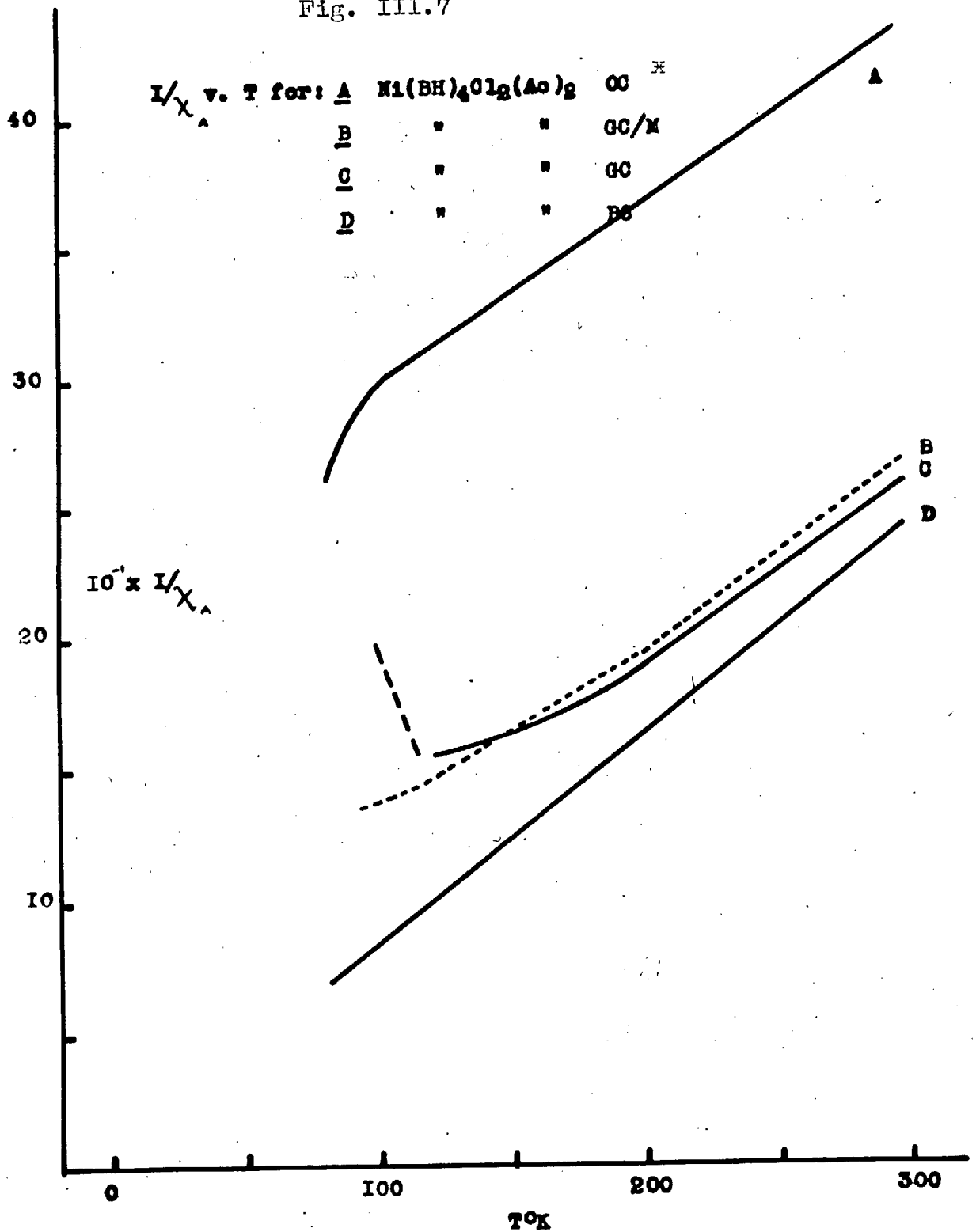
Notes

- (a) Calcd. from Curie Law
- (b) See p.      for symbols
- (c) i.e. Curie-Weiss Law behaviour over range of measurements, 80-300<sup>o</sup>K
- (d) GC after a prior cooling to 77<sup>o</sup>K, and warming to RT.
- (e) Reversed temperature measurement, i.e. starting at 77<sup>o</sup>K

are found for many six-coordinate nickel (II) complexes, and can not be taken as indicating any specific structural, or electronic, feature.<sup>11</sup>

The magnetic moment (294°K) of 3.05 B.M. for GC is lower than expected for six-coordinate nickel (II). This low moment can be correlated with the large negative  $\theta$  value, the origin of which is discussed below. When a freshly prepared sample of GC, made up of small well formed crystals, was used for the magnetic studies, the results followed the full line (for GC) in Fig. III.7. In the region of 100°K the susceptibility values showed a sudden drop, and this is marked with the dashed trace at the low temperature end of the full line, as the detailed behaviour of the susceptibility in this region is not known. On removing the Gouy tube after the magnetic measurements, the initial crystalline solid was found to be reduced to an amorphous powder, without loss of acetone (as indicated by analysis, see experimental data section in Chapter VI). This crystal collapse appears to be quite sudden, and has been observed on immersing a sample of GC in liquid nitrogen. It seems likely that the drop in susceptibility is associated with the crystal break up, although the connection is not at present clear.

Fig. III.7



BZ=3H

The relationship is however demonstrated by the fact that temperature range susceptibility measurements repeated on the amorphous powder show no drop at low temperature (GC/M in Fig. III.7). The magnetic behaviour of the crystalline and amorphous samples are somewhat different over the whole temperature range, though no differences in the X-ray powder patterns could be detected.

The complex OC has a room temperature moment of 2.35 B.M., which on the basis of the electronic spectrum, (as discussed in a preceding section), may be attributed to the presence of a diamagnetic species. The observed susceptibility indicates that the ratio of diamagnetic to paramagnetic species at room temperature is 0.75:1<sup>\*</sup>. An essentially Curie-Weiss plot is followed over the range 100 - 300<sup>o</sup>K with a  $\theta$  value of about -400<sup>o</sup>, the susceptibility showing a marked increase at temperatures below 100<sup>o</sup>K (Fig. III.7). Low temperature X-ray powder patterns, at present being obtained, should indicate whether this increase is due to structural changes. On some of the measurements it was found that the susceptibility in the region below 100<sup>o</sup>K showed time dependence. However experiments to investigate this were unable to detect

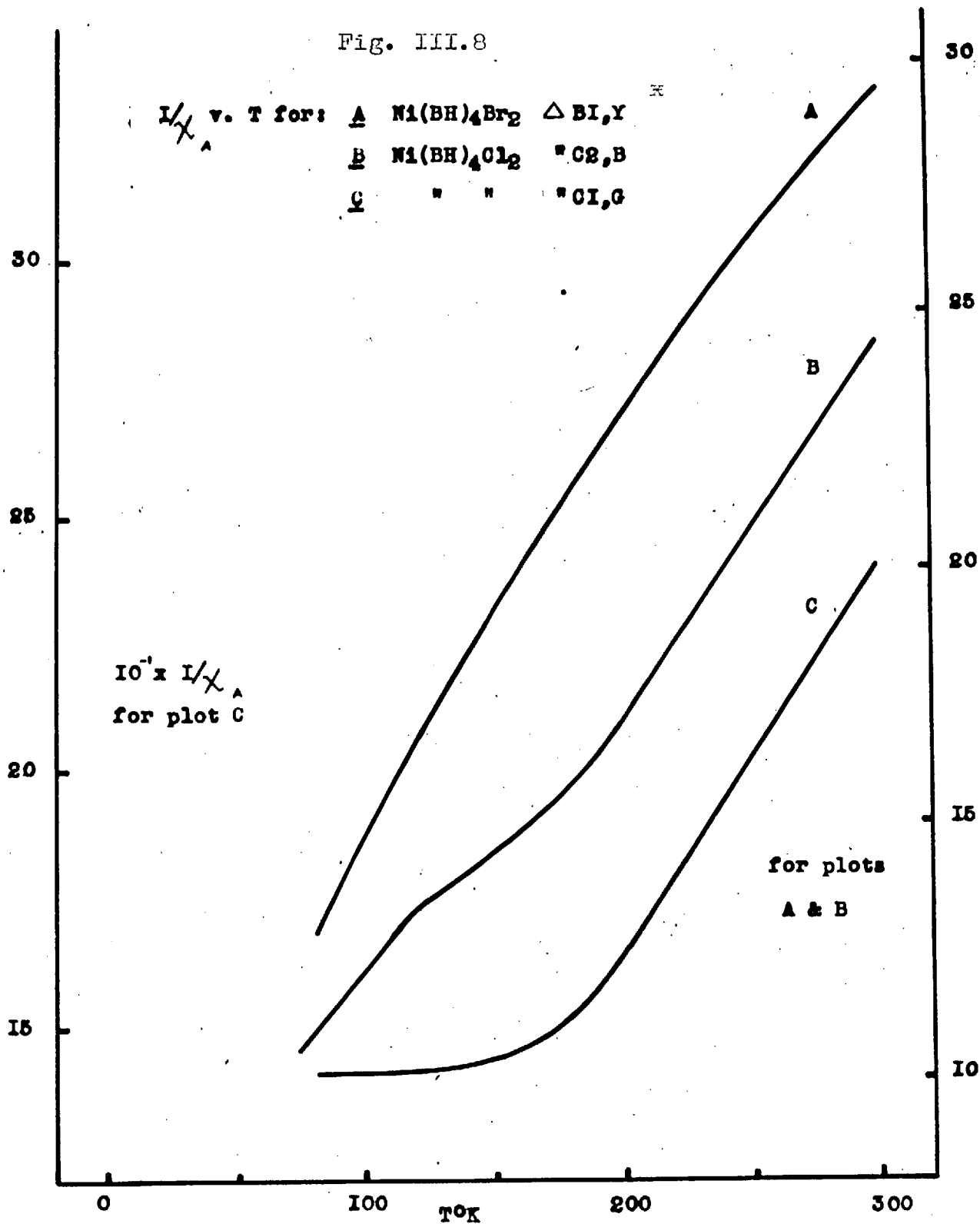
<sup>\*</sup> paramagnetic portion taken as GC



any consistent changes.

The samples of  $\Delta\text{Cl}$  ( $\Delta\text{Cl}$ , B;  $\Delta\text{Cl}$ , G;  $\Delta\text{Cl}$ , O) obtained from heating the three solvated chloride complexes (see Fig. III.1), were found to give basically similar magnetic properties, but to show some variations depending on the source. They gave normal room temperature moments of  $\sim 3.17$  B.M., and a  $\theta$  value for temperatures above  $190^\circ\text{K}$  of between  $-10^\circ$  to  $-30^\circ$ . Below  $190^\circ\text{K}$  the susceptibilities dropped off from the Curie-Weiss values, until the values were virtually independent of temperature (Fig. III.8). It was found that in the region below  $190^\circ\text{K}$ , the results showed some dependence on the rate of change of temperature. (General details on the timing of measurements may be found in Chapter VI, Physical Measurements). If the readings were taken at  $30^\circ$  intervals, (with one of the points being around  $180^\circ\text{K}$ ), then the discontinuity appeared to be sharper, and the value of the temperature independent susceptibility higher, than if measurements were taken at  $10^\circ$  intervals, at temperatures below  $190^\circ\text{K}$ . In some cases where there had been a more rapid lowering of temperature, on decreasing the temperatures towards  $77^\circ\text{K}$ , the susceptibilities appeared to drop back towards the

Fig. III.8



H

DZ=BH

values obtained using a slower cooling rate. The susceptibilities, at a given temperature, under these conditions, were not however time dependent. The effects arising with the various rates of cooling may be due to some form of supercooling.

Temperature range values of the susceptibility, using two different rates of temperature change, are given for  $\Delta\text{Cl, G}$  (Table 3.6), this sample showing the most marked variation with cooling rate. For  $\Delta\text{Cl, G}$  data is also given (Table 4.6) for measurements taken in the reverse direction, i.e. starting at  $77^\circ\text{K}$ . The results obtained were essentially the same as those found for decreasing temperatures.

The most plausible explanation of the magnetic behaviour seen in the complexes  $\Delta\text{Cl}$ , was that a phase change occurred between  $190 - 150^\circ\text{K}$ , and this was shown to be the case from room temperature, and low temperature X-ray powder patterns (Fig. III.2).

The susceptibility of the low temperature phase was essentially independent of temperature, and it was considered of interest to establish whether this behaviour was continued below liquid nitrogen temperatures. Professor B.R. Coles, of the Physics Dept., Imperial College, measured the susceptibility of  $\Delta\text{Cl, B}$  from liquid

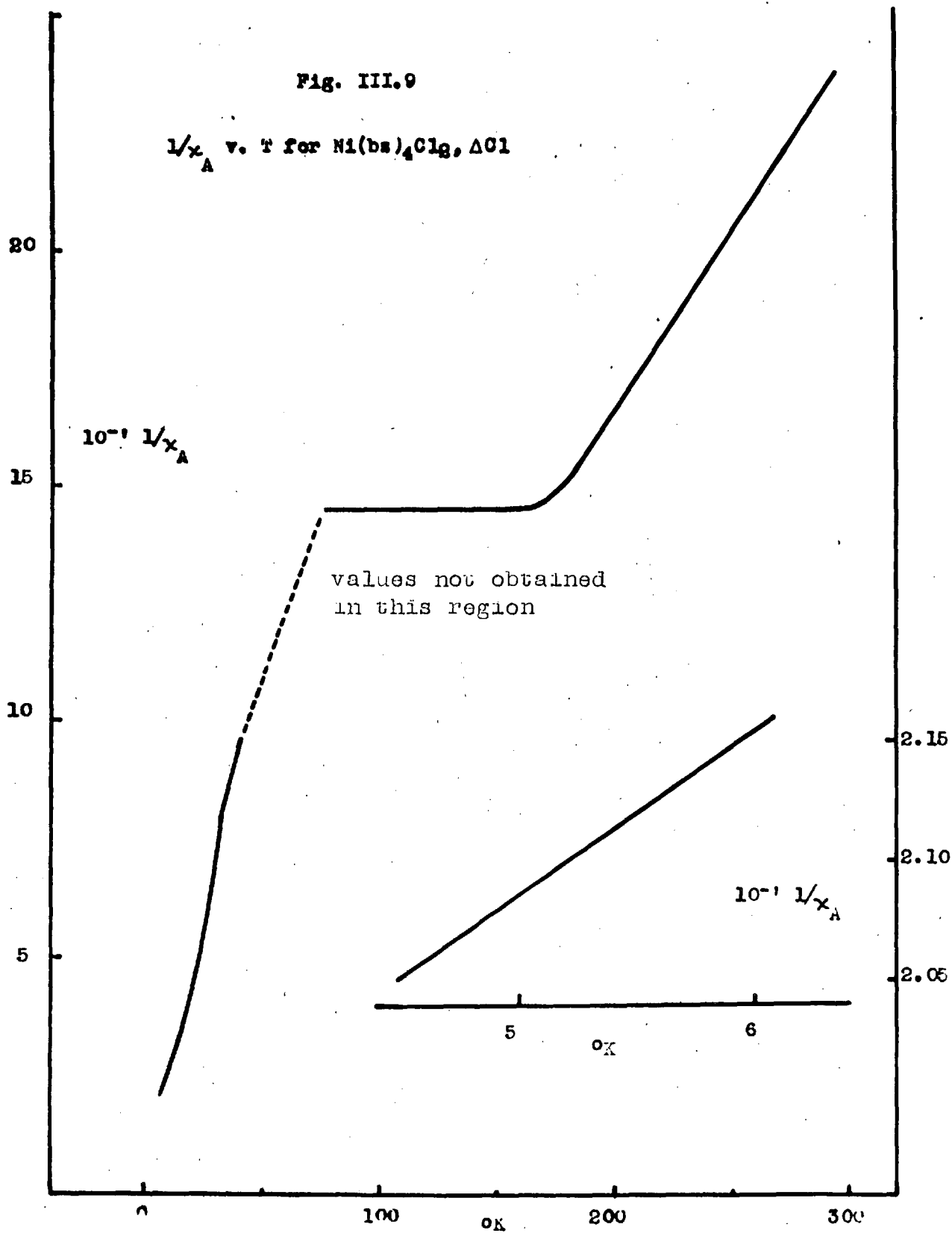
nitrogen ( $77^{\circ}\text{K}$ ), to liquid helium temperatures ( $4.2^{\circ}\text{K}$ ) Table 3.8 Fig. III.9.

A susceptibility independent of temperature was maintained for a few degrees below  $77^{\circ}\text{K}$ , then on further lowering of temperature the susceptibility showed a marked, and rapid increase, until at liquid helium temperatures the values were close to those that would have been seen if the Curie-Weiss behaviour, shown at temperatures above  $190^{\circ}\text{K}$ , had been maintained from  $190 - 4.2^{\circ}\text{K}$ . In the region of liquid helium temperatures the susceptibility approximates to a Curie-Weiss behaviour (Fig. III.9) with a  $\theta$  value similar to that shown by the compound at temperatures above  $190^{\circ}\text{K}$ . The susceptibility also shows a marked field dependence at these very low temperatures, (Table 3.8), a feature associated with coupling of ferromagnetic sign, and it is possible that the increase in susceptibility at temperatures below  $74^{\circ}\text{K}$  may be due to the onset of coupling of this type. Alternatively the increase might arise from a second phase change, but it has not been possible to obtain X-ray powder data at temperatures below that of liquid nitrogen.

The plot of  $1/\chi_A$  v.T for  $\Delta\text{C2}$  (Fig. III.8) shows

Fig. III.9

$1/x_A$  v.  $T$  for  $\text{Ni}(\text{bs})_4\text{Cl}_2, \Delta\text{Cl}$



two discontinuities such that for temperatures above  $190^{\circ}\text{K}$  Curie-Weiss behaviour is found, with a  $\theta$  of  $-42^{\circ}$ , while for temperatures below  $110^{\circ}\text{K}$ ,  $\theta$  is  $-105^{\circ}$ . In the light of the results from  $\Delta\text{C1}$  this behaviour may indicate two phase changes, and low temperature powder patterns are being obtained.

The complexes  $\Delta\text{C3}$  and  $\Delta\text{B2}$  have normal magnetic properties as expected for six-coordinate nickel (II), (Table 3.5).

The desolvated bromide complex  $\Delta\text{B1,X}$  gave a room temperature susceptibility of  $2770 \times 10^{-6}$  c.g.s.u. It was found that this susceptibility was independent of temperature in the range  $80-300^{\circ}\text{K}$ . There were fluctuations of  $\pm 80 \times 10^{-6}$  c.g.s.u., these being entirely random. There was no dependence of the susceptibility on field strength.

The complex  $\Delta\text{B1,Y}$  gave a room temperature susceptibility of  $3450 \times 10^{-6}$  c.g.s.u, somewhat larger than that for  $\Delta\text{B1,X}$ . The plot of  $1/\chi_A$  v.  $T$  was a curve (Fig. III.8). The X-ray powder pattern, at room temperature, for  $\Delta\text{B1,Y}$  suggested that the latter might be a mixture of  $\Delta\text{B,X}$  and  $\Delta\text{B2}$  (Table 3.2), and the magnetic properties can be interpreted in terms of such a mixture, (Table 3.7). While the agreement seems very

satisfactory, some recent preliminary results on the low temperature powder pattern for  $\Delta B_{l,Y}$  indicate that there may be some change in structure on cooling, in contrast to  $\Delta B_{l,X}$  which shows no alteration. If this is the case, then any such structural changes might be associated with the observed magnetic behaviour. This point is at present under investigation.

Table 3.6

Magnetic Susceptibility Data over a Temperature Range  
for the Complexes not showing Curie-Weiss behaviour.

<u>Ni(bz)<sub>4</sub>Cl<sub>2</sub>·2 Ac. GC. Crystalline</u>		<u>Ni(bz)<sub>4</sub>Cl<sub>2</sub>·2 Ac GC/M. amorphous*</u>		<u>Ni(bz)<sub>4</sub>Cl<sub>2</sub>·2 ac. GC</u>		<u>Ni(bz)<sub>4</sub>Cl<sub>2</sub> ΔCl,B</u>	
T°K	10 <sup>6</sup> χ <sub>A</sub> <sup>**</sup> (c.g.s.u)	T°K	10 <sup>6</sup> χ <sub>A</sub> (c.g.s.u)	T°K	10 <sup>6</sup> χ <sub>A</sub> (c.g.s.u)	T°K	10 <sup>6</sup> χ <sub>A</sub> (c.g.s.u)
293	3940	292.5	3820	294	2330	294	4220
271	4190	271	4070	271.5	2410	270	4600
243	4550	243	4430	241.5	2530	241.5	5090
212	5030	212	4910	213	2660	211	5810
181	5525	180	5440	182	2320	185	6500
149	6080	147	6100	148	2980	172.5	6790
121	6360	119	6730	121	3190	161	6920
93	4750	91	7270	98	3360	151	7010
		79	7450	78	3730	142	7010
						132	7010
						119	6900
						95	6910

\* after prior cooling to 77°K

\*\* molar susceptibilities corrected for ligand and metal ion diamagnetism



Table 3.6 (continued)

Ni(bz) <sub>4</sub> Cl <sub>2</sub>								
<u>ΔCl, G</u>								
(a)	T°K	10 <sup>6</sup> χ <sub>A</sub> (c.g.s.u)	(b)	T°K	10 <sup>6</sup> χ <sub>A</sub> (c.g.s.u)	(c)	T°K	10 <sup>6</sup> χ <sub>A</sub> (c.g.s.u)
	295	4210		298	4100		97	7120
	272	4540		273	4470		117	7140
	242	5070		243	4990		140	6960
	215	5750		210	5740		162	6750
	181	6660		182	6380		181	6540
	147	7440		170	6580		216	5780
	118	7400		158	6760		253	4990
	96	7400		150	6900		295	4320
				139	7030			
				129	7070			
				120	7100			
				107	7100			
				94	7100			
				81	7100			

Table 3.6 (continued)

Ni(bz) <sub>4</sub> Cl <sub>2</sub> <u>ΔCl, 0</u>		Ni(bz) <sub>4</sub> Cl <sub>2</sub> <u>ΔCl</u>		Ni(bz) <sub>4</sub> Br <sub>2</sub> <u>ΔBl, Y</u>	
T <sup>0</sup> K	10 <sup>6</sup> χ <sub>A</sub> (c.g.s.u)	T <sup>0</sup> K	10 <sup>6</sup> χ <sub>A</sub> (c.g.s.u)	T <sup>0</sup> K	10 <sup>6</sup> χ <sub>A</sub> (c.g.s.u)
297	4230	297	4170	293	3450
271	4590	271	4520	272	3620
243	5050	241	4990	242	3840
217	5580	213	5540	214	4140
199	6060	182	6340	181	4600
179	6500	162	6690	148	5230
166	6660	146	7020	119	6060
157	6750	130	7310	96	7000
146	6780	113	7620	82	7680
120	6750	96	8250		
96	6730	85	8760		
		78	9080		

Table 3.7

Observed and Calculated Susceptibilities for  
Ni(bz)<sub>4</sub>Br<sub>2</sub> ; ΔB<sub>1</sub>,Y

For calculated values

Ni(bz)<sub>4</sub>Br<sub>2</sub> ; ΔB<sub>1</sub>,X :  $\chi_A = 2770 \times 10^{-6}$  c.g.s.u. Indep. of temp.

Ni(bz)<sub>4</sub>Br<sub>2</sub> ; ΔB<sub>2</sub> :  $\chi_A = 4170$  " " " at 294°K  
 $\theta = -16^\circ$

Ratio ΔB<sub>2</sub> : ΔB<sub>1</sub>,X is 0.96 : 1

T°K	$\chi_A \times 10^6$ c.g.s.u.	
	<u>Observed</u>	<u>Calculated</u>
295	3450	3450
250	3790	3790
200	4330	4350
150	5200	5300
100	6860	6870

Table 3.8

Magnetic Susceptibility Data for Ni(benzimidazole)<sub>4</sub>Cl<sub>2</sub>;  
 $\Delta$ Cl,B from Liquid Nitrogen to Liquid Helium Temperatures<sup>\*</sup>

<u>T<sup>o</sup>K</u>	<u>10<sup>6</sup><math>\chi_M</math></u> <sup>(a)</sup> (c.g.s.u)	Field Strength dependence of magnetic susceptibility at 4.2 <sup>o</sup> K	
		<u>Field (Kgauss)</u>	<u>10<sup>6</sup><math>\chi_M</math></u> (c.g.s.u)
77	7000 <sup>(b)</sup>		
74	6900		
41	10,500		
36	11,440	2.3	58,425
32	12,780	3.4	52,580
28	14,970	4.6	49,570
23	18,250	5.5	47,680
6.6	46,135	6.3	45,425
5.9	46,530	6.8	43,820
5.3	47,555	7.3	43,760
5.0	47,900	7.9	43,210
4.8	48,250	8	42,875
4.5	48,690		

(a) 4.6 Kgauss field

(b) Found independent of field strength

<sup>\*</sup> Measured by Professor B.R. Coles of the Physics Dept.  
Imperial College.

Discussion of Magnetic Results.

It is apparent that the magnetic states arising in the present system are finely balanced. The different spin states in various samples of 4:1 complexes with the same anion presumably arise from probably small changes in structural characteristics, which in turn are critically dependent on the method of preparation. The anomalous magnetic behaviour seen in some of the compounds is likely to be caused by electron spin coupling.

Two mechanisms which may lead to lowering of magnetic moment are antiferromagnetism, and partial spin-pairing due to ligand field effects. The properties of systems in which there are antiferromagnetic interactions, and the mechanism of this interaction, are well covered in the literature<sup>11, 39, 49, 77, 78, 79</sup>. Ligand field spin pairing, and the conditions for spin state equilibria do not seem to be so adequately treated, and a brief outline of these topics is given below.

The spin pairing of electrons in octahedral fields of suitable strength is known, or theoretically possible, for all first row transition metal ions containing between four and seven d electrons. It arises

in these cases from the raising of the degeneracy of the five d orbitals into doublet ( $e_g$ ) and triplet ( $t_{2g}$ ) levels, such that for a certain value of the cubic field the splitting of the levels is greater than the spin pairing energy. In the present case for nickel (II), ( $d^8$ ), the pairing arises from tetragonal distortion of six-coordinate complexes. If the complex is of the type  $NiL_4X_2$ , then the z axis may be taken as unique. From a strong field picture the distortion along the z axis raises the degeneracy of the  $e_g$  level, made up of the  $d_{x^2-y^2}$  and  $d_{z^2}$  orbitals. For a suitable splitting the two electrons will be paired in the  $d_{z^2}$  orbital, this being stabilised with a weak axial field. For certain values of the splitting energy the singlet and triplet spin states might be separated by an energy of the order of thermal energies, when a thermal distribution between the spin states would arise.

Most of the work on this topic has been done using the crystal field approach. Both Maki<sup>9</sup> and Ballhausen<sup>80</sup> have shown that even with the axial ion, or dipole, at infinite distance the complex may be paramagnetic if the in-plane field is within certain values. Maki<sup>9</sup>,<sup>10</sup> has given energy level diagrams for singlet and triplet states as a function of in-plane dipoles, and bond

lengths. Such calculations show the dipole strengths necessary to produce a spin state degeneracy for a given value of the bond lengths. This would then describe the electronic spectra, as by the Franck-Condon principle transitions are expected without appreciable change in bond length. In the case of spin-state equilibria however the energy terms will be the total molecular state energies, for the molecules with equilibrium bond lengths in the two spin states.

For the transfer of an electron in  $O_h$  symmetry, from the  $e_g$  to the  $t_{2g}$  level, through the decreased occupancy of the antibonding orbitals, there is a reduction in  $\Delta$  of  $\sim 20\%$  <sup>81</sup>. For  $D_{4h}$  symmetry the removal of an electron from the  $x^2_{x^2-y^2}$  orbital into the  $d_{z^2}$  orbital, may lead to a reduction in the equilibrium ion-dipole distance in the plane, and an increase axially, in the absence of steric effects or rigid ring systems. Thus for the total energy a three dimensional potential energy surface is needed. For this present system the spin-pairing energies may be comparable to changes in bond energies etc., that occur on going from the singlet to the triplet state.

The alteration in the electrostatic crystal field

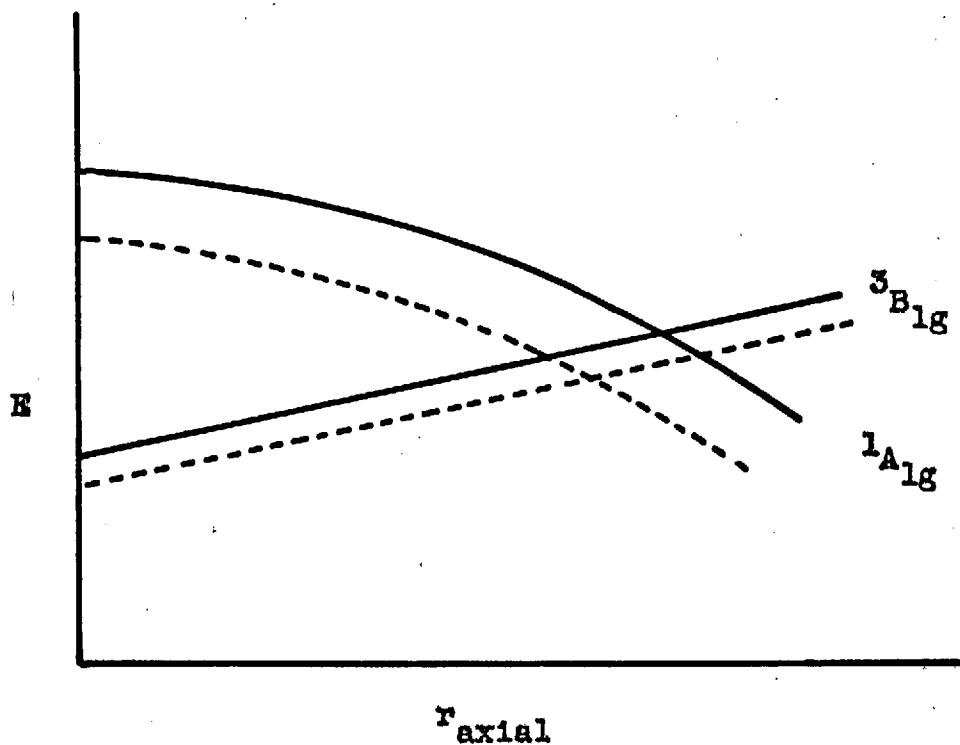
interactions on changing the ion-dipole distance may be found from the energy level diagrams of Maki<sup>9</sup>, <sup>10</sup>. The energies of the singlet and triplet ground states, as a function of axial ion-dipole distance, for fixed dipole strengths and in-plane ion-dipole distance, are shown by the full lines in Fig. III.10. On spin-pairing the action of an increased in-plane field will be to lower the energies of both the singlet and the triplet levels, the former more than the latter (dashed trace in Fig. III.10). It will be seen that if a degeneracy of the spin states is to occur, then it will be for a value of  $r_{\text{axial}}$ , for the paramagnetic state, that is considerably shorter than that at the cross over point of the full lines, the axial bond length being greater in the diamagnetic complex.

If on spin pairing there is a shortening of the in-plane ion-dipole distance then it may be considered that there will be an increase in bond energy.

For the case where there is little or no movement of the in-plane groups, then the electronic energy levels will follow the full lines in Fig. III.10. It might be supposed that there would be some increase in the axial ion-dipole distance leading to a stabilisation of the spin-paired state. If there is no



Fig. III.10



Nickel(II) electronic ground state energies in terms of the axial bond length, indicating the effect of a change in the in-plane bond lengths on going from the paramagnetic to the diamagnetic state

— paramagnetic  
----- diamagnetic

change in the in-plane bond lengths then the in-plane bond energies might remain similar, or show a decrease, on spin pairing.

Thus in principle the total potential energy curves for the molecules in the two spin states may be degenerate at the position of the equilibrium bond lengths, but this will require a fine balance of various factors. It is clear that in most 4:1 nickel (II) complexes the magnetic properties correspond to one spin state or the other, although apparently small changes may give rise to a change in the spin state, as evidenced by the Lifschitz compounds.<sup>82</sup>

Two examples have recently been given of spin-state equilibria in the solid state. One of these involved a rigid macrocycle providing the in-plane field<sup>83</sup> and the other dichlorotetrakis(N, N'-diethylthiourea) nickel (II)<sup>84</sup>.

The magnetic behaviour of a system in which there is an equilibrium between the singlet and triplet states will be considered.

If the total energy separation of the molecules in the two spin states is  $\Delta E_T$ , then there will be a Boltzman distribution between the states, the populations given by the usual expression:

$$N_T/N_S = 3 e^{-\Delta E_T/kT}$$

$N_T$  = number of molecules in triplet state

$N_S$  = " " " " singlet "

$\Delta E_T$  =  $E_T$  (triplet) -  $E_T$  (singlet)

A factor which could affect the change in distribution with temperature is the alteration in the partition coefficients of the vibration modes in the two states, and this might be corrected for. If the paramagnetic state is regarded as essentially obeying the Curie Law then the observed susceptibility  $\chi_A$  is given by.

$$\chi_A = \frac{2g^2\beta^2N}{3kT} [1 + \frac{1}{3} e^{\Delta E/kT}]^{-1} + N\alpha$$

$N\alpha$  is the correction for temperature independent paramagnetism, and the other symbols have the usual significance.

If the magnetic properties of the paramagnetic portion are known, and follow the Curie-Weiss Law then the coefficient of the bracket may be replaced by  $C/T-\theta$ . An equilibrium constant (K) may be written:

$$K = \frac{[T/3]}{[S]} \quad \begin{array}{l} T = \text{no. of molecules in triplet state} \\ S = \text{" " " " singlet "} \end{array}$$

K will be related to the thermodynamic parameters by :

$$- RT \ln K = \Delta E = \Delta H - T \Delta S$$

A plot of  $\ln K$  v.  $1/T$  would then give, if linear, values for  $\Delta H$  and  $\Delta S$ . If entropy (S) is given by<sup>87</sup>

$$S = k \ln P \quad P = \text{thermodynamic probability of state}$$

then for spin alone a gain of entropy of  $k \ln 3$  or  $\sim 0.77 \text{ cm}^{-1}/^{\circ}\text{C/mol}$  is expected for the change from the singlet to the triplet state.

The 4:1 benzimidazole complexes which show anomalous magnetic behaviour will be examined below in the light of antiferromagnetism, and the possibility of singlet-triplet equilibria.

The compound GC shows Curie-Weiss behaviour with  $\theta$  around  $-70^{\circ}$ . This may be indicative of an antiferromagnetic interaction, for the compound at temperatures well above the Néel point. The electronic spectrum indicated that there is a large tetragonal distortion, with a weak axial field. The halide ions would provide the most obvious path for any superexchange mechanism, and it is possible that only one halide ion is coordinated, and is bridging, the other halide ion considered as

ionic. This would provide  $180^\circ$  anion-metal-anion bonding which is expected to give coupling of antiferromagnetic sign for nickel (II)<sup>49</sup>. The curvature away from the Curie-Weiss plot at temperature below  $100^\circ\text{K}$  (Fig. III.7) would be consistent with the expected behaviour of an antiferromagnetic system as it approached a temperature region not much in excess of the Néel point.

Considering next the compound OC, the electronic spectrum indicates the presence of both paramagnetic and diamagnetic species, the former giving a spectrum as for GC, though the powder pattern data showed that OC was not a mechanical mixture of GC with a diamagnetic species (Table 3.1). If the ratio of paramagnetic to diamagnetic ions was static, and the paramagnetic ions had magnetic properties similar to GC, then a  $\theta$  value of around  $-70^\circ$  would be expected for OC. The observed  $\theta$  value of  $-400^\circ$  might indicate that there was extensive antiferromagnetic coupling between the paramagnetic ions, which obeyed the Curie-Weiss law with a  $\theta$  of  $-400^\circ$ . This seems unlikely however in that the probable presence of a diamagnetic species indicates that the paramagnetic portion has a room temperature magnetic moment greater than that

observed for OC, of 2.35 B.M., whereas a  $\theta$  value of  $-400^\circ$  would require the paramagnetic portion to have a room temperature moment of  $\sim 2.0$  B.M.

Two explanations of the observed behaviour might be considered. First that OC contains diamagnetic nickel ions together with paramagnetic ions in which the coupling is such that the susceptibility is almost independent of temperature, the room temperature susceptibility of the paramagnetic ions being close to that shown by magnetically dilute six-coordinate nickel (II). That such a paramagnetic species might exist is shown by the temperature independent susceptibility of  $\Delta\text{B1}$ , and the  $74\text{-}180^\circ\text{K}$  phase of  $\Delta\text{Cl}$ . The sudden increase in the susceptibility of OC at temperatures below  $100^\circ\text{K}$ , might then be similar to the marked increase seen for  $\Delta\text{Cl}$  at temperatures below  $74^\circ\text{K}$ . If the magnetic properties are due to this type of structure, then the lattice must be ordered to enable coupling to take place which might otherwise be interrupted by diamagnetic ions.

A second explanation might be that there is a thermal distribution between the spin states. The energy differences between the states that would be required to describe the observed behaviour, are given below,

but should not be taken as indicating that such an equilibrium exists, but merely as showing that a reasonable scheme can be derived. To explain the marked increase in susceptibility at  $\sim 100^\circ\text{K}$  a phase change would be invoked.

In order to obtain values for the energy separation of the spin states some knowledge of the magnetic properties of the paramagnetic species is required. The paramagnetic portion in OC gave a spectrum as for GC. However in GC if there is a thermal equilibrium between the spin states, and the distribution was random the next neighbour at any time might be in a spin singlet state, and hence coupling would not occur over any distance. Thus two sets of values were calculated, one assuming that the paramagnetic ions had  $\mu_{\text{eff.}}(295^\circ\text{K}) = 3.15 \text{ B.M.}$ ,  $\theta = -10^\circ$ ; the other taking  $\mu_{\text{eff.}}(295^\circ\text{K}) = 3.05 \text{ B.M.}$ ,  $\theta = -77^\circ$ , it being expected that an actual system would lie between these limits. The residual paramagnetism of the diamagnetic ions was taken as 250 c.g.s.u.

Equilibrium constants can be calculated at each temperature, as given above, then following the equation given, values of  $\Delta E$  may be found. Plots of

$\log K$  v.  $1/T$  gave curves for both sets of parameters, and from the tangents values of  $\Delta H$  and  $\Delta S$  were obtained. The results taking  $\mu_{\text{eff.}}(2.95^\circ\text{K}) = 3.2$  B.M.,  $\theta = -10^\circ$  are given in Table 3.9, similar results were found taking  $\mu_{\text{eff.}}(295^\circ\text{K}) = 3.05$  B.M.,  $\theta = -77^\circ$  with the values of  $\Delta H$  and  $\Delta S$  reduced by  $\sim 20\%$ .

Table 3.9

Parameters required by a Singlet-Triplet Equilibrium description of the Magnetic Properties of  $\text{Ni}(\text{bz})_4$

$\text{Cl}_2 \cdot 2$  Acetone, OC.

For the Paramagnetic ions:  $\mu_{\text{eff.}}(295^\circ\text{K}) = 3.15$  B.M.  $\theta = -10^\circ$   
 " " Diamagnetic "  $\chi_A = 250$  c.g.s.u (temp. Indep.)

T ( $^\circ\text{K}$ )	$\Delta E$ ( $\text{cm}^{-1}$ )	$\Delta H$ ( $\text{cm}^{-1}$ )	$-\Delta S$ ( $\text{cm}^{-1}/^\circ\text{C}$ )
295	205	208	$\sim 0$
250	205	168	0.148
200	197	126	0.355
150	177	95	0.546
100	145	83	0.65



It has not been possible to distinguish which of the two postulated mechanisms applies for OC, antiferromagnetism or a spin state equilibrium. In the second case, on cooling there is expected to be a change in the relative proportions of the two spin states. Thus the ratio of diamagnetic to paramagnetic ions is required to be 0.9:1 at 295°K and 2.75:1 at 100°K. If the proportion of diamagnetic species increased around three times, then a significant change in the intensity of the band at 21,300  $\text{cm}^{-1}$  would be expected. Some increase in intensity is observed (Fig. III.4) but to a lesser extent than would be anticipated for a singlet-triplet equilibrium, though the relative intensities of the electronic spectra for the paramagnetic and diamagnetic ions might alter with temperature apart from any change in the proportions of the species.

The compounds  $\Delta\text{Cl}$ , B, G and O, may be considered together. Their magnetic behaviour above 190°K is essentially as expected for magnetically dilute six-coordinate nickel (II). The phase of  $\Delta\text{Cl}$  between 70 and 190°K shows a susceptibility that is independent of temperature. A similar property is seen for  $\Delta\text{Bl}$  over the temperature range 77-300°K. As discussed in

the previous section,  $\Delta\text{Bl}$  and the low temperature phase of  $\Delta\text{Cl}$  show similarities in powder pattern, and it is considered likely that the structure, which gives rise to the interactions causing the observed magnetic behaviour, is comparable in both.

It was also noted that the electronic spectra of  $\Delta\text{Bl}$  and GC were similar, an antiferromagnetic coupling having been postulated in the latter. It would then be reasonable that a similar coupling could occur in  $\Delta\text{Bl}$ , and the low temperature phase of  $\Delta\text{Cl}$ . Thus it may be that there is a bridging halide in all three compounds, though there is no evidence for this. If this is the case then while the X-ray powder pattern data indicate that there is a phase change in  $\Delta\text{Cl}$  at  $\sim 190^\circ\text{K}$ , the electronic spectra shows that the axial distortion is large in both phases. Thus if a bridging halide is postulated for the low temperature phase of  $\Delta\text{Cl}$ , then this would also be the case for the phase above  $190^\circ\text{K}$ . This being so the latter phase would be expected to show antiferromagnetic coupling. However the electronic spectra show that the band splitting is greater, and the average ligand field weaker for  $\Delta\text{Cl}$  ( $> 190^\circ\text{K}$ ) compared with GC. Thus it might be suggested that the axial bonding is weakened in  $\Delta\text{Cl}$  ( $> 190^\circ\text{K}$ )

to a point where superexchange is diminished such that the compound approximates to a magnetically dilute system. The  $\Theta$  value of  $-30$  in  $\Delta\text{Cl}_2$  may be indicative of weak coupling.

Two other less likely possibilities for the origin of the temperature independent susceptibility may be mentioned. A singlet-triplet distribution of the type discussed above, is improbable here, as there is no diamagnetic band distinguishable in the room temperature, or  $77^\circ\text{K}$ , spectrum. Further the conditions under which an equilibrium of this type would have a susceptibility independent of temperature are very closely defined, and it would be surprising for it to occur in the complexes with two different anions.

A second possibility is that there is a temperature independent paramagnetism (T.I.P), arising from the second order Zeeman effect mixing a spin singlet ground state and a spin triplet state close above the ground state, (but separated by more than  $kT$ ). However the electronic spectra are clearly consistent with a spin triplet ground state.

T.I.P might also arise from the second order Zeeman effect operating on a spin triplet ground state, the spin degeneracy of which had been raised

by second order spin-orbit coupling with a split excited state. However while the splitting of the ground state is large for  $\Delta\text{Cl}$ ,  $\sim 70 \text{ cm}^{-1}$ , it is not sufficient to cause a temperature independent susceptibility term, even if the splitting placed the spin singlet level lowest.

Thus the observed behaviour is probably due to antiferromagnetism. The extension of a temperature independent susceptibility over  $\sim 100^\circ$  for the chloride complex  $\Delta\text{Cl}$ , and over at least  $200^\circ$  for the bromide complex  $\Delta\text{Br}$  is a feature that is not seen in antiferromagnetic systems such as the metal oxides and fluorides. The Néel point, which represents the temperature at which an antiferromagnet shows its maximum susceptibility, may become broad in some systems in which there are a large number of interacting centres, this however would not give a constant susceptibility over any significant range of temperatures.

Figgis has given<sup>11</sup>, the results of calculations, following the method of Van Vleck<sup>77</sup>, for the magnetic moments of systems of spins coupled in linear chains, when the interaction is with the nearest neighbours. The calculated results would approximately describe the present observed temperature independent susceptibility for the bromide  $\Delta\text{Br}$ , in the temperature

range 100 - 250°K, using a value of J (exchange integral) of  $\sim 80 \text{ cm}^{-1}$ , and chain lengths of 10 units. For the chloride  $\Delta\text{Cl}$ , an approximate fit may be obtained in the region 100 - 150°K using a J value about half that for the bromide.

CHAPTER IVStructural Factors in Nickel (II) ComplexesIntroduction

An outline of the background relating to the question of what should be considered as the main factors in determining the structures adopted by nickel (II) complexes, was given in the Introduction (p. 8 ). Steric factors,<sup>3,4</sup> differing amounts of  $\sigma$  and  $\pi$  bonding<sup>4a,6,7</sup>, and lattice energies<sup>4a,7</sup>, have been cited as possible causes of differences in structure between closely related compounds.

During the present studies complexes within each of the stereochemical classes, octahedral, tetrahedral, and planar, have been prepared, and these complexes will be reviewed to see if they throw any light on the structural factors. Steric and lattice effects will be considered in the general discussion at the end of this chapter, and spectral evidence for the nature of the bonding in the octahedral complexes reviewed first.

The splitting of electronic spectral bands, arising when the symmetry of a complex is lowered from cubic, has been the subject of some discussion in the literature.

As with the energy levels in cubic symmetry, the splittings on lowering symmetry may be considered from a crystal, or ligand field viewpoint, or by using a molecular orbital method. In the absence of appreciable covalency similar results should be obtained by both approaches, though the development and qualitative interpretation may not be so readily expressed in the two cases. The literature references to some of the main contributions are outlined below, together with such results as are pertinent to evaluating the splittings observed for the present complexes.

Chronologically discussion of band splittings in terms of crystal field and molecular orbital approximations have been developed in parallel; some authors using both as complementary methods.<sup>88</sup> Most of the discussion has related to the spectra of spin-paired cobalt (III), as the electronic spectra of numerous complexes of this type were available.<sup>89</sup> However the energy separations derived may be used for interpreting the splittings of the orbital triplet levels, arising from the free ion ground state term, for the spin-free  $d^2$ ,  $d^3$ ,  $d^7$  and  $d^8$  electron configurations, by suitable choice of sign.<sup>90</sup>

There was a number of papers during 1955-6 dealing with the energy levels in tetragonally distorted complexes<sup>91,92,93</sup>. Yamatera,<sup>88</sup> in a paper which also contains the basis of a molecular orbital approach, gives a crystal field calculation based on the use of the Slater free ion radial wave functions, which are now viewed as unsatisfactory<sup>94,95,96</sup>. In the earlier publications<sup>93</sup>, and in more recent contributions from Piper<sup>97,98</sup>, the radial parameters were considered as empirical.

The molecular orbital approach has been through the use of the angular overlap method<sup>99</sup>, and consideration of d orbital, and complex ion, symmetry. Contributions from Griffith and Orgel,<sup>100</sup> Yamatera<sup>88</sup>, McClure<sup>101</sup>, and Schäffer and Jorgensen<sup>90</sup>, have been of this type, and the results derived essentially equivalent.

For both the crystal field and the angular overlap approaches the problem is essentially that of finding the one-electron orbital energies, then taking suitable combinations of one-electron wave functions to give levels of the correct symmetry for the many electron system. This procedure will be outlined below to show the relation between the two sets of results.

In the crystal field approximation the field of the electron is expanded in a series of normalised spherical



harmonics, and the cubic field splitting parameter  $Dq$  is associated with the fourth-order term. On lowering the field symmetry from  $O_h$  to  $D_{4h}$ , a further term in the fourth-order, and a term in the second-order harmonic are required. These latter two terms may be associated with two radial parameters that have been termed  $Ds$  and  $Dt$ <sup>93</sup>. The perturbations of the one-electron orbital energies on going from the cubic field to  $D_{4h}$  symmetry are then given by linear combinations of these parameters<sup>102</sup>

$$E(b_{1g}) = (d_{x^2-y^2} | V_t | d_{x^2-y^2}) = 2Ds - Dt \quad [1]$$

$$E(a_{1g}) = (d_z^2 | V_t | d_z^2) = -2Ds - 6Dt$$

$$E(b_{2g}) = (d_{xy} | V_t | d_{xy}) = 2Ds - Dt$$

$$E(e_g) = (d_{xz} | V_t | d_{xz}) = (d_{yz} | V_t | d_{yz}) = -Ds + 4Dt$$

For nickel (II) in a cubic field, the free ion ground state term  ${}^3F$  gives rise to levels of  ${}^3A_{2g}$ ,  ${}^3T_{2g}$ , and  ${}^3T_{1g}$  symmetry (Fig.I.2). In  $D_{4h}$  symmetry the orbitally degenerate levels will split:

$${}^3T_{1g} \rightarrow {}^3A_{2g} + E_g$$

$${}^3T_{2g} \rightarrow {}^3B_{2g} + E_g$$

The following combinations of one-electron wave functions will then transform with the required symmetries (for two electron system):

$$\begin{aligned}
 {}^3A_{2g} & : |(xy)(x^2-y^2)| & [2] \\
 {}^3E & : -1/2 |(xz)(x^2-y^2)| + \frac{\sqrt{3}}{2} |(xz)(z^2)| \\
 & : -1/2 |(yz)(x^2-y^2)| - \frac{\sqrt{3}}{2} |(yz)(z^2)| \\
 {}^3B_{2g} & : |(xy)(z^2)| \\
 {}^3E & : -1/2 |(xz)(z^2)| - \frac{\sqrt{3}}{2} |(xz)(x^2-y^2)| \\
 & : -1/2 |(xz)(z^2)| + \frac{\sqrt{3}}{2} |(xz)(x^2-y^2)|
 \end{aligned}$$

The energy levels then follow as in equations 1

$$E({}^3A_{2g}) = 4Ds - 2Dt \quad [2a]$$

$$E({}^3E_g) = -2Ds - 3/4 Dt$$

$$E({}^3B_{2g}) = -7Dt$$

$$E({}^3E_g) = +7/4 Dt$$

Then for the splittings in nickel (II), the signs having been reversed for  $d^8$  (two position) system,\*

$$\Delta E({}^3T_{1g}, O_n) = E({}^3A_{2g}) - E({}^3E_g) = 5/4 Dt - 6Ds \quad [3]$$

$$\Delta E({}^3T_{2g}, O_h) = E({}^3B_{2g}) - E({}^3E_g) = 35/4 Dt$$

\*The off-diagonal terms are not included.

Thus the splitting of the first excited state depends only on the fourth-order term. Then following Piper:<sup>97,103</sup>

$$O_h : Dq = 1/6 \rho_4 = \Delta/10 \quad [4]$$

$$D_{4h} : Ds = 2/7 (\rho_2^{xy} - \rho_2^z) \quad [5]$$

$$Dt = 2/21 (\rho_4^{xy} - \rho_4^z)$$

Where  $\rho_n$  is a radial parameter, taken as empirical, associated with the splitting term for the nth order harmonic

$$\rho_n = e \cdot q \langle r^n / R^{n+1} \rangle \quad [6]$$

e = electronic charge

q = ligand charge

r = electronic radius

R = ligand-metal ion distance

Thus from equations 3, 4, and 5;  $E(^3T_{2g}) = 1/2(\Delta_{\text{plane}} - \Delta_{\text{axial}})$  [7]

It may be noted that in the crystal field treatment the tetragonal distortion is viewed as a perturbation of the cubic field, the in-plane field considered as remaining constant.

Thus from the splitting of the  $\nu_1$  and  $\nu_2$  bands, ( $\nu_1$  and  $\nu_2$  as defined on p.16 ), the values of  $D_s$  and  $D_t$  may be found (equations 3), and hence the splitting of the one electron atomic orbitals (equations 1)

In theory it would be possible to use the expression given above for the radial parameters, as a function of ion-dipole strengths and separations, to check whether the observed values for the splittings are consistent with a reasonable model for the complex. This may not however be satisfactory, as it is not easy to estimate likely values for the various parameters involved.<sup>104</sup> The radial parameters are thus best viewed as empirical.

Turning next to the angular overlap model. It is considered that overlap will occur for the metal ion  $t_{2g}$  orbitals with ligand orbitals of  $\pi$  symmetry, and for the  $e_g$  orbitals with ligand orbitals of  $\sigma$  symmetry. The energies of the one-electron orbitals are then evaluated in terms of the interaction between metal ion d orbitals and the total ligand orbital density, of the correct symmetry, along the axes of the d orbitals. The antibonding energy is taken to be approximately equal to the square of the overlap integral<sup>88,90,99,105</sup>

The relative contributions to the antibonding energy of a metal ion orbital, from the ligands along the various axes, may thus be evaluated. The results as given by Yamatera<sup>88</sup> and McClure<sup>101</sup> are shown in Fig.IV.1 (after McClure).

The one-electron orbital energies are thus known in terms of the  $\sigma$  and  $\pi$  antibonding contributions of the various ligands. The splittings of the  ${}^3T_{1g}$  and  ${}^3T_{2g}$  levels may then be found using the same combinations of one-electron atomic wave functions as given previously for the crystal field treatment.

Then for nickel (II) in  $D_{4h}$  symmetry:

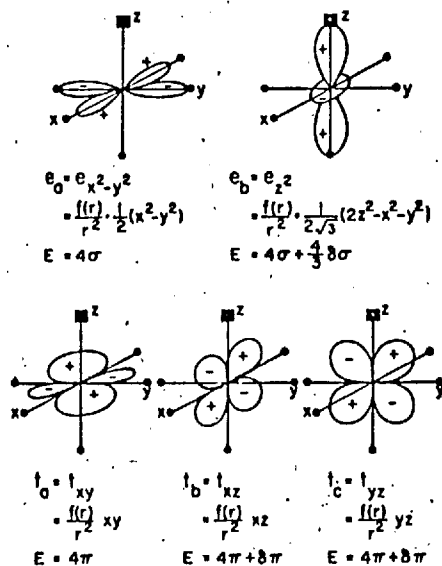
$$\Delta E({}^3T_{1g}, O_h) = E({}^3A_{2g}) - E({}^3E_g) = 2(\delta\pi + \delta\sigma) \quad [8]$$

$$\Delta E({}^3T_{2g}, O_h) = E({}^3B_{2g}) - E({}^3E_g) = 2(\delta\pi - \delta\sigma)$$

The off-diagonal elements are again ignored, though these have been given by Schäffer and Jorgensen<sup>90</sup>, and could be allowed for if the E state interaction is considered significant.

Thus the relation between the splitting of the one-electron energy levels, and the splitting of the spectral bands is the same for both the crystal field and the

Fig. IV.1



Interaction of the five d-orbitals with the ligands. The example given here is that of a monosubstituted octahedral complex. It can be seen that, due to their orientation, the various orbitals are perturbed by the substituent by different amounts. The formula for the distribution of the orbital in space and its energy in the array of ligands is given in each case.

(from ref. 101)

angular overlap approaches, the same expressions being used in both cases. The difference between the two methods lies in the interpretation of the origin of the splitting of the  $e_g$  and  $t_{2g}$  one-electron energy levels. In the one case this is seen as arising from a perturbation of the cubic field potential, and in the other as due to differences in  $\sigma$  and  $\pi$  bonding capacities of the ligands.

In general however the splitting will depend on changes in both electrostatic and antibonding energies. It will not be possible, on the basis of the observed splittings of the spectral bands for the present complexes, to decide which term is in fact dominant. Thus a useful parameter will be the calculated splitting energies of the one-electron orbitals, in that these are independent of the bond type, and depend only on the symmetry of the complex. Thus for a monosubstituted complex:

$$\delta e_g = E(a_{1g}) - E(b_{1g}) = -(4Ds + 5Dt) = \frac{4}{3} \delta\sigma \quad [9]$$

$$\delta t_{2g} = E(e_g) - E(b_{2g}) = -3Ds + 5Dt = \delta\pi$$

$\delta\sigma$  and  $\delta\pi$  can thus be related to the radial parameters  $\rho_n$  and to values of ion-dipole strengths and separations.<sup>90</sup>

Further relationships may be seen, such as by considering a complex  $MY_6$  going to  $MX_6$  then:<sup>103</sup>

$$\Delta_X - \Delta_Y = 4(\delta\sigma - \delta\pi) \quad [10]$$

∴

$$\text{Splitting of the } {}^3T_{2g} = 2(\delta\pi - \delta\sigma) = \frac{1}{2}(\Delta_Y - \Delta_X) = \frac{1}{2}\delta \Delta$$

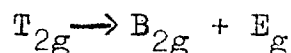
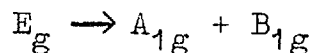
This being the same result as obtained above (Eqn.7) using the crystal field approximation. This relationship between  $\delta$ ,  $(\delta\sigma - \delta\pi)$ , and  $Dt$  may also be obtained by considering the change in the average ligand field for a monosubstituted complex, it being noted that the change in the average field is dependent only on  $Dt$ .

On a first inspection it might be considered that the ordering of the splitting of the  $t_{2g}$  level would be inverted on using the two approaches, thus for say  $M(NH_3)_4 Cl_2$ , as the halide ion is lower in the spectrochemical series than ammonia, the  $d_{xz}$  and  $d_{yz}$  might be anticipated as stabilised with respect to the  $d_{xy}$  orbital. While on a molecular orbital approach the halide ion might be viewed as a stronger  $\pi$  donor than ammonia, hence giving the reverse order of stability.<sup>103</sup>



However the more detailed crystal field theory shows that, (as given above), the sign of the splitting of the  $t_{2g}$  level depends on the difference in the values of  $D_s$  and  $D_t$ . Thus if  $D_s < \frac{5}{3} D_t$  the splitting order will be as for the molecular orbital approach.

Considering next the complexes with iron (II), the  $^5D$  free ion ground state will give rise to  $^5T_{2g}$  and  $^5E_g$  levels in a cubic field. In  $D_{4h}$  symmetry these levels will split:



These levels then have the same symmetries as the metal ion d orbitals in  $D_{4h}$ . The splittings of the electronic spectral bands will therefore be as for the splitting of the one-electron energy levels, i.e. for a monosubstituted complex:

$$\Delta E(^5E_g, O_h) = E(^5A_{1g} - ^5B_{1g}) = -(4D_s + 5D_t) = \frac{4}{3} \delta_\sigma [11]$$

$$\Delta E(^5T_{2g}, O_h) = E(^5E_g - ^5B_{2g}) = -3D_s + 5D_t = \delta_\pi$$

Thus the splitting of the spectral band should give a direct measure of the splitting of the  $e_g$  level. It is

then of interest to compare the splittings obtained for the iron (II) and nickel (II) analogs of the complexes. While the absolute bond strengths for the complexes with the two metal ions may differ somewhat, it might well be the case that the splittings of the one electron orbitals, in  $D_{4h}$  symmetry, would be similar. If this was so, and the values of  $\delta\sigma$  were approximately the same for the complexes with the two metals, then it would be reasonable to assume that the splitting of the ground state for the iron (II) complex, should be given by a value of  $\delta\pi$  that could be taken from the spectral data for the nickel (II) complex. Such calculated splittings might then be correlated with values of the ground state splitting obtained by independent methods, such as quadrupole splittings in Mössbauer spectra.

Certain of the electronic spectra are given at both room temperature and  $77^{\circ}\text{K}$ , and a brief note may be made at this point in connection with the changes expected on cooling. On lowering the temperature any vibrations will tend to occupy lower energy states. Thus owing to the anharmonicity of the vibrations, the mean bond lengths will shorten. As the value of

$Dq$  is proportional to  $R^{-5}$  for ionic ligands (equation 6), (or to  $R^{-6}$  for dipoles), it will be very sensitive to any changes in the separation of the ligand and metal ion.

For a metal ion in a cubic field, the effect of lowering the temperature on the energy ( $E$ ) of a given electronic level will then depend on the sign and magnitude of  $dE/dDq$ . For the spin-allowed bands for iron (II) and nickel (II), (Fig.I.2) this term is positive.

Considering the effect of change of temperature on the observed splittings of the spectral bands. This will depend on the relative energy distributions, and anharmonicities, of the vibrational modes for the axial and in-plane bonds. A generalisation as to the likely relative magnitudes of these factors is probably not possible.

From a crystal field viewpoint a shortening of the bond length will have a similar effect on both  $Dq$  and  $Dt$  as both depend on  $R^{-5}$ , while  $Ds$  is a function of  $R^{-3}$  (equations 5). Then in a situation where  $Dt$  is positive, and the relative shortening of the in-plane bond is more significant than that of the axial, an increase in  $Dt$ ,

and hence of the splitting of the  ${}^3T_{2g}$  level, is expected.  $D_s$  will also increase but probably to a lesser extent than  $D_t$ , however as the splitting of the  ${}^3T_{1g}$  level is given by  $5/4D_t - 6D_s$  the splitting will become more negative, if  $D_s$  is appreciable.

## Six Coordinate Iron (II) Complexes

### Preparation of Compounds

The compounds prepared were of the type  $\text{FeL}_2\text{X}_2$  (L = 3,5-dichloropyridine, 4-cyanopyridine, benzothiazole; X = Cl, Br.);  $\text{FeL}_4\text{X}_2$  (L = benzothiazole, X = Br)  $\text{Fe}(\text{benzimidazole})_4\text{Br}_2 \cdot 3 \text{ Acetone}$ , and  $\text{Fe}(\text{imidazole})_4\text{Cl}_2 \cdot 2\text{H}_2\text{O}$ . The electronic spectra are included of complexes prepared by others in this department. (See, D.M.L. Goodgame, M. Goodgame, M.A. Hitchman, and M.J. Weeks, ref. 106).

The method of preparing the 2:1 complexes given above was by addition of an ethanolic solution of the ligand, to a freshly reduced ethanolic solution of the ferrous halide. Details of the methods used to reduce oxidation, and of the preparation of the other ferrous complexes, may be found in the collected preparative data in Chapter VI.

### Electronic Spectra

It has been indicated<sup>106</sup> on the basis of isomorphism studies that  $\text{Fe}(\text{pyridine})_2\text{Cl}_2$  has the same trans-octahedral polymeric structure as is known to occur in  $\text{Co}(\text{pyridine})_2\text{Cl}_2$ <sup>107</sup>. The 2:1 complexes given above, (except  $\text{Fe}(\text{benzothiazole})_2\text{Br}_2$ ), give electronic spectra which are similar

to that given by  $\text{Fe}(\text{pyridine})_2\text{Cl}_2$  suggesting that they also have a trans-octahedral structure.

The spectra of some 4:1 and 2:1 complexes are shown in Fig . IV 2 .

The spectral data are given in Table 4.1, together with the values of  $\delta\sigma$ . The splitting of the one-electron  $e_g$  level is given by  $8/3 \delta\sigma$ , i.e. the same as the splitting of the spectral band (equations 9 and 11).

The signs given for  $\delta\sigma$  are based on the assumption that the halide ions might be expected to have a smaller  $\sigma$  antibonding effect than the nitrogen heterocyclic. Thus for the 4:1 complexes the  ${}^5B_{1g}$  is considered to be higher in energy than the  ${}^5A_{1g}$ , and vice versa for the 2:1 complexes.

As the splitting of only one electronic band is available from the spectra of the iron (II) complexes, values of  $D_s$  and  $D_t$  can not be found. However it may be seen that, for the 4:1 complexes, a positive value of  $D_t$  will be expected from equations 4 and 5, if the halide ion is lower in the spectrochemical series than the heterocycle. It is also anticipated that  $D_s$  will be positive<sup>103</sup>, thus, (from equation 9), leading to the same ordering for the splitting of the  $e_g$  and  $E_g$  levels as given above for  $\sigma$  bonding.

Table 4.1

Electronic Spectra of the Iron (II) Complexes

<u>Compound</u>	<u>Absorption Maxima (cm<sup>-1</sup>)<sup>*</sup></u>		<u><math>\delta\sigma</math>(cm<sup>-1</sup>)<sup>**</sup></u>
Fe(py) <sub>4</sub> Cl <sub>2</sub>	10,300	; ~8550(sh)	- 650
Fe(py) <sub>4</sub> Br <sub>2</sub>	10,650	; 7750	- 1100
" " " 77°K	11,500	; 8200	- 1250
Fe(isoqn) <sub>4</sub> Cl <sub>2</sub>	10,950	; ~9100(sh)	- 700
Fe(isoqn) <sub>4</sub> Br <sub>2</sub>	11,450	; 7800	- 1350
Fe(isoqn) <sub>4</sub> I <sub>2</sub>	11,750	; ~5900 <sup>(a)</sup>	- 2200
Fe(bth) <sub>4</sub> Br <sub>2</sub>	9400	; 6950	- 900
" " " 77°K	9900	; 8100	- 1050
Fe(im) <sub>4</sub> Cl <sub>2</sub> ·2H <sub>2</sub> O	12,450	; 8950	- 1300
Fe(bz) <sub>4</sub> Br <sub>2</sub> ·3Ac	11,600	; 6900	- 1750
Fe(py) <sub>2</sub> Cl <sub>2</sub>	9900	; ~5850 <sup>(a)</sup>	+ 1500
Fe(py) <sub>2</sub> Br <sub>2</sub>	9550	; ~5200 <sup>(a)</sup>	+ 1650
Fe(4-CNpy) <sub>2</sub> Cl <sub>2</sub>	9850	; 6250	+ 1350
Fe(4-CNpy) <sub>2</sub> Br <sub>2</sub>	9780	; ~5850 <sup>(a)</sup>	+ 1450
Fe(3,5-diClpy) <sub>2</sub> Cl <sub>2</sub>	9350	; 6300	+ 1150
Fe(3,5-diClpy) <sub>2</sub> Br <sub>2</sub>	9050	; 5870	+ 1200
" " " 77°K	9300	; 6300	+ 1125
Fe(bth) <sub>2</sub> Cl <sub>2</sub>	9050	; 6600	+ 900
Fe(bth) <sub>2</sub> Br <sub>2</sub>	~17,600(w.sh);	15,300(w)	
	~12,600(w.sh);	6330	

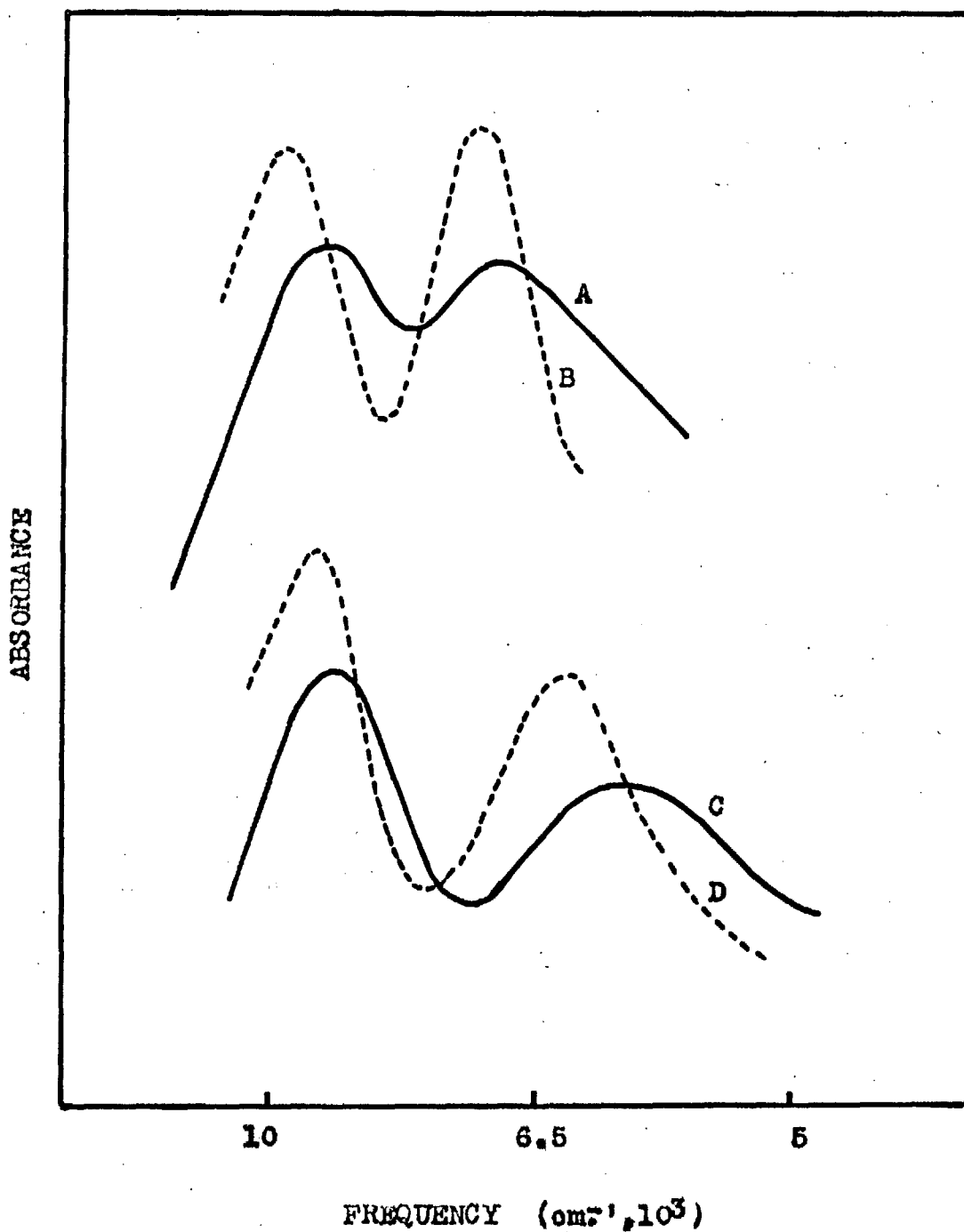
\* At room temperature unless otherwise stated

\*\* Splitting of e<sub>g</sub> level ( $\delta e_g$ ) is 8/3  $\delta\sigma$

(a) Approximate value due to presence of vibrational bands

Fig. IV.2

Spectra of:  $\text{Fe}(\text{benzothiazole})_4\text{Br}_2$  A. at RT  
B. at 77°K  
 $\text{Fe}(\text{3,5-dichloropyridine})_2\text{Br}_2$  C. at RT  
D. at 77°K





It may perhaps be noted, as discussed in the introduction, that  $\delta\sigma$ ,  $\delta\pi$  and  $D_s$ ,  $D_t$  are empirical parameters required by a covalent and electrostatic model respectively. The observed parameter is  $\delta e_g$ , the splitting of the one-electron level. Any changes in this latter parameter may be seen in terms of likely alterations in covalent or electrostatic bonding.

For the 4:1 complexes, the trends on varying the anion are established by the series  $\text{Fe}(\text{pyridine})_4\text{X}_2$ , ( $\text{X} = \text{Cl}, \text{Br}$ ) and  $\text{Fe}(\text{isoquinoline})_4\text{X}_2$ , ( $\text{X} = \text{Cl}, \text{Br}, \text{I}$ ). The  $\delta\sigma$  values are found to increase for the anions  $\text{Cl}^- < \text{Br}^- < \text{I}^-$ . This may be due either to decreasing  $\sigma$  bonding capacities for the halide ions, or to steric effects pushing the increasingly bulky anions out from the metal ion, or to both of these effects simultaneously.

This result might also be anticipated from the crystal field approach either on account of the iodide ion lying lower in the spectrochemical series than the chloride ion, or if the point charge for the iodide is considered further from the metal ion. It is then to be expected that  $D_s$  and  $D_t$  would both increase, from chloride to iodide, leading to a greater splitting of the  $e_g$  and  $E_g$  levels for the latter.

As might be expected for the band assignments given above, the position of the lower energy component ( ${}^5A_{1g}$ ) is most affected on changing the anion.

On the crystal field picture outlined in the introduction to this chapter, the bonding of the in-plane ligands is considered to remain unchanged on altering the axial field. Thus from equations 1 it will be seen that the energy for exciting an electron from the  $b_{2g}$  ( $d_{xy}$ ) level to the  $b_{1g}$  ( $d_{x^2-y^2}$ ) is not altered on going from  $O_h$  to  $D_{4h}$  symmetry. This is similarly found for the angular overlap approach, thus from Fig. IV.1 the energies of the  $d_{xy}$  and  $d_{x^2-y^2}$  orbitals will necessarily be dependent on the in-plane field.

Then for the present spectra, if the  $b_{2g}$  orbital lies lowest, the energy of the  ${}^5B_{1g}$  component will not alter if the in-plane field remains constant on altering the axial field. It will be seen in the next section that the values of  $\delta\sigma$  found for the iron (II) and nickel (II) complexes are generally in good agreement. It is thus not unlikely that the values of  $\delta\pi$  will also be similar for the complexes with the two metals. If so, then the value of  $\delta\pi$  will be positive, and the  $b_{2g}$  level will lie lowest.

From the data in Table 4.1, in the series  $\text{Fe}(\text{pyridine})_4\text{X}_2$  ( $\text{X} = \text{Cl}, \text{Br}$ ) and  $\text{Fe}(\text{isoquinoline})_4\text{X}_2$  ( $\text{X} = \text{Cl}, \text{Br}, \text{I}$ ), there is a progressive shift in the energy of the  ${}^5\text{B}_{1g}$  component to higher energies, as the anion is changed from chloride to iodide. This effect may be related to a greater  $\sigma$  donation by the in-plane ligands, which might be the result of a lowering of electron density in the  $d_{z^2}$  orbital, from the contribution of the halide ions, on going from chloride to iodide.

Some indication of the  $\sigma$  bonding capacity of a ligand, or on a crystal field model, of the perturbing effect of the  $\sigma$  lone pair, may be gained from the  $\text{p}K_a$  value. This must be treated with some caution however, as the  $\text{p}K_a$  value will be determined by changes in both enthalpy and entropy of protonation. A small  $\text{p}K_a$  could arise from an unfavourable entropy term which might not be reflected in the complexing bond. The  $\text{p}K_a$  values for a number of the ligands discussed in this chapter are collected in Table 4.6.

For the complex  $\text{Fe}(\text{benzothiazole})_4\text{Br}$  the  $\delta\sigma$  value (Table 4.1) is seen to be smaller than that for the pyridine complex, correlating with the considerably smaller  $\text{p}K_a$  value expected for the former ligand. The  $\text{p}K_a$  value for pyridine is somewhat less than that for

isoquinoline, and the energies of the  ${}^5B_{1g}$  component for the complexes with the former ligand come at lower energies than those with the latter. This may however be an indication of some relative  $\pi$  acceptance by the isoquinoline, lowering the energy of the  $b_{2g}$  level.

The values of  $\delta\sigma$  for the complexes  $Fe(\text{benzimidazole})_2\text{-Br}_2\cdot 3\text{Acetone}$  and  $Fe(\text{imidazole})_2\text{Cl}_2\cdot 2\text{H}_2\text{O}$ , will be discussed in the next section in conjunction with the nickel (II) analogs.

The 2:1 ferrous complexes give absolute values of  $\delta e_g$ , and  $\delta\sigma$ , which are larger than those for the corresponding 4:1 complexes. This might arise from the halide ions forming weaker  $\sigma$  bonds, (smaller effective electrostatic perturbation), when bridging, compared with a terminal position. Alternatively the heterocycle could approach closer to the metal ion, owing to smaller steric interactions in the 2:1 complexes. This latter possibility is shown not to be the case by the X-ray data on related compounds.

In the octahedral polymeric form of  $Co(\text{pyridine})_2\text{-Cl}_2$ <sup>107</sup>;  $Co\text{-Cl} = 2.49 \overset{\circ}{\text{A}}$ ,  $Co\text{-N} = 2.14 \overset{\circ}{\text{A}}$ , for  $Co(\text{pyridine})_4\text{-Cl}_2$ <sup>108</sup>;  $Co\text{-Cl} = 2.32 \overset{\circ}{\text{A}}$ ,  $Co\text{-N} = 1.99 \overset{\circ}{\text{A}}$ . Thus on going from the 4:1 to the 2:1 complex both metal-heterocycle, and metal-halide bond lengths increase by about the same

percentage. On a crystal field model, if all other factors remained constant, then from equation 6, for the bond length changes given above, the values of  $D_s$  and  $D_t$  are expected to be reduced on going from the 4:1 to the 2:1 complex. Thus the increased values of  $\delta e_g$  in the 2:1 complexes probably arise from weaker  $\sigma$  bonding, or electrostatic perturbation, by the bridging halide ions. This may be due to geometric considerations of lone pair overlap which might apply to both crystal field, and angular overlap models.

The variation in the values of  $\delta\sigma$  for the 2:1 complexes with the pyridine type ligands, containing substituents in the  $\beta$  and  $\gamma$  positions, the steric effects of which may thus be similar, are again seen to parallel the changes in  $pK_a$  values, (pyridine, 5.17; 4-cyanopyridine, 1.90; no value for the  $pK_a$  of 3,5-dichloropyridine has been found, but it is probably low as that for 3-chloropyridine is 2.84).

As discussed above the energy of the  ${}^5B_{1g}$  component may be taken as dependent on the in-plane field. For the 4:1 complexes above, with a given heterocyclic ligand, it was found that the in-plane field increased as the axial field weakened; and a similar trend is seen in the 2:1 complexes. Thus the energy of the  ${}^5B_{1g}$  component, for

the complexes with a given anion, is seen to show a progressive drop as the value of  $\delta\sigma$  increases. The explanation for this might be as suggested above for the 4:1 complexes.

A reflection of this apparent increase in the in-plane field is seen in the value of  $\Delta_{\text{average}}$ . For a  $D_{4h}$  complex the energy of the  $a_{1g}$  level is altered by  $8/3 \delta\sigma$ , thus the change in the average  $\Delta$  value ( $\Delta_{\text{av}}$ ) will be shifted by  $4/3 \delta\sigma$  if the  $b_{2g}$  level lies lowest. However for the present complexes the alteration in the axial field contribution to  $\Delta_{\text{av}}$  is offset by the change in the in-plane field. Thus for both  $\text{Fe}(\text{pyridine})_2\text{Cl}_2$  and  $\text{Fe}(\text{benzothiazole})_2\text{Cl}_2$ ,  $\Delta_{\text{av}} \sim 7,850 \text{ cm}^{-1}$ , while for the former complex  $\delta\sigma = 1,500 \text{ cm}^{-1}$ , and for the latter  $900 \text{ cm}^{-1}$ .

The amount of data available on the effects of cooling on the spectra of the iron (II) complexes is at present somewhat limited. However from the results in Table 4.1 it appears that on lowering the temperature to  $77^\circ\text{K}$ , for the 4:1 complexes the band splitting (and hence the splitting of the  $e_g$  level, and  $\delta\sigma$ ) increases by  $\sim 15\%$ . The energy shift for the  ${}^5B_{1g}$  level is greater than that for the  ${}^5A_{1g}$  component, suggesting that the increase in

$\delta e_g$  arises from a relative shortening of the in-plane bonds.

For the single result available for a 2:1 complex at low temperature, the  $\delta\sigma$  value is seen to decrease on cooling, this being due to the  ${}^5B_{1g}$  component again undergoing a greater shift to higher energies than the  ${}^5A_{1g}$  component.

## Six- Coordinate Nickel (II) Complexes

### Preparation of Compounds

Studies were made of the electronic spectra of various 2:1 and 4:1 six-coordinate nickel (II) complexes. The 1:1 six coordinate complexes while giving spectra potentially suitable for evaluation in terms of the splitting parameters, did not show any features not seen in the 2:1 complexes, and as the band splittings in the former were too small to be of quantitative use, the 1:1 complexes are not considered.

Compounds were prepared of the type  $NiL_2X_2$  (L = pyridine (Ch. I), benzothiazole (Ch. I), 3,5-dichloropyridine, X = Cl, Br),  $NiL_4X_2$  (L = 4-cyanopyridine, X = Cl, Br; L = benzothiazole, X = Br, L = benzimidazole (Ch. III) X = Cl, Br) and  $NiL_4X_2 \cdot 2S$  (L = benzimidazole, (Ch. III), X = Cl, Br, I; S = acetone; L = imidazole, X = Cl, S =  $H_2O$ ), also  $Ni(imidazole)_6(ClO_4)_2$ .

The method of preparation of the 2:1 and 4:1 complexes was essentially by mixing ethanolic solutions of ligand and nickel halide in stoichiometric proportions. Details may be found in the collected experimental data in Chapter VI.



The electronic spectra are included of complexes prepared by others in this department (see D.M.L. Goodgame, M. Goodgame, M.A. Hitchman and M.J. Weeks; ref. 106).

### Electronic Spectra

The usual designations of;  ${}^3A_{2g} \rightarrow {}^3T_{2g} = \nu_1$ ,  ${}^3A_{2g} \rightarrow {}^3T_{1g}({}^3F) = \nu_2$  and  ${}^3A_{2g} \rightarrow {}^3T_{1g}({}^3P) = \nu_3$ ; will be used for the transitions arising for nickel (II) in an octahedral field.

The 2:1 complexes will be considered first. The electronic spectra, at room temperature, for  $NiL_2X_2$  (L = pyridine, benzothiazole, X = Cl, Br) are given in Table 1.1. The spectra of certain of these latter complexes at 77°K, and the spectra of the remainder of the 2:1 complexes listed above, are given in Table 4.2.

Assignments for the spectrum of  $Ni(\text{pyridine})_2Cl_2$  were given in Chapter I, (p. 22), and the reflectance spectrum is shown in Fig. I.1. The further 2:1 complexes examined in this chapter gave similar spectra to that of  $Ni(\text{pyridine})_2Cl_2$ , and may be assigned likewise.

If the splitting of the  $\nu_1$  and  $\nu_2$  bands in  $D_{4h}$  symmetry are  $\Delta E(\nu_1)$  and  $\Delta E(\nu_2)$  respectively, with a positive splitting taken as that which places the

orbital singlet component at higher energy, then the band splittings on the crystal field model are given by equations 3:

$$\Delta E(\nu_2) = 5/4 Dt - 6 Ds$$

$$\Delta E(\nu_1) = 35/4 Dt$$

and for the angular overlap approach, from equations 8:

$$\Delta E(\nu_2) - \Delta E(\nu_1) = 4 \delta\sigma \quad [12]$$

$$\Delta E(\nu_2) + \Delta E(\nu_1) = 4 \delta\pi$$

Thus from the observed splittings of the  $\nu_1$  and  $\nu_2$  bands, values of the splitting parameters may be obtained.

To find these parameters however unambiguous assignments, and reasonably accurate values for the positions of the components are required. While the components of the  $\nu_1$  band are clearly resolved (Figs. I.1, and IV.3), any splitting of the  $\nu_2$  band gives rise to a shoulder on the low energy side of the main component of  $\nu_2$ . The spectra were examined at 77°K, but no significant improvement in the resolution of  $\nu_2$  was seen, (Fig. IV.3).

The shoulder on  $\nu_2$  might be taken as the  ${}^3A_{2g}$  component, there is however a spin-forbidden band expected in this region ( ${}^1E_g$  in  $O_h$  symmetry). While this is

Table 4.2Electronic Spectral Data for the Nickel (II) Complexes

<u>Compound</u>		<u>Absorption Maxima</u> ( $\text{cm}^{-1}$ ) <sup>*</sup>
Ni(py) <sub>2</sub> Cl <sub>2</sub> <sup>**</sup>	77°K	14,650; ~13,100(sh); 8700; 6400
Ni(bth) <sub>2</sub> Cl <sub>2</sub> <sup>**</sup>	77°K	14,100; ~13,00(sh); 8550; 7000
Ni(3,5-diClpy) <sub>2</sub> Cl <sub>2</sub>		23,500; ~18,900(sh); 13,600; ~12,450(sh); 8100; ~6600 (br.n.r)
Ni(3,5-diClpy) <sub>2</sub> Br <sub>2</sub>		22,600; ~19,250(sh); ~18,500 (sh); 13,300 ~11,500(sh); 8000; ~6500 (br.n.r)
" " "	77°K	13,700; ~12,700(sh); 8350; 6700
Ni(py) <sub>4</sub> Cl <sub>2</sub>		25,800; 16,050; ~14,500(sh); ~11,000(sh); 8700

<sup>\*</sup> At room temperature unless otherwise stated

For the majority of the complexes spectra are only available in the region 5000-18,000  $\text{cm}^{-1}$

<sup>\*\*</sup> Room temperature spectrum given in Chapter I, Table 1:1

Table 4.2 (continued)

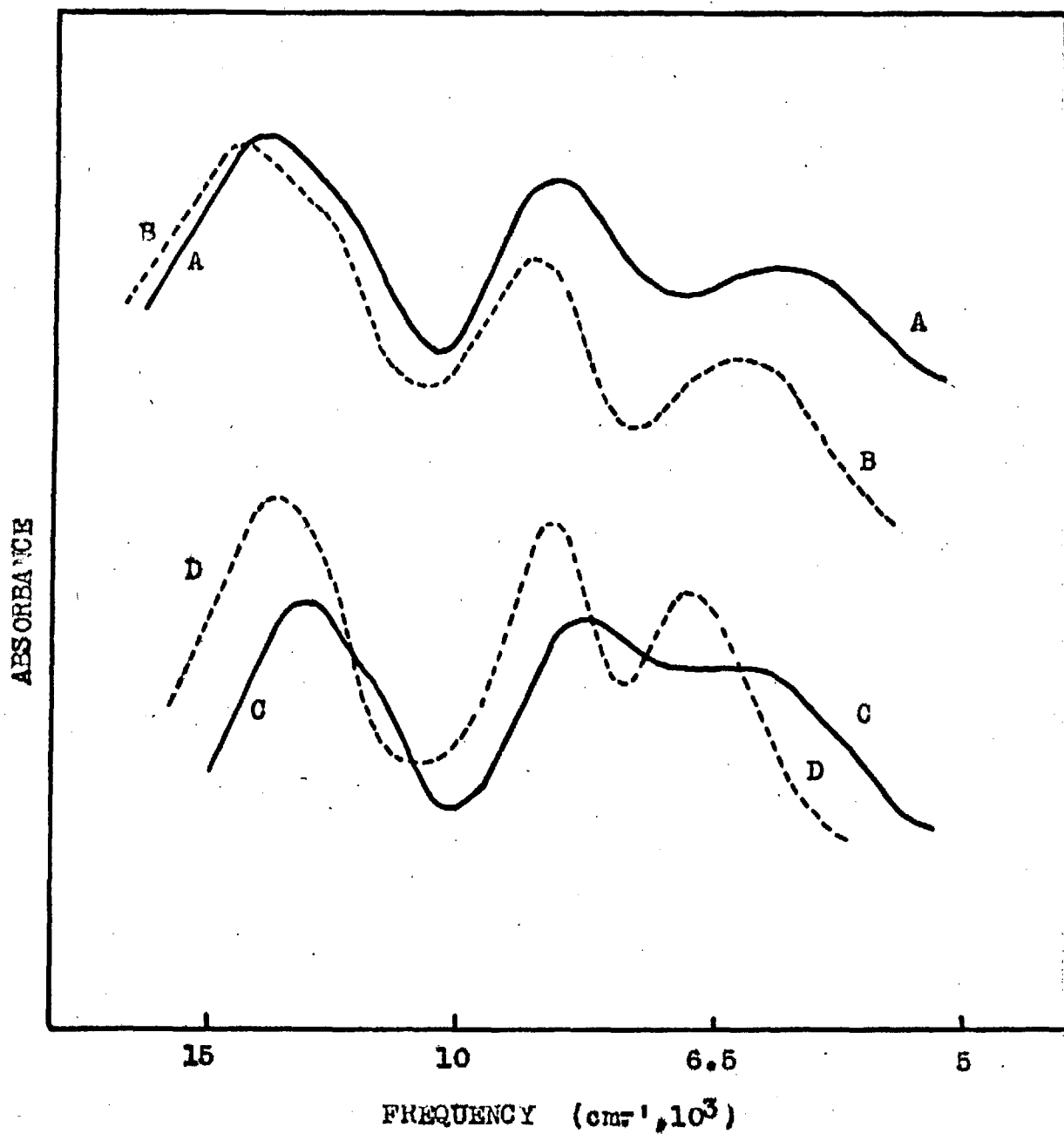
<u>Compound</u>		<u>Absorption Maxima (cm<sup>-1</sup>)</u>
Ni(py) <sub>4</sub> Cl <sub>2</sub>	77°K	16,800; ~15,300; 11,900; 9000
Ni(py) <sub>4</sub> Br <sub>2</sub>		25,200; 15,700; ~13,700(sh); 11,000; 8100
" " "	77°K	16,650; 14,300; 11,700; 8500
Ni(py) <sub>4</sub> I <sub>2</sub>		15,800; 12,300; ~11,000(sh); 7520
" " "	77°K	16,500; 12,500(br); ~11,000(sh); 7900; ~7100(sh)
Ni(isoqn) <sub>4</sub> Cl <sub>2</sub>		16,050; ~14,700(sh); ~11,000 (sh); 8770
" " "	77°K	16,900; ~15,000(sh); 12,300; 8,850
Ni(isoqn) <sub>4</sub> Br <sub>2</sub>		16,000; ~13,700(sh); ~11,200 (sh); 8100
" " "	77°K	16,900; 14,400; 12,350; 8400
Ni(isoqn) <sub>4</sub> I <sub>2</sub>		16,000; 12,700; ~11,500(sh); ~10,900(sh); 7500

Table 4.2 (continued)

<u>Compound</u>		<u>Absorption Maxima (cm.<sup>-1</sup>)</u>
Ni(isoqn) <sub>4</sub> I <sub>2</sub>	77°K	16,700; 13,100; ~12,600(s.sh); ~10,900(w.sh); 7900
Ni(4-CNpy) <sub>4</sub> Br <sub>2</sub>		15,400; ~11,900(w.sh); ~10,400(sh); 8550
" " "	77°K	16,150; ~11,800(n.r); ~10,700(n.r); 8700
Ni(4-CNpy) <sub>4</sub> I <sub>2</sub>		15,650; ~11,600(w); ~11,000(w); 8000
" " "	77°K	16,400; ~14,200(sh); 12,000; 8400
Ni(bth) <sub>4</sub> Br <sub>2</sub>		24,000; ~20,400(sh); 14,400; ~12,500(sh); ~9,500(sh); 7650
" " "	77°K	14,850; ~13,050(sh); 9650; 7,900
Ni(im) <sub>4</sub> Cl <sub>2</sub> ·2H <sub>2</sub> O		27,000; 21,500(w); 16,950; ~14,350(sh); 11,200; 9000
" " " "	77°K	18,000; 14,800; 12,000; 9200

Fig. IV.3

Spectra of:  $\text{Ni}(\text{pyridine})_2\text{Cl}_2$  A. at RT  
B. at 77°K  
 $\text{Ni}(\text{3,5-dichloropyridine})_2\text{Br}_2$   
C. at RT  
D. at 77°K



normally expected to be weak, it could gain intensity in proximity to the spin-allowed band of the same symmetry, if the distortion is not too large.

If in the first instance the shoulder is assigned to the  ${}^3A_{2g}$  component, the splitting of  $\nu_2$  is negative, with the splitting of  $\nu_1$  also negative. Using this assignment, and the band positions given in Table 1.1, then for  $\text{Ni}(\text{pyridine})_2\text{Cl}_2$ ,  $\delta\sigma = \sim + 200$ ,  $\delta\pi = \sim - 1000 \text{ cm}^{-1}$ , and for  $\text{Ni}(\text{pyridine})_2\text{Br}_2$ ,  $\delta\sigma = \sim + 50$ ,  $\delta\pi = \sim - 1100 \text{ cm}^{-1}$ .

It will be seen that these derived values of  $\delta\sigma$  are not at all similar to those found for the corresponding iron (II) complexes (Table 4.1). This might be the result of differences in the bond lengths for the iron (II) and nickel (II) complexes, such that the heterocycle was further from the metal ion in the latter, and also acted as a  $\pi$  acceptor. Such marked differences would however be surprising, and the lack of agreement of  $\delta\sigma$  values probably arises from other causes.

Two features may be seen that would affect the observed band splittings. Firstly there is the interaction between the two E components arising from the splitting of the  $\nu_1$  and  $\nu_2$  bands, which will depend on the energy separation of these components. From the ferrous complexes it appears that  $\delta\sigma$ , for a 2:1 complex, is likely to be large and

positive. The 4:1 nickel (II) complexes, examined below indicate that  $\delta\pi$  values are likely to be small, and for the 2:1 complexes  $\delta\pi$  will probably be negative (i.e. the halide ions are considered better  $\pi$  donors than the heterocycles). Thus, from equations 8, the splitting of  $\nu_1$  will place the E component to higher energy, and the splitting of  $\nu_2$  is expected to place the E component to lower energy. The separation of the E states, if there was no interaction, might therefore not be large. Then as a result of the interaction the separation of the two E components may be significantly increased. The splitting of the  $\nu_2$  band is expected to be smaller than that for the  $\nu_1$  band, (see equation 8,  $\delta\sigma$  and  $\delta\pi$  considered as having opposite signs), and thus it would not be surprising if the E state interaction in fact placed the E component of  $\nu_2$  at higher energy than the A component, or at least rendered the apparent splitting of  $\nu_2$  very small.

A second factor which may tend to affect the splitting of the  $\nu_2$  band is the mixing of the  ${}^3T_{1g}({}^3F)$  and  ${}^3T_{1g}({}^3P)$  levels, (for  $O_n$  symmetry). The splitting of the former level in  $D_{4h}$  symmetry is predicted to be the inverse of the splitting for the latter level,<sup>109</sup> and it has been suggested<sup>52</sup> that the interaction of these states may lead to the net splitting being small.



It is found that by assuming reasonable values for  $\delta\sigma$ ,  $\delta\pi$  and the interaction energy of the E states from  $\nu_1$  and  $\nu_2$ , the observed spectra may be rationalised. Owing to the interactions however, the spectra are not immediately suitable for the determination of empirical band splitting parameters.

In the absence of any E state interaction the splitting of the  $\nu_1$  band will be given by  $2(\delta\pi - \delta\sigma)$ , while the difference in the value of the average ligand field from the value of the field for the in-plane ligands, is given by  $4/3(\delta\sigma - \delta\pi)$ , from equations 10. Thus as the observed value of the splitting of the  $\nu_1$  band decreases, for the 2:1 complexes with a given anion, the value of the average ligand field should also decrease. This however is not found to be the case, and the value of the average energy of the  $\nu_1$  band shows little change e.g. for both  $\text{Ni}(\text{pyridine})_2\text{Cl}_2$  and  $\text{Ni}(\text{benzothiazole})_2\text{Cl}_2$  the average energy of  $\nu_1$  is  $\sim 7600 \text{ cm}^{-1}$ , while the splitting of  $\nu_1$  for the former complex is  $2400 \text{ cm}^{-1}$ , and for the latter  $\sim 1400 \text{ cm}^{-1}$ . This situation is thus analogous to that found for the iron (II) complexes, and it would appear that for the 2:1 nickel (II) complexes the in-plane field also effectively increases as the axial field decreases.

As for the ferrous complexes, the transition which corresponds to the exciting of an electron from the  $d_{xy}$  to the  $d_{x^2-y^2}$  orbital should have an energy which depends only on the value of the in-plane field. Such a transition would leave unpaired spin in the  $d_{xy}$  and  $d_{z^2}$  orbitals, and hence will correspond with the  ${}^3B_{2g}$  component (see equations 2). (This is consistent with the crystal field results. The wave function for the ground state ( ${}^3A_{2g}$  in  $O_h$  symmetry), on going to  $D_{4h}$  symmetry, will be given by  $|(x^2-y^2)(z^2)|$ , (the ground state being  ${}^3B_{1g}$  in  $D_{4h}$ ), the energy shift as for equations 1, is then  $-7 Dt$ . The shift of the  ${}^3B_{2g}$  level is also  $-7 Dt$ , from equations 2a, the net change then being zero.)

Thus the energy of the  ${}^3B_{2g}$  component of  $\nu_1$  should give an indication of the in-plane field. For the complexes  $NiL_2Cl_2$  the splitting of the  $\nu_1$  band varies for the various ligands in the order: pyridine > 3,5-dichloropyridine > benzothiazole. The energy of the  ${}^3B_{2g}$  component increase in the reverse order, thus suggesting that, as indicated by the average field values, there may be an increase of the in-plane field as the axial field decreases.

Turning next to the 4:1 complexes. Here the signs of  $\delta\sigma$  and  $\delta\pi$  will be the reverse of those for the 2:1

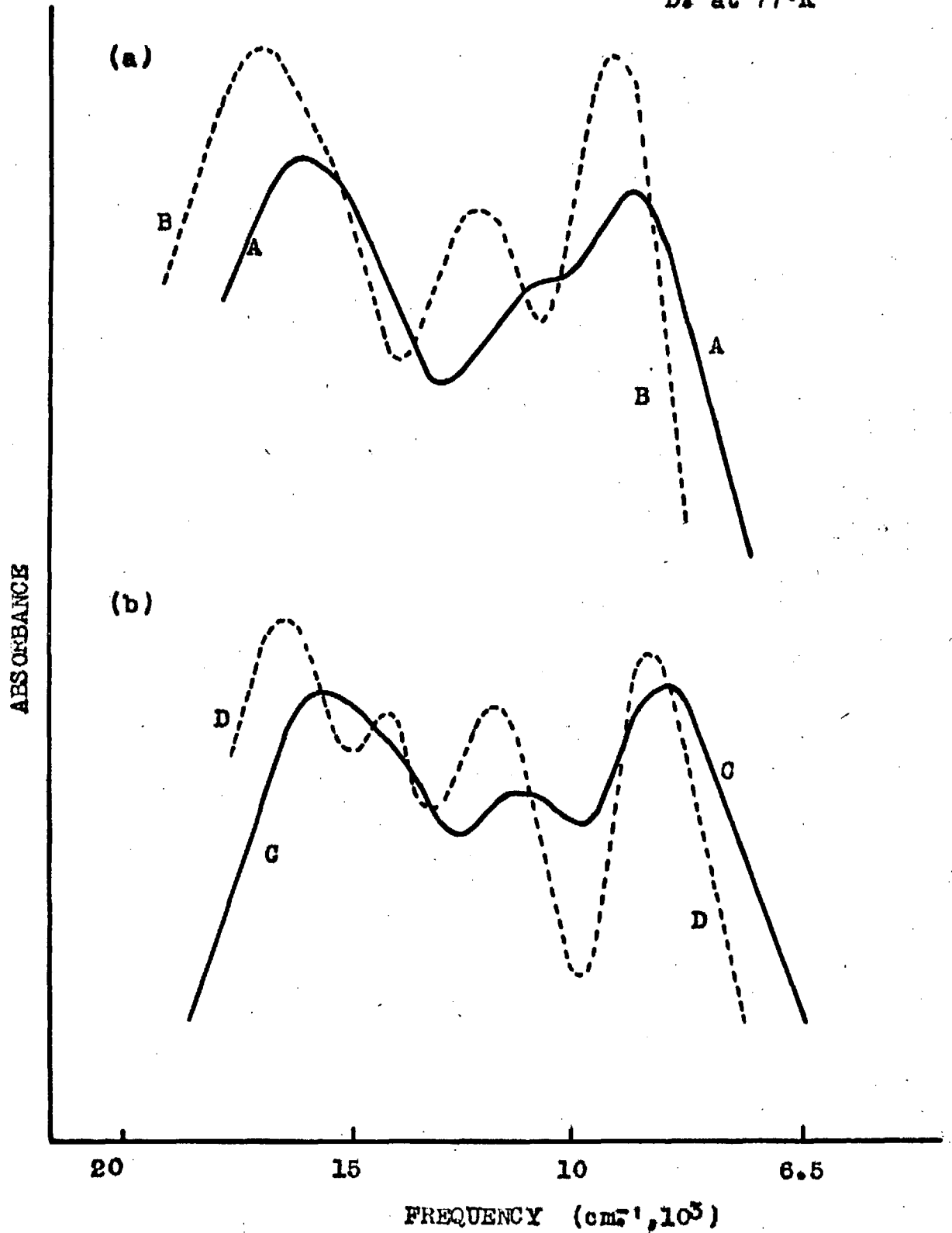
complexes, hence the signs of the splittings of the  $\nu_1$  and  $\nu_2$  bands are also reversed, placing the E components considerably further apart than in the 2:1 complexes, and hence leading to a marked reduction in any E state interaction.

Considering the complexes with the pyridine type ligands, a typical spectrum in the  $\nu_1$  and  $\nu_2$  regions may be considered as that of  $\text{Ni}(\text{pyridine})_4\text{Br}_2$  (Fig. IV.4.b), the band positions being markedly clarified at  $77^\circ\text{K}$ . A spin-forbidden band is again expected between  $\nu_1$  and  $\nu_2$ . This has the symmetry  $E_g$  in  $O_h$ , splitting to  $A_{1g} + B_{1g}$  in  $D_{4h}$ . It seems most unlikely that the two bands seen in the present spectrum, between the main components of  $\nu_1$  and  $\nu_2$ , would arise from this spin-forbidden transition. Firstly on account of their relative intensity, and secondly because if this were the case it would mean that the spin-allowed band splittings were small, which would not be consistent with the data from the ferrous complexes.

Thus for the  $77^\circ\text{K}$  spectrum the bands may be assigned  
 ${}^3B_{1g} \rightarrow {}^3E_g$  at  $8,500 \text{ cm}^{-1}$ ;  ${}^3B_{1g} \rightarrow {}^3B_{2g}$  at  $11,600$ ;  
 ${}^3B_{1g} \rightarrow {}^3A_{2g}$  at  $14,300$ ; and  ${}^3B_{1g} \rightarrow {}^3E_g$  at  $16,650 \text{ cm}^{-1}$   
 The position of the orbital singlet components in the room temperature spectrum is not so clear. This was also the

Fig. IV.4 (a) & (b)

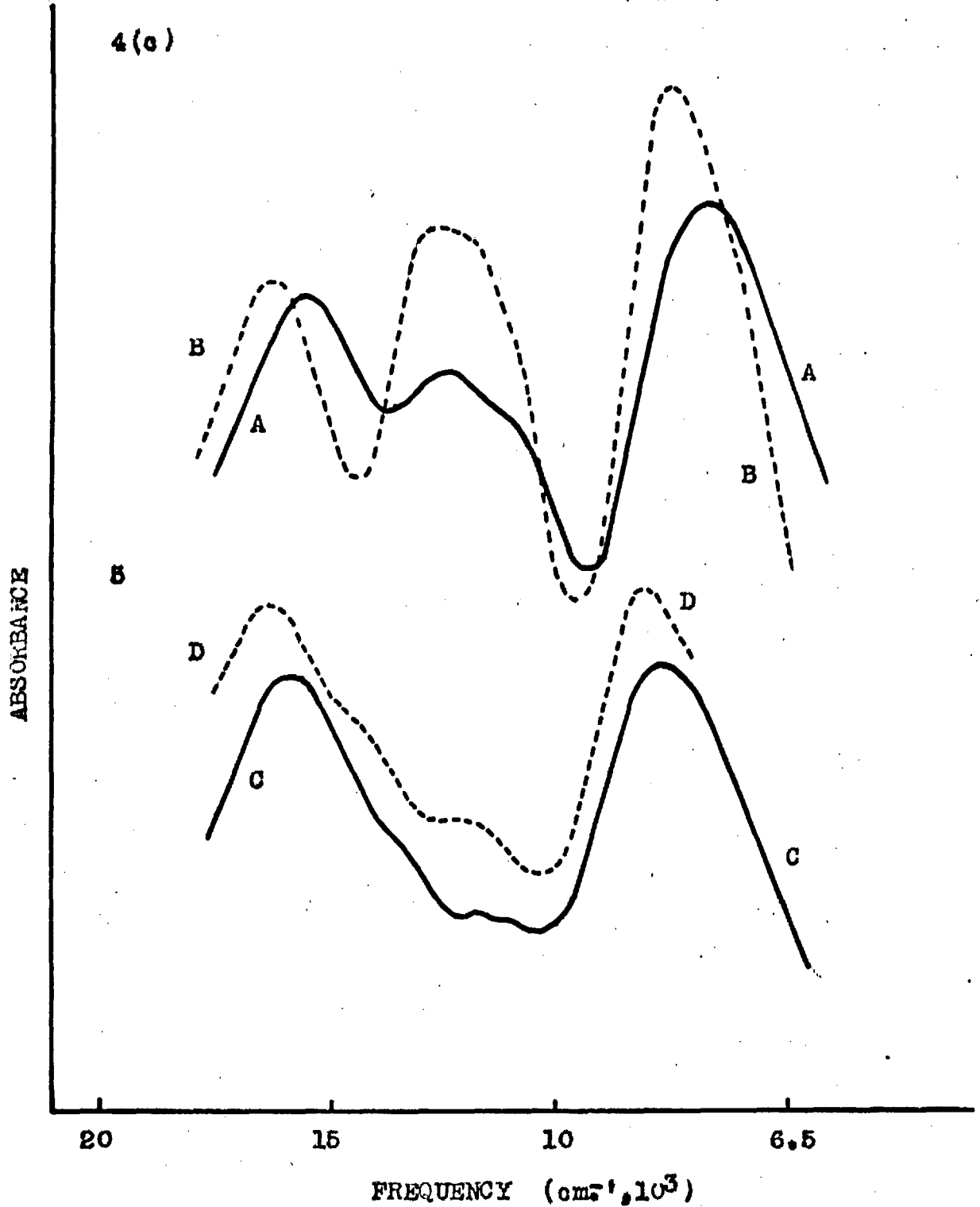
Spectra of:  $\text{Ni}(\text{pyridine})_4\text{Cl}_2$  A. at RT  
B. at 77°K  
 $\text{Ni}(\text{pyridine})_4\text{Br}_2$  C. at RT  
D. at 77°K



Figs. IV.4 (c) & IV.5

Spectra of:  $\text{Ni}(\text{pyridine})_4\text{I}_2$  A. at RT  
B. at 77°K

$\text{Ni}(\text{4-cyanopyridine})_4\text{I}_2$   
C. at RT  
D. at 77°K



case for the chloride complex, the position of the  ${}^3A_{2g}$  component of  $\nu_2$  being most uncertain in both room temperature, and  $77^\circ\text{K}$  spectra, (Fig. IV 4.a). For the complex  $\text{Ni}(\text{pyridine})_4\text{I}_2$  the two orbital singlet components appear to have overlapped, a single band being seen between the two stronger components (Fig. IV 4.c).

The electronic spectra of the isoquinoline complexes are very similar to those of the corresponding pyridine complexes.

For the 4:1 complexes with 4-cyanopyridine the band splittings are considerably smaller, such that the components of  $\nu_1$  are barely resolvable (Fig. IV.5). Estimates ~~have~~ been made for the positions of the  $\nu_1$  components, but these ~~must~~ be considered approximate. The splitting of  $\nu_2$  is assumed to be small, less than  $1000\text{ cm}^{-1}$ .

Values of the band splittings were found from the spectra of the complexes at room temperature and  $77^\circ\text{K}$ , then following equations 3 and 12 values of  $D_s$ ,  $D_t$  and  $\delta\sigma$ ,  $\delta\pi$  may be found, these are given in Table 4.3.

The values from the  $77^\circ\text{K}$  spectra are probably the more accurate ~~as~~ the bands are better resolved. While there appear to be systematic changes in the parameters on cooling from room temperature to  $77^\circ\text{K}$ , as will be

Table 4.3

Tetragonal Field Splitting Parameters<sup>x</sup>

<u>Compound</u>	<u>Ds</u>		<u>Dt</u>		<u>-δσ</u> (a)		<u>δπ</u> (b)	
	RT	77°K	RT	77°K	RT	77°K	RT	77°K
Ni(py) <sub>4</sub> Cl <sub>2</sub>	310	320	225	330	950	1,080	170	350
Ni(py) <sub>4</sub> Br <sub>2</sub>	400	460	320	360	1,200	1,350	200	200
Ni(py) <sub>4</sub> I <sub>2</sub>	670	780	420	530	1,800	2,200	50	155
Ni(isoqn) <sub>4</sub> Cl <sub>2</sub>	310	650	230	400	1,000	1,330	200	400
Ni(isoqn) <sub>4</sub> Br <sub>2</sub>	440	520	380	450	1,380	1,630	300	350
Ni(isoqn) <sub>4</sub> I <sub>2</sub>	640	710	450	530	1,800	2,100	170	250
Ni(4-CNpy) <sub>4</sub> Br <sub>2</sub>		230		270		850		300
Ni(4-CNpy) <sub>4</sub> I <sub>2</sub>		450		400		1,400		350
Ni(bth) <sub>4</sub> Br <sub>2</sub>		340		200		900		0
Ni(bz) <sub>4</sub> Cl <sub>2</sub> .2Ac [BC]	500	520	370	420	1,500	1,600	180	300

<sup>x</sup> Where values are not given, the positions of the components, in the electronic spectra, were too uncertain to allow calculation of parameters.

(a) Splitting of e<sub>g</sub> level is 8/3 δσ (see eqn. 9, p. 159)

(b) " " t<sub>2g</sub> " " 2 δπ " " " " "

discussed below, the trends on alteration of anion or heterocycle are the same for both sets of results.

Considering first the alterations on changing the anion. These are shown by the series  $\text{NiL}_4\text{X}_2$  (L = pyridine, isoquinoline, X = Cl, Br, I). The trends and numeric values of  $\delta\sigma$  (Table 4.3) are seen to follow those found for the ferrous analogs (Table 4.1), and may be interpreted as for the latter, i.e. that the  $\sigma$  donor capacity of the halide decreases, and the metal anion distance increases.

The values of  $\delta\pi$  for the nickel (II) complexes do not show such a clear trend, this being probably due to inaccuracy. The  $\delta\sigma$  values are large, arising from the addition of the two splitting terms, as these have different signs (see equations 12), whereas  $\delta\pi$  is from the small difference between the values of the band splittings, and hence more sensitive to the energies taken. The figures given for  $\delta\pi$  in the Table 4.3 represent reasonable values, however whether in fact the order of  $\delta\pi$  is  $\text{Cl} < \text{Br} > \text{I}$ ,  $\text{Cl} > \text{Br} > \text{I}$ , or another permutation, depends on the position taken for the orbital singlet component of  $\nu_2$  for the chloride complex, this being seen as a shoulder on the low energy side of the main component (Fig. IV.4a), and also on where the two overlapping orbital singlet components in the iodide complex spectrum, are positioned.



The choice of these band positions does not however affect the ordering of the  $\delta\sigma$  values.  $\delta\pi$  is clearly small, and may well decrease in the same order as  $\delta\sigma$ , from chloride to iodide.

It is found that the cubic field splitting parameter  $Dq$  associated with a particular ligand, shows only a small variation between the complexes with the various metal ions of a given transition group, if the oxidation states of the metal ions are the same. The similarity of  $\delta e_g$  and  $\delta\sigma$  for the complexes with iron (II) and nickel (II) suggests that the parameters  $Ds$  and  $Dt$  may also be comparable for the complexes with these metal ions (equations 9 and 11).  $Dt$  depends on the fourth order harmonic, as does  $Dq$  (equations 5), and hence a similarity for the former parameter might be expected.

The values of  $Ds$  and  $Dt$  are both positive, (Table 4.3), and of similar order of magnitude, as required for a large negative splitting of the  $e_g$  level, and a small splitting of the  $t_{2g}$  level (equations 9). Positive values for these parameters may not be unreasonable from a consideration of likely models for these complexes<sup>104</sup>. From equations 5 it is seen that if the halide ions are lower in the spectrochemical series than the nitrogen donors, then  $Dt$  will be positive. This is also reasonable

if the halide ion is considered as attracting electron density to the region of the fourfold axis, this being described by the localised fourth order, harmonic  $Dt$ <sup>93</sup>.

Concerning the relative values of  $D_s$  and  $D_t$ , it has been suggested that for tetragonally distorted complexes the second order term may be the most significant<sup>111</sup>. This is clearly not the case for the present complexes. If the origin of the tetragonal perturbation is considered to lie mainly in the difference of the strengths of the point charges in the plane and along the axis, then from equations 5 and 6 the ratio of  $D_t/D_s = 1/3 \bar{r}^2/\bar{R}^2$  where  $\bar{r}$  = average electronic radius, and  $\bar{R}$  = average ligand distance. Then any increasing significance of the fourth order term might be associated with increased delocalisation (covalence), or a shortening of the metal ligand distance. The implications of this type of approach for tetragonally distorted hexa-aquo complexes have been worked through by Van Vleck<sup>104</sup>. It may be noted however that, from equations 5 and 6, any increase in the axial bond lengths over that of the in-plane bond lengths will tend to increase the ratio  $D_t/D_s$ . In the previous section on the iron (II) complexes, the bond lengths in  $\text{Co}(\text{pyridine})_4\text{Cl}_2$  were given (p.172), indicating that the metal-halide bond lengths are significantly longer than those for the metal-nitrogen.

From equations 9 any  $\sigma$  bonding will be reflected in an increase in both  $D_s$  and  $D_t$  over the values for the purely electrostatic interaction, the effect being relatively greater for  $D_s$ . For  $\pi$  bonding  $D_t$  will increase in relation to  $D_s$ . As  $\delta\pi$  is small, the trends in the calculated values of  $\delta\sigma$  and  $D_s$ ,  $D_t$  will be the same.

The increase in the magnitudes of  $D_s$  and  $D_t$  may be seen in terms of the point charge for the iodide ion being further from the metal ion than the chloride ion.

It is of interest to compare the values of the splitting parameters for the present complexes, with those for related compounds. While there do not seem to be any studies on nickel (II) or iron (II) complexes, there have been a number of investigations on the spectra of spin-paired cobalt (III) complexes, as noted in the introduction to this chapter. On raising the oxidation state of a metal ion the  $\Delta$  value increases, and a figure of  $\sim 2$  has been suggested for the ratio of the  $\Delta$  values for cobalt(III) and nickel (II) complexes<sup>110</sup>. Thus as  $35/4 D_t = \frac{1}{2} (\Delta_{\text{plane}} - \Delta_{\text{axial}})$ , (from equations 3 and 7), the value of  $D_t$  may also be expected to double on going from nickel (II) to cobalt(III). Wentworth and Piper<sup>103</sup> found the following values for  $D_t$ : for  $\text{trans-Co(NH}_3)_4\text{X}_2$

and trans-Co(ethylenediamine)<sub>2</sub>X<sub>2</sub>, X = Cl, Dt ~ 600; X = Br, Dt ~ 700. These are then roughly twice the values found for the 4:1 nickel (II) complexes with these anions (Table 4.3).

For consideration of the changes in the splitting parameters, on altering the heterocyclic ligand, a comparison between pyridine and isoquinoline is best made for the bromide complexes, where fairly accurate bond energies are available for all components. The data (Table 4.3) indicates that isoquinoline may be a somewhat better  $\sigma$  donor, and  $\pi$  acceptor, than pyridine, the former result also being found for the ferrous complexes (p.171 ).

The values of  $\delta\sigma$  for the complexes with 4-cyanopyridine are considerably smaller than those for the corresponding complexes with pyridine, correlating with the smaller  $pK_a$  value for the former ligand (Table 4.6).

The effects that lowering of temperature may have on the band energies and band splittings, were discussed briefly in the introduction to this chapter (p. 162 ). The examination of any shifts on cooling for the present spectra may be rendered more difficult by the fact that there is extensive overlapping of the bands. Then changes in band shapes may also lead to shifts in apparent band maxima.

It is expected that the electronic spectral bands will be broader at room temperature compared with 77°K, as higher energy vibrational levels will be occupied, and hence greater variations in bond lengths will occur during bond vibrations. At higher temperatures there may also be sequences based on excited vibrational levels, leading to further broadening<sup>112</sup>.

There is a considerable reduction in band widths for the spectra of the present complexes on cooling to 77°K, (Fig. IV.4), and a number of features suggest that the observed shifts in the energies of the band maxima may be correlated with changes in the actual band energies.

The  ${}^3E_g$  component of  $\nu_1$  shows a definite shift to higher energies on cooling, this component being fairly well resolved from the  ${}^3B_{2g}$  component. An approximate value may then be taken for the shift in the average energy of  $\nu_1$ , and it is found that this shift is similar to that calculated for the average energy of the  $\nu_2$  band, using the observed shifts in the energies of the components of  $\nu_2$ .

It is further found that the shifts on cooling calculated from the observed spectra are in general agreement with those found for the ferrous complexes.

The changes in the apparent position of the bands, for those portions of the spectra which are extensively overlapped, are thus taken to be as for the changes in band energies.

Individual results must be treated with caution, in that for a number of cases it is most uncertain where the shoulders should be placed. However from a consideration of all the spectral data certain changes appeared consistently, thus on cooling from room temperature to 77°K:

Splitting of $\nu_1$	increases	10-30%
" " $\nu_2$	" "	" "
Average Energy of $\nu_1$	"	3-6 %
" " " $\nu_2$	"	" " "
	$\delta\sigma$	" 10-20%

For the  $\nu_1$  band the shift of  ${}^3B_{2g}$  component is in general greater than that for the  ${}^3E_g$  component. As the energy of the former component depends on the value of the in-plane field, this may indicate that the lowering of temperature produces a more effective shortening of the in-plane bonds relative to the axial, hence leading to the increase in band splitting,  $\delta e_g$ , and the splitting parameters (Table 4.3).

This result is also supported by the data from the ferrous complexes, where the shift of the band depending on the in-plane field, again appears to be more significant than that of the band for which the energy depends on both axial and in-plane fields.

From the data at present available, (Tables 4.1 and 4.3) it would appear that the fractional change in  $\delta e_g$  and  $\delta o$  for the 4:1 complexes, on cooling, is essentially the same for the iron (II) and nickel (II) complexes, suggesting similar changes in bond lengths for the complexes with the two metals.

If the energy of the  ${}^3B_{2g}$  component gives a value for the energy of the in-plane field, then in conjunction with the observed  $\nu_1$  band splitting, the equation 7 should give a figure for the axial field.

Applying this to the complexes  $NiL_4X_2$  (L = pyridine, isoquinoline), the results are obtained as given in Table 4.4.

The value of  $\Delta$  for the chloride ion, at room temperature, is very similar to that found from  $[NiCl_3]^-$  of  $6600\text{ cm}^{-1}$  (see Chapter I, Table 1.2), however the values are in general probably not quantitatively significant. There is a trend towards lower values for the axial field on cooling, which may be a reflection of greater steric interaction of the halide ions with the heterocycles,

if the metal-nitrogen bond shortens, causing the rings to rotate further out of the metal-nitrogen plane.

Table 4.4

<u>Complex Type</u>	<u>X</u>	<u><math>\Delta</math>, heterocycle (cm.<sup>-1</sup>)</u>		<u><math>\Delta</math>, halide (cm.<sup>-1</sup>)</u>	
		RT	77°K	RT	77°K
Ni(py) <sub>4</sub> X <sub>2</sub>	Cl	11,000	11,900	6500	6100
	Br	11,000	11,700	5200	5300
	I	11,200	12,400	3800	3400
Ni(isoqn) <sub>4</sub> X <sub>2</sub>	Cl	11,000	12,200	6500	5400
	Br	11,200	12,350	5000	4400
	I	11,500	12,500	3500	3200

For the complex Ni(pyridine)<sub>4</sub>Br<sub>2</sub>, at room temperature, the planes of the pyridine rings lie at angles of 45-55° to the M-N<sub>4</sub> plane<sup>113</sup>.

It was noted above that the  $\Delta$  values for iron (II) and nickel (II) complexes are frequently similar. As discussed in the section on the ferrous complexes, for the spectra of the latter, the energy of the <sup>5</sup>B<sub>1g</sub> component (the higher energy component of the split E<sub>g</sub> level for the 4:1 complexes) should give a value of  $\Delta$  for the in-plane field.



Comparison of the energies of the  ${}^5B_{1g}$  component (Table 4.1), and  $\Delta$  values from Table 4.4, for the analogous 4:1 complexes of the two metals with pyridine and isoquinoline, indicates that  $\Delta$  may be somewhat larger for the iron complexes, as is frequently found to be the case<sup>110</sup>.

For the complexes with both metals the same trend is seen towards larger in-plane  $\Delta$  values as the axial field decreases. If this is a result of increased bond strength in the plane it might be shown in the N-Metal vibrational frequencies.

However measurements have been made of the N-Ni stretching frequencies for  $Ni(pyridine)_4X_2$  ( $X = Cl, Br$ )<sup>71</sup>, and these were found to be essentially the same for the complexes with both anions. X-Ray structural determinations for these latter two complexes<sup>108,72</sup>, have indicated that the N-Ni bond lengths are also the same ( $2.00\overset{\circ}{\text{A}}$ ).

Thus these two results do not demonstrate any marked alteration in the in-plane bonding on going from the chloride to the bromide complex, though the modifications associated with an increase in  $\Delta$  of the order suggested by the electronic spectra, might not be reflected in observable changes in vibrational frequencies or bond lengths.

The value of  $\delta\sigma$  for  $\text{Ni}(\text{benzothiazole})_4\text{Br}_2$  (Table 4.3) is in good agreement with the value found for the ferrous analog (Table 4.1). The  $\delta\sigma$  is again considerably smaller than that for the pyridine complex consistent with the low  $\text{pk}_a$  value for benzothiazole (Table 4.6). The  $\delta\pi$  of zero may indicate some  $\pi$  donation by the heterocycle, or be due to the greater steric effect of the benzothiazole increasing the metal-anion distance.

For  $\text{Ni}(\text{imidazole})_4\text{Cl}_2 \cdot 2\text{H}_2\text{O}$  the  $\delta\sigma$  value is again in good agreement with the figure obtained from the ferrous complex.

The electronic spectra of a number of the 4:1 complexes with benzimidazole studied in Chapter III show definite splittings of the  $\nu_1$  and  $\nu_2$  bands. The spectra are given in Table 3.3.

For the blue solvated complex  $\text{Ni}(\text{benzimidazole})_4\text{Cl}_2 \cdot 2\text{Acetone}$ , [BC], the positions of the components are fairly clear (Fig. III.3), and values for the splitting parameters are given in Table 4.3. The value of  $\delta\sigma$  from the ferrous complex is very similar to that for the nickel complex, as also are the energies of the  ${}^5\text{B}_{1g}$  component (ferrous), and  ${}^3\text{B}_{2g}$  component (nickel (II)).

Following the approach given above, in connection with the 4:1 pyridine complexes, for determining the  $\Delta$

value for the axial ligands from the in-plane field and the splitting of the  $\nu_1$  band, it appears that the large splittings for the above complex arise from a fairly strong in-plane field, with a weak axial field ( $\Delta_{\text{axial}} \sim 5,000 \text{ cm}^{-1}$ ).

For the remaining 4:1 benzimidazole complexes the assignments are too uncertain, (see discussion of Electronic Spectra in Chapter III), to merit the determination of splitting parameters, however certain features may be noted. For the complexes  $\text{Ni}(\text{benzimidazole})_4\text{Cl}_2$ . [  $\Delta$  C3 ] and  $\text{Ni}(\text{benzimidazole})_4\text{Br}_2$ . [  $\Delta$  B2 ], (see Fig.III.1 for symbols); which were magnetically normal; following the assignments suggested in Chapter III, the values of  $\delta\sigma$  and  $\delta\pi$  are similar to those found for the corresponding pyridine complexes.

For  $\text{Ni}(\text{benzimidazole})_4\text{Cl}_2 \cdot 2\text{Acetone}$  [GC],  $\text{Ni}(\text{benzimidazole})_4\text{Cl}_2$  [  $\Delta$  C1 ], and  $\text{Ni}(\text{benzimidazole})_4\text{Br}_2$  [  $\Delta$  B1 ] the values of  $\delta\sigma$  appear to be large, following the assignments in Chapter III. If the axial field is determined for the latter complexes, using the method indicated above for the blue solvated chloride, then this is found to be zero or negative, suggesting that the approximations on which the calculations are based are not valid when the

distortions become large. Thus the values given in Table 4.4, for the field of the halide ions, may be too low, though the qualitative trends observed could be valid.

## Structural Factors in Nickel (II) Complexes

The structures of some of the compounds prepared during the present studies, and of some related complexes reported in the literature, are collected in Table 4.5. The factors that might influence structure, as given in the introduction to this chapter, will be considered in turn.

It is perhaps worth mentioning that in this discussion the concern is not with which is the most stable complex formed by a system, but with a consideration of the stereochemistries of the complexes that may be obtained in the solid state, for a given coordination number.

Turning first to the effects of changes in the ligand field strengths of the ligands in the complex. From a molecular orbital viewpoint this may be considered in terms of the  $\sigma$  and  $\pi$  bonding for a given ligand. On the crystal field picture, while there are two parameters  $D_s$  and  $D_t$  for describing the splitting of the cubic field levels on going to  $D_{4h}$  symmetry, there is the single parameter,  $D_q$ , related to the crystal field strength of an individual ligand,  $D_q = \frac{2}{5} (\sigma - \pi)$ .

Table 4.5Structures of Nickel (II) Complexes

<u>Ligand</u>	<u>2:1 Complexes</u>			<u>4:1 Complexes</u>		
	<u>Cl</u>	<u>Br</u>	<u>I</u>	<u>Cl</u>	<u>Br</u>	<u>I</u>
NH <sub>3</sub> (1)	0	0	-	-	-	-
imidazole	-	-	-	0	P	P
pyridine	0	0	O/T	0	0	0
3,5-dichloropyridine	0	0	..	..	..	..
4-cyanopyridine	0 <sup>(1)</sup>	0 <sup>(1)</sup>	..	..	0	0
isoquinoline	0	0	T	0	0	0
aniline	0	0	0	-	0	0
benzothiazole	0	0 <sup>(2)</sup>	T	..	0	..
⊗4-methylpyridine (a)	-	0	T	0	0	0
N-methylimidazole	..	T	..	..	0	..
2-methylimidazole	..	T	..	..	0	..
⊗3,4-dimethylpyridine (b)	-	T	T <sup>(c)</sup>	0	0	P
benzimidazole	-	T	T	O/P	O/P	P
⊗quinoline (d)	O/T	T	P	(3)		
⊗2-methylpyridine (a)	T	T	P			
3-methylisoquinoline	T	T	P			
2-methylbenzothiazole	-	P <sup>(2)</sup>	P			
⊗2,5-dimethylpyridine (e)	P	P	P			



Table 4.6pK<sub>a</sub> values for the Heterocyclic Ligands<sup>‡</sup>

<u>Heterocycle</u>	<u>pK<sub>a</sub></u>	<u>Heterocycle</u>	<u>pK<sub>a</sub></u>
imidazole	6.95	benzimidazole	5.53
2-methylimidazole	7.86	2-methylbenzimidazole	6.19
N-methylimidazole	7.33	5,6-dimethylbenzimidazole	5.98
thiazole <sup>(1)</sup>	2.53	quinoline	4.87
pyridine	5.17	isoquinoline	5.40
2-methylpyridine	5.97		
4-methylpyridine	6.02		
3,4-dimethylpyridine	6.46		
2,5-dimethylpyridine	6.40		
3-chloropyridine <sup>(2)</sup>	2.84		
4-cyanopyridine	1.90		

(1) no value has been found for benzothiazole, but comparing imidazole and benzimidazole, the value for benzothiazole is probably < 2.53.

(2) no value has been found for 3,5-dichloropyridine.

<sup>‡</sup> The values are taken from the collected data of ref.114.



However in discussing the changes of structure, the feature of significance will be the difference between the bonding of the ligands present. Hence in considering a series of complexes with the same anion, the splitting of the  $e_g$  and  $t_{2g}$  one-electron orbitals may be used as a guide, the splitting being seen as due either to anti-bonding or electrostatic effects.

From the preceding section it would appear that the splitting of the  $e_g$  level (i.e.  $\sigma$  bonding, or electrostatic interactions following the spectrochemical series) is the most significant factor. As  $\delta\sigma$  and  $\delta\pi$  are directly proportional to the splitting of the one-electron orbitals, (Fig.IV 1), discussion will be in terms of these parameters, though not implying complete covalent bonding.

It was found for those 4:1, and octahedral 2:1, complexes where other factors might be expected to be similar, that the observed  $\sigma$  donor strengths of the ligands were related to the  $pK_a$  values. This correlation has also been shown by examination of  $F^{19}$  shielding parameters, in platinum (II) fluorophenyl complexes, which could be related to the  $\sigma$  and  $\pi$  bond strengths of other ligands in the complexes.<sup>115</sup> It may then be a reasonable extrapolation to consider that this relation

will also apply in tetrahedral and planar configurations. The  $pK_a$  values of most of the ligands given in Table 4.5, are collected in Table 4.6.

It would appear that there is no correlation between the  $pK_a$  of a ligand, and the ability to adopt a 4:1 structure, or with the change in structure of the 2:1 complexes from octahedral polymeric, to tetrahedral, or planar.

It is noticeable that those with low basicity, benzothiazole, 3,5-dichloropyridine and 4-cyanopyridine, form the 4:1 complex with more difficulty, a polymeric 2:1 complex tending to be obtained, suggesting that when the bonding become weak it is energetically more favourable to adopt the latter structure.

Spin-pairing will occur for nickel (II) complexes if the splitting of the  $e_g$  level is greater than the spin-pairing energy. Thus the 4:1 complexes where  $\delta\sigma$  is large may be diamagnetic, this being shown by the imidazole complexes. While N-methyl- and 2-methylimidazole have  $pK_a$  values greater than that for imidazole, the 4:1 bromide complexes are paramagnetic, presumably because steric effects from the methyl group increase the metal-nitrogen distance.

Metal- ligand  $\pi$  bonding has been suggested as a significant factor in determining the change from 6 to 4 coordination in cobalt complexes analogous to those examined here.<sup>67</sup> This conclusion was based on observations of entropy terms for solution equilibria. An explanation of this data on the basis of steric effects has however been put forward.<sup>116</sup>

It might be expected that in the event of metal to ligand  $\pi$  bonding there would be a drop in the energy of the ligand  $\pi \rightarrow \pi^*$  transitions. Attempts were made to examine the ultraviolet spectra of some of the present complexes to evaluate any shifts in the energies of transitions of this latter type. Satisfactory spectra were however not obtained, and no conclusions could be drawn. Using similar complexes, spectra in the ultraviolet region have been observed by others<sup>117</sup> which were interpreted as indicating  $\pi$  bonding between the metal and ligand.

The relative contributions of electrostatic and antibonding interactions to the splitting of the  $t_{2g}$  level, are not known from the splitting of the electronic spectral bands. For the molecular orbital approach the splittings in fact depend on the differences in  $\pi$

bonding, but as the values of  $\delta\pi$  remain similar, and small, through a range of anions and heterocycles, this would indicate that the total  $\pi$  bonding is small.

The spectral data indicates that the heterocycles are weaker  $\pi$  donors than the halide ions. That the halide ions act as  $\pi$  donors has been shown by the measurements on  $F^{19}$  shielding effects mentioned above. The heterocycles might then be weak  $\pi$  donors or weak  $\pi$  acceptors.

There is little independent evidence relating to the  $\pi$  bonding of the heterocyclic ligands in complexes of the present type. A study has been made of the proton contact shifts (see Chapter V) in the adducts of pyridine with cobalt (II) and nickel (II) acetylacetonates<sup>118</sup>. For the cobalt complexes where there is unpaired spin in orbitals of  $\pi$  symmetry, it was found that the observed shifts could be rationalised in terms of  $\sigma$ -contact and pseudocontact interactions (the effect of  $t_{2g}$  electrons being through anisotropy rather than  $\pi$  bonding). For the nickel complexes the results were similarly explained. While no spin of  $\pi$  symmetry is expected for nickel (II), that there is some mixing has been shown by the results from the adducts with phosphines<sup>119</sup>.

The  $\pi$  bonding appears to be small in the octahedral complexes, but might be more significant in tetrahedral and planar complexes, though it has been suggested that this would not be the case for the tetrahedral configuration<sup>67</sup>. Studies on the contact shifts seen for the tetrahedral complexes  $\text{Ni L}_2\text{I}_2$  (L = pyridine, picoline),<sup>120</sup> have indicated that there may be some slight  $\pi$  acceptance by the heterocycle, although any observed  $\pi$  effects may arise from indirect mechanisms.

Turning to steric effects, a detailed study has recently been made of the nickel (II) complexes with the mono- and dimethylpyridines.<sup>4,4a,5</sup> These ligands have a range of  $\text{pK}_a$  values, but the results were rationalised in terms of the steric effects of the methyl groups in the various ring positions. The general conclusions of that study are in agreement with those found for the present complexes.

The steric effects depend to some extent on whether the donor nitrogen is in a five- or six-membered ring.

Considering first the six-membered rings and the 2:1 complexes. It is found that for those ligands with no substituent in the position  $\alpha$  to the nitrogen, the

chloride and bromide complexes are six-coordinate (octahedral polymeric), the iodide complexes being tetrahedral. If there is an  $\alpha$ -substituent then the complexes are four-coordinate, with the iodides planar.

It would seem that increasing steric hinderance, by crowding of the atoms close to the metal ion, causes a change first from 6- to 4-coordination, and then from tetrahedral to planar forms. This latter change is reasonable if the different packing requirements of the neutral and anionic ligands are considered. With four roughly spherical ligands, such as halide ions, the tetrahedron will be preferred on geometric grounds. However with heterocyclic ligands, and in particular when there are  $\alpha$ -substituents, a trans-planar arrangement of metal-ligand bonds, with the planes of the aromatic rings perpendicular to the plane of the bonds, will introduce less steric strain. This idea is supported by the fact that when there are two  $\alpha$ -substituents e.g. 2,5-dimethylpyridine, all the complexes are planar. For this latter type of ligand the rings might well be inclined at an angle to the plane of the metal-ligand bonds.

It may be noted that while the ligands giving marked steric hinderance do not form polymeric 2:1 complexes, they do give polymeric 1:1 complexes in many cases, in which there is considerable distortion of the lattice (see chapter I).

For the 4:1 complexes with the donor nitrogen in a six-membered ring, those ligands which cause the least steric strain, as evidence by the formation of octahedral  $\text{Ni L}_2\text{Br}_2$  and tetrahedral  $\text{Ni L}_2\text{I}_2$ , readily form 4:1 complexes which are paramagnetic. With somewhat greater steric hinderance  $\text{Ni L}_2\text{Br}_2$  is tetrahedral, and some of the 4:1 complexes are diamagnetic (though this latter effect also depends on the  $\sigma$  donor strength). If the steric effects are sufficient to force a planar structure for  $\text{Ni L}_2\text{I}_2$ , then halide complexes with more than two neutral ligands are rarely formed.

The bond angles in five-membered rings differ from those of the pyridine type ring, such that any substituent  $\alpha$ -to the nitrogen is further removed from the region of the metal-nitrogen bond.

The data available on steric effects in five-membered ring heterocycles is limited by the fact that imidazole

and benzimidazole have specific characteristics, possibly associated with hydrogen bonding, as discussed below, which significantly affect their properties.

The octahedral  $\text{Ni}(\text{benzothiazole})_2\text{Br}_2$  suggests a steric effect from the heterocycle which is closer to that of isoquinoline than quinoline. The planar structure of  $\text{Ni}(2\text{-methylbenzothiazole})_2\text{Br}_2$  then indicates rather more steric interaction than would be expected. However a tetrahedral configuration is readily adopted by this complex in solution, and the planar solid state structure may be due to contributions from lattice effects, and possibly  $\pi$  bonding.

Imidazole and benzimidazole behave similarly as ligands, but stand in contrast to benzothiazole. The  $\text{pK}_a$  for the latter ligand is considerably less than that for benzimidazole, which might account for the differing magnetic properties of the 4:1 complexes. This would not however seem to rationalise the formation of a polymeric 2:1 bromide complex by benzothiazole, the corresponding benzimidazole complex being tetrahedral.

Tetrahedral 2:1 complexes are readily formed by imidazoles, and benzimidazoles in solvents such as



acetone, which suggests that hydrogen bonding may be of some importance in determining the structures adopted by complexes with these ligands. It is not however clear why this effect should favour a tetrahedral rather than a planar, or polymeric configuration. The action of hydrogen bonding is shown by the frequent occurrence in the complexes, of solvents such as acetone or water.

In concluding this section it may be noted that though steric requirements appear to influence markedly the structures adopted by nickel (II) complexes, they do not rigidly require for example a planar rather than a tetrahedral structure. This is shown by the fact that where the analogous cobalt (II) complexes have been studied, they are in most cases tetrahedral. It thus seems that in nickel (II) the balance of electronic factors renders the structures which are adopted susceptible to effects such as steric strain.

## Chapter V

### Contact Shifts in the Proton N.M.R. Spectra of the Tetrahedral 2:1 Nickel (II) Complexes

#### Introduction

The isotropic contact shifts observed for n.m.r. proton resonances in the paramagnetic complexes with certain transition metals, can be a source of information on electronic structure and the nature of the metal-ligand bonding. Thus some studies were undertaken of contact shift phenomena in complexes with imidazoles, knowledge of spin distribution in ligands of this type being potentially of some biological significance.<sup>16</sup>

The study of contact shifts in transition metal complexes has been developed during the past six years, and review material is at present not very extensive, though outlines have been given by some authors.<sup>40,41</sup> A brief summary of the essential features is given below, together with relevant equations, the origins of which may be found in the references cited.

The fine structure seen in the n.m.r. spectra of

diamagnetic materials is not normally observed in the presence of unpaired electron spin, any lines then being broad. The line width is determined by the lifetime in a given state, (uncertainty principle), and electron relaxation together with electron-nucleus relaxation, then leads to extensive line broadening for the proton resonance. However if the electron relaxation time ( $T_{1e}$ ) is fast, or if there is a rapid interchange of electron spin states ( $T_{ex}$ ), then n.m.r. lines may be seen which have undergone an time average isotropic contact shift.

The proton experiences an electron-nucleus Fermi contact interaction, in which the contact interaction constant ( $A_i$ ) is given by

$$A_i = \frac{8\pi}{3h} g_e g_H \beta_e \beta_H [\psi(0)]^2 \quad [1]$$

where  $g_e$  and  $g_H$  are the electron and proton  $g$  values, and  $\beta_e$  and  $\beta_H$  are the Bohr and nuclear magnetons,  $\psi(0)$  is the wave function for the unpaired spin at the nucleus.

The conditions for observation of time-averaged contact shifted lines have been related to the contact interaction constant;<sup>121</sup>

$$\text{either } 1/T_{1e} \gg A_i, \text{ or } 1/T_{ex} \gg A_i \quad [2]$$

These conditions are found to be satisfied for the proton resonances in the complexes with a number of transition metals.<sup>122</sup> For nickel (II) complexes there may be a spin singlet-triplet equilibrium leading to short relaxation times. Thus Phillips et al.<sup>126</sup> in their studies on the nickel (II) aminotroponeiminates observed very sharp lines due to a tetrahedral-planar interconversion. For other tetrahedral nickel (II) complexes, such as those with pyrromethenes<sup>127</sup>, there is no such interconversion. LaMar<sup>128</sup> has reviewed the mechanisms that might lead to short relaxation times, and has concluded that the main factor is a coupling of the zero field splitting with the tumbling motion in solution.

The line width will depend on the relaxation time, and an expression has been given by Luz and Meiboom<sup>129</sup>,

$$1/T_{2m} = 1/15 \frac{S(S+1) \gamma_I^2 g^2 \beta^2}{r^6} \left[ 4t_c + \frac{3t_c}{1+\omega_I^2 t_c^2} + \frac{13t_c}{1+\omega_S^2 t_c^2} \right] + 1/3 \frac{S(S+1)A_i^2}{\hbar^2} \left[ T_e + \frac{T_e}{1+\omega_S^2 t_e^2} \right] \quad [3]$$

where  $\omega_s$  and  $\omega_I$  are the Larmor precession frequencies for the electron and nucleus respectively,  $t_c$  and  $t_e$  are the correlation times for the dipolar and hyperfine interactions respectively, and  $\gamma_I$  the magnetogyric ratio for the nucleus.

When the inequalities given in 2 hold, then the isotropic shift is given by,<sup>121</sup>

$$\left(\frac{\Delta H}{H}\right)_i = \left(\frac{\Delta f}{f}\right)_i = -A_i \gamma_e / \gamma_H \frac{g\beta S(S+1)}{3kT} \quad [4]$$

where  $H, (f)$  is the applied field (frequency),  $\Delta H(\Delta f)$  is the observed isotropic field (frequency) shift of the  $i^{\text{th}}$  proton,  $\gamma_e$  and  $\gamma_H$  are the magnetogyric ratios for the electron and proton respectively.

The direction of the shift in resonance frequency will depend on the sign of the spin density at the nucleus, positive spin giving a down field shift. Spin density may be transmitted through the ligand by  $\sigma$  or  $\pi$  orbitals. This point is considered further in the section that follows, though it may be noted here that positive spin density at a point in a  $\pi$  system gives rise to negative spin at a proton attached to the ring, owing to the indirect interaction.

If there is anisotropy in the  $g$  tensor for the complex, then the proton will experience a fluctuating field that does not average to zero in solution. This field has been given for an axially symmetric system<sup>123</sup>, and following these authors<sup>123</sup>, LaMar obtained<sup>124,125</sup> equation 5 for  $C_{2v}$  symmetry, for the case where  $1/T_{1e} \gg t_e$  (where  $t_e$  is the electron correlation time).

$$\begin{aligned}
 (\Delta H/H)_i = - \left\langle (g_1 + g_2 + g_3) \left[ (g_1 - \frac{1}{2}g_2 - \frac{1}{2}g_3) \left( \frac{3\cos^2\chi_i - 1}{R_i^3} \right) \right. \right. \\
 \left. \left. + \frac{3}{2}(g_2 - g_3) \left( \frac{\sin^2\chi \cos 2\phi}{R_i^3} \right) \right] \right\rangle \quad [5] \\
 \left\langle = \frac{\beta^2 S(S+1)}{27kT}
 \end{aligned}$$

where  $g_1$  is the  $g$  factor along the  $C_2$  axis,  $g_2$  and  $g_3$  the  $g$  factors in the two mirror planes, and  $\phi$  the angle that the projection of the radius vector,  $R$ , in the  $g_2g_3$  plane makes with the  $g_2$  axis,  $\chi$  is the angle the radius makes with the  $C_2$  axis, (Fig. V.1 (b)).

For protons in non-equivalent positions, the resonance frequency separation of which is  $(\nu_A - \nu_B)$ , if there is rapid exchange between sites, then the spectrum will consist of a single line. The expected

Fig. V.1(a)

(from ref. 131)

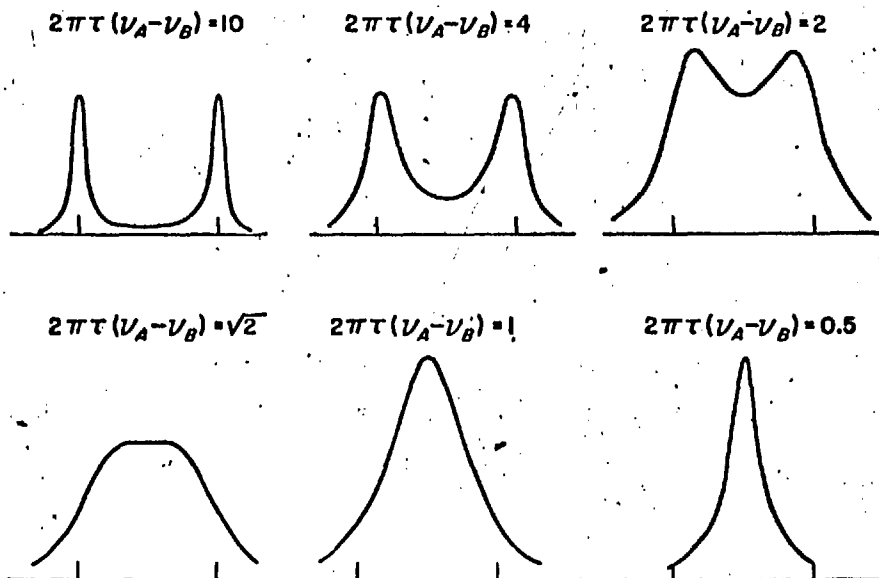
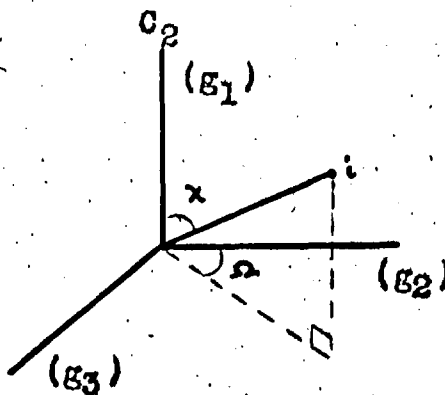


FIG. 10-1. Change of shape function  $g(\nu)$  for increasing exchange rate between two positions with equal populations. (Note that  $\tau$  is half of the lifetime of either site. The intensities are not on comparable scales.)

Fig. V.1(b) Location of a proton (1) within the symmetry coordinates of the complex. ( $C_{2v}$ )



line shapes for various ratios of  $t$ , (the average time between exchange), to  $\nu_A - \nu_B$ , have been given<sup>130</sup>, and are shown in Fig. V.1(a) (from ref. 131).

### Contact Shift Spectra

A general examination is being made of contact shift spectra from complexes of the type  $ML_2X_2$  (M = nickel or cobalt, L = imidazole, benzimidazole, and various methyl substituted imidazoles, and benzimidazoles, X = Br, I). These studies are at present incomplete, and at this point a brief outline of the data for the 2:1 nickel (II) complexes with benzimidazole and methylsubstituted benzimidazoles will be given, to illustrate the type of results obtained.

Considering first the spectra of the free ligands, these are shown for acetone solutions in Fig. V.2. (Throughout this section all line positions are given in cycles per second (cps) from tetramethylsilane (TMS), at 56.4 mcs., and are downfield, (negative), unless specified.

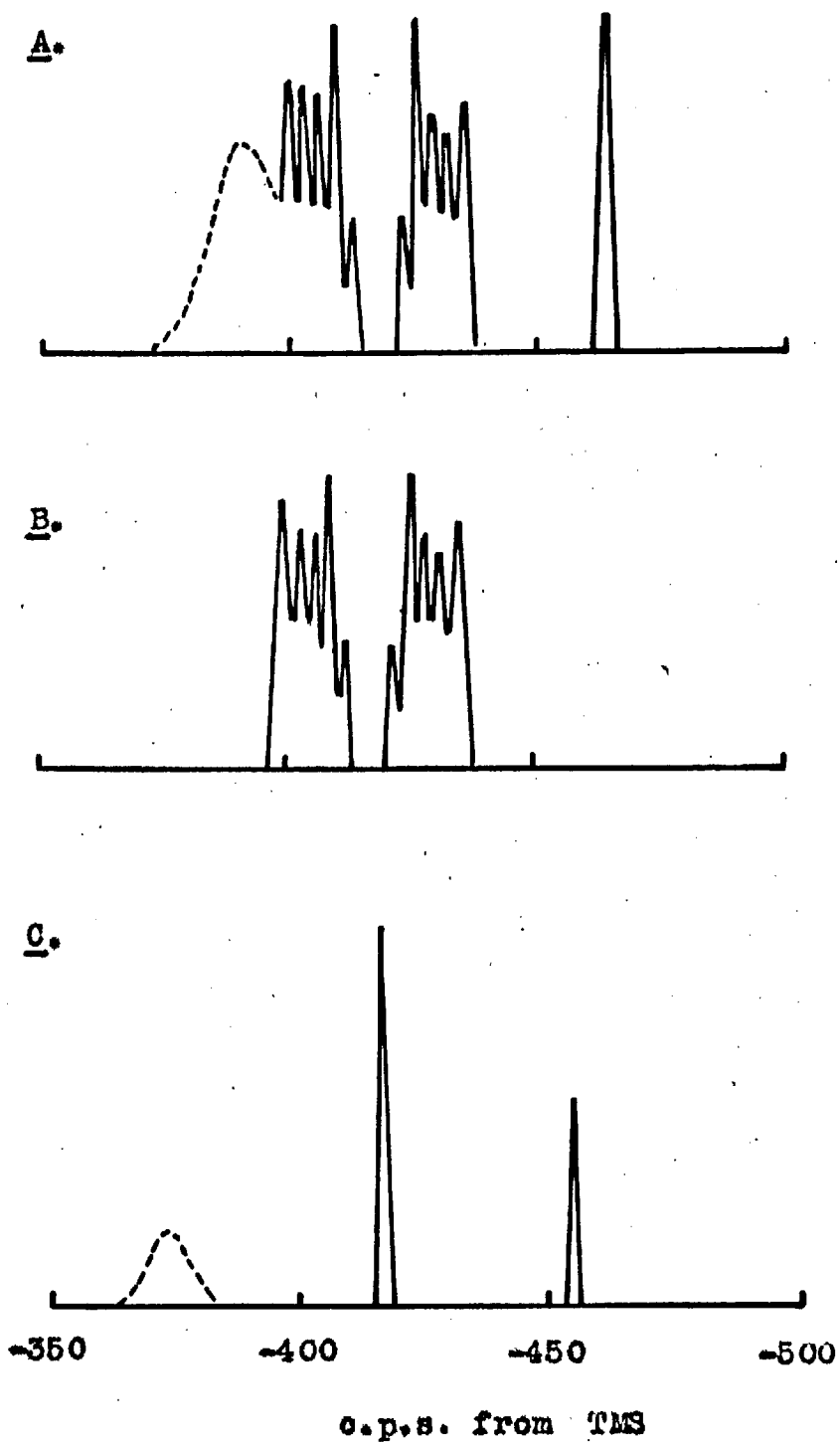
The pyrrole type proton undergoes rapid exchange, and a line from this proton, (393 cps for benzimidazole, 375 cps. for 5,6-dimethylbenzimidazole), is only seen within certain concentration limits. The N-H resonance



Fig. V.2

Proton n.m.r. Spectra of Free Ligands in  
Acetone Solution

- A. Benzimidazole
- B. 2-Methylbenzimidazole
- C. 5,6-Dimethylbenzimidazole



would also be broadened by the quadrupole of nitrogen.

For benzimidazole the line at 463.5 cps may be assigned to the proton in the 2 position. Owing to the rapid exchange of the proton between the two nitrogens of the imidazole ring, the benzimidazole molecule in solution has effectively  $C_{2v}$  symmetry. The pair of multicomponent systems centered at  $\sim 410$  and  $\sim 430$  cps are then due to the  $A_2B_2$  system of the 5,6 and 4,7 positions. These line positions agree well with those found by Black and Heffernan<sup>132</sup>.

For 2-methylbenzimidazole the resonances from the 5,6 and 4,7 protons are shifted slightly upfield. 5,6-Dimethylbenzimidazole gives a sharp line (418 cps) for the 4,7 protons, there being no coupling with the 5,6 positions.

Contact shift spectra were measured on acetone and nitromethane solutions for concentrations of  $\sim 0.05 - 0.15M$ . The effect of addition of free ligand, and dilution, on line positions were checked for each solution. The benzimidazole complexes were sufficiently soluble only in solvents of the above type, which can not readily be obtained in non-proton containing forms. Hence the solvent lines are strong, and with the high R.F. power required for observing contact shifted lines,

the region  $\pm$  200 cps from the solvent line can not be examined.  $\text{Ni}(\text{benzimidazole})_2\text{Br}_2$  and  $[\text{Ni}(\text{benzimidazole})\text{Br}_3]^-$  gave very similar spectra, three lines being observed, with a fourth seen to low field under certain conditions, Fig. V.3.

Such a spectrum would be consistent with the ligand being considered as  $C_{2v}$ , any shifts arising from an essentially  $\sigma$  contact mechanism, when the spin density would fall off as the number of bond lengths from the metal ion increased. The order of positions showing increasing shift would then be  $5,6 < 4,7 < 2$ . From this generalisation the shift of the NH proton would be less than that for the proton in the 2 position. This however is not usually the case, owing to the more electronegative nitrogen atom placing more spin on the bonded proton than would be the case for a carbon atom in the same position. The fact that the appearance of the fourth line depends on the conditions, further indicates that it may arise from the NH proton.

As a check on the ordering of the shifts, the spectrum of benzimidazole in acetone was examined as small portions of nickel bromide solution were added. It was found that the shifts followed the above order,

Fig. V.3

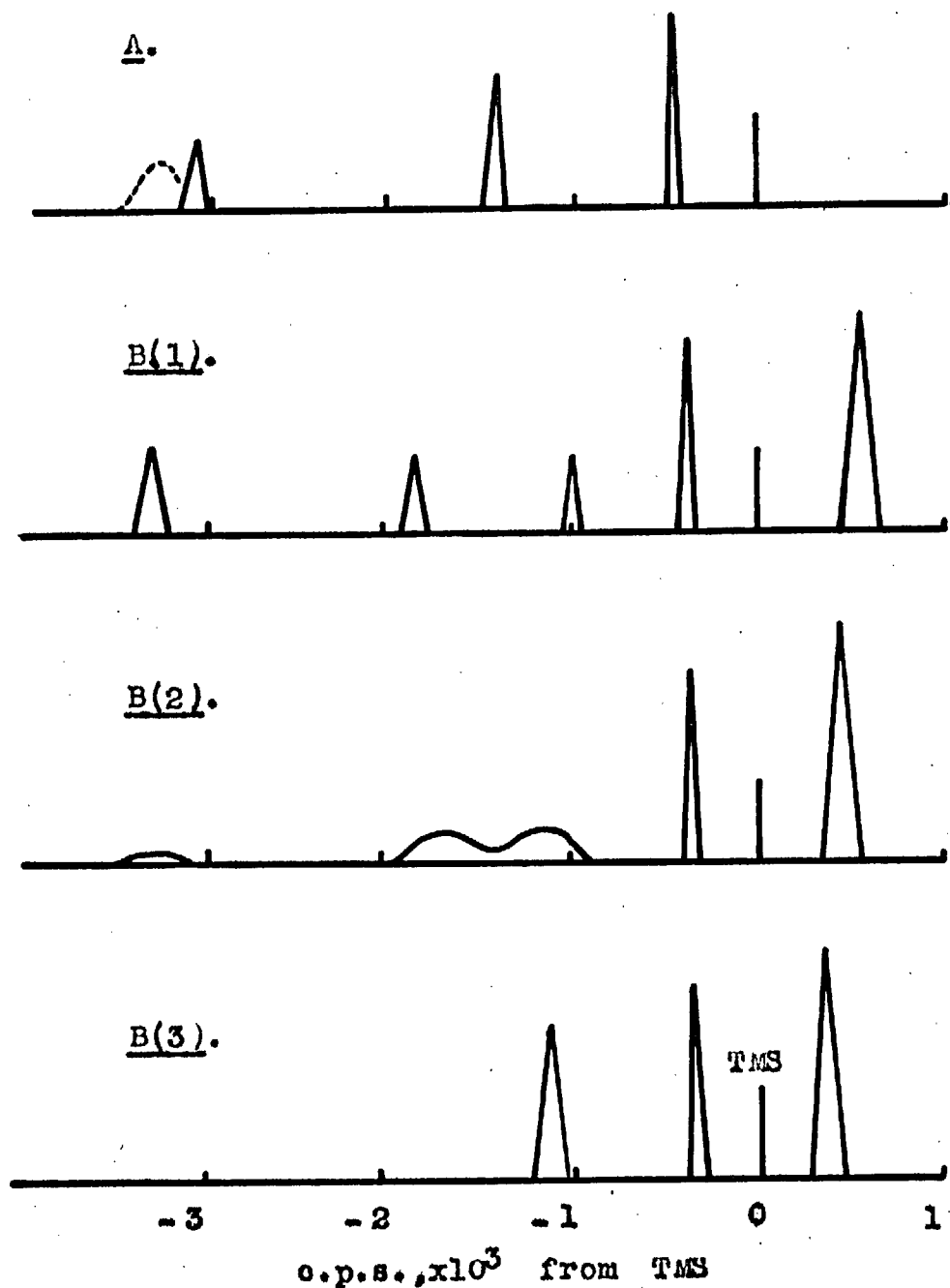
Proton n.m.r. Spectra (Schematic)

A.  $\text{Ni}(\text{benzimidazole})_2\text{Br}_2$

B(1).  $\text{Ni}(\text{2-methylbenzimidazole})_2\text{Br}_2$

(2). as above, plus slight excess ligand

(3). " " " further ligand



with the 5,6 protons being virtually unaffected, though the addition of nickel bromide could not be carried very far, owing to the precipitation of the 4:1 complex. (The species in solution under these conditions may be significantly of a 4:1 type, however the ordering of the shifts will probably be as for the  $C_{2v}$  complex).

The methyl substituted benzimidazole complexes were investigated to establish whether the changes in the spectrum would be consistent with the above assignments.  $Ni(5,6\text{-dimethylbenzimidazole})_2Br_2$  then gave a spectrum in which the lines assigned to the 4,7 and 2 position protons, occur at the same frequency as for the benzimidazole complex, while the line at 430 cps. could no longer be seen.

For  $Ni(2\text{-methylbenzimidazole})_2Br_2$  the spectrum, Fig. 3(B), does not immediately fall into the above assignment scheme, there being a greater number of lines downfield of acetone than anticipated. The line at 3300 cps. may however be assigned to the NH proton, and it will be seen that the average frequency of the two lines at 1880 and 1070 cps is 1475 cps, which is very similar to the position of the line assigned to the 4,7 protons in the spectrum of the benzimidazole complex, Fig. V.3(A). Thus it may be that the two

lines seen for the 2-methylbenzimidazole complex arise from the protons in the 4,7 positions being rendered non-equivalent.

This situation might arise from two causes. Firstly the rate of exchange of the ligand molecules could be less than 500 cps ( $800 \times \pi / 5$ , Fig. V.1(a)), the difference in the shifts for the 4,7 positions then not being time-averaged. Secondly the rate of exchange of the NH protons for the non-complexed ligand could be less than 500 cps, then while the exchange rate for the ligand might be greater than this latter value, the effective rate of alternation of the two nitrogen bonding sites would be below 500 cps. It has not been possible as yet, to distinguish between these two possibilities.

The addition of a small quantity of free ligand to a solution of the 2:1 2-methylbenzimidazole complex causes collapse of the line at 3300 cps, and the broadening and merging of the lines at 1880 and 1070 cps., to give a single line which shifts upfield as further free ligand is added (Figs. V.3 B(1)-(3)).

These changes would be seen as due to the presence of free ligand increasing the rate of proton exchange, causing the disappearance of the line at 3300 cps,

and also increasing the rate of exchange between nitrogen bonding sites, the 4,7 positions then becoming averaged. Comparison of the spectra in Figs. V.3(B), for the lines from the 4,7 position protons, with the calculated line shapes of Fig. V.1(a) shows good agreement.

The shift of the resultant single line for the 4,7 protons indicates that the rate of ligand exchange is  $\nu \sim 1100x\pi/5$ . This rate however may well have altered from the value in the 2:1 complex solution, and hence does not necessarily differentiate between the above mechanisms for the non-equivalence of the 4,7 protons.

A line is seen upfield of TMS for the 2-methylbenzimidazole complex, which may be assigned to the  $\text{CH}_3$  protons. The position of this line will be discussed below.

Thus while the evidence is not conclusive the assignments given above for the spectrum of  $\text{Ni}(\text{benzimidazole})_2\text{Br}_2$ , appear to be generally consistent with the spectra of the complexes with the methyl substituted benzimidazoles, and further discussion will be made on this basis.

Isotropic shifts (shifts in c.p.s, at 56.45 m.c.s,

of the proton resonance for the complex relative to the free ligand) are given in Table 5.1. A note is also made of whether there is any change in the spectrum on addition of free ligand. Before discussing the contact shifts the data on the iodide complexes will be introduced.  $\text{Ni}(\text{benzimidazole})_2\text{I}_2$  gives a spectrum Fig. V.4(A) in which the 4,7 protons again appear to be non-equivalent, the lines at 1770 and 1220 cps being assigned to the protons in these latter positions. The line at 3170 cps is probably due to the overlapping of the proton resonances from the NH and 2 positions. On addition of the free ligand the lines originally at 1770 and 1220 cps. broaden and coalesce, as described above for the complex with 2-methylbenzimidazole, the lines shapes being very similar to those calculated, as in Fig. V.1(a). For an estimate of the amount of free ligand used, between the various spectra of Fig. V.4, about 3-5 small crystals of ligand were added to  $\sim 0.6\text{ml.}$  of a  $\sim 0.15\text{M}$  solution of the 2:1 complex.

The complex  $\text{Ni}(2\text{-methylbenzimidazole})_2\text{I}_2$  gave a spectrum which was very similar in appearance to that of the bromide complex (Fig. V.3(B)). The action of added ligand was also as for that complex.



Table 5.1

Isotropic shifts<sup>⊛</sup> for 2:1 complexes in Acetone

Complex	NH	Proton(or Methyl)Position					Affect	Fig
		2	4	7	5	6 Ligand		
Ni(bz) <sub>2</sub> Br <sub>2</sub>	(2880)	2550		1020		25	NS	V.3
[Et <sub>4</sub> N][Ni(bz)Br <sub>3</sub> ]	(3330)	2680		1060		30	NS	(d)
Ni(5,6-dinebz) <sub>2</sub> Br <sub>2</sub>		2540		1020			NS	(e)
Ni(2-nebz) <sub>2</sub> Br <sub>2</sub>	2900 <sup>(b)</sup>	+580 <sup>(c)</sup>	1445		665	45	S	V.3
Ni(bz) <sub>2</sub> I <sub>2</sub>	~2750		1340		790	5	S	V.4
Ni(2-nebz) <sub>2</sub> I <sub>2</sub>	2760 <sup>(b)</sup>	+550 <sup>(c)</sup>	1340		665	5	S	(f)

⊛ Shifts in c.p.s, at 56.4 m.c.s., from line positions in diamagnetic ligand, probably accurate to ± 10 c.p.s., shifts negative unless specified.

(a) NS = no shift (in line position) ; S = shift

(b) Line from NH proton not seen in spectrum of diamagnetic ligand, the value taken from benzimidazole spectrum.

(c) Line from CH<sub>3</sub> proton not seen in spectrum of diamagnetic ligand, the value taken from spectrum of 2-methylimidazole in CHCl<sub>3</sub> (80 c.p.s. from T.M.S)

(d) Spectrum similar to V.3(A)

(e) " " " " , line at 430 c.p.s. absent

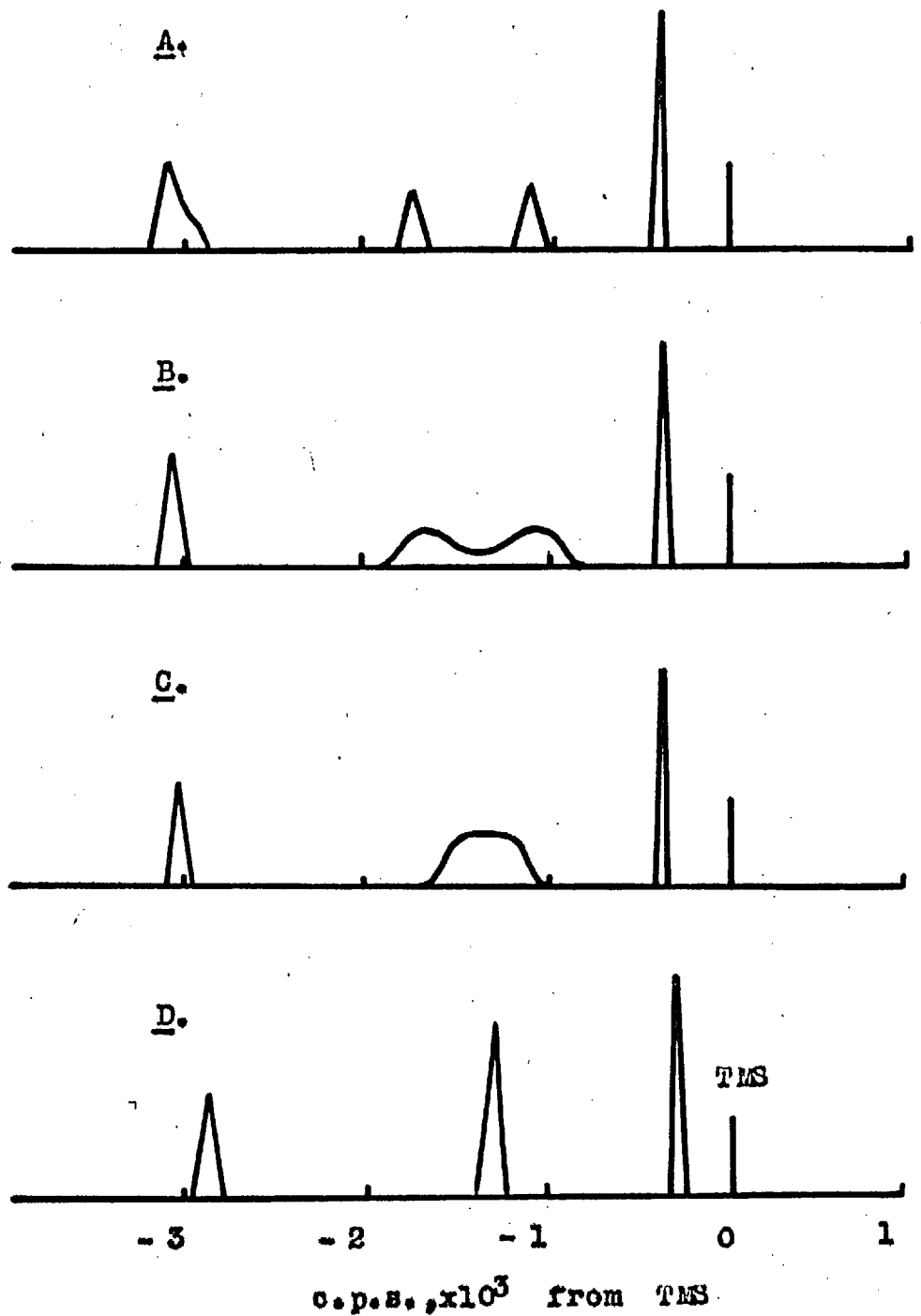
(f) " " " V.3(B)

Fig. V.4

Proton n.m.r. Spectra. (Schematic)

A.  $\text{Ni}(\text{benzimidazole})_2\text{I}_2$

B, C, and D show the effects of successive additions of small quantities of ligand.



Turning next to a general consideration of the isotropic shifts. As noted in the introduction to this chapter, the isotropic shifts can arise from contact interaction through a  $\sigma$  or  $\pi$  system, or through a pseudocontact interaction due to dipolar interaction between the nuclear moment and electron spin on the metal ion. The observed downfield shifts, decreasing as the proton is separated from the metal ion by a greater number of bonds, are indicative of predominantly  $\sigma$  contact interaction.

The presence of  $\alpha$  (aligned with applied field) spin density in the  $\pi$  system would tend to give up-field shifts in an alternant system. Shifts might be small or downfield, if spin correlation was important. If the system was effectively odd-alternant, e.g. a molecular orbital extending over the benzene ring and a nitrogen, then a clear alternation in spin density sign would be expected, with positive spin at the 4 and 6 positions for the above case. If by an indirect mechanism, possibly via depolarisation on the nitrogen atom,  $\beta$  spin was introduced into the  $\pi$  system, downfield shifts would result, but for either  $\alpha$  or  $\beta$  spins there would be no necessary correlation of the magnitude of spin density with the separation from the metal ion

The mechanism by which delocalisation occurs will be related to the relative energies of the molecular orbitals on the ligands, and the metal ion d orbitals<sup>122</sup>. For nitrogen heterocyclic azines the highest energy bonding orbital is the  $\sigma$  orbital localised on the nitrogen,<sup>133</sup> and this is probably also the case for the azole ring considered here. A transfer of  $\beta$  spin from the  $\sigma$  orbital on the ligand, to the metal ion, would then not be unreasonable.

Holm et al.<sup>120</sup> examined the contact shifts in the tetrahedral complexes  $NiL_2I_2$  (L = pyridine, picoline), and observed large downfield shifts. The ordering of the molecular orbitals in pyridine were calculated, and the results were consistent with a  $\sigma$  contact term.

It would appear that for nitrogen heterocyclics, such as pyridine<sup>118,120</sup>, and o-phenanthroline<sup>34</sup>, and also for amines and amino acids<sup>135,136</sup>, that the contact is primarily via a  $\sigma$  molecular orbital. This is not however general for nitrogen donor ligands as is demonstrated by the complexes with the aminotropone-ininates<sup>135</sup> porphyrins<sup>127</sup> and pyrromethenes<sup>127</sup>, where delocalisation is via the  $\pi$  system. It has been suggested<sup>122,127</sup> that the relative energies of the

$\pi$  M.O.'s are such that ligand to metal electron transfer occurs for the first of these ligands, and from metal to ligand for the latter two.

In the above discussion pseudocontact shifts have not been considered. This latter effect would also give shifts which decrease as the proton becomes further separated from the metal ion, however as will be discussed below the observed shifts do not in the main arise from this interaction.

From equation 5 it will be seen that the magnitude of the pseudocontact term will depend on the difference in the three principle g values, and also on the geometric terms for a given proton. For nickel (II) in  $C_{2v}$  symmetry some anisotropy in the g tensor will be expected. However contact shift studies on complexes of the type  $Ni(PH_3P)_2X_2$  have indicated that there the pseudocontact term is small<sup>124</sup>. It was suggested that this may be due to the terms  $(g_1 - \frac{1}{2}g_2 - \frac{1}{2}g_3)$   $(3\cos^2\chi_i - 1)/R_i^3$  and  $\frac{3}{2}(g_2 - g_3)(\sin^2\chi_i \cos 2\alpha_i)/R_i^3$ , being of the same magnitude and sign, and hence giving a small pseudocontact interaction. LaMar<sup>136</sup> has demonstrated a definite pseudocontact contribution in certain  $C_{3v}$  phosphine complexes.

An evaluation of the relative pseudocontact terms for the present complexes has been made, to give some estimate of likely shift contributions from this effect, and also to enable comparison of shifts for the cobalt(II) and nickel(II) complexes, the pseudocontact term being anticipated as larger for complexes with the former ion<sup>118,124,136</sup>.

The relative pseudocontact shifts for the protons at the various ring positions will depend on the geometric terms in equation 5. These latter terms were thus calculated for the ligands relating to the present studies. The method used is outlined in the appendix to this chapter. The values of the geometric terms, FN1 and FN2, being the first and second geometric terms in eqn. 5, were found for various values of the structural parameters. It was found that small changes ( $\pm 2^\circ$ ,  $\pm 0.05\overset{\circ}{\text{A}}$ ), in the ligand structure did not produce significant alterations in the geometric terms. More marked is the effect of changing the values of the metal-ligand bond length and the tetrahedron angles, particularly the latter, as given in Table 5.2.

Horrocks and LaMar<sup>125</sup> found that the ratios of the geometric terms were very similar for both FN1 and FN2 for given structural parameters. For the

present calculations it was found that these ratios were identical in absolute magnitude, though differing in sign (Table 5.2). It was further found that the ratio  $FN1/FN2$  depends only on the value of the metal-ligand bond length. Thus while the values of the geometric terms are markedly dependent on the value of the tetrahedron angles, the ratios are not affected by changes in this parameter (Table 5.2). This result may be demonstrated on geometric grounds from consideration of Fig. V.5(b).

For any set of  $g$  values, within normal limits, the pseudocontact shifts will be small in relation to the observed shifts. LaMar found  $g_{1\uparrow} > g_{\downarrow}$  for the  $C_{3v}$  phosphine complexes, and for the present complexes it might be further assumed that  $g_2 > g_3$  (Fig. V.5(a)). Then for  $g$  values in the region  $g_1 \approx 2.40$ ,  $g_2 \approx 2.25$ ,  $g_3 \approx 2.1$  the pseudocontact shift for the proton in the 2 position will be of the order of 100 c.p.s. at 56.4 mcs, and correspondingly less for the protons in the other positions.

It will be noted in Fig. V.3(B) that the resonance of the methyl protons is observed upfield of TMS. Being separated from the metal ion by the same number of bond lengths as the proton in the 4 position, a

Table 5.2

Geometric Terms for Pseudocontact Interaction

$$AVFN1 = \left\langle \frac{(\cos^2 \chi_i - 1)}{R_i^3} \right\rangle_{\theta}, \quad AVFN2 = \left\langle \frac{\sin^2 \chi_i \cos 2\alpha_i}{R_i^3} \right\rangle_{\theta}$$

FA,  $\phi$ , as in Fig. V.5(a)

<u>AVFN,</u> x10 <sup>-21</sup> , cm <sup>-3</sup>	<u>FA</u>	<u><math>\phi^{\circ}</math></u>	<u>2</u>	<u>Me<sup>‡</sup></u>	<u>4</u>	<u>5</u>	<u>6</u>	<u>7</u>
AVFN1	2.0	35	-0.144	0.041	0.058	-0.005	-0.024	-0.048
			-1	0.28	0.40	-0.03	-0.17	-0.335
AVFN2	2.0	35	7.40	-2.10	-2.98	0.25	1.25	2.47
			1	-0.28	-0.40	0.03	0.17	0.335
AVFN1	2.1	35	-0.146	0.028	0.042	-0.006	-0.024	-0.046
			-1	0.19	0.29	-0.04	-0.16	-0.315
AVFN2	2.1	35	7.50	-1.43	-2.15	0.32	1.22	2.36
			1	-0.19	-0.29	0.04	0.16	0.315
AVFN1	2.0	32	-1.74	0.49	0.70	-0.059	-0.29	-0.580
			-1	0.28	0.40	-0.03	-0.17	-0.335
AVFN2	2.0	32	7.93	-2.25	-3.2	0.27	1.34	2.65
			1	-0.28	-0.40	0.03	0.17	0.335
R( $\overset{\circ}{A}$ )	2.0	35	3.13	3.8 <sup>‡</sup>	3.18	5.59	5.80	6.35

<sup>‡</sup> Value averaged over methyl rotation



downfield shift might have been expected for the methyl protons. A pseudocontact shift of some hundreds of c.p.s could occur, but this seems inadequate to explain the observed position. It is possible that there is negative spin density in the  $\pi$  system. This would result in a downfield shift for a proton attached to the ring, hence contributing to the  $\sigma$  shift, but would give an upfield shift for the methyl protons. Similar upfield shifts have been seen in methyl substituted pyridine complexes.<sup>118,120</sup>

In Table 5.3 line widths are given for the spectra of certain of the present complexes. Values are not given for the remaining complexes as there is extensive broadening from exchange, and other lines overlap. An expression for the line width in terms of dipolar and exchange correlation times is given in equation 3. It has been suggested by Luz and Meiboom<sup>129</sup>, and others,<sup>137,128</sup> that the dipolar term is the most significant. This latter term is a function of  $r^{-6}$ , and hence critically dependent on the separation of the proton from the metal ion. Values of R for the various proton positions are given in Table 5.2, and ratios of  $R^{-6}$ , together with the observed line widths in Table 5.3. While there is some agreement

Table 5.3n.m.r. Spectral Line Widths (c.p.s. at 56.4 m.c.s.)

<u>Compound</u>	<u>2</u>	<u>4,7</u>	<u>5,6</u>
bz	~ 5	~ 5	~ 5
Ni(bz) <sub>2</sub> Br <sub>2</sub>	140	125	12
	1	0.9	0.05
[Et <sub>4</sub> N][Ni(bz)Br <sub>3</sub> ]	155	120	14
Ni(5,6-dimebz) <sub>2</sub> Br <sub>2</sub>	145	190	
<u>Ratio of 1/R<sub>av</sub><sup>6</sup></u>	1	0.43	0.02

between the ratio of  $R^{-6}$  and the line width for the 5,6 protons, this is not the case for the 4,7 protons, as might be expected if the two proton positions are not completely time-averaged. There will be some broadening of all resonances from ligand exchange<sup>138</sup>.

From equation 3 a value of the electron dipolar correlation time may be found of  $\sim 10^{-16}$  sec. for the complexes listed in Table V.3. This is of a similar order of magnitude to the value of  $10^{-13}$  sec. found by LaMar for the  $C_{2v}$  phosphine complexes<sup>137</sup>,

and may be identified directly with the electron relaxation time.<sup>129,137</sup> If this is the case then the conditions for equation 5 to be valid do not hold,<sup>123,137</sup> and an alternative expression should be used<sup>122,123</sup>, which will lead to slightly larger, or smaller calculated shifts, depending on the  $g$  values.

Appendix Chapter VCalculation of Pseudocontact Terms

To calculate the geometric terms reasonable values for bond lengths and angles are required. X-ray structural data is available for imidazole<sup>140</sup>, and for benzimidazole extrapolations were made from the fairly extensive data available for purines<sup>141</sup>. Any further structural parameters were taken from ref. 141. For the metal-ligand bond length an initial value of 2.0<sup>0</sup>Å seemed reasonable, this being the value found for the 4:1 pyridine complexes<sup>72</sup>. In this outline detailed geometric considerations are not given, but may be followed through from the diagrams of Fig. V.5 and the program of Fig. V.6, the lettering being the same in both.

Considering the case of a proton in the 2 position Fig. V.5(a). The complex  $NiL_2X_2$  is initially considered to have regular tetrahedral bond angles, with the metal-ligand bond lying in the xz plane. The location of a proton in the coordinate framework, and relative to the metal-nitrogen axis was fixed by the parameters R, D, and S, which may be calculated from standard

trigonometric relationships for given structural parameters. If the imidazole ring is rotated  $\theta^\circ$  out of the xz plane, Fig. V.5(b), the geometric terms may be calculated following method of subroutine PSUCON (Fig. V.6). In the latter, values of the geometric terms are found at  $10^\circ$  intervals, though for some proton positions larger intervals could be used without loss of accuracy to four figures.

For the methyl substituted complex rotation of the methyl group must be included. This may be treated as equivalent to altering the values of R, D, and S. If the methyl proton is considered as remaining in the xz plane as the methyl rotates, then the imidazole ring becomes inclined to the xz plane. When Y is the projection of i in the plane of the imidazole ring, values of RY and DY may be found which are equivalent to R and D for i in the xz plane, Fig. V.5(c) and (d). Then from the known inclination of the ring to the latter plane, R, D and S may be found, as shown in the main program of Fig. V.6.

Average values of the geometric terms for all rotations of the methyl group and the imidazole ring were found.

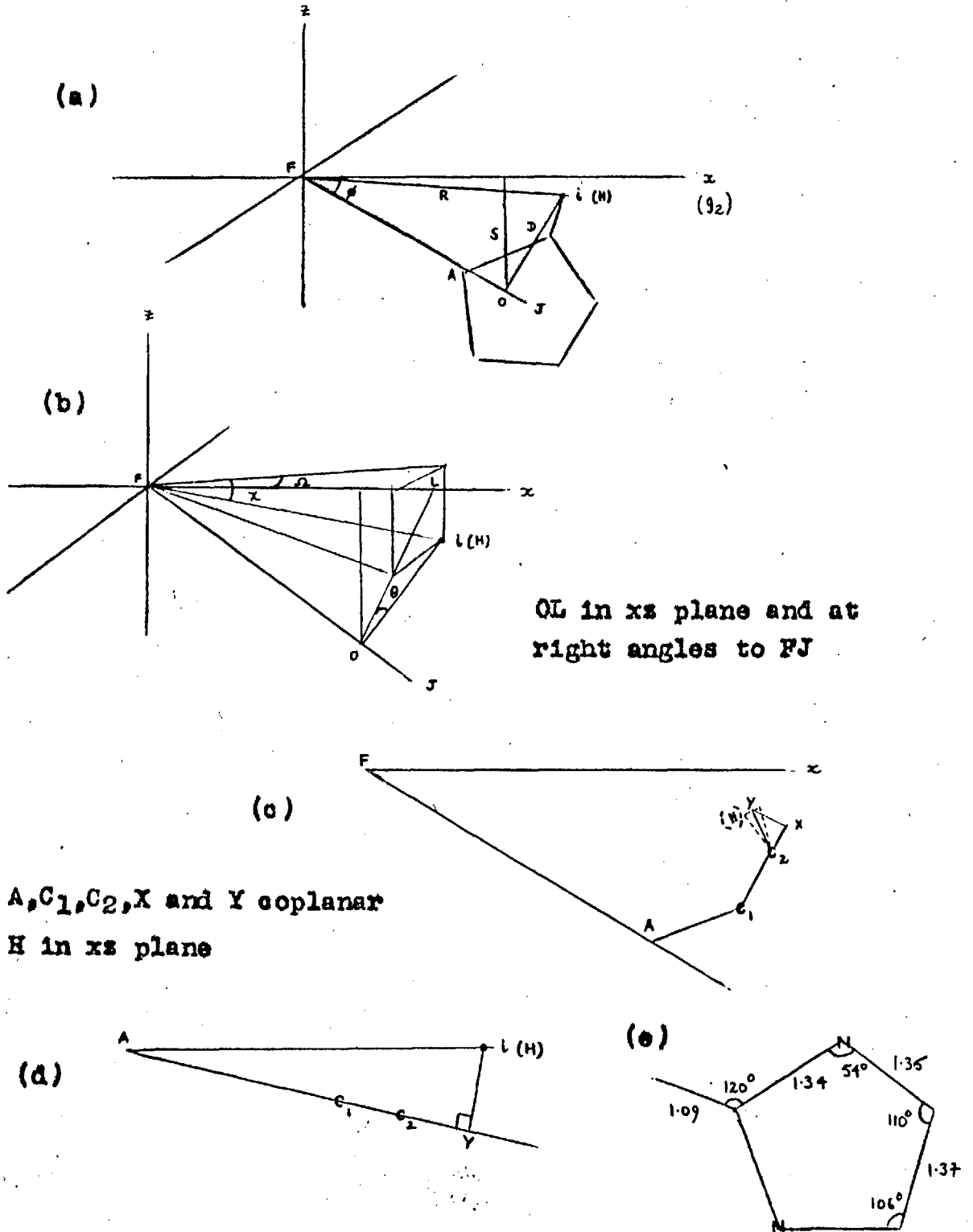
Calculations of the geometric terms for protons

in other positions of the imidazole and benzimidazole rings were carried out by suitable modifications of the above procedure. It was found that small variations in the structural parameters did not significantly affect the relative values of the derived geometric terms. For the set of results given in Table 5.2 the bond angles and bond lengths for the benzene ring were taken to be as in benzene, while those for the imidazole ring were as in Fig. V.5(e). The C-C bond length for the 2-methyl substituted ligand was 1.55 Å.

The geometric terms may be calculated by a number of other approaches, such as taking orthogonal axes, one of which is coincident with the metal-ligand bond, and using the usual matrix transform to the complex symmetry axes. This would not give a significant difference in machine time over the above method.<sup>149</sup>

Fig. V.5

Geometric Aspects for Pseudocontact Interactions.



```

C      CALCULATE PARAMETERS 2 METHYL
C      ARCSINE
      ASNF(T) = ATAN (T/SQRT( 1.- T*T))
C      TRIANGLE SINE FORM
      TSNF (A,B,C) = A* SIN(B)/C
C      TRIANGLE SIDE COS FORM
      TSLF (U,V,W)   = SQRT(U*U+V*V-2.*U*V*COS(W))
C      RADIANS
      RD = 57.296
      INTEGER SYST
      READ (5,50) IB
50     FORMAT (I3)
42     READ ( 5,43)  SYST
43     FORMAT (I4)
      WRITE (6,44) SYST
44     FORMAT(20H  RNME2  SYSTEM NO. 14 // )
17     READ (5,36) GAM,ACC,XCH,PHI,FA,AC1,CC,C2H
36     FORMAT ( 6F10.4 / 2F10.4 )
      WRITE (6,24)  GAM,ACC,XCH,PHI,FA,AC1,CC,C2H
240    FORMAT ( 7H  GAM= F10.4, 7H  ACC= F10.4, 7H  XCH= F10.4,
1       7H  PHI= F10.4, 6H  FA= F10.4, 7H  AC1= F10.4, /
2       6H  CC= F10.4 , 7H  C2H= F10.4 ///)
      GAM =GAM/RD
      ACC =ACC/RD
      XCH =XCH/RD
      PHI =PHI/RD
C      SAVFN = SUM AVFN
      COMMON SAVFN1,SAVFN2
      QR = 0.
      SAVFN1 = 0.
      SAVFN2 = 0.
C      SMR6 = SUM OF R**6
      SMR6 = 0.
      M = 20
      DO 40 MU= 1,360,M
      EMU= FLOAT(MU)
      EMU =EMU/RD
      XH = C2H*SIN(XCH)
      XY = XH*COS(EMU)
      YH = XH* SIN(EMU)
      C2Y = SQRT(C2H*C2H - YH*YH)
C      SINE XCY
      SNXCY = XY / C2Y
C      COS XCY
      CSXCY = SQRT(1.- SNXCY**2)
      C1Y2 = CC*CC + C2Y*C2Y + 2.*CC*C2Y*CSXCY
      C1Y = SQRT(C1Y2)
      SNNU = C2Y*SNXCY/ C1Y
      ENU = ASNF(SNNU)
      ALF = ACC- ENU
      AY = TSLF( AC1, C1Y, ALF)
      SNTET = TSNF( C1Y,ALF,AY)
      TET = ASNF(SNTET)
      BET = GAM + TET
      DY = AY * SIN(BET)
      AO = AY* COS(BET)
      FO = FA + AO
      YH2 = YH*YH
      DY2 = DY*DY
      D = SQRT(DY2 + YH2)
      RY = SQRT( DY2 + FO*FO )
      R = SQRT(RY*RY + YH2)
      S = FO * SIN(PHI)
      R6 = R**6
      SMR6 = SMR6 + R6
      CALL PSUCON ( R, D, S, PHI )
      QR = QR+1.
40     CONTINUE

```



```

XAVFN1 = SAVFN1/QR
XAVFN2 = SAVFN2/QR
AVSMR6 = SMR6 / QR
WRITE (6,82) XAVFN1,XAVFN2
82  FORMAT ( 10H  XAVFN1= E15.4, 10H  XAVFN2= G15.4 // )
WRITE (6,233) AVSMR6
233  FORMAT (10H  AVSMR6= E15.4 ////)
      IB = IB + 1
      IF (10-IB) 47,47,42
47   CONTINUE
      STOP
      END
      SUBROUTINE PSUCON ( R, D, S, PHI )
      COMMON SAVFN1,SAVFN2
C     ARCSINE
C     ASNF(T) = ATAN (T/SQRT( 1.- T*T))
      RADIANS
      RD = 57.296
      CSPHI = COS(PHI)
10   SUMFN1=0.
      SUMFN2=0.
      CD = 0.
      G=0.
      N = 45
      L = 360
      DO 8 J= 1,L,N
      THETA = FLOAT (J)
      THETA = THETA/RD
      Q = D* COS(THETA)
      Z = Q * CSPHI
      A=S-Z
      C = D* SIN(THETA)
      SNCHI = A/R
      CHI = ASNF (SNCHI)
      X=R**3
      Y=SNCHI**2
      FN1=(3.*Y-1.)/X
      SUMFN1=SUMFN1+FN1
      P = R* COS(CHI)
      SNOMG = C/ABS(P)

      OMEGA = ASNF(SNOMG)
      CSCHI=1.-Y
      FN2=CSCHI*(1.-2.*SNOMG**2)/X
      SUMFN2=SUMFN2+FN2
      G = G+1.
8   CONTINUE
      AVFN1 = SUMFN1/G
      AVFN2 = SUMFN2/G
      SAVFN1 = SAVFN1 + AVFN1
      SAVFN2 = SAVFN2 + AVFN2
      RETURN
      END

```

CHAPTER VIExperimentalPhysical Measurements

The solid state diffuse reflectance spectra were measured on either a Beckman D.K.2 recording spectrophotometer in the region 4,000 - 28,000  $\text{cm}^{-1}$ , or on a Unicam S.P. 500 spectrophotometer in the region 10,000 - 28,000  $\text{cm}^{-1}$ .

Reflectance spectra at low temperatures were obtained on the former machine, the sample being immersed in liquid nitrogen, or a suitable cooling mixture, using a dewar type apparatus, similar to that described by J.P. Fackler<sup>143</sup>. A cross sectional diagram of this apparatus, and the sample mounting, is shown in Fig. Vl.1. The front silica plate is attached with standard silicone grease. It was found that this type of grease was not suitable for sealing the junction of the back, inner, plate with the apparatus as when immersed in liquid nitrogen, the solidification and fracturing of the grease at points where it was appreciably thick, led to loss of vacuum. Other commercial greases tried

were also unsatisfactory, however a grease compounded of a 15% solution of soap in glycerine<sup>144</sup> was found to be effective. The sample is held in an aluminium dish, which is attached to the back silica plate by a layer of silicone grease round the flattened rim of the dish.

A section of standard white tile replaces the sample for base line measurements at room and low temperatures. It was found that to obtain spectra giving the same relative intensities as those given by spectra taken under normal operating conditions, a compensating tube lined with aluminium foil had to be placed on the reference port, to balance the tube in the apparatus. Aluminium has a weak band at  $\sim 12,500 \text{ cm}^{-1}$ , which increases in intensity on lowering the temperature, this was balanced by increasing the length of the tube on the reference port.

Solution spectra were taken on a Perkin-Elmer 350 recording spectrophotometer in the range 8,000 - 28,000  $\text{cm}^{-1}$ , or on a Unicam S.P. 500 in the range 10,000 - 28,000  $\text{cm}^{-1}$ .

For magnetic susceptibility measurements at room temperature, a standard Gouy balance, with a permanent magnet, was used. To determine suscep-

tibilities in the temperature range 77 - 300°K, use was made of a Gouy balance with a cryostat unit, set up by Dr. D. Forster, of essentially the same design as that described by Figgis and Nyholm<sup>145</sup>. The magnetic fields given by the electro-magnet for various currents were calibrated using an aqueous solution of 'Analar' nickel chloride, the susceptibility of which is accurately known<sup>146</sup>. The found field values then gave gram susceptibilities of  $16.52(\pm 0.25) \times 10^{-6}$  c.g.s.u at 293°K for  $\text{CoHg}(\text{SCN})_4$  and  $10.75(\pm 0.18) \times 10^{-6}$  c.g.s.u at 298°K for  $\text{Ni}(\text{ethylenediamine})_3\text{S}_2\text{O}_3$ , in agreement with the literature values of  $16.44 \times 10^{-6}$ <sup>147</sup> and  $10.82 \times 10^{-6}$ <sup>148</sup>, respectively at these temperatures.

The thermocouple, for temperature measurements, was calibrated with  $\text{CoHg}(\text{SCN})_4$ , taking a  $\theta$  value of  $-10^\circ(\pm 1^\circ)$ <sup>147</sup>. The Gouy tubes used were made from Perspex.

It is estimated that the error on the field value, at 8 amps, was  $\sim \pm 1.5\%$ . Weighings were made to  $\pm 0.00005\text{g}$ .

A note may be made here in connection with the timing of measurements, as this is of some significance in connection with the compounds discussed in Chapter III. The measuring of the susceptibilities at various fields, for a given temperature, occupied about

15-20 minutes. Lowering the temperature  $30^{\circ}$  in the region of  $300^{\circ}\text{K}$  took a few minutes, and at  $150^{\circ}\text{K}$  about 15 minutes. The sample was allowed to equilibrate, at a given temperature, for about 30 minutes before measurements were taken.

Nuclear magnetic resonance spectra were obtained on a Varian Associates spectrometer operating at 56.4 m.c.s. (Some of the spectra were also measured at 40 m.c.s.). The spectra were calibrated by the standard modulated side band technique, using tetramethylsilane (TMS) as an internal reference.

Solution susceptibilities were measured by the n.m.r. method of Evans<sup>65</sup>, using spinning concentric tubes, and TMS as internal reference.

Infrared spectra, in the region  $4,000 - 400 \text{ cm}^{-1}$ , were taken on a Grubb-Parsons Spectromaster grating spectrometer, using potassium bromide discs and Nujol, or hexachlorobutadiene, as mulling agent. In the region  $450-200 \text{ cm}^{-1}$ , spectra were measured with a Grubb-Parsons D.M.2 double-beam grating instrument, using polythene discs and Nujol as mulling agent.

X-ray powder photographs were taken on an Enraf-Nonius Guinier-De Wolff camera, or a Phillips Debye-Scherrer camera, using fine beam iron or copper  $K_{\alpha}$

radiation.

Powder photographs, to detect phase-changes, were taken at room temperature and at  $\sim 140^{\circ}\text{K}$ , using a front plate camera. The sample was mounted in a Lindemann tube, and cooled by a stream of dry nitrogen gas, which had been passed through a bath of liquid nitrogen. Temperatures were measured with a calibrated thermocouple.

Conductances were measured with a Philips PR 9500 bridge, and a standard cell.

Fig. VI.1

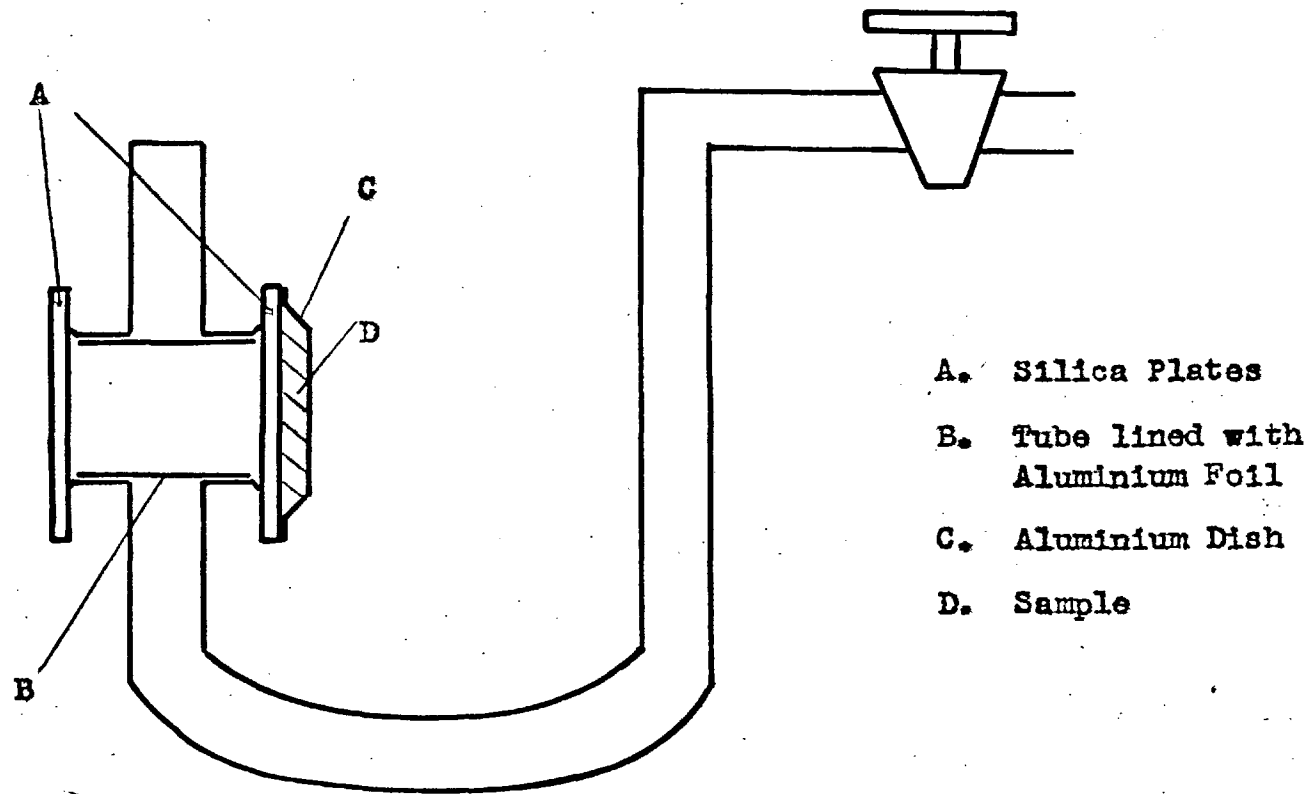


Fig. VI.1 Dewar Unit for Low Temperature Reflectance Spectra.

## Analyses

(For details on the analytical methods see Ref.85)

Metals were determined as follows

Nickel (II): gravimetrically, following precipitation  
with dimethylglyoxime

Cobalt (II): volumetrically, EDTA using murexide  
indicator

Iron (II): volumetrically, ceric sulphate and  
back titration with ferrous ammonium  
sulphate; o-phenanthroline indicator.

Halides and thiocyanates were determined volumetrically  
by Volhard's method.

Carbon, hydrogen, nitrogen and oxygen analyses were  
carried out by the Microanalytical Laboratory, Imperial  
College.

## Preparation of the Compounds

### Chapter I

#### Ni(pyridine)<sub>2</sub>Cl<sub>2</sub>

A solution of pyridine (1.2 g.) in ethanol (5 ml.),  
was added to a solution of nickel chloride hexahydrate  
(3.55 g.) in ethanol (20 ml.). The heavy pale yellow-  
green precipitate, which formed with evolution of heat,  
was filtered off, washed with ethanol containing a small  
amount of pyridine, and dried in vacuo.



(Found: C, 41.6; H, 3.6; Cl, 24.2; Ni, 20.2.

Calc. for  $C_{10}H_{10}Cl_2N_2Ni$ : C, 41.9; H, 3.5; Cl, 24.4;

Ni, 20.4%).

Ni(pyridine)<sub>2</sub>Br<sub>2</sub>

The pale yellow compound was obtained by a method analogous to that for Ni(pyridine)<sub>2</sub>Cl<sub>2</sub>.

(Found: C, 31.5; H, 2.8; Br, 42.1; Ni, 15.3.

Calc. for  $C_{10}H_{10}Br_2N_2Ni$ : C, 31.9; H, 2.7; Br, 42.4;

Ni, 15.6%)

Ni(benzothiazole)<sub>2</sub>Cl<sub>2</sub>

The pale yellow solid was obtained by a method analogous to that for Ni(pyridine)<sub>2</sub>Cl<sub>2</sub>.

(Found: C, 42.6; H, 2.85; Cl, 17.5; Ni, 14.6.

Calc. for  $C_{14}H_{10}N_2S_2Cl_2Ni$ : C, 42.0; H, 2.5; Cl, 17.7;

Ni, 14.7%).

Ni(benzothiazole)<sub>2</sub>Br<sub>2</sub>

Benzothiazole (2.73 ml.) was added to a solution of nickel bromide hexahydrate (3.27 g.) in ethanol

(25 ml). The resultant green solution was kept at 5°C, when yellow needles slowly crystallised out.

(Found: C, 34.1; H, 2.0, Calc. for  $C_{14}H_{10}N_2S_2Br_2Ni$ :  
C, 34.4; H, 2.1%).

### Ni(pyridine)Cl<sub>2</sub>

Ni(pyridine)<sub>2</sub>Cl<sub>2</sub> was heated at 120°C to constant weight (Weight loss, 27.5; calc. 27.5%).

(Found: C, 28.6; H, 2.4; Ni 28.2. Calc. for  $C_5H_5Cl_2NNi$ : C, 28.8; H, 2.4; Ni, 28.2%).

### Ni(imidazole)Cl<sub>2</sub>

A solution of nickel chloride hexahydrate (4.75 g.) and imidazole (1.4g.) in ethanol (15 ml) was evaporated to dryness. The pale yellow solid obtained was washed with acetone and ethanol, and dried at 120°C.

(Found: Cl, 35.8; Ni, 29.7. Calc. for  $C_3H_4N_2Cl_2Ni$ :  
Cl, 35.9; Ni, 29.7%).

The methods for the preparation of Ni(imidazole) Br<sub>2</sub> (pinkish-orange), Ni(benzimidazole) Cl<sub>2</sub> (yellow), and Ni(benzimidazole) Br<sub>2</sub> (pinkish-orange) were exactly

analogous to that for  $\text{Ni}(\text{imidazole})\text{Cl}_2$ .

$\text{Ni}(\text{imidazole})\text{Br}_2$

(Found: Br, 55.6; Ni, 20.45. Calc. for  $\text{C}_3\text{H}_4\text{N}_2\text{Br}_2\text{Ni}$ :  
Br, 55.8; Ni, 20.5%).

$\text{Ni}(\text{benzimidazole})\text{Cl}_2$

(Found: C, 34.45; H, 2.4; Cl, 28.5; Ni, 23.6. Calc.  
for  $\text{C}_7\text{H}_6\text{N}_2\text{Cl}_2\text{Ni}$ : C, 34.0; H, 2.5; Cl, 28.7; Ni, 23.7%).

$\text{Ni}(\text{benzimidazole})\text{Br}_2$

(Found: C, 24.7; H, 1.9; Br, 47.7; Ni, 17.4. Calc.  
for  $\text{C}_7\text{H}_6\text{N}_2\text{Br}_2\text{Ni}$ : C, 25.0; H, 1.8; Br, 47.45; Ni, 17.4%)

$\text{Ni}(\text{quinoline})\text{Cl}_2$

$\text{Ni}(\text{quinoline})_2\text{Cl}_2^2$  was heated at  $120^\circ\text{C}$  to constant weight (weight loss, 33.1; calc. 33.4%), to give a pink product.

(Found): C, 42.0; H, 2.6; Ni, 22.7. Calc. for  
 $\text{C}_9\text{H}_7\text{NCl}_2\text{Ni}$ : C, 41.75; H, 2.7; Ni 22.7%).

Ni(quinoline)Br<sub>2</sub>

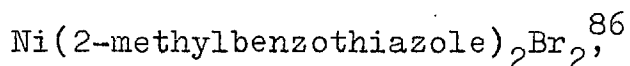
Ni(quinoline)<sub>2</sub>Br<sub>2</sub><sup>2</sup> was heated at 100°C to constant weight (weight loss, 27.1; calc., 27.1%), to give a pink product.

(Found: C, 31.0; H, 2.1; Br, 46.05; Ni, 16.9. Calc. for C<sub>9</sub>H<sub>7</sub>Br<sub>2</sub>NNi: C, 31.1; H, 2.0; Br, 46.0; Ni, 16.9%).

Ni(2-methylbenzothiazole)Cl<sub>2</sub>

The method of preparation was analogous to that used for Ni(imidazole)Cl<sub>2</sub>. The pink product was formed just before the solution reached dryness, and was filtered off.

(Found: C, 34.8; H, 2.8; Cl, 25.5; Ni, 21.2. Calc. for C<sub>8</sub>H<sub>7</sub>NSCl<sub>2</sub>Ni: C, 34.5; H, 2.5; Cl, 25.4; Ni, 21.05%).

Ni(2-methylbenzothiazole)Br<sub>2</sub>

was heated at 120°C to constant weight, with the formation of a pink product. (Weight loss, 29.1; calc., 28.9%).

(Found: Br, 43.6; Ni, 16.0. Calc. for C<sub>8</sub>H<sub>7</sub>NSBrNi: Br, 43.5; Ni, 15.9%).

A sample of Ni(2-methylbenzothiazole)Br<sub>2</sub> was also prepared following the method given for Ni(imidazole)Cl<sub>2</sub>.

(Found: Br, 43.5; Ni, 15.8%. Calc. as above).

Ni(3-methylisoquinoline)Cl<sub>2</sub>

Pink solid prepared by method analogous to that for Ni(imidazole)Cl<sub>2</sub>. (Found: Cl, 26.0; Ni, 21.5. Calc. for

C<sub>10</sub>H<sub>9</sub>NCl<sub>2</sub>Ni: Cl, 26.0; Ni, 21.5%).

Ni(3-methylisoquinoline)Br<sub>2</sub>

Pink solid prepared by method analogous to that for Ni(imidazole)Cl<sub>2</sub>.

(Found: Br, 44.25; Ni, 16.25. Calc. for C<sub>10</sub>H<sub>9</sub>NBr<sub>2</sub>Ni:

Br, 44.2; Ni, 16.2%).

Chapter II

Ni(N-methylimidazole)<sub>2</sub>Br<sub>2</sub>

A solution of N-methylimidazole (1 ml.) in acetone (3 ml.) was added to a solution of nickel bromide hexahydrate (3.27 g.) in acetone (10 ml.), to give a deep

blue solution. On standing a green oil was formed, which on stirring gave a green amorphous solid. This solid was filtered off, and washed with a little acetone. The infrared spectrum of this compound indicated the presence of water and acetone, and it was heated at 100°C till rapid weight loss ceased, (weight loss 10.3%), an intense blue product being formed.

(Found: C, 25.2; H, 3.3; Br, 42.0. Calc. for  $C_8H_{12}N_2Br_2Ni$ : C, 25.1; H, 3.2; Br, 41.8%).

Ni(2-methylimidazole)<sub>2</sub>Br<sub>2</sub>

It was not found possible to prepare this complex directly, but it was obtained by heating the 4:1 complex, which was prepared as follows.

A solution of 2-methylimidazole (3.2 g.) in acetone (8 ml.) was added to a solution of nickel bromide hexahydrate (3.27 g.) in acetone (10 ml.). A deep blue solution was formed, from which a green solid crystallised out on standing. This was filtered off, washed with a small quantity of cold acetone, and dried in vacuo.

(Found: Br, 29.2; Ni, 10.7: Calc. for  $C_{16}H_{24}N_8Br_2Ni$ :  
Br, 29.2; Ni, 10.7%).

This green compound was heated at 150°C for 3 days, to give a dark blue solid (Weight loss, 30; calc. 30%).

(Found: C, 25.4; H, 3.5. Calc. for  $C_8H_{12}N_2Br_2Ni$ :  
C, 25.1; H, 3.2%).

Some of the complexes examined in this chapter were prepared by Dr. M. Goodgame. The methods of preparation have been published for the following nickel complexes  $NiL_2X_2$  (L = 2-methylbenzimidazole, X = Cl, Br)<sup>86</sup> (L = 3-methylisoquinoline, X = Cl, Br)<sup>86</sup>. Three of the complexes have not been reported,  $NiL_2X_2$  (L = benzimidazole, X = Br, I) and  $[Et_4N][Ni(\text{benzimidazole})Br_3]$ . The experimental details are given below.

#### $Ni(\text{benzimidazole})_2Br_2$

A solution of benzimidazole (2.4 g) and nickel bromide hexahydrate (3.5 g.) in ethanol (5 ml.) was evaporated to dryness. The resulting solid was dissolved in acetone (8 ml.), filtered, and the solution heated to boiling. Hot carbon tetrachloride (15 ml.) was added, and the solvent decanted, leaving a blue oil. This was triturated with successive portions of hot carbon tetrachloride until it solidified, when

it was filtered off, and dried in vacuo at 100°C.

(Found: C, 36.9; H, 2.6; Ni, 12.4. Calc. for  $C_{14}H_{12}N_4Br_2Ni$ : C, 37.0; H, 2.7; Ni, 12.3%).

Ni(benzimidazole)<sub>2</sub>I<sub>2</sub>

A solution of nickel nitrate hexahydrate (3.2 g.) in acetone (5 ml.) was added to a solution of sodium iodide (3.3 g.) in acetone (20 ml.), chilled and dried over molecular sieves for several hours, then filtered into a solution of benzimidazole (2.36 g.) in acetone (25 ml.). The deep green solution was evaporated to dryness, and the resultant solid dried at 120°C. It was then extracted with 20 ml. of acetone, the filtered extract heated to boiling, and the solid precipitated by addition of hot carbon tetrachloride (50 ml.). The hygroscopic solid was washed by decantation with hot carbon tetrachloride, and dried in vacuo.

(Found: C, 30.6; H, 2.25; Ni, 10.8. Calc. for  $C_{14}H_{12}I_2N_4Ni$ : C, 30.6; H, 2.20; Ni, 10.7%).



[Et<sub>4</sub>N][Ni(benzimidazole)Br<sub>3</sub>]

A solution of benzimidazole (1.18 g.) and tetramethylammonium bromide (2.10 g.) in n-butanol (10 ml.) was added to one of Nickel bromide trihydrate (2.73 g.) in n-butanol (30 ml.). Benzene (10 ml.) was added, and the solution slowly evaporated to about 20 ml., when a blue oil began to form. It was left to cool, when the oil crystallised. The solvent was decanted, the crystals were washed with benzene, and dried in vacuo.

(Found: C, 33.0; H, 5.1; N, 7.45. Calc. for C<sub>15</sub>H<sub>26</sub>Br<sub>3</sub>N<sub>3</sub>Ni: C, 32.95; H, 4.80; N, 7.7%).

[CH<sub>3</sub>(C<sub>6</sub>H<sub>5</sub>)<sub>3</sub>As]<sub>2</sub>[NiCl<sub>4</sub>]

Prepared following the method of D.M.L. Goodgame et al.<sup>53</sup> (Found: C, 54.1; H, 4.2; Ni, 7.0. Calc. for C<sub>38</sub>H<sub>36</sub>As<sub>2</sub>Cl<sub>4</sub>Ni: C, 54.1; H, 4.3; Ni, 7.0%).

Ni(benzothiazole)<sub>2</sub>I<sub>2</sub>

A solution of nickel iodide (0.01 M), in acetone (22 ml.) was prepared as described above for the preparation of Ni(benzimidazole)<sub>2</sub>I<sub>2</sub>. Benzothiazole (2.2 ml.) was added to the filtered nickel iodide solution,

and the resultant brown solution evaporated to about 8 ml., when a dark brown solid was precipitated. This was filtered off, washed with dichloromethane containing a small quantity of benzothiazole, and dried in vacuo.

(Found: C, 28.8; H, 1.65; Ni 10.0. Calc. for  $C_{14}H_{10}N_2S_2I_2Ni$ : C, 28.85; H, 1.7; Ni, 10.1%).

Ni(2-methylbenzimidazole) $_2I_2$

This dark green complex was prepared by a method analogous to that for Ni(benzimidazole) $_2I_2$ , except that benzene was used as the tritulant.

(Found: C, 33.4; H, 2.8; Ni, 10.0. Calc. for  $C_{16}H_{16}N_4I_2Ni$ : C, 33.4; H, 2.8; Ni, 10.2%).

The preparations of some of the cobalt complexes examined in Chapter II have been given previously.  $CoL_2X_2$  (L = benzimidazole, X = Cl, Br)<sup>62</sup> and  $[Et_4N][Co(benzimidazole)Br_3]$ <sup>62</sup>.

Co(N-methylimidazole) $_2Cl_2$

N-methylimidazole (1 ml.) in ethanol (2 ml.) was added to a solution of cobalt chloride hexahydrate (2.37 g.) in ethanol (5 ml.). A blue crystalline solid was

precipitated which was filtered off, washed with a small quantity of ice cold ethanol, and dried in vacuo.

(Found: Cl, 24.1; Co, 20.3. Calc. for  $C_8H_{12}N_4Cl_2Co$ :  
Cl, 24.1; Co, 20.3%)

Co(N-methylimidazole)<sub>2</sub>Br<sub>2</sub>

Method analogous to that for the chloride complex, but using acetone as the solvent. The blue precipitate was formed after allowing the mixed solutions to stand for some minutes.

(Found: Br, 41.9; Co, 15.4. Calc. for  $C_8H_{12}N_4Br_2Co$ :  
Br, 41.8; Co, 15.6%).

Co(2-methylimidazole)<sub>2</sub>X<sub>2</sub>, (X = Cl, Br) were prepared by Miss K.A. Price of this Department, using similar methods to those given above for the N-methylimidazole complexes. Cobalt and halide analyses were good.

Co(2-methylbenzimidazole)<sub>2</sub>Cl<sub>2</sub>

A solution of 2-methylbenzimidazole (2.64 g.) in ethanol (8 ml.) was added to a solution of cobalt chloride hexahydrate (2.37 g.) in ethanol (5 ml.).

The blue solution obtained was evaporated to about 5 ml., benzene added (4 ml.), and the solution evaporated to a small bulk. The oil formed was triturated with benzene, and the intense blue solid obtained dried at 120°C.

(Found: Cl, 18.1; Co, 14.75. Calc. for  $C_{16}H_{16}N_4Cl_2Co$ :  
Cl, 18.0; Co, 14.95%).

Co(2-methylbenzimidazole)<sub>2</sub>Br<sub>2</sub>

A solution of 2-methylbenzimidazole (2.64 g.) in ethanol (8 ml.), was added to a solution of cobalt bromide hexahydrate (3.27 g.) in ethanol (5 ml.). The deep blue solution was placed in an ice box for 24 hours., when an intense blue crystalline solid was formed. This was filtered off, washed with a little ice cold ethanol, and dried in vacuo.

(Found: Br, 32.7; Co, 12.2. Calc. for  $C_{16}H_{16}N_4Br_2Co$ :  
Br, 33.1; Co 12.2%).

Chapter III (See Fig.3.1 for symbols associated with  
the compounds)

Ni(benzimidazole)<sub>4</sub>Cl<sub>2</sub>. 2 Acetone [BC]

Benzimidazole (8.3 g.) was dissolved in acetone

75 ml.). This solution was added to powdered nickel chloride hexahydrate (3.6 g.), and the mixture refluxed for 36 hours.

The immediate product of initial refluxing was a pale white precipitate, which altered to a bright green solid after 15 minutes. As the refluxing was continued the product became darker, and finally attained an olive-green colour after about 15 hours, which remained unchanged during the remainder of the reflux.

The flask containing the solid products and solution, was corked and allowed to stand for 12 days, when there was a slow change to a blue crystalline solid. This was filtered off, washed with acetone, and dried for a short time in vacuo.

(Found: C, 54.7; H, 5.05; N, 15.4; O, 4.24; Cl, 9.6; Ni, 8.0. Calc. for  $C_{34}H_{36}N_8O_2Cl_2$ : C, 56.85; H, 5.05; N, 15.6; O, 4.45; Cl, 9.9; Ni, 8.2%).

Ni(benzimidazole)<sub>2</sub>Cl<sub>2</sub> · 2 Acetone [GC]

The blue isomer BC was dissolved in boiling acetone (70 ml.) till the solution was saturated. Benzimidazole (1.5 g.) in boiling acetone (40 ml.) was added, and the solution allowed to cool slowly. (The flask was placed

in a heating mantle, the temperature of which was reduced from  $\sim 50^{\circ}\text{C}$  to room temperature over a period of 12 hours). Green monoclinic crystals were formed, which were filtered off, washed with a small quantity of ice-cold acetone, and dried for a short time in vacuo.

(Found: C, 56.75; H, 4.85; O, 4.5; Ni, 8.15%. Calc. as above).

The amorphous sample produced on cooling GC to  $77^{\circ}\text{K}$  (see Chapter III) was analysed to check for loss of acetone.

(Found: O, 4.8, Cl, 9.5%. Calc. as above).

Ni(benzimidazole)<sub>4</sub>Cl<sub>2</sub> · 2 Acetone [OC]

This was prepared following the first part of the preparation for the blue isomer given above. The olive-green compound was filtered off, washed with a small quantity of acetone, and dried for a short time in vacuo.

(Found: C, 55.5; H, 5.0; O, 4.3; Ni, 8.2%. Calc. as above).

Ni(benzimidazole)<sub>4</sub>Cl<sub>2</sub> · ~1 Acetone. [YC]

This was obtained from the olive-green solvate, given above, by allowing the latter to stand at room temperature and pressure for many days, or under vacuum for 2 days.

(Found: O, 2.6; Cl, 10.6. Calc. for C<sub>31</sub>H<sub>30</sub>N<sub>8</sub>OCl<sub>2</sub>Ni:  
O, 2.4; Cl, 10.7%).

Ni(benzimidazole)<sub>4</sub>Br<sub>2</sub> · 2 Acetone [BB]

Benzimidazole (6 g.) was dissolved in acetone (50 ml). This solution was added to powdered nickel bromide hexahydrate (3.27 g.), and the mixture refluxed for 4 hours. A green precipitate was formed initially, which on further refluxing altered to a pale blue solid. The resulting mixture was allowed to stand for three days, the product then being filtered off, washed with a small quantity of acetone, and dried for a short time in vacuo.

(Found: C, 47.0; H, 4.5; O, 3.9; Br; 19.8; Ni, 7.2. Calc. for C<sub>34</sub>H<sub>36</sub>N<sub>8</sub>O<sub>2</sub>Br<sub>2</sub>Ni: C, 50.5; H, 4.5; O, 4.0; Br, 19.8; Ni, 7.3%).

Desolvated CompoundsChloride Complexes

These were obtained by heating a solvated complex in a container formed by drawing out an ignition tube, so that the aperture at the top of the tube was small. The tube was filled to about  $\frac{1}{4}$  of its length, and placed in a weighing bottle, which was partially filled with porcelain chips. The sample was heated till there was no further loss of weight.

The product, starting material, temperature of desolvation, weight loss on heating, and analysis of the product, are summarised in the Table below.

Type	Ni(benzimidazole) <sub>4</sub>	Cl <sub>2</sub>	Calc. Weight loss %	Calc. Analysis %		
Product Compound	Starting Material	Temp. (°C)	Found Wt. Loss	Found C	Found H	Analysis Ni
	(C <sub>28</sub> H <sub>24</sub> N <sub>8</sub> Cl <sub>2</sub> Ni)		16.2%	55.85	3.8	9.75
ΔCl, B	BC	130	16.0	55.7	3.8	9.7
ΔCl, G	GC	130	16.1	55.7	3.8	9.7
ΔCl, O	OC	110	16.0	55.4	4.1	9.8
ΔC2	BC	110	15.8	55.65	4.4	9.7
ΔC3	BC	75	16.1	55.9	4.3	9.8



Bromide Complexes

These were obtained by heating the solvate in a similar manner to that described above for the chloride complexes. There were specific conditions in connection with the preparation of certain of the complexes, these being given in the notes below the table.

Type	Ni(benzimidazole) <sub>4</sub> Br <sub>2</sub>	Calc. Weight loss	Calc. Analysis C.	H.	% Ni	
	(C <sub>28</sub> H <sub>24</sub> N <sub>8</sub> Br <sub>2</sub> Ni)	14.4%	48.7	3.5	8.5	
Product Compound	Starting Material	Temp. (°C)	Found Wt. Loss	Found C.	Analysis H.	Ni
ΔB1, X <sup>(a)</sup>	BB	140/160	14.2	48.1	3.8	8.5
ΔB1, Y <sup>(a)</sup>	"	140/160	14.3	48.7	3.45	8.4
ΔB2	"	140	14.4	48.7	3.6	8.4
ΔB3 <sup>(b)</sup>	"	140	14.3	48.6	3.5	8.5

(a) The solvate BB was heated at 140°C for about 15 minutes, in a vessel as described above, the colour changing from pale blue to blue-brown. The sample was then transferred, without cooling, to 160°C for 1 hour, when the compound turned to a green colour. On cooling the complex assumed a pale yellow-green colour.

(b) The solvate BB was heated in an uncapped weighing bottle.

Ni(benzimidazole)<sub>4</sub>Br<sub>2</sub> · 3 CHCl<sub>3</sub>

A sample of Ni(benzimidazole)<sub>4</sub>Br<sub>2</sub> · 2 Acetone [BB] was placed in chloroform, and sealed up. Over a period of about three months, the blue crystalline acetone solvate changed to well formed orange crystals.

(Found: C, 35.8; H, 2.55; Br, 15.4; Ni 5.35. Calc. for C<sub>31</sub>H<sub>37</sub>N<sub>8</sub>Cl<sub>9</sub>Br<sub>2</sub>Ni: C, 35.5; H, 2.6; Br, 15.2; Ni, 5.6%). On heating at 110°C the orange crystals gave a blue-green product (Weight loss, 33.7; Calc., 34.1%).

(Found: C, 49.5; H, 3.35. Calc. for C<sub>28</sub>H<sub>24</sub>N<sub>8</sub>Br<sub>2</sub>Ni.  
C, 48.7; H, 3.5%).

Ni(benzimidazole)<sub>4</sub>I<sub>2</sub> · 3 Acetone

Ni(benzimidazole)<sub>2</sub> I<sub>2</sub> (1 g.), (see Chapter II above), was dissolved in acetone (25 ml.) and the solution filtered. Benzimidazole (1 g.) was dissolved in the filtrate and the resultant solution chilled for seven days. Pale green crystals were formed which were filtered off, washed with a small quantity of acetone, and dried for a short time in vacuo.

(Found: O, 4.9; I, 26.5. Calc. for C<sub>37</sub>H<sub>42</sub>N<sub>8</sub>O<sub>3</sub>I<sub>2</sub>Ni:  
O, 5.0; I, 26.5%).

Ni(benzimidazole)<sub>4</sub>I<sub>2</sub>

On heating the above acetone solvate at 110°C an orange compound was obtained (Weight loss, 18.0, Calc. 18.2%)

(Found: C, 43.5; H, 3.0. Calc. for C<sub>28</sub>H<sub>24</sub>N<sub>8</sub>I<sub>2</sub>Ni:

C, 42.8; H, 3.1%)

Chapter IVIron (II) Complexes

Certain general features in the preparation of the iron (II) complexes may be noted. The solvents used were deoxygenated by boiling, and passing of nitrogen gas. Ferrous chloride solutions were reduced by standing over iron powder, under nitrogen gas, for 12 hours before use. Ferrous bromide was prepared directly in solution by the addition of 'Analar' bromine, in small portions, to excess iron powder in ethanol, under nitrogen gas, then shaking till a green solution was obtained. This was then filtered directly into the solution of ligand.

Fe(benzothiazole)<sub>2</sub>Cl<sub>2</sub>

Ferrous chloride (1.95 g.) in ethanol (10 ml.) was filtered under nitrogen, into a solution of benzothiazole (2.16 ml.) in ethanol (5 ml.). A yellow precipitate was rapidly formed, this was filtered off, washed with a small quantity of ethanol, and dried in vacuo.

(Found: Cl, 17.75; Fe, 14.0. Calc. for C<sub>14</sub>H<sub>10</sub>N<sub>2</sub>S<sub>2</sub>Cl<sub>2</sub>Fe:  
Cl, 17.85; Fe, 14.1%).

Ferrous (benzothiazole)<sub>2</sub>Br<sub>2</sub>

Pale yellow crystalline solid prepared by a method analogous to that for the chloride.

(Found: Br, 32.7; Fe, 11.5. Calc. for C<sub>14</sub>H<sub>10</sub>N<sub>2</sub>S<sub>2</sub>Br<sub>2</sub>Fe:  
Br, 32.9; Fe, 11.5%)

The complexes Fe L<sub>2</sub>X<sub>2</sub> (L = 4-cyanopyridine, 3,5-dichloropyridine; X = Cl, Br) were prepared by methods analogous to that given above for Ni(benzothiazole)<sub>2</sub>Cl<sub>2</sub>.

Fe(4-cyanopyridine)<sub>2</sub>Cl<sub>2</sub>

(Found: Cl, 20.85; Fe, 16.85. Calc. for C<sub>12</sub>H<sub>8</sub>N<sub>4</sub>Cl<sub>2</sub>Fe:  
Cl, 21.15; Fe, 16.7%)

Fe(4-cyanopyridine)<sub>2</sub>Br<sub>2</sub>

(Found: Br, 37.25; Fe, 12.75. Calc. for C<sub>12</sub>H<sub>8</sub>N<sub>4</sub>Br<sub>2</sub>Fe:  
Br, 37.70; Fe, 13.2%)

Fe(3,5-dichloropyridine)<sub>2</sub>Cl<sub>2</sub>

(Found: Cl, (anionic) 16.5; Fe, 12.7 Calc. for  
C<sub>10</sub>H<sub>6</sub>Cl<sub>6</sub>N<sub>2</sub>Fe: Cl, (anionic) 16.7; Fe, 13.1%)

Fe(3,5-dichloropyridine)<sub>2</sub>Br<sub>2</sub>

(Found: C, 23.2; H, 1.40; Br, 31.05 Calc. for  
C<sub>10</sub>H<sub>6</sub>N<sub>2</sub>Cl<sub>4</sub>Br<sub>2</sub>Fe: C, 23.5; H, 1.2; Br, 31.2%)

Fe(benzothiazole)<sub>4</sub>Br<sub>2</sub>

Ferrous bromide (3.3 g.) in ethanol (8 ml.) was filtered into a solution of benzothiazole (10 ml.) in ethanol (4 ml.). A yellow solid was precipitated, this was filtered off, washed with a small amount of ethanol, and dried in vacuo.

(Found: Br, 20.8; Fe, 7.5. Calc. for C<sub>28</sub>H<sub>20</sub>N<sub>4</sub>S<sub>4</sub>Br<sub>2</sub>Fe:  
Br, 21.1; Fe, 7.4%)

Fe(benzimidazole)<sub>4</sub>Br<sub>2</sub> · 3 Acetone

Ferrous bromide (2.3 g.) in acetone, was filtered into a solution of benzimidazole (4.72 g.) in acetone (35 ml.). The resultant solution was chilled for 24 hours, when yellow-brown crystals were formed. These were filtered off, washed with a small quantity of acetone, and dried in vacuo.

(Found: O, 5.45; Br, 18.6; Fe, 6.5. Calc. for C<sub>37</sub>H<sub>42</sub>N<sub>8</sub>O<sub>3</sub>Br<sub>2</sub>Fe: O, 5.6; Br, 18.5; Fe, 6.5%)

Fe(imidazole)<sub>4</sub>Cl<sub>2</sub> · 2 H<sub>2</sub>O

Ferrous chloride tetrahydrate (1 g.) in acetone (20 ml.), was filtered into a solution of imidazole (2.3 g.) in acetone (15 ml.)

An orange-brown solid was formed, this was filtered off after 15 minutes, washed with acetone, and dried in vacuo.

(Found: C, 32.3; H, 4.7; O, 7.35; Cl, 16.3. Calc. for C<sub>12</sub>H<sub>20</sub>N<sub>8</sub>O<sub>2</sub>Cl<sub>2</sub>Fe: C, 33.1; H, 4.6; O, 7.35; Cl, 16.3%).

Nickel (II) ComplexesNi(3,5-dichloropyridine)<sub>2</sub>Cl<sub>2</sub>

A solution of 3,5-dichloropyridine (2.96 g.) in ethanol (7 ml.) was added to a solution of nickel chloride hexahydrate (2.37 g.) in ethanol (8 ml.). A pale yellow precipitate was immediately formed, which was centrifuged off, washed with ethanol, and dried in vacuo.

(Found: N, 6.2; Cl, (anionic), 16.5; Ni, 13.7. Calc. for C<sub>10</sub>H<sub>6</sub>N<sub>2</sub>Cl<sub>6</sub>Ni: N, 6.6; Cl, (anionic) 16.65; Ni, 13.75%)

Ni(3,5-dichloropyridine)<sub>2</sub>Br<sub>2</sub>

Method of preparation analogous to that for the chloride complex.

(Found: N, 5.0; Br, 31.0; Ni, 11.3. Calc. for C<sub>10</sub>H<sub>6</sub>N<sub>2</sub>Cl<sub>4</sub>Br<sub>2</sub>Ni: N, 5.45; Br, 31.1; Ni, 11.4%)

Ni(4-cyanopyridine)<sub>4</sub>Br<sub>2</sub>

A solution of nickel bromide hexahydrate (1.6 g.) in ethanol (4 ml.) was added, with stirring, to a warm solution of 4-cyanopyridine (3.2 g.) in ethanol (14 ml.). A green crystalline solid was obtained, which was allowed

to stand in the solution for 2 hours. The complex was then filtered off, washed with a small quantity of ice cold ethanol, and dried in vacuo.

(Found: C, 45.1; H, 2.4; Br, 25.2. Calc. for  $C_{24}H_{16}N_8Br_2Ni$ : C, 45.4; H, 2.7; Br, 25.2%)

Ni(4-cyanopyridine)<sub>4</sub>I<sub>2</sub>

A solution of nickel iodide in ethanol was prepared metathetically, as described above for Ni(benzimidazole)<sub>2</sub>I<sub>2</sub>. The 4:1 complex was then prepared following a method analogous to that given above for the bromide.

(Found: C, 40.05; H, 2.4; I, 34.5. Calc. for  $C_{24}H_{16}N_8I_2Ni$ : C, 39.55; H, 2.2; I, 34.8%).

Ni(benzothiazole)<sub>4</sub>Br<sub>2</sub>

Benzothiazole (12 ml.) was added to a solution of nickel bromide hexahydrate (3.27 g.) in acetone (10 ml.), and the solution chilled overnight. A pale green solid was obtained, this was filtered off, washed with a small quantity of ice cold acetone, and dried for a short time in vacuo.



(Found: C, 44.5; H, 2.9; Ni, 7.7. Calc. for  
 $C_{28}H_{20}N_4S_4Br_2Ni$ : C, 44.3; H, 2.65; Ni, 7.7%)

$Ni(imidazole)_4Cl_2 \cdot 2H_2O$

A hot solution of imidazole (2.8 g.) in ethanol (10 ml.) was added to a hot solution of nickel chloride hexahydrate (2.37 g.) in ethanol (10 ml.). The resulting solution was boiled for 2 minutes, then allowed to cool slowly. A pale blue solid crystallised out. This was filtered off, washed with ice-cold ethanol, and dried in vacuo.

(Found: C, 33.0; H, 4.6; O, 8.6; Cl, 16.2; Ni, 13.5.  
 Calc. for  $C_{12}H_{20}N_8Cl_2O_2Ni$ : C, 32.9; H, 4.6; O, 7.3;  
 Cl, 16.2; Ni, 13.4%)

$Ni(imidazole)_6(ClO_4)_2$

A solution of nickel perchlorate hexahydrate (1.83 g.) in acetone (5 ml.), was added to a solution of imidazole (2.75 g.) in acetone (7 ml.). The blue solution formed was evaporated to about 5 ml. and chilled for 12 hours, when a blue solid crystallised out. This was filtered off, washed with acetone, and dried in vacuo.

(Found: C, 32.2; H, 3.9; Ni, 8.8. Calc. for  
 $C_{18}H_{24}N_{12}Cl_2O_8Ni$ : C, 32.45; H, 3.6; Ni, 8.8%)

REFERENCES

1. L.M. Venanzi, J. Chem. Soc., 719 (1958);  
M.C. Browning, J.R. Mellor, D.J. Morgan,  
S.A.J. Pratt, L.E. Sutton, and L.M. Venanzi,  
J. Chem. Soc., 693 (1962).
2. D.M.L. Goodgame and M. Goodgame, J. Chem. Soc.,  
207 (1963).
3. W. Ludwig and G. Wittmann, Helv. Chim. Acta.,  
47, 1265 (1964).
4. S. Buffagni, L.M. Vallarino, and J.V. Quagliano,  
Inorg. Chem., 3, 480 (1964); (a) idem, ibid.,  
3, 671 (1964).
5. L.M. Vallarino, W.E. Hill, and J.V. Quagliano,  
Inorg. Chem., 4, 1598 (1965).
6. H.C.A. King, E. Körös, S.M. Nelson, and T.M. Shepherd,  
Proc. 8 I.C.C.C., Vienna (1964).
7. A.B.P. Lever, ibid. (1964).
8. A.D. Liehr and C.J. Ballhausen, Ann. Phys. (N.Y.),  
6, 134 (1959).
9. G. Maki, J. Chem. Phys., 28, 651 (1958).
10. idem, ibid., 29, 1129 (1958).
11. B.N. Figgis and J. Lewis, Progr. Inorg. Chem., 6,  
37 (1964).
12. D. S. McClure, "Advances in the Chemistry of the  
Coordination Compounds", S. Krschner, Ed.,  
The Macmillan Co., New York, N.Y., 1961, p.498.
13. B.N. Figgis, Nature, 182, 1568 (1958).
14. B.N. Figgis, J. Lewis, F. Mabbs, and G.A. Webb,  
Nature, 203, 1138 (1964).

15. E.A. Barnard and W.D. Stein, *Advan. Enzymol.*, 20, 51 (1958).
16. D.W. Urrey and H. Eyring, *J. Theoret. Biol.*, 8, 198 (1965).
17. A.C. Hollinshead and P.K. Smith, *J. Pharmacol. Exp. Therap.*, 123, 54 (1958); D.G. O'Sullivan and A.K. Wallis, *Nature*, 198, 1270 (1963); D.G. O'Sullivan, D. Pantic, and A.K. Wallis, *Nature*, 205, 262 (1965).
18. D.E. Burton, A.J. Lambie, J.C.L. Ludgate, G.T. Newbold, A. Percival, and D.T. Siggers, *Nature*, 208, 1166 (1965).
19. E. Wundt, *Chem. Ber.*, 11, 826 (1878).
20. O. Fischer, *ibid.*, 22, 637 (1889).
21. E. Bamberger and J. Lorenzen, *Ann. Chem.*, 273, 267 (1893); E. Bamberger and B. Berle, *ibid.*, 273, 303 (1893).
22. S. Skraup, *ibid.*, 419, 70 (1919).
23. B. Ghosh, *J. Indian Chem. Soc.*, 28, 7710 (1951).
24. R. Dutta and S. Lahiry, *Sci. Cult. (Calcutta)*, 26, 139 (1960).
25. M. Goodgame and F.A. Cotton, *J. Am. Chem. Soc.*, 84, 1543 (1962).
26. J.E. Bauman, Jr., and J.C. Wang, *Inorg. Chem.*, 3, 368 (1964).
27. J. Brigando and D. Colaitis, *Compt. Rend.*, 256 5574 (1963).
28. Y. Nozaki, F.R.N. Gurd, R.F. Chen, and J.T. Edsall, *J. Am. Chem. Soc.*, 79, 2123 (1957).
29. J.T. Edsall, G. Felsenfeld, D.S. Goodman, and F.R.N. Gurd, *ibid.*, 76, 3054 (1954).

30. R.B. Martin and J.T. Edsall, *ibid.*, 80, 5033 (1958).
31. R.H. Carlson and T.L. Brown, *Inorg. Chem.* 5 268 (1966).
32. T.R. Harkins, J.L. Walters, O.E. Harris, and H. Freiser, *J. Am. Chem. Soc.*, 78, 260 (1956).
33. T.J. Lane and K.F. Quinlan, *ibid.*, 82, 2994 (1960).
34. R.S. Milner and L. Pratt, *Discussions Faraday Soc.*, 34, 88 (1962).
35. M.V. Artemenko and K.F. Slyusarenko, *Zh. Neorg. Khim.*, 10, 1145 (1965).
36. C.K. Jørgensen, "Absorption Spectra and Chemical Bonding in Complexes", Pergamon Press, Oxford, 1962; (a) D.S. McClure, *Solid State Phys.* 9, 399 (1959).
37. J. Lewis and R.G. Wilkins (Ed.), "Modern Coordination Chemistry", Interscience, 1960, p.232.
38. C.J. Ballhausen, "Introduction to Ligand Field Theory", McGraw-Hill, New York, 1962.
39. A.H. Morrish, "The Physical Principles of Magnetism", John Wiley, New York, 1965.
40. E.L. Muetterties and W.D. Phillips, *Advan. Inorg. Chem. Radiochem.*, 4, 231 (1962); and references given therein.
41. *Discussions Faraday Soc.* 34 Pt.II, 74-103 (1962).
42. F.A. Cotton, O.D. Faut, and D.M.L. Goodgame, *J. Am. Chem. Soc.*, 83, 344 (1961).
43. Y. Tanabe and S. Sugano, *J. Phys. Soc. Japan*, 9, 753 (1954).
44. N.S. Gill, R.S. Nyholm, G.A. Barclay, T.I. Christie, and P.J. Pauling, *J. Inorg. Nucl. Chem.*, 18, 88 (1961).

45. M. Ciampolini, *Inorg. Chem.*, 5, 35 (1966).
46. ref. 38, p. 142.
47. B.N. Figgis, *Trans. Faraday Soc.*, 56, 1553 (1960).
48. C. Starr, F. Bitter, and A.R. Kauffmann, *Phys. Rev.*, 58, 977 (1940).
49. J. Kanamori, *J. Phys. Chem. Solids*, 10, 87 (1959).
50. I. Tsubokawa, *J. Phys. Soc. Japan*, 15, 2109 (1960).
51. S.M. Nelson and T.M. Shepherd, *Inorg. Chem.*, 4, 813 (1965).
52. A.P.B. Lever, S.M. Nelson, and T.M. Shepherd, *ibid.*, 4, 810 (1965).
53. D.M.L. Goodgame, M. Goodgame, and F.A. Cotton, *J. Am. Chem. Soc.*, 83, 4161 (1961).
54. H.A. Weakliem, *J. Chem. Phys.*, 36, 2117 (1962).
55. P.J. Pauling, unpublished observation,
56. D.M.L. Goodgame and M. Goodgame, *Inorg. Chem.*, 4, 139 (1965).
57. D. Forster and D.M.L. Goodgame, *J. Chem. Soc.*, 2790 (1964).
58. *idem*, *Inorg. Chem.*, 4, 823 (1965).
59. *idem*, *J. Chem. Soc.*, 454 (1965).
60. E.U. Condon and G.H. Shortley, "The Theory of Atomic Spectra", Cambridge Univ. Press, 1951, p.177.
61. reff. 36(a), p.411.
62. M. Goodgame and F.A. Cotton, *J. Am. Chem. Soc.*, 84, 1543 (1962).

63. C.K. Jørgensen, *J. Inorg. Nucl. Chem.*, 24, 1571 (1962).
65. D.F. Evans, *J. Chem. Soc.*, 2003 (1959).
66. L.I. Katzin, *J. Chem. Phys.*, 35, 467 (1961).
67. H.C.A. King, E. Körös, and S.M. Nelson, *J. Chem. Soc.*, 5449 (1963).
68. idem, *ibid.*, 4832 (1964).
69. D.A. Fine, *Inorg. Chem.*, 4, 345 (1965).
70. A.B.P. Lever, J. Lewis, and R.S. Nyholm, *J. Chem. Soc.*, 5042 (1963).
71. R.J.H. Clark and C.S. Williams, *Inorg. Chem.*, 4, 350 (1965).
72. M. Delepine, *Ann. Chim. (Paris)*, 19, 145 (1923);  
idem, *Bull. Soc. Chim. France*, 45, 235 (1929).
73. C.W. Frank and L.B. Rogers, *Inorg. Chem.*, 5, 615 (1966).
74. P.C.H. Mitchell and R.J.P. Williams, *J. Chem. Soc.*, 1912 (1960).
75. J. Lewis, R.S. Nyholm, and P.W. Smith, *ibid.*, 4590 (1961).
76. M.M. Chamberlain and J.C. Bailar, Jr., *J. Am. Chem. Soc.*, 81, 6412 (1959).
77. J.H. Van Vleck, "Electric and Magnetic Susceptibilities", Oxford Univ. Press, N.Y., 1932.
78. J.B. Goodenough, "Magnetism and the Chemical Bond", John Wiley and Sons, N.Y., 1963.
79. V. Halpern, *Proc. Roy. Soc. (London)*, Ser. A, 291, 113 (1966).

80. C.J. Ballhausen and A.D. Liehr, J. Am. Chem. Soc., 81, 538 (1959).
81. L.E. Orgel, J. Chem. Phys., 23, 1958 (1955).
82. I. Lifschitz and K.M. Dijkema, Rec. Trav. Chim., 60, 581 (1941); and references given therein.
83. G.A. Melson and D.H. Busch, J. Am. Chem. Soc., 86, 4830 (1964).
84. S.L. Holt, Jr., R.J. Bouchard, and R.L. Carlin, *ibid.*, 86, 519 (1964).
85. A.I. Vogel, "Quantitative Inorganic Analysis", 3rd Edn., Longmans, Green, 1961.
86. M. Goodgame and M.J. Weeks, to be published, J. Chem. Soc.
87. S. Glasstone, "Thermodynamics for Chemists", D. Van Nostrand, N.Y., 1947, p.185.
88. H. Yamatera, Bull. Chem. Soc. Japan, 31, 95 (1958).
89. M. Linard and M. Wiegel, Z. Anorg. Allgem. Chem., 264, 321 (1951); and references given therein.
90. C.E. Schäffer and C.K. Jørgensen, Mat. Fys. Medd. Dan. Vid. Selsk., 34, nr.13, (1965).
91. H. Hartmann and H. Kruse, Z. Physik. Chem., N.F., 5, 9 (1955).
92. C.J. Ballhausen and C.K. Jørgensen, Mat. Fys. Medd. Dan. Vid. Selsk., 25, nr.14, (1955).
93. C.J. Ballhausen and W. Moffitt, J. Inorg. Nucl. Chem., 3, 178 (1956).
94. R.L. Belford and M. Karplus, J. Chem. Phys., 31, 394 (1959).
95. D.P. Craig and F.A. Magnusson, Discussions Faraday Soc., 26, 116 (1958).

96. C.K. Jørgensen, *ibid.*, 26, 110, 172 (1958).
97. T.S. Piper and R.L. Carlin, *J. Chem. Phys.*, 33, 1208 (1960).
98. R.A.D. Wentworth and T.S. Piper, *ibid.*, 41, 3884 (1964).
99. C.E. Schäffer and C.K. Jørgensen, *Mol. Phys.*, 9, 401 (1965).
100. J.S. Griffith and L.E. Orgel, *J. Chem. Soc.*, 4981 (1956).
101. D.S. McClure, "Advances in the Chemistry of the Coordination Compounds", S. Kirschner, Ed., The Macmillan Co., New York, N.Y., 1961, p.498.
102. ref. 38., p. 99-101.
103. R.A.D. Wentworth and T.S. Piper, *Inorg. Chem.*, 4, 709 (1965), *idem*, *ibid.*, 4, 1524 (1964).
104. J.H. Van Vleck, *J. Chem. Phys.*, 7, 72 (1939).
105. M. Wofsiberg and L. Helmholz, *ibid.*, 20, 837 (1952).
106. D.M.L. Goodgame, M. Goodgame, M.A. Hitchman and M.J. Weeks, *Inorg. Chem.* 5, 635 (1966).
107. J.D. Dunitz, *Acta Cryst.*, 10, 307 (1957).
108. M.A. Porai-Koshits, *Tr. Inst. Krist. Akad. Nauk SSSR*, 10, 117 (1954).
109. C.K. Jørgensen, *Advan. Chem. Phys.*, 5, 33 (1963).
110. ref. 36, p.113.
111. B.N. Figgis, *J. Chem. Soc.*, 4887 (1965).
112. ref. 37, p. 282.
113. A.S. Antsishkina and M.A. Porai-Koshits, *Kristallografiya*, 3, 676 (1958).



114. A.R. Katritzky, (Ed.), "Physical Methods in Heterocyclic Chemistry", Academic Press, N.Y., 1963. Vol.I, p.65-103.
115. G.W. Parshall, J. Am. Chem. Soc., 88, 704 (1966).
116. D.P. Graddon and E.C. Watton, Aust. J. Chem., 18, 507 (1965).
117. C.K. Jørgensen, Act. Chem. Scand., 11, 151 (1957); idem, *ibid.*, 11, 166 (1957); E. König and H.L. Schläfer, Z. Physik. Chem., N.F, 26, 371 (1960).
118. J.A. Happe and R.L. Ward, J. Chem. Phys., 39, 1211 (1963).
119. W.D. Horrocks, Jr., R.C. Taylor, and G.N. LaMar, J. Am. Chem. Soc., 86, 3031 (1964).
120. R.H. Holm, G.W. Everette, Jr., W.D. Horrocks, Jr., *ibid.*, 88, 1071 (1966).
121. H.M. McConnell and D.B. Chesnut, J. Chem. Phys., 28, 107 (1958).
122. D.R. Eaton, J. Am. Chem. Soc., 87, 3097 (1965).
123. H.M. McConnell and R.E. Robertson, J. Chem. Phys., 29, 1361 (1958).
124. G.N. LaMar, W.D. Horrocks, Jr., L.C. Allen, *ibid.*, 41, 2126 (1964).
125. W.D. Horrocks, Jr. and G.N. LaMar, Proc. 8 I.C.C.C., 1964, p.52.
126. D.R. Eaton, A.D. Josey, W.D. Phillips, and R.E. Benson, J. Chem. Phys., 39, 3513 (1963).
127. D.R. Eaton and E.A. LaLancette, *ibid.*, 41, 3534 (1964).
128. G.N. LaMar, J. Am. Chem. Soc., 87, 3567 (1965).
129. Z. Luz and S. Meiboom, J. Chem. Phys., 40, 1058, 1066 (1964).

130. H.S. Gutowsky, D.W. McCall, and C.P. Slichter, *ibid.*, 21, 279 (1953).
131. J.A. Pople, W.G. Schneider, and H.J. Bernstein, "High Resolution Nuclear Magnetic Resonance", McGraw Hill, New York, 1959, p.223.
132. P.J. Black and M.L. Heffernan, *Australian J. Chem.*, 15, 862 (1962).
133. R. Hoffman, *J. Chem. Phys.*, 40, 2745 (1964).
134. L. Pratt, *Boll. Sci. P.c. Chim. Ind. Bologna*, 21, 72(1963).
135. W.D. Phillips and R.E. Benson, *J. Chem. Phys.*, 33, 607 (1960).
136. G.N. LaMar, *J. Chem. phys.*, 41, 2992 (1964).
137. *idem*, *J. Phys. Chem.* 69, 3212 (1965).
138. L.H. Piette and W.A. Anderson, *J. Chem. Phys.*, 30, 899 (1959).
139. E.A. LaLancette and D.R. Eaton, *J. Am. Chem. Soc.*, 86, 5145 (1964).
140. S. Martinez-Carrera, *Acta. Cryst.*, 20, 783 (1966).
141. L.E. Sutton, Ed., "Tables of Interatomic Distances and Configurations in Molecules and Ions", Chem. Soc. Special Publication, Burlington House, London, 1958.
142. A.F. Wells, "Structural Inorganic Chemistry", 2nd Edn., Clarendon Press, Oxford, 1950, Chapter II.
143. J.P. Fackler and D.G. Holah, *Inorg. Chem.*, 4, 954 (1965).
144. F.E. Hoar, L.C. Jackson, and N. Kurti, *Experimental Cryophysics*, Butterworths, London, 1961, p.132.
145. B.N. Figgis and R.S. Nyholm, *J. Chem. Soc.*, 331 (1959).

146. H.R. Nettledon and S. Sugden, Proc. Roy. Soc. (London), Ser. A, 173, 313 (1939).
147. B.N. Figgis and R.S. Nyholm, J. Chem. Soc., 4190 (1958).
148. N.F. Curtis, *ibid.*, 3147 (1961).
149. M.G.B. Drew, private communication.